# PRECLINICAL PHARMACOLOGICAL AND TOXICOLOGICAL STUDY OF NOVEL INHIBITORY KAPPA B KINASE ALPHA (IKKα) INHIBITOR COMPOUNDS IN PROSTATE CANCER

By

KHALID S. ALHARBI

A thesis presented in fulfillment of the requirements for the degree of Doctor of Philosophy

June 2016

Strathclyde Institute for Pharmacy and Biomedical Sciences

University of Strathclyde, Glasgow, UK

***"This thesis is the result of the author's original research. It has been composed by the author and has not been previously submitted for examination which has led to the award of a degree.***



***Signed:*** ***Date:***

## ACKNOWLEDGMENTS

*"This Thesis is dedicated to the memory of my father, who passed away before the completion of this effort. He was really special person, and I thank him for his affection and support. Words cannot heal the pain of losing you. How I miss you"*

*First and foremost I would like to thank Allah (God) for giving me the power to believe in myself and pursue my dreams. I could never have done this without the faith I have in you.*

*I would like to express my sincere gratitude to my advisor Dr Marie Boyd for the continuous support of my PhD study and related research, for her patience, motivation, and immense knowledge. Her guidance helped me throughout the research and writing of this thesis. I could not have imagined having a better advisor and mentor for my PhD study. I have been extremely lucky to have a supervisor who cared so much about my work, and who always responded to my questions and queries so promptly. I also would like to thank my second supervisor, Prof Robin Plevin.*

*I would also like to submit my sincere debt of gratitude to the government of Saudi Arabia represented by the Ministry of Health and the Saudi Cultural Bureau in London for providing me with this great opportunity to undertake this rather challenging and inspiring project for which they provided the financial support.*

*Thank you to everyone who helped me in the lab. Tony and Annette gave me lots of advice when I first started my Ph.D. Their professional and enthusiastic attitude in science showed me a good model of being a PhD student. For my last year of Ph.D. study, Gary and Ahlam have helped me a lot and shared advices and ideas with me. Also, I will never forget my friends: Pamela, Paul, Mohammad, Abdulfattah, Omar, David and Lindsey.*

*A special thanks to my family. Words cannot express how grateful I am to my mother for all of the sacrifices that you've made on my behalf, without her continuous support and encouragement I never would have been able to achieve my goals. Thank you to my brothers and sisters for their endless advice and support. My deepest appreciation is expressed to my wife for her continuous support and love and to my sons for their love and patience and for giving me the courage to make it.*

*"Allah makes the way to Heaven easy for him who treads the path in search of knowledge." ~ Prophet Mohammad (PBUH)*

# Publications

## Poster presentations

**K Alharbi,** A McCluskey, A Sorensen, S McKay, A Paul, R Plevin, J Edwards, A Rosweir, N. Anthony, J. Baiget, G. Berretta, D. Breen, J. Huggan, K. Ho, S. Lang, L Young,CJ Suckling, M Boyd (2014). Assessing the Anti-tumour Efficacy of IKKα inhibitors Against Prostate Cancer. Postgraduate Research day. Strathyclyde University, Glasgow, UK.

**K Alharbi,** A McCluskey, A Sorensen, S McKay, A Paul, R Plevin, J Edwards, A Rosweir, N. Anthony, J. Baiget, G. Berretta, D. Breen, J. Huggan, K. Ho, S. Lang, L Young,CJ Suckling, M Boyd (2014). Assessing the Anti-tumour Efficacy of IKKα inhibitors Against Prostate Cancer. Cell Biology, Cardiovascular and Neuroscience Postgraduate Research Day, Strathyclyde University, Glasgow,UK.

**K Alharbi,** A McCluskey, A Sorensen, S McKay, A Paul, R Plevin, J Edwards, A Rosweir, N. Anthony, J. Baiget, G. Berretta, D. Breen, J. Huggan, K. Ho, S. Lang, L Young,CJ Suckling, M Boyd (2015). Assessing the Anti-tumour Efficacy of IKKα inhibitors Against Prostate Cancer. SIPBS Annual Research Symposium, Strathyclyde University, Glasgow,UK.

## Publications relating to this thesis

**K Alharbi,** A McCluskey, A Sorensen, M Boyd, (2016). Radiosensitisation effect of novel IKKα inhibitor (SU1261) in castration resistant prostate cancer (CRPC). (In preparation)

# Table of Contents

# List of Figures

# List of Tables

# Abbreviations

| | |
|---|---|
| ANOVA | Analysis of variance |
| BAD | Bcl-2 assoicated death promoter |
| BAFF | B cell activation factor |
| Bcl-2 | B-cell lymphoma-2 |
| BPH | Benign Prostatic Hyperplasia |
| BSA | Bovine serum albumin |
| CBP | CRE binding protein |
| CRPC | Castrate-resistant prostate cancer |
| DMEM | Dulbecco's Modified Eagle Medium |
| DMSO | Dimethyl sulfoxide |
| DNA | Deoxyribonucleic acid |
| DRE | Digital Rectal Examination |
| DTT | Dithiothreitol |
| EGFR | Epidermal growth factor receptor |
| FCS | Foetal calf serum |
| FDA | Food drug administration |
| HLH | Helix-loop-helix |
| IKK | Inhibitory kappa B kinase |
| IκB-α | Inhibitory kappa B alpha |
| LTα1β2 | Lymphotoxin alpha 1 beta 2 |
| Luc | Luciferase |

| | |
|---|---|
| MAPK | Mitogen-activated protein kinase |
| MAPKK | Mitogen activated protein kinase kinase |
| MEF | Mouse Embryonic Fibroblast |
| MEM | Minimum essential media |
| mRNA | Messenger Ribonucleic acid |
| mRNA | Messenger Ribonucleic acid |
| NEMO | NF-κB essential modulator |
| NF-κB | Nuclear factor kappa B |
| NIK | NF-κB inducing kinase |
| NLS | Nuclear localisation sequence |
| NMR | Nuclear Magnetic Resonance |
| PAGE | Polyacrylamide gel electrophoresis |
| PBS | Phosphate buffered saline |
| PCa | Prostate cancer |
| PSA | Prostate specific antigen |
| SDS | Sodium dodecyl sulphate |
| shRNA | Short hairpin interfering RNA |
| siRNA | Small interfering RNA |
| TNF-α | Tumour necrosis factor |
| TRAF | TNF receptor-associated factor |

## Abstract

Prostate cancer (PCa) is the most frequently diagnosed cancer and the second most common cause of cancer deaths in men in the UK, despite the progress that has been made in PCa treatment. Nuclear Factor kappa B (NF-κB) regulates several genes involved in immune response, inflammation, proliferation and apoptosis. Overexpression of NF-κB has been shown to be involved in tumour progression and radiation therapy resistance of PCa. One potential approach in PCa cancer treatment therefore involves targeting IκB kinases (IKKs) which are key regulators of the NF-κB signaling pathway. Whilst IKKβ regulates the canonical NF-κB pathway involving degradation of IκB-α and phosphorylation of p65, IKKα regulates the non-canonical NF-κB pathway by mediating the processing of p100 to p52. Inhibition of NF-κB signaling by targeting IKKβ is a sub-optimal treatment choice as it has been shown to be associated with multiple serious toxicities. However, IKKα is of interest in PCa therapy as it has been implicated in PCa survival, proliferation, invasion and metastasis. In addition, the non-canonical NF-κB pathway, which is regulated mainly by IKKα, has been demonstrated to drive the development of radioresistance in PCa cells. Therefore, targeting IKKα is a new approach for the development of novel therapies for PCa.

In Chapter 3, the pharmacological characteristics of novel first-in-class IKKα inhibitors (SU compounds) developed in-house were investigated in terms of selectivity against IKKα and IKKβ in PCa cell lines using Western blot analysis. In Chapter 4, the phenotypic impact of the selective IKKα inhibitors (SU compound) in PCa and normal prostate cell lines was interrogated using cell growth assay, cell viability assay, clonogenic assay, caspase-3 assay and cell cycle analysis, and the radiosensitisation potential of selective IKKα inhibitor SU compounds in PCa cell lines were investigated using clonogenic assay, cell cycle assay and combination index methods. In Chapter 5, the cytotoxicity and radiosensitisation effects of non-pharmacological inhibition of IKKα and IKKβ using small interfering RNAs (siRNAs) in PCa cell lines were also investigated using cell growth assay, clonogenic assay, cell cycle analysis and linear quadratic analysis.

These studies demonstrated that among investigated SU compounds, SU1261 most selectively inhibits the non-canonical NF-κB pathway biomarker p52 at lower concentrations than the canonical NF-κB pathway biomarkers, IκB-α degradation and phosph-p65, demonstrating selectivity of this compound for IKKα over IKKβ. Furthermore, SU1261 showed a highly cytotoxic profile in term

of inhibition of growth rate, reduction in cell viability and clonogenicity, and induced apoptosis in both PCa (PC3M-luc-C6 and PC3) and normal prostate (PNT2A) cell lines. However, SU1261 exhibited lower cytotoxicity against normal prostate epithelium cells (PNT2A) compared with PCa cells (PC3M-luc-C6 and PC3), suggesting that inhibition of IKKα may offer a therapeutic differential in cancer versus normal cells. Furthermore, a combination of SU1261 and X-ray irradiation delivered to PC3M-luc-C6s showed a synergistic interaction which resulted in an enhanced radiation-induced colony survival inhibition arrest of the cell cycle at the G2/M phase. On the other hand, knockdown of the IKKα protein in PC3M-luc-C6s using siRNA only impacted the growth rate of cells, but silencing of IKKβ inhibited both growth rate and clonogenicity of PC3M-luc-C6 cells as well as inducing apoptosis. In addition, knockdown of both kinases did not show significant enhancement in radiation cytotoxicity in PC3M-luc-C6 cells.

These data taken together represent one of the first interrogations of the phenotypic effect of IKKα inhibition and suggest that SU1261 is a first-in-class novel selective IKKα inhibitor compound. Pharmacological inhibition of IKKα using SU1261, but not with siRNA against IKKα, as a single agent or in combination with radiation may be a useful approach for PCa treatment.

# Chapter 1

# General Introduction

## 1.1 Introduction to cancer

### 1.1.1 The incidence of cancer

Cancer is a major public health problem in the United Kingdom and worldwide. In 2012, GLOBOCAN estimated that around 14.1 million people were diagnosed with cancer, with 8.2 million deaths; of these, 57% of incidences and 65% of mortalities were recorded in developing countries (Torre *et al.,* 2015). Despite the advances in cancer therapy which have led to increased survival rates, deaths from cancer worldwide are predicted to continue increasing, with an expected 13 million deaths occurring due to cancer in 2030 (Ferlay *et al*., 2010).

According to the most recent statistics available from Cancer Research UK, 352,197 people were diagnosed with cancer in 2013, which equates to about 962 cases a day, and more than 40 cases per hour (Figure 1.1) (Cancer Research UK, 2016). Nowadays, there are more than 200 different types of cancer identified, but four of them — breast, prostate, lung and colorectal — account for over half (53%) of all new cases in the UK in 2013 (Cancer Research UK, 2016). In addition, the incidence rates for cancer in the UK increased by 25%, with a 14% increase in incidence rates in men and a 32% increase in women between 1979–1981 and 2007–2009, with only 50% of people diagnosed with cancer surviving for more than 10 years. In 2012, 161,823 people died from cancer in the UK (Cancer Research UK, 2016), suggesting that there is an urgent need for the development of novel anti-cancer therapies to reduce cancer mortality rates.

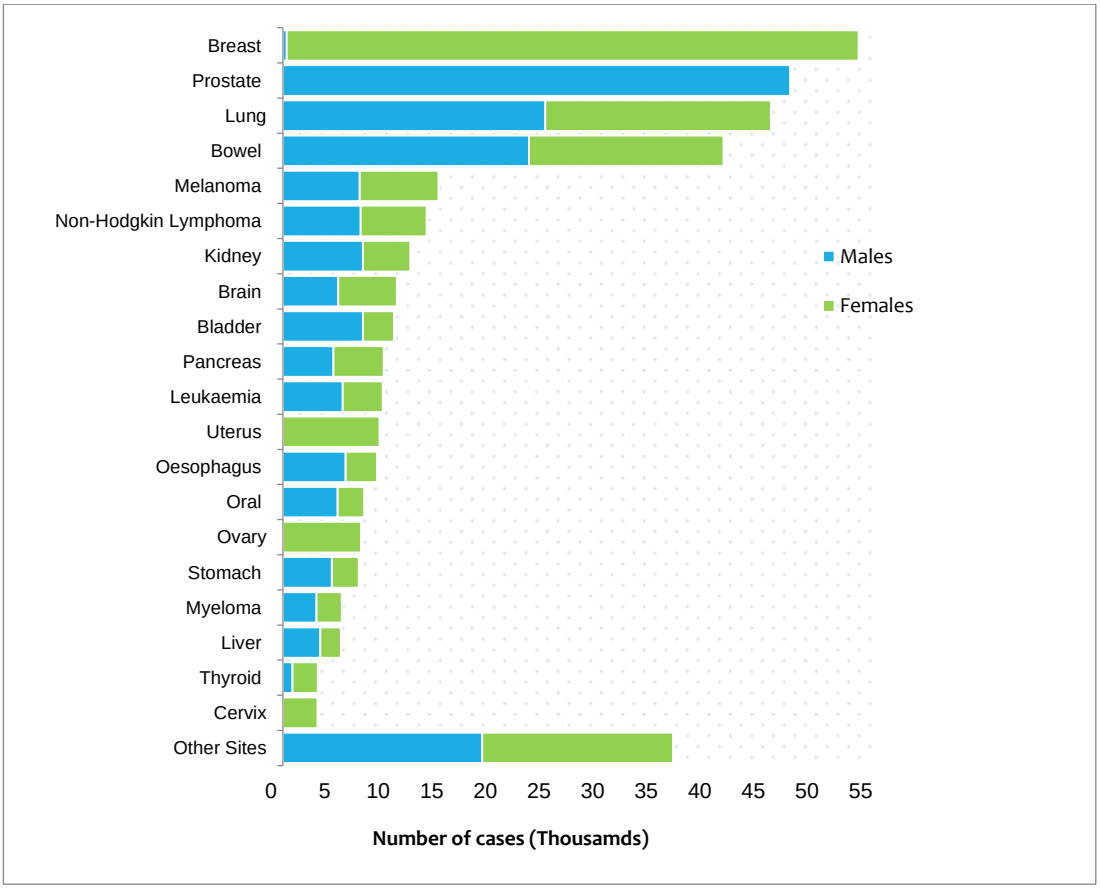


**Figure 1.1: Number of registered cancer cases for males and females in the UK in 2013.** (Figure adapted from Cancer Research UK, 2016).

### 1.1.2 The development of cancer

Cancer means ‘crab’ in Latin. In ancient times, the word was used to describe the crab-like way that cancer cells spread throughout the body. In scientific terms, cancer (malignant neoplasm) is defined as a complex genetic disease in which a group of cells exhibit ‘uncontrolled growth’ (division beyond the normal limits), ‘invasion’ (intrusion on and destruction of adjacent tissues) and sometimes ‘metastasis’ (spread to other locations in the body via lymph or

blood). These three malignant properties of cancers distinguish them from benign tumours, which are self-limited and do not invade or metastasise (Akanni *et al*., 2010). These alterations are caused mainly by abnormalities in the genetic material (DNA) of the transformed cells and consequently lead to an inability of these cells to carry out their normal functions. These abnormalities in the genetic material (mutations) are often caused by cancer-causing agents (carcinogens), such as tobacco smoke, radiation, chemicals or infectious agents. However, other cancer-promoting genetic abnormalities may be inherited or acquired through errors in DNA replication.

Cancer is caused mainly by two classes of genes, oncogenes and tumour suppressor genes (TSGs), which each have an essential role in normal cells. Oncogenes are derived from mutated forms of normal cellular genes (called proto-oncogenes) that control cell proliferation, survival and spread. The expression of proto-oncogenes is strictly regulated in normal cells to prevent uncontrolled cell growth. However, in cancer, activated mutations of proto-oncogenes lead to uncontrolled cell division, enhanced survival and dissemination (Rogers *et al*., 2005). TSGs or anti-oncogenes [such as *TP53 (p53)*, *BRCA1*, *BRCA2*, *APCA* and *RB*] are genes that are responsible for inhibition of cell proliferation and survival. In their unmutated state, the protein products of these genes are mainly involved in controlling cell cycle progression and programmed cell death (apoptosis). In the presence of DNA damage due to irradiation, chemical or infectious agents, proteins encoded by tumour

suppressor genes arrest the cell cycle until the damage is repaired. However, if damage in the cell is not repaired, apoptosis is induced. For example, p53 as a transcription factor induces a G1 arrest of the cell cycle by regulating the expression of p21WAF1/CIP1/Sdi1, an inhibitor of the cyclin-dependent kinases (CDKs) 2, 3, 4 and 6. p53 also mediates apoptosis through regulation of apoptotic protein BAX, a member of the BCL-2 protein family gene (Koutsodontis *et al*., 2005; Shaw, 1996). When TSGs are mutated, cells can grow out of control, which can lead to cancer.

Key changes occur in cancers that can be seen as mostly responsible for driving their malignant behaviour. The first of these is growth factor independence. Cancer cells can grow and divide without external normal growth signals, and some cancer cells can create their own growth signals. For example, glioblastomas can produce their own platelet-derived growth factor (PDGF), and sarcomas can produce their own tumour growth factor α (TGF-α). Second, cancer cells develop insensitivity to anti-growth signals. The growth inhibition of normal cells is controlled by growth inhibitors in the surrounding environment, in the extracellular matrix and on the surfaces of nearby cells. Cancer cells can also avoid apoptosis through their ability to ignore signals sent through the extrinsic pathways or by resetting the balance of intracellular pro-apoptotic and anti-apoptotic molecules (Harrington *et al*., 2010). However, normal cells evaluate their viability by assessing the balance of survival (anti-apoptotic) and death (pro-apoptotic) signals that they receive.

Cancer cells also induce sustained angiogenesis, the process by which new blood vessels are formed. Cancer cells can create their own blood vessels to maintain an adequate supply of oxygen and nutrients for cancer cells to progress. Angiogenesis is controlled by inducers and inhibitors. Inducers include vascular endothelial growth factor (VEGF) and basic fibroblast growth factor (FGF 1/2), which bind to transmembrane tyrosine kinase receptors on endothelial cells. An inhibitor of angiogenesis is thrombospondin-1, which binds to CD36. A further distinguishing feature of cancer cells is their ability to immortalise or to have limitless reproductive potential. Normal cells die after a certain number of divisions (about 25–50 doublings). This limit is mediated by the pRb, p16INK4a and p53 pathways, and further replication subsequently leads to telomere (chromosome end) loss. However, most cancer cells are able to grow and divide without limit through their ability to upregulate telomerase, the enzyme that maintains telomeres. Finally, cancer cells have the ability to invade adjacent tissues and metastasise to distant sites, through loss of cell–cell contacts (cadherins) and increased production of matrix metalloproteinases (Hanahan and Weinberg, 2000).

## 1.2 Prostate cancer (PCa)

### 1.2.1 Prostate cancer incidence and risk factors

Prostate cancer (PCa) is cancer in the prostate gland. It is a major public health problem facing men in the United Kingdom and many other parts of the world. In the UK, cancer of the prostate is the second most common cancer after breast cancer, and the most common cancer in men (Cancer Research UK, 2016). Among the 352,197 diagnosed cancer cases in the UK in 2013, out of 200 types of cancer, PCa accounted for 47,300 cases, nearly 13% of the cases that year (Cancer Research UK, 2016). PCa is the second most common cause of cancer death in UK men, after lung cancer. In 2012, around 10,800 men died from PCa in the UK, which equates to 30 deaths per day (Cancer Research UK, 2016).

Age is the most important risk factor, and the highest rates of PCa are found in the oldest patients with approximately 85% of diagnosed men being over 65, and less than 0.1 percent being younger than 50 (Patel and Klein, 2009). Post-mortem prostate autopsy data also show that nearly 50% of all tested men in their 50s have a histological indication of PCa and this figure increases to 80% by age 80 (Haas *et al*., 2008).

Race is also considered a risk factor in PCa. For instance, African Americans have a 50% higher rate of incidence and prognosis of PCa than white Americans (Bostwick *et al*., 2004). However, Asian Americans tend to develop a more advanced stage of the disease than white Americans, and are predisposed

to the development of more advanced stages than non-Hispanic (NH) whites (Lichtensztajn *et al*., 2014, Oakley-Girvan *et al*., 2003). The mortality rate from PCa in African-Americans has also been reported to be twice that of white men (Powell, 2007).

Family history or heredity is another risk factor for PCa. The incidence of PCa doubles in males whose fathers have or had the disease, and triples for those with a brother who has or had the disease (Kicinski *et al*., 2011). Some inherited genetic mutations might pose an increased risk for PCa, but only in a small percentage of cases. Females with the BRCA1 or BRCA2 genes are at greater risk of developing breast and ovarian cancers and it has been reported that the presence of mutations in these genes may increase the risk of PCa in men (Cavanagh and Rogers, 2015). Additionally, in men with Lynch syndrome (also known as hereditary non-polyposis colorectal cancer, or HNPCC), a condition caused by inherited gene germline mutation of the mismatch repair (MMR) genes, the risk of PCa is increased fivefold (Haraldsdottir *et al*., 2014). Other risk factors that may be linked to PCa include diet, lifestyle and environment. A positive correlation has been found between obesity and risk of PCa metastasis and mortality in middle aged males (Gong *et al*., 2007). High body mass index (BMI) in men is linked with higher prostate mass and higher pathological stages of PCa (Goris Gbenou *et al*., 2016) and conversely increased physical activity is associated with a lower risk of high-stage PCa (De Nunzio *et al*., 2015). High consumption of dairy products is associated with high incidence of PCa and

other environmental factors, including smoking and alcohol intake, may have a role in PCa progression (Baglietto *et al*., 2006; Jones *et al*., 2016; Fowke *et al*., 2015), but the results from studies interrogating these links have been inconsistent.

### 1.2.2 Prostate gland anatomy, function and pathophysiology

The prostate is a tubuloalveolar exocrine gland of the male sex reproductive system that includes the prostate, seminal vesicles and bulbourethral glands. It is a walnut-sized gland, and weighs 20–30 g in men between the ages of 20 and 50. The prostate gland is located in the pelvis, under the urinary bladder and in front of the rectum (Figure 1.2) (Fine and Reuter, 2012).

The main function of the prostate gland is the secretion and storage of 25% of the seminal fluid, which carries spermatozoa made by the testicles. The prostate gland has a metabolic function that regulates testosterone, the male sex hormone. The prostate converts less active testosterone to the active form dihydrotestosterone (DHT) (Kumar and Majumder, 1995).

In pathology, the prostate gland is divided into three major regions: the peripheral zone (PZ), the central zone (CZ) and the transition zone (TZ) (McNeal, 1981). The clinical importance of this classification is to understand which parts of the prostate are susceptible to benign and malignant tumours (Fine and Reuter, 2012). The PZ is the main part (70%) of the prostate; more than 70% of PCa originates in this zone. The CZ constitutes 20% of the

prostate; roughly 2.5% of PCa develops in this portion. The TZ makes up only 5% of the prostate and is responsible for 10–20% of PCa. Beyond middle age, this zone becomes enlarged, causing a condition called benign prostatic hyperplasia (BPH), or enlargement of the prostate gland (Fine and Reuter, 2012).

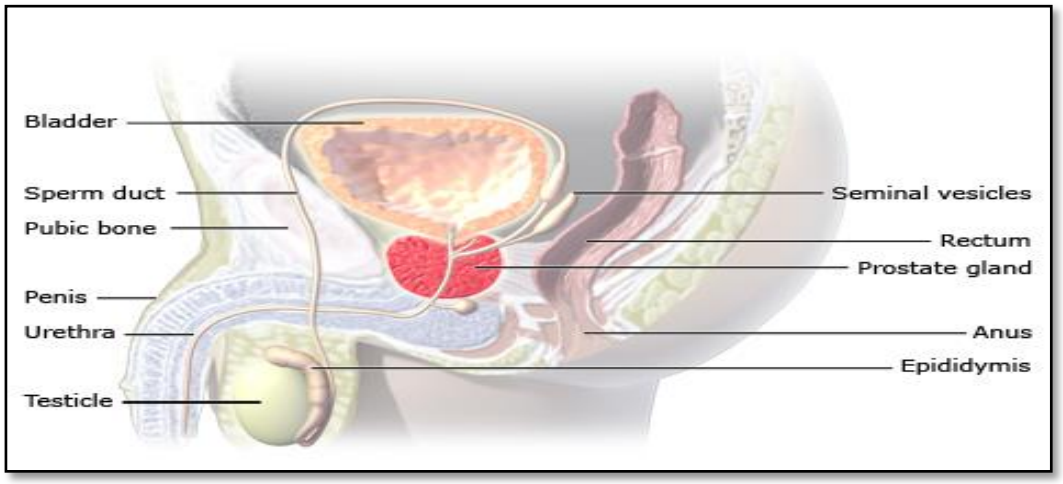


**Figure 1.2. Prostate gland location.** The prostate position and the surrounding organs (Image from informedhealth.org at https://www.informe dhealth.org).

### 1.2.3 Prostate cancer progression and pathogenesis

More than 90% of all PCa cases are adenocarcinoma which is a cancer that generates from the epithelial cells of the organs and arises from the peripheral zone of the prostate (Borges *et al*., 2016). Small cell carcinoma, another form of PCa, is formed mainly by the hormone secreting cells (neuroendocrine cells). In the early stages, small cell carcinoma is hard to detect by pathologists, as it is

not accompanied by a raised prostate-specific antigen (PSA), which is the diagnostic marker of PCa (Hirai *et al*., 2015). Similarly, squamous cell carcinoma is a fast growing tumour and may not elevate PSA levels (Acosta *et al*., 2016). Sarcomas and transitional cell carcinoma are rare forms of PCa. The latter is a secondary tumour which derives from distal tumours developed in the urinary tract system (bladder or urethra), but rarely originates in the prostate (Arista-Nasr *et al*., 2016).

The growth of prostate gland and PCa cells both need physiological levels of androgen to stimulate proliferation and inhibit apoptosis. Androgens (male hormones), which are synthesised mainly in the testicles, are responsible for up to 80% of PCa growth (Chuu *et al*., 2011). Androgens mediate the translocation of androgen receptor (AR) into the nucleus where it binds with androgen response elements and subsequently induces PCa growth and inhibition of apoptosis (Figure 1.3) (Semenas *et al*., 2012). Thus, initial therapy for PCa consists of anti-androgen therapy; however, this is only a palliative treatment with an effective duration of between 12 and 18 months (Harris *et al*., 2009, Maroto *et al*., 2016). After this duration, the PCa develops to an androgen-insensitive stage called castration-resistant PCa (CRPC) and will progress independently of androgens. CRPC is an advanced stage of PCa for which no full cure therapies are available, and it is therefore associated with high mortality rates. The mechanisms underlying the development of castration-resistant PCa are still poorly understood. A number of studies have shown that CRPC cells

continue to express androgen-responsive genes and AR protein (Dutt and Gao, 2009). AR gene amplification and AR mutation are possible mechanisms that may be involved in PCa progression and development of castration resistance, even with low androgen levels (Dutt and Gao, 2009). AR gene amplification is present in 20–52% of CRPC specimens which suggests the possible role of AR in the castration-resistance mechanism (Robinson *et al*., 2015).

PCa is a highly metastatic cancer which spreads outside the prostate capsule particularly to the bones (90%), lung (46%), liver (25%), pleura (21%), and adrenal glands (13%) (Conde Moreno *et al*., 2014). Approximately 10% of PCa is metastatic at diagnosis, and 25% of cases with localised or locally advanced tumours will progress to the metastatic stage during the disease period (Suarez *et al*., 2014). The bony metastasis is highly frequent (90%) with PCa, and associated with highly significant disease symptoms including pain, fractures, nerve compression syndromes, and hypercalcemia prior to a patient's death. The network of veins that surrounds the prostate gland (Batson's plexus) which connects to the veins of the spine is the potentially cause of the bone being the most common metastatic site of PCa (Ye *et al*., 2007). Current treatments for those patients are only palliative, symptomatic treatment to improve quality of life. Unfortunately the median survival of metastatic CRPC remains poor, at less than 19 months (Husson *et al*., 2014).

The exact mechanism of metastatic potential of PCa is still not fully understood. The metastasis of prostate tumour cells has been found to correlate with the

expression of several angiogenic genes, including vascular endothelial growth factor (VEGF), basic fibroblast growth factor (bFGF), interleukin 8 (IL-8) and matrix metalloproteases (MMP-2 and MMP-9) (Uehara *et al*., 2005). The MMPs proteins are essential in the metastasis process by their ability to degrade the extracellular matrix, thereby allowing the invasive PCa cells to metastasize to distal organs via the lymph node and blood vessels (Dasgupta *et al*., 2012). In addition, this protease activity of MMPs not only permits cell metastasis, but also has a role in facilitating angiogenesis. In bone, the PCa metastatic cells allow for angiogenesis via the MMP9 derived from osteoclasts (Bruni-Cardoso *et al*., 2010). Some of the MMPs members such as MMP-2 and MMP-9 have a higher expression in metastatic PCa samples, suggesting the involvement of these proteins in PCa progression and metastasis (Gong *et al*., 2014).

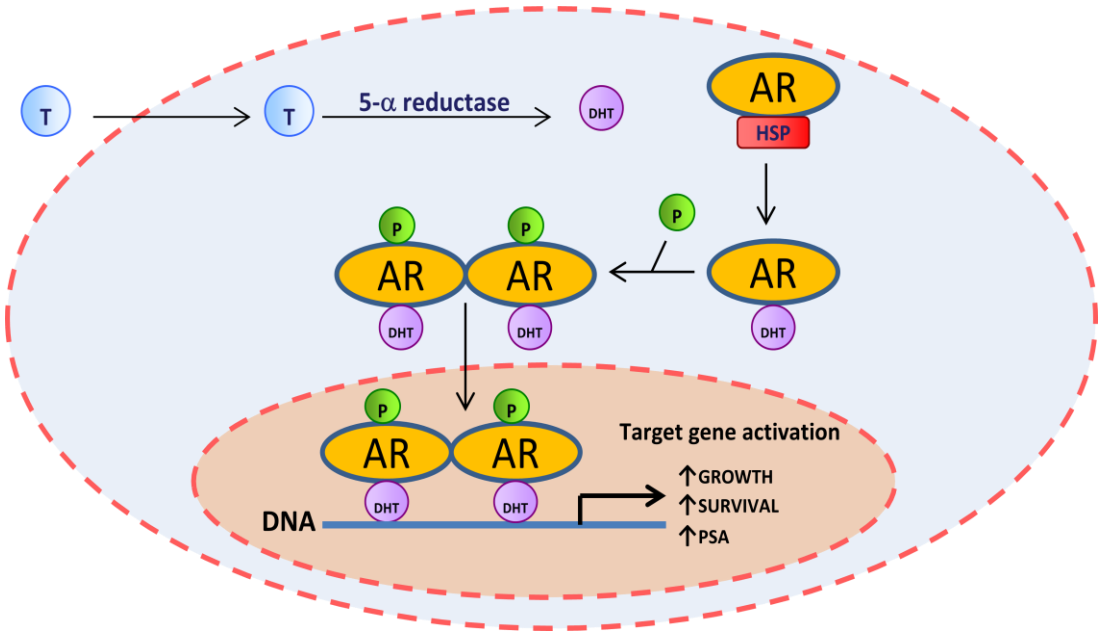


**Figure 1.3 Role of androgens in PCa cell survival and growth**. In the cytoplasm of prostatic epithelial cells, 5α-reductase converts testosterone to dihydrotestosterone (DHT). AR is released from inhibitory heat shock proteins (HSPs) and binds to DHT resulting in phosphorylation and translocation of the AR homo-dimer into the nucleus where it binds with androgen response elements in the promoter regions leading to transcriptional activation, and subsequently induced survival and growth of the cell and expression of PSA.

### 1.2.4 Prostate tumour staging

Tumour staging refers to the degree to which the tumour has involved the prostate gland or has spread. Once a patient has been diagnosed with a prostate tumour, the cancer must be staged to determine if it has spread beyond the prostate. Staging also provides better insight into the risk of the disease spreading further, which helps to identify the correct treatment option. The Tumour Node Metastasis (TNM) system is used to determine the stage of the

cancer; that is, how far it has spread from the prostate. The TNM classification system breaks tumour stage into three components. The tumour (T) stage reflects the extent of disease at the primary site; the node (N) stage reveals if the cancer has spread to nearby lymph nodes in the pelvic region and the metastasis (M) component indicates whether the cancer has spread to other parts of the body, such as the bones. This information, combined with the Gleason score, is pivotal in the selection of the best treatment approach. The 2009 TNM classification for PCa is used for staging cancer of the prostate and is shown in Table 1.1 (Chi et al., 2009).

### 1.2.5 Prostate tumour grading: The Gleason Score

Tumour aggressiveness can be determined by a pathologist's examination of the cancer cells under a microscope. Normal tissue has an ordered pattern of growth, but in cancer tissue the pattern is not ordered, due the unpredictable nature of cancer cell growth and differentiation. The most commonly used system for grading cancer of the prostate is the Gleason grading system (Chi *et al*., 2009). This system assigns a grade for each PCa from 1 (least aggressive) to 5 (most aggressive), based on the degree of architectural differentiation of the tumour.

Tumours often show multiple grade “patterns” within the prostate or even within a single core biopsy (Gleason *et al*., 2002). To account for this, the Gleason scoring system is used to show how abnormal or different the cancer tissue is,

compared with normal tissue. The two most common patterns of growth seen in the biopsy sample are each given a number from 1 to 5, and these two numbers are added together to give the Gleason grade (e.g., 4+3=7). The greater the difference between the cancer and normal tissue patterns, the higher the Gleason Score, and the more aggressive the cancer. This score has been shown to provide significant prognostic information in PCa treatment (Gleason *et al*., 2002).

**Table 1.1:** TNM classification of PCa staging (adapted from Chi *et al*., 2009).

| **T – Primary tumour** | | |
|---|---|---|
| TX | | Primary tumour cannot be assessed |
| T0 | | No evidence of primary tumour |
| T1 | Clinically unapparent tumour not palpable or visible by imaging | |
| | T1a | Tumour incidental histological finding in 5 percent or less of tissue resected |
| | T1b | Tumour incidental histological finding in more than 5 percent of tissue resected |
| | T1c | Tumour identified by needle biopsy (e.g. because of elevated PSA level) |
| T2 | Tumour confined within the prostate (**1)** | |
| | T2a | Tumour involves one half of one lobe or less |
| | T2b | Tumour involves more than half of one lobe, but not both lobes |
| | T2c | Tumour involves both lobes |
| T3 | Tumour extends through the prostatic capsule (**2)** | |
| | T3a | Extracapsular extension (unilateral or bilateral) |
| | T3b | Tumour invades seminal vesicle(s) |
| T4 | Tumour is fixed or invades adjacent structures other than seminal vesicles: external sphincter, rectum, levator muscles, and/or pelvic wall | |
| **N - Regional lymph nodes (3)** | | |
| NX | Regional lymph nodes cannot be assessed | |
| N0 | No regional lymph node metastasis | |
| N1 | Regional lymph node metastasis | |
| **M - Distant metastasis (4)** | | |
| MX | Distant metastasis cannot be assessed | |
| M0 | No distant metastasis | |
| M1 | Distant metastasis | |
| | M1a | Non-regional lymph node(s) |
| | M1b | Bone(s) |
| | M1c | Other site(s) |
| **1** | | *Tumour found in one or both lobes by needle biopsy, but not palpable or visible by imaging, is classified as T1c* |
| **2** | | *Invasion into the prostatic apex, or into (but not beyond) the prostate capsule, is not classified as T3, but as T2.* |
| **3** | | *The regional lymph nodes are the nodes of the true pelvis, which are essentially the pelvic nodes below the bifurcation of the common iliac arteries. Laterality does not affect the N classification.* |
| **4** | | *When more than one site of metastasis is present, the most advanced category should be used* |

### 1.2.6 Symptoms and diagnostic tools of prostate cancer

Prostate tumours are usually slow growing, and symptoms may not manifest in affected individuals for many years or may indeed be misdiagnosed as due to other factors. In the early stages of PCa, there are often no symptoms. However, due to its location surrounding the urethra, symptoms of the disease commonly affect urination. PCa symptoms include frequent urination, increased urination during the night (nocturia), difficulty in maintaining a steady stream of urine, blood in the urine (haematuria) and painful urination (dysuria). It can also affect sexual function, for example, difficulty in achieving erection or painful ejaculation (Knight and Latini, 2009). Many of the urinary symptoms also occur in other prostate diseases, such as benign prostate hyperplasia and enlargement of the prostate. If the cancer is advanced, it can spread to other organs, causing bone pain in the pelvis or ribs (Thobe et al., 2011).

The main diagnostic tool used to find evidence of PCa is the serum level of PSA. The PSA test was originally approved by the FDA in 1986 to monitor the progression of PCa in asymptomatic men as well as patients diagnosed with the disease. PSA is a 33-kDa glycoprotein and a member of the kallikrein (KLK) family of serine proteases. It is secreted by normal, hyperplastic and cancerous prostatic epithelia into the seminal fluid. Its function is to digest seminogelins formed in semen after ejaculation (Balk *et al*., 2003). Elevation of PSA levels, in conjunction with histopathological and imaging examinations, confirm the presence of cancer. Imaging tools include: digital rectal examination (DRE),

trans-rectal ultrasound guided biopsy (TRUS), bone scan, computed tomography (CT) and Magnetic Resonance Imaging (MRI) scan (Smith *et al*., 2007).

### 1.2.7 Treatment of prostate cancer

The management of PCa is determined primarily according to tumour stage, patient age, the general health status of the patient, and individual patient preference. The therapeutic options available include surgical and non-surgical approaches. Treatments for early stage localized PCa can result in cure, but treatments for advanced disease such as castration resistant PCa (CRPC) are mainly used to delay disease progression or palliate symptoms (Khemlina *et al*., 2015).

#### *1.2.7.1 Watchful waiting*

The term “watchful waiting” is used to describe a treatment strategy that includes an active decision to postpone treatment until the patient begins to show symptoms of metastatic disease. This strategy is an alternative approach in the medical management of certain diseases and is offered to elderly men, especially those who have other illnesses, such as coronary heart disease or diabetes. Most often it is considered an appropriate approach to treatment of low-risk PCa. This approach offers the opportunity to delay aggressive therapies and its associated complications until the cancer progresses (Williams *et al*., 2015).

#### *1.2.7.2 Radical prostatectomy*

Radical prostatectomy (surgery to remove the prostate gland) is the standard treatment option for many men with PCa. It is widely used as the primary treatment for patients with early-stage PCa and is not useful for PCa that has spread (Wong *et al*., 2006). Radical prostatectomy is an operation to remove the prostate with localised cancer that is completely contained within the gland. The aim of a radical prostatectomy is to remove the prostate gland, the attached seminal vesicles and part of the urethra within the prostate (Hegarty *et al*., 2010). Removal of the whole prostate in early stages of cancer may stop cancer from metastasising, and may result in a complete cure. However, as for any type of surgery, there are short-term risks, such as problems with bleeding or infections, and the risk of some long-term complications, such as urinary incontinence and sexual dysfunction (Ficarra *et al*., 2012).

#### *1.2.7.3 External and internal radiotherapy*

Radiotherapy is a common approach in the treatment of all stages of PCa (Dulaney *et al*., 2016). This therapy is also used to treat bone pain due to metastatic disease. It uses high-energy rays (photons, protons or particle radiation) delivered to the tumour site (Baskar *et al*., 2012). Radiation interacts with DNA, directly causing damage, or acting indirectly by generating free radicals in the cellular water content, which leads to DNA double-strand breaks (DSBs). Both mechanisms cause double-strand and single-strand DNA breaks subsequently lead to cell cycle arrest and apoptosis mainly through the tumour

suppressor protein p53 (Baskar *et al*., 2012, Verheij, 2008). Multi-factors are involved in radiation-induced cell cycle arrest and apoptosis including p53, Poly (ADP-ribose) polymerase (PARP), DNA-dependent protein kinase (DNA-PK), and ataxia-telangiectasia-mutated (ATM). PARP, DNA-PK and ATM function upstream of p53, whereas other components such as the retinoblastoma tumour suppressor gene Rb and the cyclin kinase inhibitor p21 function downstream of p53. In response to radiation-induced DNA strand breaks, PARP binds to DNA strand breaks, leading to synthesis of a poly (ADP-ribose) chain as a signal for the DNA-repairing enzymes (Kim *et al*., 2015). ATM, which acts as an upstream activator and stabilizer of p53, is involved in the G1/S cell cycle checkpoint arrest following DNA damage through the p53-mediated stimulation of p21 and, at the G2 checkpoint, through the direct phosphorylation of the Chk2 protein (Sancar *et al*., 2004, Canman *et al*., 1998, Banin *et al*., 1998). There are different systems of radiation delivery to PCa which include external beam therapy and internal radiotherapy (brachytherapy).

External beam radiotherapy directs high energy X-ray photon beams specifically at the cancer from outside the body using machines such as linear accelerators (linacs). This option generally is used for localized tumours in early stages (stage T1 and T3). However, radiotherapy is also applied to locally advanced prostate tumours that have started to metastasise into nearby tissues, with the aim of shrinking the tumour or stopping its spread to other organs.

Although external beam radiotherapy has proven beneficial in most cancer treatment settings, its effect on adjacent normal tissues and its inadequate dosage to the tumour cells are disadvantages that limit its use.

Three-dimensional conformal radiation therapy (3D-CRT) is one of the most advanced types of external beam radiation current available in the UK. It is designed to improve the delivered doses of radiation to the tumour by directing radiation from multiple angles. Unfortunately, 3D-CRT has not fully prevented radiation-induced cytotoxicity in the surrounding normal cells (Tribius and Bergelt, 2011). However, intensity modulated radiotherapy (IMRT), a more specific technique based on the three-dimensional shape of the tumour, increases the required dose to the treated area and reduces the cytotoxicity in the surrounding normal tissue (Leibel *et al*., 2002). Generally, IMRT carries a smaller risk of damage to normal cells compared with 3D-CRT, but it still exposes a large number of normal cells to radiation (Veldeman *et al*., 2008). Focal external beam radiation therapy (RT) is a palliative therapy used for patients with castration resistant PCa (CRPC) who suffer from bone pain (Amaral *et al*., 2012).

Internal radiotherapy (also called brachytherapy or seed implantation) has become a promising approach in the field of oncology. It uses a radioactive substance (such as palladium-103, iridium-192 or cesium-137) placed inside the prostate gland to deliver a high dose of radiation. Brachytherapy is used alone in early stage, low grade PCa treatment, or combined with external beam radiation

for treating higher risk cancer which has spread outside the prostate. There are two types of prostate brachytherapy: permanent, which administers a low dose rate of radiation at a rate of up to 2 $Gy.hr^{-1}$; and temporary, which administers a high dose rate of radiation (Galalae *et al*., 2004, Moule and Hoskin, 2009)

In general, radiotherapy is associated with short-term side effects, such as bowel disorders and urinary incontinence and retention (Dearnaley, 1995). The long-term side effects include sexual disorders, such as erectile dysfunction (Hummel *et al*., 2010). Some studies have reported a risk of developing secondary cancers in the bladder, colon and rectum following radiation therapy for PCa (Wallis *et al*., 2016).

#### *1.2.7.4 Cryotherapy*

Cryotherapy, also referred as cryosurgery, cryoablation or cryosurgical ablation, is a new therapy which is applied to localised PCa that has not metastasised. It is a minimally invasive surgical technique that involves in-situ freezing by applying extremely low temperatures to kill the prostate tumour and shrink the size of the prostate. In this treatment, cryo-needles are positioned into the gland and argon gas is delivered to the prostate. This generates rapid cooling, with temperatures reaching -186°C, and results in destroying the cells (Kvorning Ternov *et al*., 2015). Cryoablation is still undergoing clinical trials due to uncertainties surrounding the treatment. Clinical trials have shown impotence occurring in 90% of patients following cryoablation (Friedman *et al*., 2014; Wallace *et al*., 2014).

### *1.2.7.5 Hormonal therapy (androgen ablation therapy)*

Hormone therapy, or androgen deprivation therapy (ADT), is one of the strategies used in the treatment of advanced stage of PCa. Androgens are responsible for up to 80% of PCa growth. Therefore, reducing the endogenous androgen levels will inhibit the progression of the tumour (Chuu *et al*., 2011).

Surgical castration (orchiectomy) is a surgical procedure to remove the testicles, where most testosterone and dihydrotestosterone (DHT) are synthesised, in order to stop the PCa from growing and to shrink the tumour. Chemical castration using luteinising hormone-releasing hormone (LHRH) analogue drugs is another strategy to decrease the level of androgens made by the testicles. These drugs include leuprolide (Lupron® and Eligard®), triptorelin (Trelstar®), goserelin (Zoladex®) and histrelin (Vantas®). They act by desensitising the pituitary GnHR receptors, leading to a decreased level of endogenous testosterone through the inhibition of the luteinising hormone and follicle-stimulating hormone synthesis (Khemlina *et al*., 2015). Abiraterone (Zytiga®) and Enzalutamide (Xtandi®) are examples of new hormone therapy drugs recently approved for the treatment of patients with CRPC (Yin *et al*., 2013). Abiraterone is an inhibitor of the CYP17 enzyme that leads to the inhibition of adrenal androgen biosynthesis. Enzalutamide is a potent androgen receptor antagonist that prevents the binding of androgen to its receptors on PCa cells and downregulates AR mRNA (Zhang *et al*., 2011).

Despite the effectiveness of hormonal therapy, almost 90% of PCa patients relapse and develop castrate resistant prostate cancer (CRPC) 12–18 months after androgen deprivation therapy (Harris *et al*., 2009, Maroto *et al*., 2016). In addition, ablation therapy is associated with numerous side effects, including: sexual dysfunction, osteoporosis, fatigue, gynecomastia, anemia, depression, cognitive dysfunction, increased risk of diabetes and cardiovascular disorder (Chuu *et al*., 2011). In addition, the cost-effectiveness studies of anti-hormonal drugs, particularly Enzalutamide, showed the high cost of these agents may limit their usefulness for many patients (Pilon *et al*., 2016).

#### *1.2.7.6 Chemotherapy*

Chemotherapy is used in patients who develop castration-resistant PCa. Several chemotherapeutic agents are available to treat PCa. Docetaxel, for example, is approved for the treatment of metastatic CRPC. Docetaxel is a taxoid that inhibits the depolymerisation of microtubules, interfering with mitosis and cell cycle arrest in the G2M phase, and inducing apoptosis (Kohli and Tindall, 2010). Cabazitaxel is another member of the taxane class used in the treatment of CRPC. It has led to better overall survival of Docetaxel-refractory metastatic CRPC, and it exerts its cytotoxicity by arresting mitosis via binding to the tubulin, leading to microtubule depolymerisation (de Bono *et al*., 2010; Yin *et al*., 2013). Another class of drugs utilised in PCa treatment is type II topoisomerase inhibitors, such as Mitoxantrone, which inhibits DNA synthesis and the DNA repair system and induces apoptosis in both normal and cancer cells (Boland *et*

*al*., 2000). It has been used as a second line treatment for metastatic CRPC, in combination with the steroid prednisone (Tannock *et al*., 1996; Green *et al*., 2015). Eribulin is a synthetic analogue of the marine macrolide halichondrin B recently used in metastatic PCa treatment, acting as a microtubule inhibitor leading to G(2)/M phase cell-cycle arrest and apoptosis (Preston and Trivedi, 2012).

Unfortunately, none of the current therapies described provide a cure for advanced metastasis CRPC; their role is restricted to improving overall survival, symptom relief and prolonging bone metastasis-free survival (Yin *et al*., 2013). At present, the progression and metastasis of PCa are common, and the rate of cancer-related mortality remains high (Semenas *et al*., 2012). In addition, the overall median survival period of patients with metastatic CRPC is less than 19 months, and only 10% of patients survive 10 years after diagnosis (Husson *et al*., 2014). Currently, the standard treatments for advanced metastatic CRPC include radiotherapy, chemotherapy and hormonal therapy, which shows little benefit. Resistance to these treatments occurs in the long term (Yin *et al*., 2013). Novel therapies are urgently sought for the treatment of CRPC. The process of finding new drugs for use in combination with existing therapies requires examination of alternative molecular pathways that may be involved in tumour progression.

#### *1.2.7.7 Summary of current PCa treatment*

The primary therapies for early stage, localized tumour PCa include radiotherapy and prostatectomy, which aims to remove tumour burden (Zejnullahu *et al*., 2016). However, almost half of people who develop PCa are diagnosed in more advanced stages, where tumours have become castration-resistant and have often metastasised to other organs. For these cases, the aims of treatment are symptom palliation and delaying tumour advancement, and pharmacological or surgical hormonal ablation therapy in combination with radiation therapy are often implemented. Within approximately months of post-hormonal therapy, most of the PCa patients develop highly metastatic CRPC carcinoma, which is associated with poor outcome and limited therapeutic options (Maroto *et al*., 2016). Bone metastases are a hallmark of metastatic CRPC in more than 90% of patients, and are associated with a high mortality rate (Frieling *et al*., 2015). A regimen of chemotherapeutic agents, hormonal deprivation drugs and radiation therapy are the current options for those patients in terms of palliative, symptomatic treatment to improve survival and to reduce pain related to bone metastasis. Despite the availability of these therapies, the median survival of metastatic CRPC remains poor, at less than 19 months (Husson *et al*., 2014).

As no curative therapies are available for metastatic, androgen resistant PCa, effective new therapeutic agents and combinations are urgently needed. Developing new therapies and identifying novel targets require an understanding

of the molecular mechanisms underlying PCa progression. One such molecular change correlated with carcinogenesis of PCa is the nuclear factor-kappaB (NF-κB) transcription factor and its signaling pathways. Many studies demonstrate that activation of NF-κB signaling in PCa cells is associated with PCa progression and with castration-resistant and metastatic statuses (Jin *et al*., 2008, Jin *et al*., 2014, McCall *et al*., 2012). In the next section of this introduction, we will highlight the role of NF-κB and its signaling pathways in PCa development.

## 1.3 Nuclear factor-κB (NF-κB)

### 1.3.1 Biological significance of NF-κB

Nuclear factor-kappa B (NF-κB) is the generic term for a family of dimeric eukaryotic transcription factors, composed of members of the Rel family of DNA-binding proteins. NF-κB is a transcriptional factor which controls important biological processes including inflammation, apoptosis, cell proliferation, growth, and cell cycle (Bonizzi and Karin, 2004; Bours et al., 2000; Karin et al., 2002). NF-κB was first identified by Sen and Baltimore in 1986 as a B cell-specific nuclear factor that bound to an enhancer element in the immunoglobulin kappa (κ) light chain gene (Sen and Baltimore, 1986). NF-κB proteins has been found as first-line defense in all cell types and are involved in the regulation of a remarkably large number of genes in response to infections, inflammation, and other stressful conditions. In response to stress signalling, activation of the NF-κB pathway induces a rapid reprograming of gene expression for several outcomes. Firstly, activation may promote the expression of genes that are important for the immune response, including genes encoding for proinflammatory cytokines such as IL-1 and IL-6, chemokines including IL-8 and RANTES, and the adhesion molecules intercellular adhesion molecule-1 and E-selectin (Mogensen, 2009). A second potential role for NF-κB is to protect cells from cell death induction through the expression of anti-apoptotic genes including X-linked inhibitor of apoptosis protein (XIAP) and cellular inhibitor of apoptosis protein (c-IAP) and pro-survival factors such as bcl-2 (Fulda, 2014). A

third potential role is to generate anti-oxidant proteins such as superoxide dismutase 2 (SOD2) and ferritin heavy chain which are able to control the production of reactive oxygen species (ROS) shielding the cells from death (Pham et al., 2004; Sakon et al., 2003).

In addition to its physiological role, NF-κB has been shown to be involved in various pathophysiological processes, including cancer, inflammation and atherosclerosis. Abnormal NF-κB activation has been shown to contribute to the pathogenesis of several human malignancies including PCa. In cancer, NF-κB has been shown to play pivotal roles in the control of growth, differentiation and apoptosis (Hoesel and Schmid, 2013). NF-κB has been found to be related to the initiation and progression of PCa through activation of various target genes, including c-myc, cyclin D and IL-6 which promote growth, anti-apoptotic (pro-survival) genes such as bcl-2, and angiogenesis genes such as IL-8 and VEGF, and MMP9 which promotes invasion and metastases (Suh and Rabson, 2004, Huang *et al*., 2001). Expression of NF-κB has been found to be elevated in different human cancers, including PCa (Gasparian *et al*., 2002; Braunstein *et al*., 2008), and is an independent prognostic factor in PCa relapse (Domingo-Domenech *et al*., 2005). For instance, inhibition of NF-κB using an adenoviral vector that contains the IκB gene (an inhibitor of NF-κB) reduced the colony formation of prostate cancer PC3 cells (Pajonk *et al*., 1999). NF-κB blockage was also shown to result in increased apoptosis in LNCaP cells, and increased sensitivity to apoptosis was induced by TNF-α in PC3 cells (Gasparian *et al*.,

2002). This observation has led to the hypothesis that NF-κB activation may be linked to carcinogenesis and may provide tumour cells with a survival advantage and appropriate stimuli required for cell proliferation and invasiveness (DiDonato *et al*., 2012; Vlahopoulos *et al*., 2015).

### 1.3.2 The NF-κB members

The NF-κB family of transcription factors consists of five closely related DNA binding proteins that includes the NF-κB1 (p50/p105), NF-κB2 (p52/p100), RelA (p65), c-Rel and RelB genes, which function as various homodimers and heterodimers. All five NF-κB members share a highly conserved 300-amino-acid-long N-terminal Rel homology domain (RHD), which is responsible for their dimerisation, nuclear translocation, DNA binding, and also interaction with the inhibitors of NF-κB. RelA, RelB, and c-Rel subunits contain transactivation domains within the C-terminal RHD (Hayden and Ghosh, 2008). However, the precursors p105 and p100 do not have a transactivation domain and instead they contain a number of ankyrin repeats (protein motifs that facilitate protein–protein binding) that act like IκB-inhibitory proteins which are proteolytically cleaved to produce the active subunits p50 and p52, respectively (Hayden and Ghosh, 2008). There is an N-terminal leucine zipper-like region in the p105 and p100 subunits which facilitates their physical binding. In its unstimulated state, NF-κB is retained inactive in the cytoplasm through binding with the inhibitory proteins (IκBs) which block their nuclear localization sequence (NLS). IκBα, IκBβ and IκBε are the most IκBs prominent, whereas Bcl-3 and IκBζ are atypical

members of the IκBs family, which stimulate and regulate the NF-κB in the nucleus. IκBs consists of multiple ankyrin repeats which mediate their binding to the RHD of NF-κB (Figure 1.4).

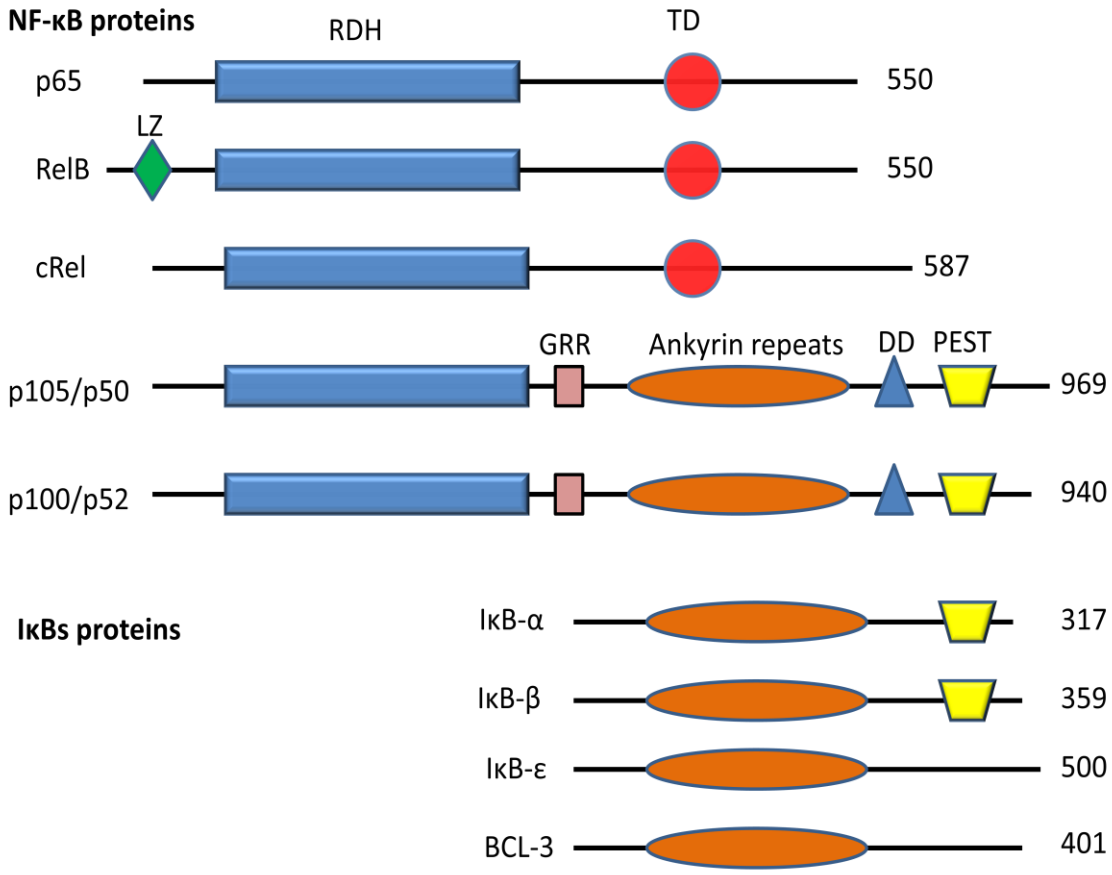


**Figure 1.4 The structures of various subunits of NFκB and IκB members**. The number of amino acids is shown next to each NF-κB and IκB member. LZ: leucine zipper; TD: transactivation domain; Rel: homology domain; PEST region: polypeptide sequence enriched in proline (P), glutamic acid (E), serine (S) and threonine (T) region; GRR: glycine-rich region; DD: death domain.

### 1.3.3 The IKKs

The inhibitory kappa B kinases (IKKs) are the major regulatory kinases within the NF-κB pathways. Five members of IKK enzymes have currently been identified. IKKα and IKKβ are the major catalytically active kinase subunits. Both kinases (IKKα and IKKβ) are highly homologous proteins, sharing 52% of their protein sequence identity (Israel, 2010). IKKα and IKKβ proteins have an N-terminal kinase domain, a C-terminal helix-loop-helix (HLH) domain that acts in controlling the kinase activity, and a leucine-zipper (LZ) region which facilitates the homo- or hetero-dimerisation of the kinases (DiDonato *et al*., 1997). A further member, IKKγ, also known as NF-κB essential modulator (NEMO), is a non-catalytic 48 kDa enzyme. Despite the lack of kinase activity of IKKγ, it plays a major scaffolding or regulatory function in the canonical NF-κB pathway (Rothwarf *et al*., 1998; Solt *et al*., 2009). The N-terminal region of NEMO is responsible for interaction with the carboxyl terminus of the IKKα and IKKβ subunits (Figure 1.5) (May *et al*., 2002). The last member of this family are TANK-binding kinase 1 (TBK1) and IKK-ε (or IKK-i). Both kinases sharing 64% of protein sequence identity. TBK1 and IKK-ε consist of an N-terminal kinase domain, a ubiquitin-like domain (ULD), a LZ, HLH region and C-terminal coiled-coil domain that assists interaction with adaptor proteins such as TANK protein (Shimada *et al*., 1999; Pomerantz and Baltimore 1999; Ikeda *et al*., 2007).

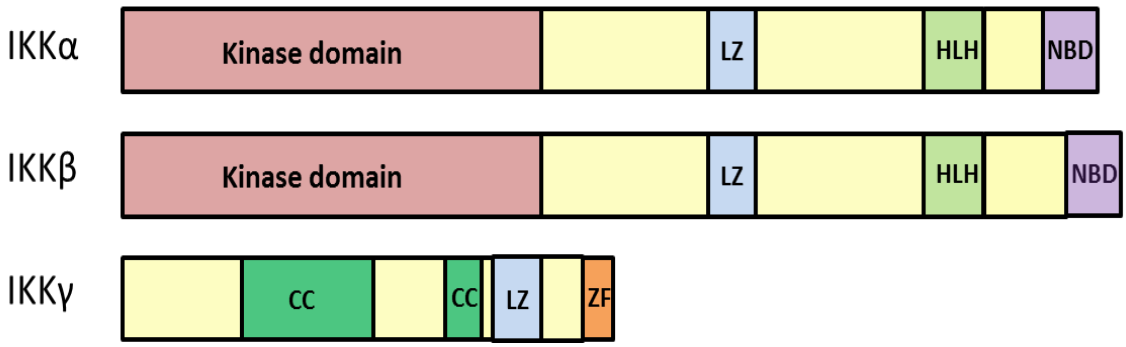


**Figure 1.5** Schematic representation of the principal structural motifs of the IKKs IKKα, IKKβ and IKKγ (NEMO). Abbreviations: CC: coiled coil region; LZ: leucine zipper motif; ZF: zinc-finger domain; HLH: helix-loop-helix domain; NBD: NEMO-binding domain.

### 1.3.4 The canonical NF-κB pathway

IKKs have been found to be key kinases involved in the regulation of NF-κB. However, activation of the NF-κB pathway should be mediated through intermediates which trigger initial cellular activation from the extracellular to the intracellular IKKs. Cytokine receptors including TNFR1 and the IL-1β receptor and toll-like receptors (TLRs) have been recognised to activate the canonical NF-κB pathway in a number of various cell types (Plotnikov *et al*., 2011). The canonical NF-κB pathway is triggered by various stimuli, such as tumour necrosis factor α (TNFα), lipopolysaccharides (LPS), and interleukin-1 β (IL-1β) (Hayden and Ghosh, 2008). Following stimulation, the IKK complex is activated by a member of the mitogen-activated protein/ERK kinase 3 family (MAP3K)

known as transforming growth factor β-activated kinase 1 (TAK-1) (Sakurai *et al*., 1999).

IKKβ kinase is a crucial part of this pathway. *In vivo* studies demonstrated that in IKKβ-deficient mice, there was a massive reduction in RelA (p65) and NF-κB1 (p50/p105) subunits activity following either TNF-α or IL-1α stimulation (Li *et al*., 1999). The main regulatory step in the canonical pathway is the activation of the IKK complex by the multiple aforementioned inflammatory signals. The IKK complex consists of catalytic kinase subunits (IKKα and IKKβ), and the regulatory subunit IKK-γ/NEMO. Most agents that activate NF-κB employ a common pathway based on the phosphorylation of the two N-terminal serines in IκBs, targeting them for ubiquitination and degradation by the 26S proteasome (Kisselev and Goldberg, 2001). As shown in Figure 1.6, IKKβ phosphorylates the IκBα bound to the p65 NLS region of p65/p50 dimers which results in degradation of the IκBα subunits and the subsequent translocation of p65-containing heterodimers into the nucleus where they regulate transcription of various genes that are involved in innate immunity (Malek *et al*., 1998; Oeckinghaus and Ghosh, 2009). The transcriptional activity of nuclear NF-κB p65 is also regulated by IKKβ-induced phosphorylation (Denk *et al*., 2001).

Conversely, IKKα is not essential for upstream activation of the canonical NF-κB pathway. In IKKα knockout mice, stimulation of the canonical NF-κB pathway with TNF-α, IL-1β and LPS activates the IKK complex and induces IκBα degradation and p65 nuclear translocation in keratinocytes and hepatocytes (Hu

*et al*., 1999). However, other researchers found that IKKα can regulate the expression of some p65-dependant genes, including chemokines such as interleukin-8 (IL-8) and endothelial adhesion molecules such as vascular cell adhesion molecule-1 (VCAM-1) and E-selectin (Denk *et al*., 2001; Gloire *et al*., 2007; Huang *et al*., 2007).

NEMO is a non-catalytic enzyme that lacks kinase activity. It acts as scaffolding or regulatory protein for both IKKβ and IKKα kinase activity. NEMO activates the IKK complex through interaction with a specific domain called NEMO-Binding Domain (NBD) in the IKKβ (May *et al*., 2002). The presence of mutations in the C-terminal or in the NBD domains of NEMO was reported to block the activation of both the IKK complex and the canonical NF-κB pathway (Solt *et al*., 2009).

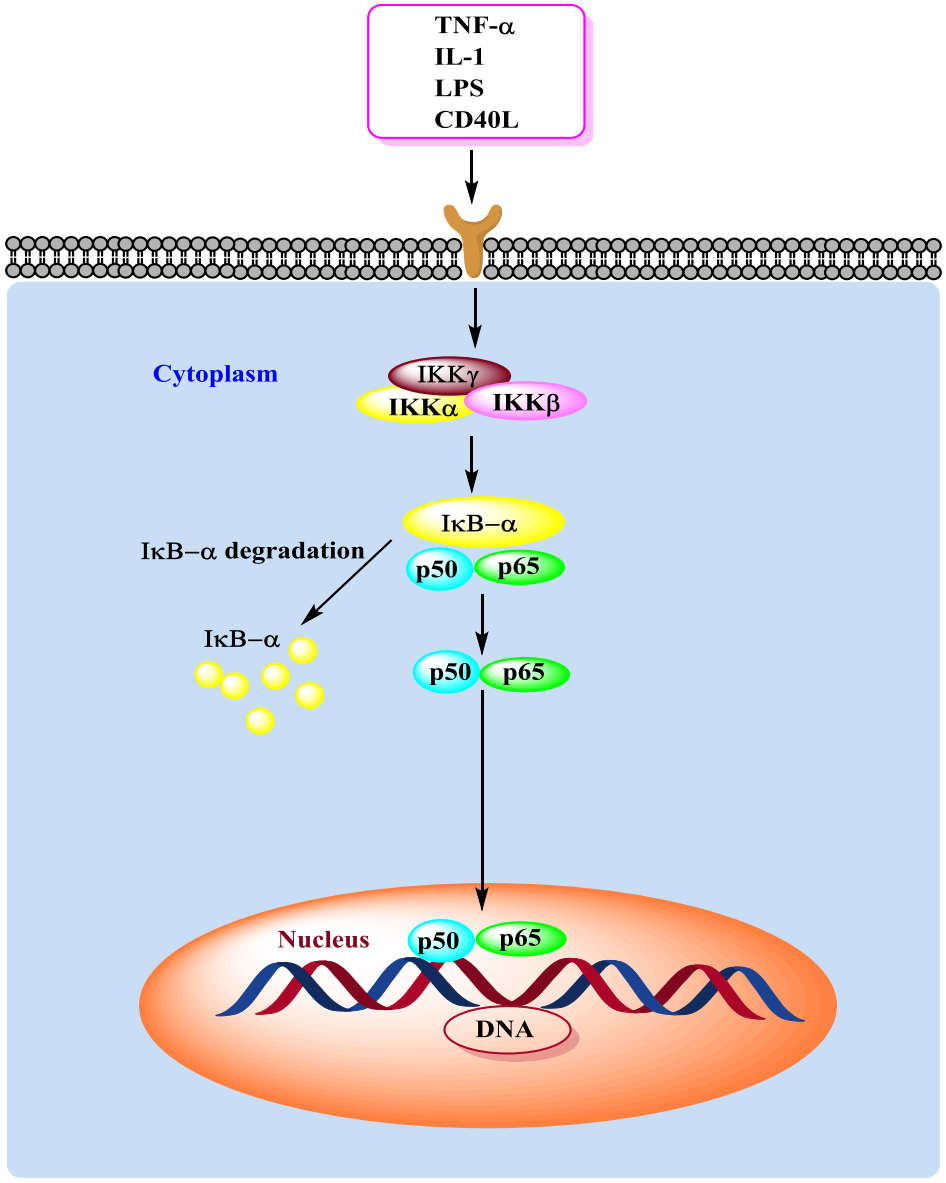


**Figure 1.6: Schematic diagram of the canonical NF-κB pathway.** This pathway is triggered by different stimuli, such as TNF, leading to phosphorylation of the IKK complex, which subsequently activates IκBα and induces the translocation of p65-containing heterodimers into the nucleus.

### 1.3.5 The non-canonical NF-κB pathway

The non-canonical, alternative NF-κB pathway, NF-κB-inducing kinase (NIK) or IKKα-dependent pathway, is triggered by specific TNF family cytokines, such as CD40 ligand (CD40L), B cell activating factor (BAFF) and lymphotoxin β (LTβ), that are primarily developmental signals (Hayden and Ghosh, 2008). This pathway can also be activated by receptor activator of nuclear factor kappa-B ligand (RANKL) to regulate osteoclast differentiation during bone formation (Novack *et al*., 2003).

As shown in Figure 1.7, upon stimulation by these inducers, NIK induces activation of cytoplasmic IKKα homodimers by phosphorylation on Ser177 and Ser188 (Senftleben *et al*., 2001). Subsequently, this activation of IKKα kinases leads to the processing of p100 on Ser866 and 870 to generate active p52-RelB heterodimers which then translocate into the nucleus and activate gene expression (Solan *et al*., 2002). The NIK-dependent IKKα-mediated phosphorylation of p100 is regulated by TNF receptor-associated factors 2 and 3 (TRAF2 and TRAF3) adaptor proteins and ubiquitin ligase enzymes (Gardam *et al*., 2008). IKKα-induced NIK phosphorylation serves as a negative feedback signal preventing excess accumulation or overactivity of NIK within noncanonical NF-κB signaling (Razani *et al*., 2011).

The non-canonical NF-κB signaling controls a wide variety of developmental phenotypes including adaptive immunity, B-cell survival and maturation,

dendritic cell activation, and bone metabolism (Dejardin, 2006). In contrast to the canonical pathway, which is characterized by a rapid and transient response, activation of the alternative pathway is slow and persistent (Israel, 2010). The fact that the non-canonical pathway is mainly IKKα dependent and does not require IKKβ or NEMO suggests a lack of requirement for the classical IKK complex (Luftig *et al*., 2004, Israel, 2010).

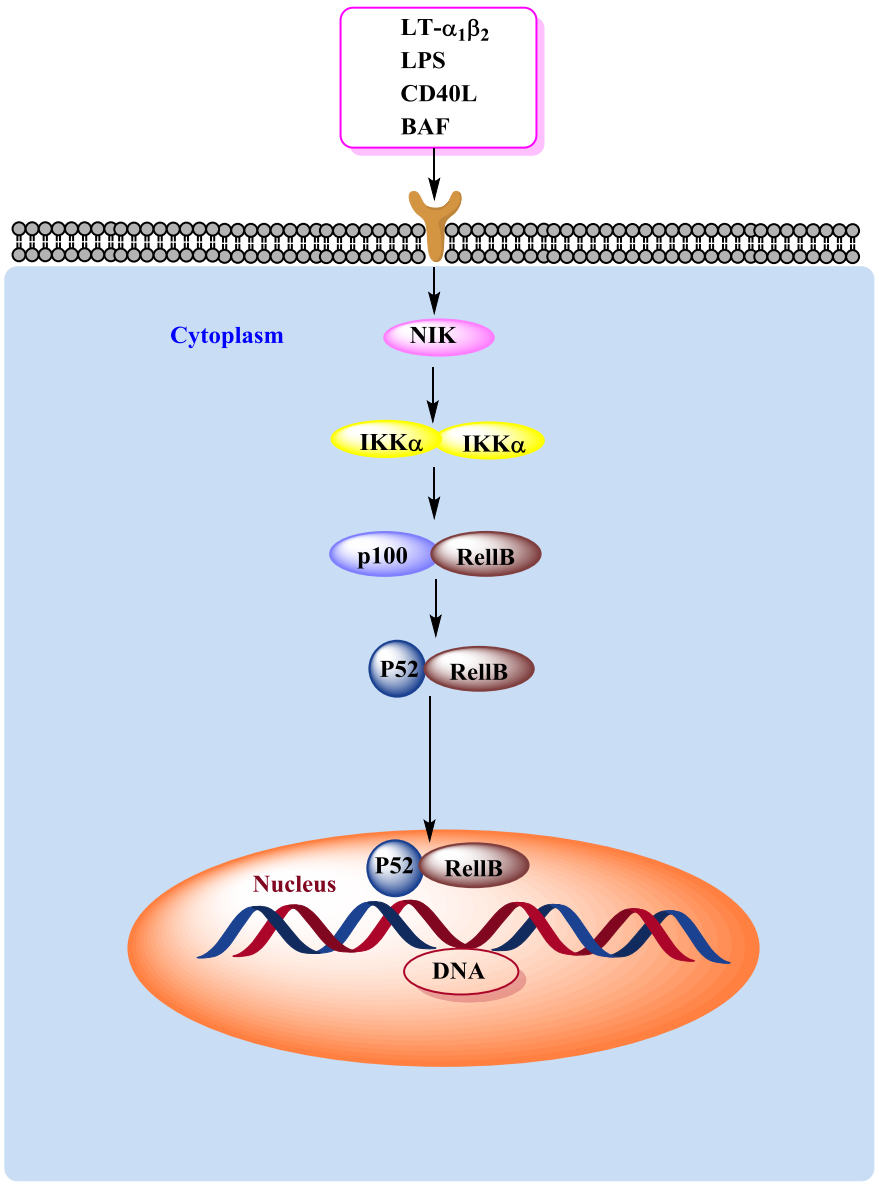


**Figure 1.7: Schematic diagram of the non-canonical NF-κB pathways.** This pathway is stimulated by various molecules, such as lymphotoxin β (LTβ), which phosphorylates IKKα subunits, leading to the processing of p100 to p52 and generating active p52-RelB heterodimers.

### 1.3.6 Role of IKKs in cancer progression

The IKKs play an important role in regulating numerous physiological processes such as inflammation, immunity, cell proliferation or control of cell death through the activation of NF-κB subunits (Senegas *et al*., 2015). Moreover, these kinases have been linked with various human diseases, including cancer (Yang *et al*., 2010; Senegas *et al*., 2015; Huang *et al*., 2007). The IKKs have been shown to play an essential role in tumour survival, proliferation, metastasis, angiogenesis and the activity of cell adhesion molecules which may play roles in cancer progression (Lee and Hung, 2008). Different studies provide strong evidence showing that altered IKK function results in profound signalling modifications that may lead to the development of cell transformation and cancer. For example, IKKβ induces tumourigenesis in different cancer types through the control of numerous genes which are involved in cell proliferation, anti-apoptotic 'cell survival' invasion and angiogenesis (Basseres and Baldwin, 2006). In mice, studies have shown that ablation of IKKβ expression inhibited the development of melanoma tumours, resulting in decreased expression of the mitotic kinase Aurora A protein, inhibition of G2/M transition and stabilisation of tumour suppressor protein p53, accompanied by lower levels of IL-6 and induction of apoptosis (Yang *et al*., 2010). In breast cancer, IKKβ has been shown to mediate the degradation of forkhead box O3a (FOXO3a), a transcription factor that acts as an inhibitor of the cell cycle and a promoter of apoptosis (Hu *et al*., 2004). In addition, IKKβ has been found to increase tumour angiogenesis and tumour progression in breast cancer by phosphorylation of the

tumour suppressor protein tuberous sclerosis 1 (TSC1) which subsequently upregulates mTOR activity (Lee *et al*., 2007). Furthermore, β-carboline (PS-1145), an IKKβ inhibitor, was able to suppress TNFα-mediated NF-κB activation via suppression of IκBα phosphorylation and induced cytotoxicity in multiple myeloma cells (Castro *et al*., 2003; Hideshima *et al*., 2002).

IKKα has also been reported to influence apoptosis, cell cycle progression and tumour progression in various types of cancer including colorectal, breast, pancreatic, gastric and prostate cancer (Fernandez-Majada *et al*., 2007; Park *et al*., 2005; Shiah *et al*., 2006; Hirata *et al*., 2006; Luo *et al*., 2007). For instance, the phosphorylation of CREB-binding protein (CBP) by IKKα was found to switch the binding affinity of CBP, a histone acetyltransferase, from p53 to NF-κB, promoting tumour proliferation and growth in human lung cancer tissue (Huang *et al*., 2007). Other studies demonstrated that phosphorylation of the oncogenic transcriptional factor β-catenin by IKKα led to the stimulation of β-Catenin/T-cell factor-dependent cyclin D1 expression, a protein involved in the regulation of the cell cycle, enhancing cell proliferation in various cancer types (Carayol and Wang, 2006). In addition, IKKα may promote cell proliferation in breast cancer through phosphorylation of the oestrogen receptor-α transcriptional factor, the oestrogen receptor-α coactivator protein AIB1/SRC3, and activating oestrogen-responsive genes such as cyclin D1 and c-MYC (Park *et al*., 2005). IKKα was also found to activate survival and differentiation in human colorectal cancer cell biopsies via phosphorylation of the nuclear receptor co-repressor 2 SMRT

protein, a transcriptional coregulatory protein, which subsequently activates Notch-target survival genes *hes1* and *herp2* (Fernandez-Majada *et al*., 2007). Knocking down IKKα with shRNA vector was shown to deactivate SMRT protein which resulted in growth inhibition and apoptosis in human colorectal cancer cell *in vitro* and in nude mice *in vivo* (Margalef *et al*., 2012).

Unlike the major catalytical subunits IKKα and IKKβ, IKKε and TBK1 have limited roles in the NF-κB pathways, and their functions are restricted to phosphorylation of IFN regulatory transcription factors 3 and 7 (IRF3 and IRF7) in response to viral infections (tenOever *et al*., 2004). However, IKKε has been shown to be highly expressed in various breast and ovarian cancer cell lines (Eddy *et al*., 2005; Guo *et al*., 2009). In fact, IKKε was found to promote cell transformation by phosphorylating the tumour suppressor CYLD at serine 418 and decreasing its ubiquitinase activity (Hutti *et al*., 2009). TBK1 on the other hand, has been found to be overexpressed in lung, breast and colon cancers (Barbie *et al*., 2009; Kan *et al*., 2010). Moreover, SU-6668, a receptor tyrosine kinase inhibitor which acts as an antiangiogenic and anti-tumour drug, was found to inhibit TBK1 activity and TBK1-mediated IRF3 (Laird *et al*., 2000; Godl *et al*., 2005).

Together, these studies provide strong evidence showing that altered IKK function results in profound signalling modifications that may lead to the development of cell transformation and progression of cancer.

### 1.3.7 Role of IKKα in PCa progression

Growing evidence is showing that IKKα has a crucial role in a number of cancer types including PCa (Fernandez-Majada *et al*., 2007; Park *et al*., 2005; Shiah *et al*., 2006; Hirata *et al*., 2006; Luo *et al*., 2007). In PCa, IKKα is a key mediator in growth, metastasis and development of CRPC (Luo *et al*., 2007; Ammirante *et al*., 2010; Mahato *et al*., 2011; Jain *et al*., 2012). Unlike IKKβ which is a cytoplasmic kinase, IKKα shuttles between the cytoplasm and nucleus which leads to different cytoplasmic and nuclear molecular changes (Huang and Hung, 2013). Firstly, it controls NF-κB subunits in the cytoplasm by driving the processing of p100 to p52 which subsequently dimerises with RelB, P52-RelB then translocates to the nucleus, causes induction of expression of cancer survival and anti-apoptotic genes such as cIAP2 (Hayden and Ghosh, 2008). Secondly, nuclear IKKα regulates numerous genes involved in tumour growth, metastasis and angiogenesis (Huang and Hung, 2013; Huang *et al*., 2007; Solan *et al*., 2002; Luo *et al*., 2007).

Crosstalk between the inflammation and activation of IKKα has been reported in the emergence of castration-resistant PCa. One study demonstrated that approximately 90% of human PCa samples, but not normal tissue, contain B lymphocytes which is required for IKKα activation and the rapid emergence of CRPC (Karin, 2009). In models of PCa, a siRNA-induced blockade of IKKα expression was shown to delay the development of castration-resistant PCa in the murine myc-CaP cell line (derived from *c-myc* transgenic mouse bearing

PCa) (Ammirante *et al*., 2010). Furthermore, Ammirante *et al*. (2010) demonstrated that infiltrating B cells in PCa cells produces lymphotoxin which subsequently activates IKKα and signal transducer and activator of transcription 3 (STAT3) which subsequently leads to prolonging the hormone-free survival and proliferation in these cells. (Ammirante *et al*., 2010). STAT3 protein is an important event for the mediation of growth proliferation, survival and development via regulation of different anti-apoptotic and survival gene expression such as Bcl-xL and survivin genes (Yue *et al*., 2009, Darnell, 1997).

Cancer stem cells (CSCs) are cancer cells that originated within tumors that possess characteristics associated with normal stem cells, specifically the ability to self-renew and differentiate. CSCs are tumorigenic (tumor-forming), and are responsible for cancer initiation, progression, relapse and metastasis in many cancer types (Kaur *et al*., 2014). It has been previously found that PCa stem cells share properties with normal adult prostate stem cells, and have the ability to survive even in androgen ablation conditions and subsequently regenerate the tumour with a more aggressive cancer (Litvinov *et al*., 2003). The growth of PCa stem cells is found to be regulated by expression of the transcription factor Bmi-1 (B lymphoma Mo-MLV insertion region 1), which is found to be over-expressed in advanced PCa samples (van Leenders *et al*., 2007). Using $IKK\alpha^{AA/AA}$ in a transgenic adenocarcinoma of mouse prostate (TRAMP) model, it has been found that activation of IKKα by the infiltrating B cells in epithelial progenitors cells and androgen-deprived PCa mediates the nuclear

translocation of E2F1 transcription factor that associates with the coactivator CBP (CREB-binding protein) that binds to Bmil promoters, hence promoting castration-resistance tumour growth (Ammirante *et al*., 2013). These data suggest that IKKα regulates the growth and the development of CRPC cells through the IKKα-E2F1-BMI1 signalling pathway.

Overexpression of androgen receptors (AR) is associated with PCa progression, hormonal therapy resistance and development of androgen-resistant PCa (Zhang *et al*., 2009). It has been demonstrated that siRNA knockdown of IKKα significantly reduces AR activity, nuclear androgen receptor levels and AR gene expression in LNCaP PCa cell lines (Lessard *et al*., 2007). Similarly, Jain *et al.* (2012) using specific siRNA against IKKα, demonstrated a marked reduction in the expression of the AR target genes *(TMPRSS2 and PSA)* in VCaP and LNCaP cells as well as inhibition of their growth (Jain *et al*., 2012). These data suggest the possible regulatory role of IKKα on AR activity, which might be one of the mechanisms by which IKKα induces progression of PCa and development of CRPC.

Additional studies, supporting a role for IKKα in PCa, show an association between IKKα and the induction of genes responsible for regulation of PCa metastasis and growth. For instance, expression of the inactive mutant form of IKKα ($IKK\alpha^{AA/AA}$) in the TRAMP model of PCa resulted in inhibition of metastases in areas such as the lung and pelvis, delayed the cancer's progression and improving survival compared with wild type TRAMP mice,

notably by upregulating the tumour suppressor gene maspin, which is closely related to this function (Luo *et al.,* 2007). Likewise, the silencing of IKKα with siRNA in two androgen-independent prostate cell lines (PC3 and DU-145) induced the inhibition of PCa metastasis via increased expression of the maspin gene (Mahato *et al*., 2011).

The subunits involved in the non-canonical NF-κB pathway that are controlled by IKKα also contribute to PCa progression. As mentioned previously, IKKα induces processing of p100 to p52 which subsequently dimerises with RelB and translocates to the nucleus, up-regulating the expression of anti-apoptotic genes such as cIAP2, Bcl-2 and Bcl-xl, thereby promoting cancer cell survival (Hayden and Ghosh, 2008). Clinical immunohistochemical studies of PCa patient biopsies have suggested that high expression of nuclear RelB is associated with high Gleason scores (Lessard *et al*., 2005). Inhibiting the nuclear RelB level by transfection of PC3 (aggressive androgen-independent PCa cells) with dominant-negative p100 mutant markedly delayed and decreased the ability of these cells to form tumours in xenograft models (Xu *et al*., 2009). In the same study, silencing of RelB in the same cells which were subsequently placed in a nude mice model resulted in an inhibition of primary and metastatic tumour formation (Xu *et al*., 2009). Furthermore, both cytoplasmic and nuclear levels of p52 were elevated in advanced androgen-independent PCa cell lines (PC-3 and DU145) relative to androgen-dependent LNCaP cells, suggesting that the

alternative NF-κB pathway is also constitutively activated and contributes to androgen-independent PCa progression (Lessard *et al*., 2007).

### 1.3.8 The NF-κB pathways and radiation resistance

Radiotherapy, such as external beam radiotherapy (XBR) is a mainstay in the treatment of advanced prostate cancer (Dulaney *et al*., 2016). The therapeutic efficacy of radiation therapy is highly dose-dependent; however, toxicity to normal cells increases as the dose of radiation increases (Kozakai *et al*., 2012). Unfortunately, many cancer cells inherently resist the toxicity caused by ionising radiation (IR), or convert to radioresistance shortly following exposure to radiation, which results in treatment failure and relapse of the cancer (Li and Sethi, 2010; Wu *et al*., 2011). In particular, advanced-stage androgen-insensitive PCa cells are known to be radioresistant compared with hormone-sensitive cells in early stages of PCa (Xie *et al*., 2010). This characteristic of androgen-insensitive behaviour towards radiation has been documented to occur mainly through activation of NF-κB pathway subunits following radiation exposure (Kim *et al*., 2006; Baud and Karin, 2009; Li and Sethi, 2010).

The activation of NF-κB proteins is considered to be the most important factor involved in the development of cancer resistance to IR (Kim *et al*., 2015). In different *in vitro* and *in vivo* studies, IR has been found to activate IKK/NFκB pathways as well as increase the expression of NFκB mRNA levels which has been associated with tumour resistance to radiation (Rithidech *et al*., 2005;

Ahmed *et al*., 2006; Natarajan *et al*., 2006; Lewis and Spandau, 2007). IR is known as a potent DNA damaging agent, and exposure of cells to IR causes generation of free radicals and DNA DSBs which subsequently lead to cell cycle arrest and apoptosis (Baskar *et al*., 2012; Verheij, 2008; Cohen-Jonathan *et al*., 1999). The mechanism involved in the radioresistance effect of NF-κB is believed to be via activation of its target genetic programs, including the expression of many anti-apoptotic proteins including IAP1, IAP2, XIAP,cFLIP and BclxL, and antioxidant enzymes, including superoxide dismutase (SOD), manganese superoxide dismutase (MnSOD), catalase and glutathione peroxidise, thereby protecting cancer cells from radiation-induced DNA damage (Guo *et al*., 2003, Kim *et al*., 2015). For example, inhibition of classical the NF-κB pathway using three different IKKβ inhibitor agents (BMS, SC-514 and TPCA-1) significantly potentiates IR-induced clonogenic cell death and reduced the repair of IR-induced DSBs in breast cancer cells (MCF-7) and lung cancer cells (H1299 and H1648) (Wu *et al*., 2011). Furthermore, *in vitro* and *in vivo* inhibition of NF-κB in colorectal cancer cells by either the IKKβ inhibitor PS-341 or an adenovirus encoding lκBα super-repressor increased the IR-induced apoptosis (Russo *et al*., 2001). However, because NF-κB regulates important physiological functions, targeting of the classical NF-κB pathway is associated with severe complications and toxicities such as inflammation, immunosuppression, infection and/or lethality (Li *et al*., 1999; Chariot, 2009).

As well as the canonical NF-κB pathway, different studies also reveal that the non-canonical NF-κB pathway component (RelB) regulates the radioresistance of PCa cells (Holley *et al*., 2010; Kim *et al*., 2015). The mechanism involved in radioresistance of non-canonical NF-κB pathway in PCa is via the RelB protein which upregulates the expression of cIAP2, Bcl-2 and Bcl-xl anti-apoptotic proteins and MnSOD anti-oxidant enzyme (Kim *et al*., 2015). Using immunohistochemical studies, it has been demonstrated that the RelB protein is highly expressed in PCa biopsies and associated with high Gleason scores in PCa patients (Lessard *et al*., 2005). Furthermore, Josson and co-workers showed that constitutive nuclear levels of RelB are significantly higher in androgen-insensitive PCa PC-3 cells compared with androgen-insensitive LNCaP cells. They also demonstrated the expression levels of MnSOD enzyme was higher in PC3 cells compared with the LNCaP cells (Josson *et al*., 2006). These data suggest that the RelB and MnSOD proteins may be driving the radiation resistance of androgen-insensitive PCa cells.

Targeting non-canonical NF-κB pathway components by different agents leads to an increase in the radiosensitivity of PCa cells (Holley *et al*., 2010). For instance, inhibition of the p52;p100 dimer in PCa cells using STI571, an inhibitor of tyrosine kinase, resulted in enhanced sensitivity of these cells to radiation therapy (Xu *et al*., 2010). In addition, transfected human androgen-insensitive PC3 cells and mouse RM-1 cells (highly aggressive androgen-insensitive mouse PCa cells) with RelB siRNA, sensitised both cell lines to radiation-induced cell

death (Holley *et al*., 2010; Zhu *et al*., 2015). These data suggest that inactivation of the non-canonical NF-κB pathway has been identified as a mechanism involved for the radiosensitivity. Thus, new combination therapies based on radiosensitisation indeed will improve the therapeutic efficacy as well as decrease the radiation-related toxicity to normal cells in PCa treatment.

### 1.4 Aims and objectives

Despite improvements in PCa treatment, none of the current therapies are curative for metastatic CRPC and have limitations in terms of efficacy and toxicity. Therefore, new treatments are urgently sought. There is evidence to suggest that IKKα plays a role in PCa tumourogenesis and although overall this role remains to be fully ascertained, IKKα has been shown to play a role in the regulation of growth, invasion and metastasis. In addition, the non-canonical NF-κB pathway, which is regulated solely by IKKα, has been demonstrated to drive the development of radioresistance of PCa cells. Therefore, targeting IKKα might be a promising approach for the development of a novel treatment for PCa.

The specific aims of the thesis are:

1. To characterise the pharmacological effects of our novel selective IKKα inhibitors by examining their selectivity within the canonical and non-canonical NF-κB pathway in the highly metastatic human prostate cancer PC3M-luc-C6 cell line.

2. To investigate the cytotoxicity activity of specifically selected novel IKKα inhibitors against the metastatic human prostate cancer PC3 and PC3M-luc-C6 cell lines and the human normal prostate epithelium PNT2A cell line.

3. To interrogate whether pharmacological inhibition of IKKα elicits a radiosensitisation effect in the highly metastatic human prostate cancer PC3M-luc-C6 cell line.

4. To compare the outcomes from aims 1-3 above with assessment of the phenotypic and the radiosensestisation effect following knockdown of IKKα and IKKβ by siRNA in the highly metastatic human prostate cancer PC3M-luc-C6 cell line.

# Chapter 2

# Materials and Methods

## 2.1 Cell Lines

In this study, three different prostate cell lines were used, two of which were high metastatic androgen-insensitive prostate cancer PC3 (ATCC, Virginia, USA) and PC3M-luc-C6 (Caliper Life Sciences, Massachusetts, USA), and the other, the normal prostate epithelium cell lines PNT2A cells (Sigma-Aldrich, Gillingham, UK).

PC3M-luc-C6 (a human prostate carcinoma prostate cell line transfected with a luciferase reporter vector) were cultured in Eagle's minimum essential medium (EMEM) supplemented with penicillin/streptomycin (100U/ml), fungizone (2µg/ml), 200mM L-glutamine, 10% (v/v) fetal calf serum (FCS), minimum essential medium non-essential amino acids (MEM NEAA), 100mM sodium pyruvate and minimum essential medium vitamins solution. EMEM medium was obtained from Sigma® (Sigma-Aldrich, Gillingham, UK). Penicillin/streptomycin, fungizone, FCS, sodium pyruvate, minimum essential medium vitamins solution and MEM NEAA were purchased from Gibco® (Gibco, Paisley, UK). L-glutamine was purchased from Invitrogen® (Invitrogen, Paisley, UK). PC3 (human prostate cancer cell lines) were maintained in minimum essential medium (MEM), supplemented with 10% (v/v) FCS and 5% (v/v) of each of penicillin/streptomycin (10000ug/mL), fungizone (250µg/mL) and L-glutamine (200mM) (Life Technologies, Paisley, UK). PNT2A (normal human epithelial prostate cell lines) were cultured in Roswell Park Memorial Institute (RPMI) medium (containing L-glutamine (300mg/L) and 25mM 4-(2-hydroxyethyl)-1-pip

erazineethanesulfonic acid (HEPES)) supplemented with penicillin/streptomycin (100U/ml), fungizone (2µg/ml), and 10% FCS. RPMI medium was purchased from Gibco® (Paisley, UK).

### 2.2 Culture Conditions

PC3M-luc-C6, PC3 and PNT2A cell lines were cultured in 75cm$^2$ flasks (Corning B.V, Buckinghamshire, UK) until approximately 80% confluent; medium was then removed and the cells were washed with 4ml of phosphate buffer solution (PBS). The cells were detached by addition of 4ml of 0.05% trypsin (Gibco®, Paisley, UK) and incubated for 5 minutes at 5% $CO_2$ at 37°C. Once the cells had detached, 6ml of fresh media were added to inactivate the trypsin. Various concentrations of cells were then prepared (1:5, 1:10 and 1:20) in three new 75cm$^2$ flasks containing 20ml of fresh media to enable continuity of the cell line. For PC3M-luc-C6, 2µls of zeocin (200µg/ml) (Invitrogen, Paisley, United Kingdom) per 1ml of medium was added to each passage of PC3M-luc-C6 cells to maintain luciferase gene expression. The cells were gassed with 5% $CO_2$ and incubated at 37°C in a humidified atmosphere. Stocks of PC3M-luc-C6, PC3 and PNT2A cell lines were P10-18 and passages used in the whole experiments were P12-30.

To freeze cells at -80°C or liquid nitrogen (-196°C), cells were detached from the flasks by the addition of 4ml of trypsin and following the addition of complete medium (to neutralise the trypsin), were centrifuged at 1500rpm for 5 minutes and the supernatant removed before the pellets were resuspended in 1ml of

cryoprotectant medium (freezing medium) which was prepared from 10% dimethyl sulfoxide (DMSO) in full medium. The suspension containing the cells was then transferred to labelled cryovials (Thermo Fisher Scientific Inc, Surrey, UK) and stored at -80°C for 24 hours before being transferred for storage in liquid nitrogen. To defrost cells for use, vials were warmed in a water bath at 37°C and then immediately transferred to 75cm$^2$ flasks containing 15ml medium.

## 2.3 Treatment of prostate cell lines

### 2.3.1 Treatment of prostate cell lines with SU compounds

SU1261, SU1361, SU1337 and SU1257 (SU compounds) are first-in-class novel IKKα inhibitors with various potencies and selectivities which had been developed via the small molecule drug discovery programme led by Professor Simon Mackay (University of Strathclyde, Glasgow, UK). Based on the provided weight and the molecular weight (M.Wt) of these agents, a 20mM stock solution was prepared by dissolving the chemical in a calculated volume of DMSO. The prepared solutions were stored at -20$^o$C. For all SU compounds, PC3M-luc-C6 cells were treated with a dose range from 0-30μM for pharmacological characteristic study, and from 0-10μM for PNT2A, PC3 and PC3M-luc-C6 cells in the cytotoxicity study.

### 2.3.2 Treatment of prostate cancer cell lines with External Beam Radiation (XBR)

For radiosensitisation studies, PC3M-luc-C6 cells were exposed to External Beam Radiation (XBR) using a cell irradiation cabinet XRAD 225 (CT, USA) with a 225keV X-ray beam and dose rate of 2.2 Gray/minute (Gy/min) and current of 13.00mA. For treating cells with radiation as a single therapy, doses from 0 to 6Gy were used, however a dose range from 0-2Gy of XBR was used for all combination treatments.

### 2.3.3 Treatment of prostate cancer cell lines with NF-kB pathways stimulators

The canonical and non-canonical NF-kB pathways were stimulated in PC3M-luc-C6 in order to study the pharmacological effects of SU compounds on prostate cancer cells by using Western blot analysis. To do this, PC3M-luc-C6 cells were cultured at a density of $2x10^5$ cells/well in 12-well plates (Thermo Fisher Scientific Inc., Surrey, UK), to reach 90% confluency before being replaced with serum-free medium (no FCS) for 24hr to reduce the basal cellular activity. Cells were then stimulated with the ligands tumour necrosis factor alpha (TNFα) or lymphotoxin $\alpha1\beta_2$ ($LT\alpha1\beta_2$) at the appropriate concentration and time point before protein samples were collected and stored in -20°C for Western blot analysis (section 2.5).

#### *2.3.3.1 Stimulation of the canonical pathway of the NF-kB*

The canonical pathway was stimulated in PC3M-luc-C6 cells using 10ng/ml of TNF-α (Insight Biotechnology Limited, Wembley, UK). Different time points were examined (5, 15, 30, 45, 60, 90 and 120 minutes) and the optimal stimulation time of TNFα was determined on PC3M-luc-C6 cells.

#### *2.3.3.2 Stimulation of the non-canonical pathway of the NF-kB*

The non-canonical pathway was stimulated in PC3M-luc-C6 cells using 30ng/ml of LTα1$\beta_2$ (Sigma-Aldrich, Gillingham, UK). Different time points were examined (1, 2, 4, 8 and 24 hours) and the optimal stimulation time of LTα1β2 was determined on PC3M-luc-C6 cells.

### 2.4 SiRNA transfection of IKKα and IKKβ in prostate cancer cells

Small interfering RNA (siRNA) is one of the useful methods in molecular biology to study the function of different proteins in mammalian cells. siRNA belongs to a class of double stranded RNA (20-25 base pairs) which inhibits the expression of targeted genes with complementary nucleotide sequences causing mRNA to be shut down, leading to halted translation and synthesis for a particular protein (Elbashir *et al.,* 2001).

To investigate the effect of IKKα and IKKβ expression knockdown with siRNA on prostate cell lines, PC3M-luc-C6 cells were transfected with siRNA against IKKα and IKKβ using ON-TARGET*plus*® siRNA reagent (Target sequences are shown in Table 2.1) obtained from Thermo Fisher Scientific® (Thermo Fisher Scientific, Surrey, UK). Newly purchased siRNA was re-suspended in RNase-free 1x

siRNA buffer (Dharmacon, Buckinghamshire, UK). To prepare a 20µM stock, 10nmol of siRNA were resuspended with 500µl of 1x siRNA buffer and mixed by pipetting up and down 3-5 times. The diluted solution was then placed on an orbital mixer for 30 minutes at room-temperature, before being aliquoted and stored at -20°C. Cells were seeded into 6, 12 or 96 well plates (Thermo Fisher Scientific, Surrey, UK) until they reached approximately 50% confluence on the day of transfection. For each well, two labelled eppendorfs were prepared, tube 1 containing the siRNA mixture and tube 2 containing the Lipofectamine® mixture (shown in Table 2.2). Tube 1 was made up to 100µl with Opti-MEM® medium (Life Technologies, Paisley, UK) and in the second tube 5µl Lipofectamine RNAiMAX® (Invitrogen®, Paisley, UK) was diluted into 100µl Opti-MEM®. The contents of tubes 1 and 2 were then added together and mixed gently before incubation at room-temperature for 15-20 minutes to allow complex formation. Full media were then replaced with Opti-MEM® (see Table 2). After the incubation of siRNA and Lipofectamine®, transfection mixture was added to the appropriate wells dropwise. Plates were incubated for 6-8h at 37°C at 5% $CO_2$. After this period, the transfection mixture was aspirated off and replaced with full EMEM media. Cells were then incubated for 72 hrs at 37°C at 5% $CO_2$ when maximal run down had been observed as determined by Western blot analysis for the expression of IKKs protein levels. Cells were then either collected and stored in -20°C for IKKs expression levels by Western blot analysis (section 2.4) or used for phenotypic assays (clonogenic assay section

(2.8), cell cycle analysis section (2.9) and caspase 3 activity assay section (2.10).

**Table 2.1: SiRNA transfection agents.** Target gene, siRNA origin and target sequence.

| Target Gene | On-Target *plus* siRNA | Target Sequence |
|---|---|---|
| IKKα (CHUK) | Human CHUK Cat.No: J-003473-09 | GCGUGAAACUGGAAUAAAU |
| IKKβ (IKBKB) | Human IKBKB (3551) Cat.No: J-003503-13 | GAGCUGUACAG GAGACUAA |
| Non-targeting (NT) | Non-targeting Cat.No: D-001810-01-20 | UGGUUUACAUGUCGACUAA |

**Table 2.2: SiRNA and Lipofectamine® calculated volumes for each plate size.**

| Plate size | OptiMEM volume | siRNA mixture volumes (20µM stock) | | Lipofectamine mixture volumes | Final volume |
|---|---|---|---|---|---|
| 6-well plate | 1.5ml (2ml in control) | 50nM | 2.5µl+247.5µl OptiMEM | 10µl siRNA+240µl OptiMEM | 2ml |
| | | 75nM | 3.75µl+246.25µl OptiMEM | | |
| | | 100nM | 5µl+245µl OptiMEM | | |
| 12-well plate | 750µl (1ml in control) | 50nM | 1.25µl+123.75µl OptiMEM | 5µl siRNA+120µl OptiMEM | 1ml |
| | | 75nM | 1.875µl+123.125 µl OptiMEM | | |
| | | 100nM | 2.5µl+122.5µl OptiMEM | | |
| 96-well plate | 150µl (200µl in control) | 50nM | 0.25µl+24.75µl OptiMEM | 1µl siRNA+24µl OptiMEM | 200µl |
| | | 100nM | 0.5µl+124.5µl OptiMEM | | |

## 2.5 Western blot analysis

The Western blot (protein immunoblot) is an analytical technique used to measure specific proteins in a tissue homogenate or cell extract. This method was used to measure different protein levels using specific antibodies in PC3M-luc-C6 cells extracts following treatment with SU compounds or siRNA transfection.

### 2.5.1 Preparation of whole cell extracts

The PC3M-luc-C6 cells were treated with agents (TNFα or LTα1$\beta_2$ stimulators, SU compounds or siRNA) for the relevant times. Plates were then positioned on ice to stop the degradation or dephosphorylation of protein. Cells were immediately washed with PBS buffer (ice cold) followed by addition of 200µl of pre-heated Laemmli's sample buffer (63mM Tris-HCl (pH6.8), 2mM $Na_4P_2O_7$, 5mM EDTA, 10% (v/v) glycerol, 2% (w/v) sodium dodecyl sulphate (SDS), 50mM Dithiothreitol (DTT), 0.007% (w/v) bromophenol blue) to each well. The cells were then scraped and the chromosomal DNA sheared by repeatedly syringing up and down using a 21 gauge needle and transferred to eppendorf tubes. The tubes containing cell extracts were then boiled at 100°C for 5 mins to denature the proteins, helping the antibodies to access and bind efficiently with epitopes and facilitate their running through the gels. Whole cell extract samples were stored at -20°C or -80°C until use. All chemicals were obtained from Sigma-Aldrich (Sigma-Aldrich, Gillingham, UK) unless otherwise stated.

### 2.5.2 SDS-polyacrylamide gel electrophoresis (SDS-PAGE)

The principle behind gel-electrophoresis is based on the migration of negatively charged proteins (due to presence of SDS) towards the positive anode through the polyacrylamide gel. Due to the pores produced by the acrylamide, smaller proteins move faster than the large ones, thus proteins are separated by the polyacrylamide gel according to their molecular weight.

The gel electrophoresis equipment was first cleaned with 70% ethanol, then distilled $H_2O$ was added for 1 hour to test for any leaking between the glass plates. 10% (w/v) resolving gels were prepared which consisted of acrylamide 10% (w/v) (Rotiphorese® Gel 30 (37.5:1), 0.375M Tris base (pH8.8), 0.1% (w/v), SDS and 10% (w/v) ammonium persulfate (APS). Polymerisation of the gel was introduced by adding 0.05% (v/v) N, N, N', N' tetramethylethylenediamine (TEMED). The preparation was flowed between two glass plates assembled in a vertical slab pattern and overlaid with 200µl of 0.1% (w/v) SDS. When the gel polymerized, the upper-layer of 0.1% (w/v) SDS was poured off and a 10% (v/v) stacking gel (10% (v/v) acrylamide Rotiphorese® Gel 30 (37.5:1), 0.125M Tris base (pH6.8), 0.1% (w/v) SDS and 10% (w/v) ammonium persulfate (APS) and 0.05% (v/v) TEMED) was added on the resolving gel, and a teflon comb was directly inserted into the stacking gel layer. The comb was removed after the stacking gel being polymerized and the glass plates were assembled in a Bio-Rad Mini-PROTEAN 3TM electrophoresis (Bio-Rad Laboratories, Hertfordshire, UK), with both tanks filled with running buffer (25mM Tris, 129mM glycine, 0.1%

(w/v) SDS). Samples (20-30µg/ml) and prestained SDS-PAGE molecular weight marker (Bio-Rad Laboratories, Hertfordshire, UK) were then loaded into the wells using a microsyringe. The gel was run at a constant voltage of 120V for 1-1.5 hours, until the samples reached the bottom of the gel. All chemicals were obtained from Sigma-Aldrich (Sigma-Aldrich, Gillingham, UK) unless otherwise stated.

### 2.5.3 Electrophoretic transfer of proteins to nitrocellulose membrane

In order to detect proteins using primary antibodies, the proteins separated by the polyacrylamide gel were then transferred to nitrocellulose membranes (GE Healthcare, Buckinghamshire, UK) by electrophoretic blotting in wet conditions according to a standard protocol (Towbin *et al*., 1979).

A transfer cassette sandwich was assembled which comprised two sponge pads and two filter papers (GE Healthcare, Buckinghamshire, UK) and nitrocellulose membrane (Figure 2.1). It was very important to get rid of any air bubbles by gently rolling over the top surface of the sandwich. The cassette was slotted into a Bio-Rad Mini-PROTEAN 3TM electrophoresis which was filled with transfer buffer (25M Tris, 19mM glycine, 20% (v/v) methanol). Proteins were transferred to the membrane at current of 300mA for 105min. A reservoir was included in the tank to minimize the high temperature of the transfer buffer. As proteins were charged negatively by SDS in the gel, the transfer process was conducted from the gel (negative/cathode) to the nitrocellulose (positive/anode).

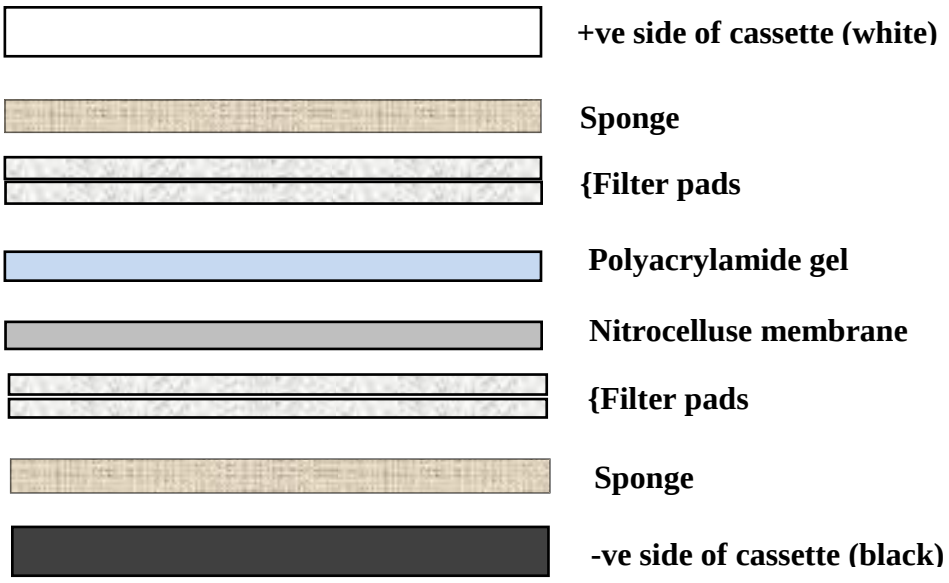


**Figure 2.1: Assembly of Western blot transfer sandwich.** Schematic demonstration of the assembly of transfer sandwich on the cassette.

### 2.5.4 Immunological detection of protein

Following transfer of the proteins to the membrane, the membrane was removed and nonspecific binding blocked by incubation in a solution of 2-3% Bovine Serum Albumin (BSA) in NaTT buffer (150mM NaCl, 20mM Tris (pH 7.4), 0.2% (v/v) Tween 20) on an orbital shaker for at least 1.5 hours. The blocking buffer was then removed and membranes were incubated overnight (at room temperature or 4°C) with specific primary antibody (antiserum) to the target protein in a solution of 0.2% BSA in NaTT buffer. Primary antibodies and conditions are listed in Table 2.3. The next day, membranes were then washed six times every 15 minutes in NaTT buffer on an orbital shaker with gentle agitation. Again, membranes were incubated at room temperature for 90

minutes with secondary antibody horseradish peroxidase-conjugated IgG (sheep anti-mouse IgG or goat anti-rabbit IgG) (Jackson ImmunoResearch Laboratories Inc, PA, USA) diluted to 1:10000 0.2% BSA in NaTT buffer. Following 6 washes in NaTT at 15 minute intervals, immuno-reactive target proteins were detected by addition of 6ml of enhanced chemiluminescence (ECL) reagent (1:1 mixture of solution 1 [1M Tris pH8.5, 250mM luminol, 250mM p-cymuric acid and water] and solution 2 [1M Tris pH8.5, 0.19% $H_2O_2$ and water]) for 2 mins with a gentle shaking. To visualise the protein bands, the membranes were placed on an exposure cassette, covered with cling film and then exposed to X-ray film (B Plus – Full Blue) in the dark room for the required time and developed using X-OMAT machine (KODAK M35-M X-OMAT Processor).

**Table 2.3: Primary antibodies used in immunoblotting and optimal conditions.** Table showing the source of antibodies used and their catalogue number, species in addition to the blocking and incubation conditions in Western blot analysis.

| Target Proteins | Antibody source | Species | Blocking Conditions | Incubation Temperature |
|---|---|---|---|---|
| IκBα | IκBα-alpha Cell signaling Technology Inc (Hertfordshire, UK) | Rabitt | 2% BSA in NaTT | Room temperature |
| phospho-p65 | p-NF-kB p65 (S536) Cell signaling Technology Inc (Hertfordshire, UK) | Rabbit | 2% BSA in NaTT | 4°C |
| p65 | NFκB p65 (C-20) Santa Cruz Biotechnology Inc (CA, USA) | Rabbit | 2% BSA in NaTT | Room temperature |
| p100/52 | Anti-NFκB p52 Millipore (CA, USA.) | Mouse | 2% BSA in NaTT | 4°C |
| IKKα | anti-IKKα Calbiochem (CA, USA) | Mouse | 3% BSA in NaTT | 4°C |
| IKKβ | IKKβ (Y466) Calbiochem (CA, USA) | Rabbit | 3% BSA in NaTT | 4°C |

### 2.5.5 Nitrocellulose membrane stripping and reprobing

To reprobe the same membranes for the detection of other cell proteins or to confirm equal loading of total proteins, nitrocellulose membranes were stripped using a stripping buffer (0.05M Tris-HCl, 2% SDS, and 0.1M of β-54

mercaptoethanol). The membrane was incubated in a heated cabinet shaker at 70°C with 15ml of stripping buffer. The buffer was then removed and the membrane washed with NaTT buffer three times at 15 minutes intervals in a fume hood sink then washed 3 times with NaTT buffer at 15min intervals to remove any remaining of stripping buffer. The membranes were then ready for incubation overnight with a new primary antibody in 0.2% BSA (w/v) in NaTT buffer followed by the immunological detection protocol mentioned in section 2.5.4.

### 2.5.6 Scanning densitometry and quantification of expression levels

Western blot films were scanned using Epson Perfection 1640SU Scanner and Adobe Photoshop 5.0.2 software. Expression of protein levels were quantified and normalised to a control by using Scion Image (Scion Corp., Maryland, USA). Fold increase in protein levels compared to control or agonist stimulated control were analysed statistically by a one-way ANOVA with Bonferroni correction post-test using GraphPad Prism software, version 6.0, 2014 (GraphPad Software Inc, CA, USA). *P* values lower than 0.05 were used to determine the significance.

## 2.6 Cell growth assay

The aim of this method was to assess the effects of SU compounds exposure on the growth and proliferation of PC3M-luc-C6, PC3 and PNT2A cells. In 6-well plates, 5 x $10^4$ cells per well were seeded with 5ml of fresh media and incubated for 48hr for at least one population doubling in a 37$^{o}$C and 5% $CO_2$ incubator.

After this period, the media were removed and 1ml of fresh media containing various concentrations of SU compounds (0-10 µM) was added for each well in each plate. The cells were incubated at 37$^{o}$C and 5% $CO_2$ with drugs at 5 time points (0h, 24h, 48h, 72h and 96h). For each concentration at each time point, the medium was removed and washed with PBS and then cells were detached by the addition of 0.5ml of trypsin EDTA (0.05%). Trypsin was then deactivated by addition of 1ml of fresh media and disaggregated through a 21G needle and then counted using a haemocytometer. The results were then plotted on a graph as cell number (y axis) versus time (x axis) and the growth Area Under the Curve (AUC) for each dose during the whole growth time was measured using Graph Pad Prism software, version 6.01, 2014 (GraphPad Software Inc, CA, USA).

### 2.7 Alamar blue cell viability assay

Alamar blue® dye (Life Technologies, Paisley, UK) is a cell viability and proliferation indicator that widely used in human and animal cell lines cytotoxicity experiments. It recruits resazurin (7-Hydroxy-3H-phenoxazin-3-one 10-oxide), a fluorescent blue dye, and when resazurin is reduced by the mitochodial NADPH dehydrogenase and NADH dehydrogenase enzymes, it is converted to the red fluorescent resorufin which can be then quantitatively measure by Fluorometry (Gloeckner *et al*., 2001).

In 25 cm$^2$ flasks, 2x10$^5$ of PC3M-luc-C6, PC3 and PNT2A cells were cultured in 5ml of complete medium and incubated at 37$^{o}$C and 5% $CO_2$. When the cells

reached 80% confluence, the medium was then removed and cells washed with PBS and detached using 1ml of trypsin (0.05%) followed by addition of 2mls of fresh medium, disaggregated through a 21G needle and then counted using a haemocytometer. A density of 1500, 2000 and 1500 cells of PC3M-luc-C6, PC3 and PNT2A cells respectively were cultured in 96 well plates (Sigma-Aldrich, Gillingham, UK) with 3 replicates of each sample and incubated at 37$^{o}$C and 5% $CO_2$ for 48 hours. For each well, medium was replaced with 100µl of fresh medium containing different concentration of SU compounds (0-10µM) and incubated at 37$^{o}$C and 5% $CO_2$. After 72hr following treatment, each well for each time point was replaced with 100µl of full medium containing 10% (v/v) Alamar blue® and kept in the incubator at 37$^{o}$C and 5% $CO_2$ for 4 hours. Fluorescence intensity was then measured using a Spectra Max Gemini XS plate reader (Molecular Devices Corporation, CA, USA) with an excitation wavelength of 570nm and an emission wavelength of 580nm and processed using SoftMax Pro software version 4.3 (Molecular Devices Corporation, CA, USA).

The results were presented as the mean percentage of cell viability (mean ± sd) compared with untreated control wells of three independent experiments. The results were plotted as percentage of cell viability on y-axis against the logarithmic dose on x-axis, and $IC_{50}$ values were calculated by using non-linear regression curve fitting of cell viability using GraphPad Prism software, version 6.01, 2014 (GraphPad Software Inc, CA, USA).

## 2.8 Clonogenic survival assay

The Clonogenic survival assay is a cytotoxic tool that is used widely to investigate the effect of cytotoxic agents (compounds or radiation) on mammalian cells. Exposure of cells to toxic agents could affect their normal division and reproduction integrity which subsequently leads to cell death. However, unaffected cells which retained the ability to divide and proliferate normally can produce large colonies (Munshi et al., 2005).

### 2.8.1 Clonogenic survival assay for the effect of SU compounds and XBR as single agents

The clonogenic assay method was conducted as described by Cunningham *et al*. (2000). In brief, PC3M-luc-C6, PC3 cells were cultured in 25cm$^2$ flasks in 5ml of complete medium at a 37$^o$C and 5% $CO_2$ incubator. When the cells reached 60-70% confluence, medium was replaced with 1ml of fresh medium containing various concentration of SU compounds (0-10µM) and incubated for 24 hours at 37$^o$C and 5% $CO_2$. However with XBR exposure, cells were treated with a dose range from 0-6Gy immediately before conducting the clonogenic assay. In both treatment flasks (SU compounds or XBR), medium was removed and cells were washed with PBS and detached using 1ml of trypsin (0.05%) followed by addition of 2mls of fresh medium before cells were disaggregated through a 21G needle and then counted using a haemocytometer. An appropriate number of cells (400 cells for PC3M-luc-C6 and 250 cells for PC3) were added to each of three 60mm petri dishes (Sigma-Aldrich, Gillingham, UK) containing 5ml of fresh

medium. This triplicate plating was carried out for each experimental condition and control and plates containing the cells were incubated at 37$^{o}$C and 5% $CO_2$. Following 10-14 days of incubation, colonies formation was assessed to ensure colonies of over 50 cells had developed in control dishes. The medium was then removed and cells were washed with PBS, fixed with 100% methanol for 10 minutes and stained with 10% Giemsa's stain solution (BDH Laboratory, Dorset, UK) for 10 minutes. The stain was carefully removed and dishes were rinsed with water and formed colonies were counted by eye. Plating efficiency (PE) and survival fraction (SF) were calculated from the following equations:

$$\mathrm{PE} = \frac{\text{average no. of control colonies formed}}{\text{no. of seeded cells}}$$

$$\mathrm{SF} = \frac{\text{average no. of colonies formed after treatment}}{\text{no. of seeded cells X PE}}$$

The experimental results were fitted to dose-response curve as the mean SF (mean ± sd) on y-axis versus treatment doses on x-axis of three independent experiments.

### 2.8.2 Clonogenic assay for the effect of SU1261 and XBR as a combination

In this experiment, clonogenic survival assays were carried out to assess the effect of SU1261 and XBR as a combination on PC3M-luc-C6 clonogenicity. PC3M-luc-C6 cells were grown in 25cm$^2$ flasks in 5ml of complete medium flask until reaching 60-70% confluence, then the medium was replaced with 1ml of fresh medium containing different concentration of SU1261 (0-10μM) and

incubated for 24 hours at 37$^{o}$C and 5% $CO_2$ followed by exposure to 0-2Gy of XBR. The cells were counted, plated and stained as describe previously in section 2.8.1.

### 2.8.3 Clonogenic assay for the effect of siRNA IKKα and IKKβ transfection alone or in combination with XBR

Clonogenic survival assays were conducted in this experiment to investigate the effect of siRNA transfection with IKKα or IKKβ siRNA alone and in combination with XBR on PC3M-luc-C6 clonogenicity. PC3M-luc-C6 cells were cultured in 6-well plates until reaching approximately 50% confluence, medium was replaced with transfection mixture (50 and 100nM) for NT, IKKα or IKKβ as described previously in section 2.4. After 72 hours of transfection, groups of wells were exposed to 0-2Gy of XBR while other groups were untreated and the cells were then counted, seeded in petri dishes and stained as described previously in section 2.8.1.

## 2.9 Assessment of the cell cycle progression by Fluorescence-Activated Cell Sorting Analysis (FACS)

Fluorescence-Activated Cell Sorting Analysis (FACS) is a specialised type of flow cytometry that is used to discriminate cells in different phases of the cell cycle. It has become a standard tool to analyse the DNA content in populations of cells and provides a description of the cell cycle distribution following treatment at any selected point of time (Schorl and Sedivy, 2007). This technique employs a Propidium Iodide dye (a fluorescent dye) which stains DNA quantitatively. The fluorescence intensity of stained cells can be then measured at a particular wavelength and reflects the DNA content of cells (Krishan, 1975).

### 2.9.1 Assessment of the effect of SU compounds on cell cycle progression by Fluorescence-Activated Cell Sorting Analysis (FACS)

The aim of the FACS method was to assess the effect of the SU agents on the cell cycle progression of PC3M-luc-C6 Cells. Cells were cultured in 25cm$^2$ flasks with 5ml of fresh medium until reaching 60-70% confluence. Medium was removed from the flasks and replaced by 1ml of fresh medium containing various concentration of SU drugs (0-10µM) and incubated for 24 hours in a 37$^o$C and 5% $CO_2$ incubator. After cells were detached by addition of 1ml of trypsin (0.05%), 2mls of fresh medium was added to counteract the effect of trypsin. The cell suspension was then spun down at 1500 RPM for 5 minutes, the supernatant was removed, cells were washed with PBS and re-pelleted at 1500rpm, for 5 minutes. Cells were fixed with 3ml 70% ice-cold ethanol and

stored at -20$^{o}$C until analysis. On the day of analysis, cells were centrifuged at 2000rpm for 10 minutes, the ethanol layer was removed and cells were resuspended and centrifuged twice with 10ml of PBS at 1500rpm for 10 minutes. The PBS was then poured off and the pellet was resuspended with 300µL PBS containing 10µg/mL Propidium Iodide (PI) (Sigma-Aldrich, Gillingham, UK) and 50ug/mL RNase (Sigma-Aldrich, Gillingham, UK). Tubes containing cell suspensions were incubated on ice in the dark for at least 1 hour. Cell cycle analysis was carried out using a FACScan (Becton Dickinson Systems, Cowley, UK) and data were analysed using BD CellQuest$^{TM}$ Pro software (version 5.1.1). Three independent experiments were carried out with a minimum of 1000 cells/sample and results presented as the percentage of the cell cycle phases (mean ± sd).

### 2.9.2 Assessment of the effect of SU1261 and XBR combination on Cell Cycle Progression by Fluorescence-Activated Cell Sorting Analysis (FACS)

Cell cycle analysis assays by FACS was conducted to investigate the effect of SU1261 and XBR combination on Cell Cycle Progression of PC3M-luc-C6. Cells were grown in 25cm$^2$ flasks in 5ml of complete medium flask until reaching 60-70% confluent, medium was replaced with 1ml of fresh medium containing different concentration of SU1261 (0-10µM). After 24 hours of treatment, flasks were exposed to 0-2Gy of XBR and incubated for 24hr at 37$^{o}$C and 5% $CO_2$.

Samples were collected and assessed for cell cycle progression through FACS as described in section 2.9.1.

### 2.9.3 Assessment of the effect of siRNA IKKα and IKKβ transfection alone or in combination with XBR on Cell Cycle Progression by Fluorescence-Activated Cell Sorting Analysis (FACS)

Cell cycle analysis assays by FACS were carried out to investigate the effect of siRNA transfection with IKKα or IKKβ alone and in combination with XBR on cell cycle progression of PC3M-luc-C6. Cells were cultured in 6-well plates until reaching approximately 50% confluent, then medium was replaced with transfection mixture (50 and 100nm) for NT, IKKα or IKKβ as described before in section 2.4. After 72 hours of transfection, wells were exposed to 0-2Gy of XBR and incubated for 24hr at 37$^{o}$C and 5% $CO_2$ or unexposed. Samples were collected and assessed for cell cycle progression through FACS as mentioned in section 2.9.1.

### 2.10 Caspase 3 activity apoptosis assays

Caspase 3 is known as a marker of early apoptosis activation as a result of DNA damage. It acts by interfering with the normal DNA repair process by breaking down (by proteolysis) the main proteins involved in repair such as poly (ADP-ribose) polymerase (PARP) (Nicholson *et al*., 1995). The amino acid sequence site at which PARP is cleaved by caspase 3, DEVD (Asp-Glu-Val-Asp), is occupied by the synthetic tetrapeptide fluorogenic substrate, DEVD-AMC, which contains the amino acid sequence for the PARP cleavage site. Caspase 3

cleaves the tetrapeptide between the DEVD and AMC leading to releasing of the fluorescent AMC which can be measured using fluorometry (Gurtu *et al*., 1997).

### 2.10.1 Caspase 3 activity apoptosis assays for the effect of SU compounds

Caspase 3 activity assays were conducted to test if the SU compounds induced caspase 3 activity on PC3M-luc-C6, PC3 and PNT2A cells as an indicator for apoptosis. In 25cm$^2$ flasks, 2x10$^5$ of PC3M-luc-C6, PC3 and PNT2A cells were cultured in 5ml of complete medium and incubated at 37$^o$C and 5% $CO_2$. When cells reached 80% confluence, the medium then was removed and washed with PBS and detached using 1ml of trypsin (0.05%) followed by 2mls of fresh medium, disaggregated through a 21G needle and then counted using a haemocytometer. A density of 3000, 3500 and 2500 cells of PC3M-luc-C6, PC3 and PNT2A cells were cultured respectively in 96 well plates with 3 replicates of each sample and incubated at 37$^o$C and 5% $CO_2$ for 48 hours. For each well, medium was replaced with 60µl of fresh medium containing different concentration of SU compounds (0-10µM) or 30µM of Staurosporine (positive control for caspase 3 activity) and incubated for 4 hours at 37$^o$C and 5% $CO_2$. Following incubation, 30µl of cell lysis buffer containing the Ac-DEVD-AMC caspase 3 fluorogenic substrate (BD Bioscience, Oxford, UK) mixture were added to each well and plates were incubated for 1 hour. The cell lysis buffer contained 150mM HEPES, 450mM NaCl, 150mM KCl, 30mM $MgCl_2$, 1.2mM EGTA, 1.5% Nonidet P40 (Fluka Chemicals, Gillingham UK), 0.3% CHAPS and 30% sucrose in distilled $H_2O$ and the pH was adjusted to 7.4. Immediately

before the assay, the caspase 3 fluorogenic substrate was prepared by adding 30mM Dithiothreitol and 3mM phenylmethanesulfonylfluoride to 10mM DEVD-AMC caspase substrate. All chemicals were obtained from Sigma-Aldrich (Sigma-Aldrich, Gillingham, UK) unless otherwise stated.

Plates were read for fluorescence intensity of free AMC by using a Spectra Max Gemini XS plate reader (Molecular Devices Corporation, CA, USA) with an excitation wavelength of 360nm, an emission wavelength of 460nm and processed using SoftMax Pro software, version 4.3 (Molecular Devices Corporation, CA, USA). The results were presented as the mean fold increase (mean ± sd) in caspase 3 activity by comparing and normalising the mean fluorescence intensity for each treated group with the fluorescence intensity of untreated control wells in three independent experiments.

### 2.10.2 Caspase 3 activity apoptosis assays for the effect of siRNA IKKα and IKKβ transfection

This experiment was carried out to assess whether siRNA transfection with IKKα or IKKβ siRNA has any role in caspase 3 activity levels after 48 and 72 hrs post-transfection in PC3M-luc-C6 cells. A density of 3000 cells of PC3M-luc-C6 were cultured in 96 well plate with 3 replicates of each sample until reaching approximately 50% confluent, when medium was replaced with transfection mixture (50 and 100nM) for NT, IKKα or IKKβ as described before in section 2.4. After 48 and 72hr of transfection, a 30µl of cell lysis buffer containing the Ac-DEVD-AMC caspase 3 fluorogenic substrate mixture were added to each well

and plates were incubated for 1 hr at 37$^{o}$C and 5% $CO_2$. The level of caspase 3 activity was measured and normalized to the untreated control as previously described in the previous section (2.10.1).

### 2.11 Combination index analysis

Mathematical evaluation of combinations of SU1261 and XBR in PC3M-luc-C6 cells was carried out using the median-effect principle and combination index analysis of Chou and Talalay (Chou and Talalay, 1984).

The Combination index analysis method is used to analyse the synergistic effect of two therapies which are both found to be cytotoxic as single agents. From the results of clonogenic assays following treatment with SU1261 and XBR as either single agents or as a combination, dose–effect curves were plotted using equation 1:

$$fa/fu = (D/IC_{50})^{m} \qquad \text{Equation 1}$$

Where D is the drug dose, fa is the fraction of cells affected by drug dose D, fu is the unaffected fraction by drug dose D, and $IC_{50}$ is the dose that inhibited 50% of colony formation.

Then, equation 1 is transformed to the *log* form (Equation 2) to convert it to a straight line equation (y=*m*x+c), where the coefficient *m* becomes the slope of the line.

$$\log[fa/fu] = m\log D - m\log IC_{50} \qquad \text{Equation 2}$$

Therefore, following treatment with SU1261 and XBR as either single agents or as a combination, $IC_{50}$ was calculated from the x-intercept ($\log IC_{50}$) and the coefficient *m* (slope) was determined for each treatment, these can then be put into the re-arranged median effect equation (Equation 3).

$$D = IC_{50}[fa/fu]^{1/m} \qquad \text{Equation 3}$$

Subsequently, the combination-index (CI) analysis was used to evaluate the efficacy of the combination (Chou and Talalay, 1984). The toxic effects caused by each agent and combination, as calculated from equation 4 were then calculated using equation 4:

$$CI = (D)_1/(Dx)_1 + (D)_2/(Dx)_2 \qquad \text{Equation 4}$$

where $(D)_1$ and $(D)_2$ are the doses of each single therapy that inhibit (x)% of cell when used in combination, and $(Dx)_1$ and $(Dx)_2$ are the doses of each drug, treated as single agents, that inhibit (x)% of growth. The resultant combination indices, were plotted against the fraction of toxicity, where CI < 1 (synergism), CI = 1 (additivity) and CI > 1 (antagonism).

### 2.12 Linear quadratic analysis

Linear quadratic analysis is another mathematical model which is used to analyse the relationship and the effectiveness of two different therapies in combination (Miller *et al*., 1992). This method was used to assess the radiosensitising effect of IKKα and IKKβ siRNA transfection to XBR on PC3M-

luc-C6 cells. As we mentioned previously, the median-effect and combination index analysis methods are applied to investigate the relationship between two different therapies when both are cytotoxic as a single agents, however the linear quadratic analysis was the best method to assess the cytotoxicity effect of the siRNA transfection and XBR combination as no significant toxicity has been found in PC3M-luc-C6 cells when transfected with siRNA IKKα alone.

The principle behind the linear quadratic model is based on two key components of cytotoxicity. These components are the linear component (α coefficient) and the quadratic component (β coefficient). The linear component represents the initial slope of the survival curve at low doses or the sub-lethal effect of radiation which is thought to result from single-ionisation events that cause DNA damage, whilst the quadratic component corresponds to the latter slope of the curve which results from multiple-ionisation events causing the severe cytotoxic effect of radiation at high doses (Barendsen, 1997; Brenner *et al*., 1998; Franken *et al*., 2001). GraphPad Prism software, version 6.0, 2014 (GraphPad Software Inc, CA, USA) was used to fit clonogenic survival data to the linear quadratic curve (equation 1), and to calculate the linear component (α coefficient) and the quadratic component (β coefficient) values (Hall and Giaccia, 2006).

$$SF = \exp(-\alpha D - \beta D^2) \qquad \text{Equation 1}$$

Where SF is the survival fraction of cells and D is the dose of radiation. The α and β coefficients are the linear and the quadratic phases of the curve respectively. Equation 2 was used to calculate the $IC_{50}$ of the radiation (dose

which caused 50% of cell death) against PC3M-luc-C6 cells treated with XBR (0-2Gy) alone or after transfection with IKKα and IKKβ siRNA (50 and 100nm).

$$IC_{50} = [- \alpha + \sqrt{} (\alpha^2 - 48 \ln 0.5]/2\beta \qquad \text{Equation 2}$$

When the values of the $IC_{50}$ were obtained from the previous equations for XBR as a single therapy or after transfecting the cells with IKKα and IKKβ siRNA, the dose enhancement factor at 50% cell death ($DEF_{50}$) was calculated from equation 3. The $DEF_{50}$ can be defined as the ratio between the $IC_{50}$ for radiation when used alone, to the $IC_{50}$ of radiation in presence of radiosensitiser (Roeske *et al*., 2007). Therefore, the higher $DEF_{50}$ ratio is the larger the radiosensitising effect, and the lower the dose of radiation needed in combination to achieve the same fraction of cell death compared to radiation alone.

$$DEF_{50} = IC_{50} \text{ (radiation alone)} / IC_{50} \text{ (radiation + radiosensitiser)} \qquad \text{Equation 3}$$

**2.13 Statistical analysis**

All data presented were carried out in at least three separate experiments. All data was analysed statistically using GraphPad Prism software, version 6.0, 2014 (GraphPad Software Inc, CA, USA). The statistical significance of differences between groups were analysed by either one-way analysis of variance (ANOVA) followed or two-way ANOVA followed by Bonferroni post-tests. *P* values lower than 0.05 were used to determine the significance.

# Chapter 3

# Pharmacological Inhibitory Effect of Selective IKKα Inhibitors (SU compounds) on NF-κB Canonical and Non-canonical Pathways

## 3.1 Introduction

As mentioned in the introduction (Chapter 1), IKKs play a major role in the regulation of NF-κB pathways (Lee and Hung, 2008). When a canonical pathway is stimulated by different stimuli, such as TNF-α, this will lead to phosphorylation of the IKK complex and subsequent activation of IκB-α degradation and the translocation of p65 into the nucleus (Oeckinghaus and Ghosh, 2009). However, stimulation of the non-canonical NF-κB pathway by various molecules such as lymphotoxin β (LTβ), leads to the processing of p100 to p52 and generation of active p52-RelB heterodimers through the phosphorylation of IKKα subunits (Oeckinghaus and Ghosh, 2009).

IKKα contributes to the pathogenesis of various types of cancer, including PCa (Fernandez-Majada *et al*., 2007; Park *et al*., 2005; Shiah *et al*., 2006; Hirata *et al*., 2006; Luo *et al*., 2007). Despite IKKα having been implicated in PCa progression, invasion, metastasis and the development of CRPC (Mahato *et al.,* 2011; Ammirante *et al.,* 2010; Jain *et al.,* 2012; Luo *et al.,* 2007), no selective IKKα inhibitor compounds have been developed which could be utilised as an approach for PCa treatment. Therefore, selective IKKα inhibitors (SU compounds) were designed and prepared chemically by our collaborator from the Medicinal Chemistry department at the University of Strathclyde. These novel compounds were tested for IKKα selectivity inhibition using *in vitro* kinase assay but not at a cellular level. Thus, the aim of this chapter was to study the pharmacological characteristics of these novel IKKα inhibitors (SU compounds)

in terms of their selectivity and the potency against canonical and non-canonical NF-κB pathways in the androgen-insensitive PCa cell line PC3M-luc-C6.

Before the assessment of the potency and the selectivity of SU compounds on IKKα at cellular level, there is an issue that should be considered first. Previous workers in our laboratory used commercial phospho-IKKα antibodies to measure the selectivity of SU agents on IKKα levels. However, these antibodies were found to be problematic in terms of specificity against IKKα and the results could not be achieved using Western blotting. Therefore, in this chapter, we assess the selectivity and the potency of SU compounds by measuring the consequences of the inhibition of the canonical and non-canonical NF-κB pathways. Phosphorylation of p65 and IκB-α degradation were used as markers of canonical NF-κB pathway inhibition, while the processing of p100 to p52 was used for the non-canonical NF-κB pathway. The canonical and non-canonical NF-κB pathways were stimulated by TNF-α (10ng/ml) and LTα1β (30ng/ml) respectively. The hypothesis was that the most selective IKKα inhibitor (SU compounds) should inhibit the non-canonical pathway rather than the canonical pathway.

## 3.2 Results

### 3.2.1 Determining the dissociation constant (Ki value) of the SU compounds

The IKKα and IKKβ inhibitory activity of SU compounds (SU1261, SU1361, SU1337 and SU1257) were determined using a dissociation-enhanced ligand fluorescent immunoassay (DELFIA) based on the protocol of HTScan™ IKKβ Kinase Assay (Cell Signaling Technology, Inc., Danvers, MA, USA) by Mrs. Louise C. Young, University of Strathclyde.

Briefly, recombinant IKKα or IKKβ, 37nM, (Millipore, Dundee, UK) was incubated with IκB-α (Ser32) (New England Biolabs, Hitchin, UK) biotinylated peptide substrate (0.375μM or 0.18 μM for IKKα and IKKβ assay respectively) and 40μM or 10μM ATP for IKKα and IKKβ respectively in assay buffer (40 mM Tris-HCl (pH 7.5), 20 mM $MgCl_2$, EDTA 1mM, DTT 2 mM and BSA 0.01mg/ml) in a V-well 96-well plate in the presence and absence of SU compound. The assay plate was incubated for 60 min at 30°C after which the kinase reaction was quenched by the addition of 50mM EDTA, pH8. The resulting mixture was transferred to a streptavidin-coated 96-well plate (Perkin Elmer, Beaconsfield, UK) and incubated for 1 hour at 30°C to immobilise the substrate peptide. The extent of phosphorylation was assessed by dissociation-enhanced lanthanide fluorescent immunoassay (DELFIA) and the time-resolved fluorescence (TRF) for three individual experiments to determine the $IC_{50}$ curves.

The dissociation constant or the Ki values (the concentration of compound at which 50% of the kinase activity is inhibited) of the lead compounds under interrogation are shown in Table 3.1. The Ki value of SU1261 for IKKα was 10nM, while the Ki value of IKKβ was approximately 70-fold higher than that of IKKα (Ki value = 680nM). Similarly, the Ki value for SU1361 on IKKα was very low (Ki value = 8nM), while the Ki value for IKKβ was 100-fold higher than IKKα (Ki value = 961nM). SU1337 was also more selective against IKKα (Ki value = 21nM) than IKKβ (Ki value = 1550nM). These data suggest that these compounds are highly selective for IKKα. Further, the Ki values of SU1257 were high for IKKα (Ki value = 9800nM) and IKKβ (Ki value = 4100nM), which make this compound useful as a negative control against other SU compounds as no inhibitory effect on kinase activity was observed on both kinases (IKKα and IKKβ) except in very high dose.

**Table 3.1: The effect of SU compounds (SU1261, SU1361, SU1337 and SU1257) on IKKα and IKKβ kinases activities.** IKKα and IKKβ were purified and the dissociation constant (Ki value) of SU compounds was assessed using a dissociation-enhanced ligand fluorescent immunoassay.

| Ki value (nM) | SU1261 | SU1361 | SU1337 | SU1257 |
|---|---|---|---|---|
| **IKKα** | 10 | 8 | 21 | 9800 |
| **IKKβ** | 680 | 961 | 1550 | 4100 |

### 3.2.2 Characterisation of SU compounds on TNF-α induced activation of the canonical NF-κB pathway in PC3M-luc-C6 cell lines

As the selectivity of SU compounds on IKKα/β were tested in an *in vitro* kinase method but not in cell based assays, SU compounds were then assessed for effects on the canonical NF-κB pathway of the PC3M-luc-C6 cell lines after induction with TNF-α (10ng/ml). The phosphorylation of the p65 subunit and the degradation of IκB-α were measured as key markers of the canonical pathway. In addition, the total p65 level was used as an indicator for the total loading protein.

#### *3.2.2.1 TNF-α induced IκB-α degradation and phosphorylation of the p65 in PC3M-luc-C6 cell lines in a time-dependent manner*

Our previous laboratory experiments showed that TNF-α (10ng/ml) activated the canonical NF-κB pathway leading to cellular degradation of the IκB-α and phosphorylation of the p65 subunits in PC3M-luc-C6 cell lines. The aim of this initial experiment was to determine the optimal time course for TNF-α induced IκB-α loss and p65 phosphorylation.

As indicated in Figure 3.1 B, IκB-α degradation was largely observed at 30min (30.43% of control basal expression) following TNF-α (10ng/ml) stimulation and levels were sustained over 45min (28.01% of basal expression) and 60min (28.23% of control basal expression). Subsequently, the expression of IκB-α

gradually increased towards basal values by 120min (70.66% of control basal expression).

In Figure 3.1 C, phosphorylation of p65 was initiated 5min following TNF-α (10ng/ml) stimulation as determined by measurement of more than a two-fold increase in protein expression (fold increase=2.24) compared with the control group. This phosphorylation continuously increased to 7-fold at 15min (fold increase=7.13) and reached a maximum at 30min, with an 8-fold (fold increase=8.01) increase compared to the unstimulated control group. The phosphorylation of p65 then gradually declined and reached 1.84-fold the levels of the control group following two hours of stimulation with TNF-α (10ng/ml).

From this data, we concluded that 30min following TNF-α (10ng/ml) stimulation was the appropriate time point to choose for canonical NF-κB pathway stimulation where the IκB-α loss and p65 phosphorylation were highly stimulated compared with the unstimulated control group.

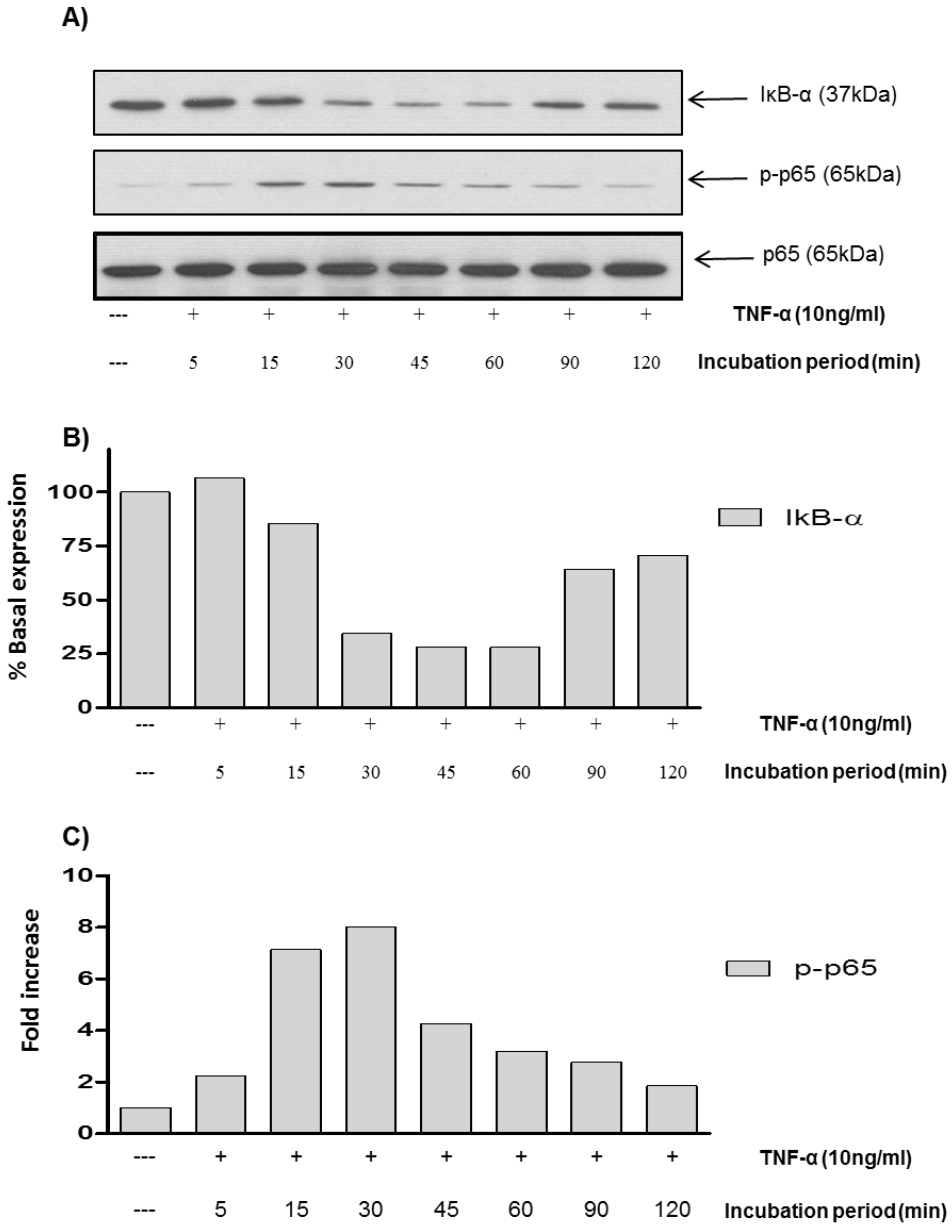


**Figure 3.1: Time course of TNF-α-mediated IκB-α degradation and p65 phosphorylation in PC3M-luc-C6.** Cells were stimulated with TNF-α (10ng/ml) for a two-hour period. A) Whole cell lysates were prepared, separated by SDS PAGE and assessed for IκB-α (37kDa), p-p65 (65kDa), and p65 (65kDa). Blots were quantified by scanning densitometry for B) IκB-α as % expression, and fold increase for C) p-p65. The results are representative of one independent experiment.

### *3.2.2.2 Effect of SU compounds on TNF-α induced IκB-α degradation and p65 phosphorylation of the canonical NF-κB pathway in PC3M-luc-C6 cell lines*

Next, the SU compounds were tested for their inhibitory effect on the canonical NF-κB pathway. The PC3M-luc-C6 cell lines were treated with SU compounds in a dose rage from 0.3 to 30μM for one hour followed by stimulation with TNF-α (10ng/ml) for 30min. The compounds interrogated included SU1261, SU1361, and SU1337, in addition to the negative control SU1257. Phosphorylation of the p65 subunits and IκB-α degradation in whole cell lysate were then assessed by Western blot as markers of the canonical NF-κB pathway. The total p65 level was used as an indicator for the total loading protein.

- **Effect of SU1257 on canonical NF-κB pathway**

Figures 3.2 and 3.3 demonstrate the effect of SU1257 on TNF-α induced p65 phosphorylation and IκB-α degradation in PC3M-luc-C6 cells. Compared with the control unstimulated group, TNF-α (10ng/ml) significantly induced IκB-α degradation by 85% (% basal expression=15.67% (±3.59), Figure 3.2, $P<0.01$). The same dose of TNF-α also stimulated the p65 phosphorylation significantly by more than two-fold (fold increase=3.59 (±0.25), Figure 3.3, $P<0.01$) compared with the untreated control group. However, increasing concentrations of the negative control SU1257 (0.3-30μM) did not significantly affect the TNF-α induced IκB-α degradation compared with cells stimulated by TNF-α alone. (Figure 3.2, $P>0.05$). Similarly, in the presence of TNF-α, the phosphorylated p65 level was not altered significantly following treatment with SU1257 up to the

maximum concentration of 30μM compared with TNF-α stimulated cells ($P$>0.05, Figure 3.3). In the absence of TNF-α, and following administration with the maximum dose of SU1257 (30μM), neither the IκB-α nor the phosphorylated p65 levels were found to be affected compared with control cells with no statistically significant difference in protein expression observed ($P$>0.05).

These results suggest that SU1257 is an ideal negative control for study of the effect SU compounds on the canonical NF-κB pathway as it did not affect the biomarkers of this pathway in any tested concentration following stimulation with TNF-α (10ng/ml).

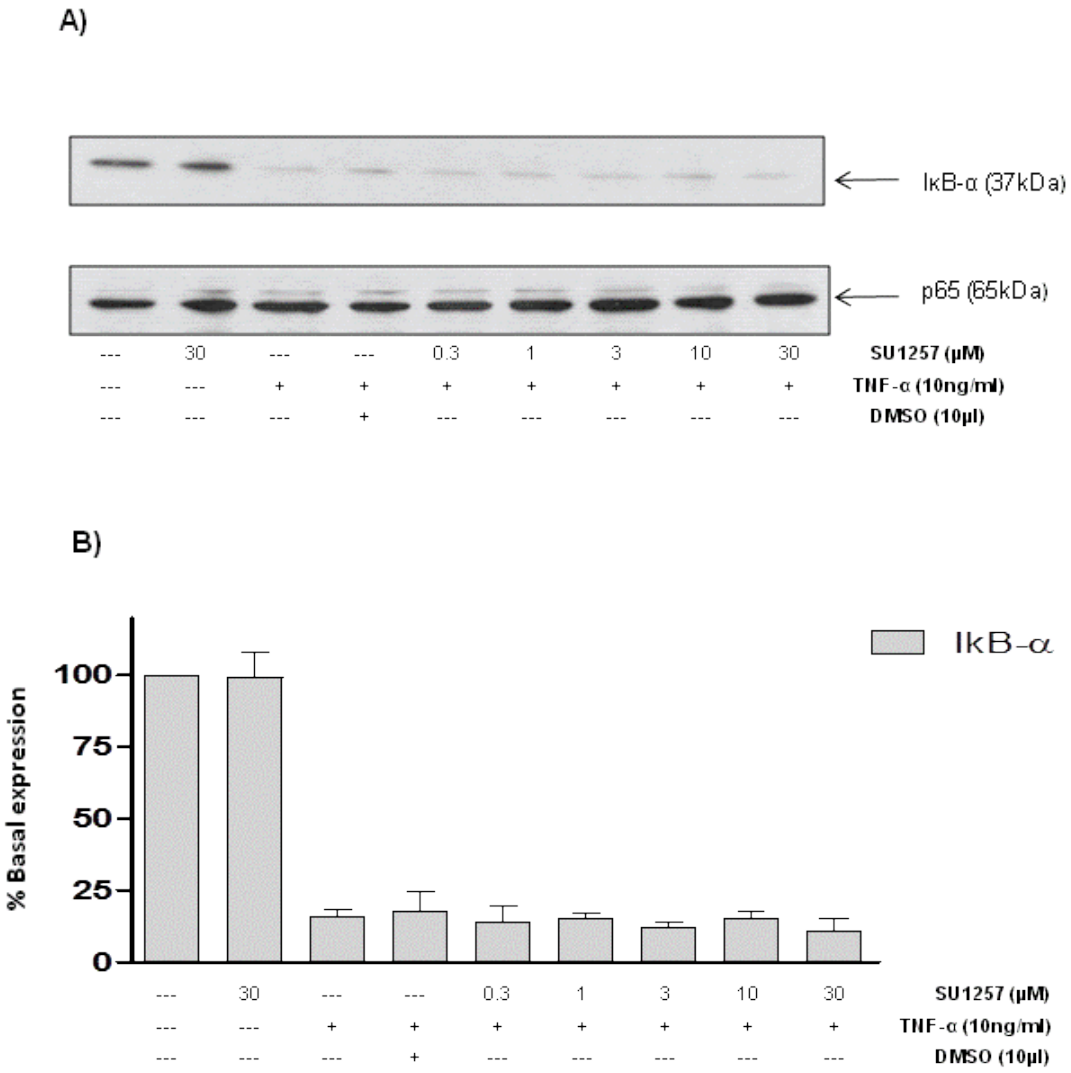


**Figure 3.2: The effect of SU1257 upon TNF-α-mediated IκB-α degradation in PC3M-luc-C6.** Cells were pre-treated with SU1257 for 1h prior to stimulation with TNF-α (10ng/ml) for 15min. A) Whole cell lysates were prepared, separated by SDS PAGE and assessed for IκB-α (37kDa) and p65 (65kDa). B) Blots were quantified for % expression by scanning densitometry; each value represents the mean ± S.E.M. The results are representative of three independent experiments.

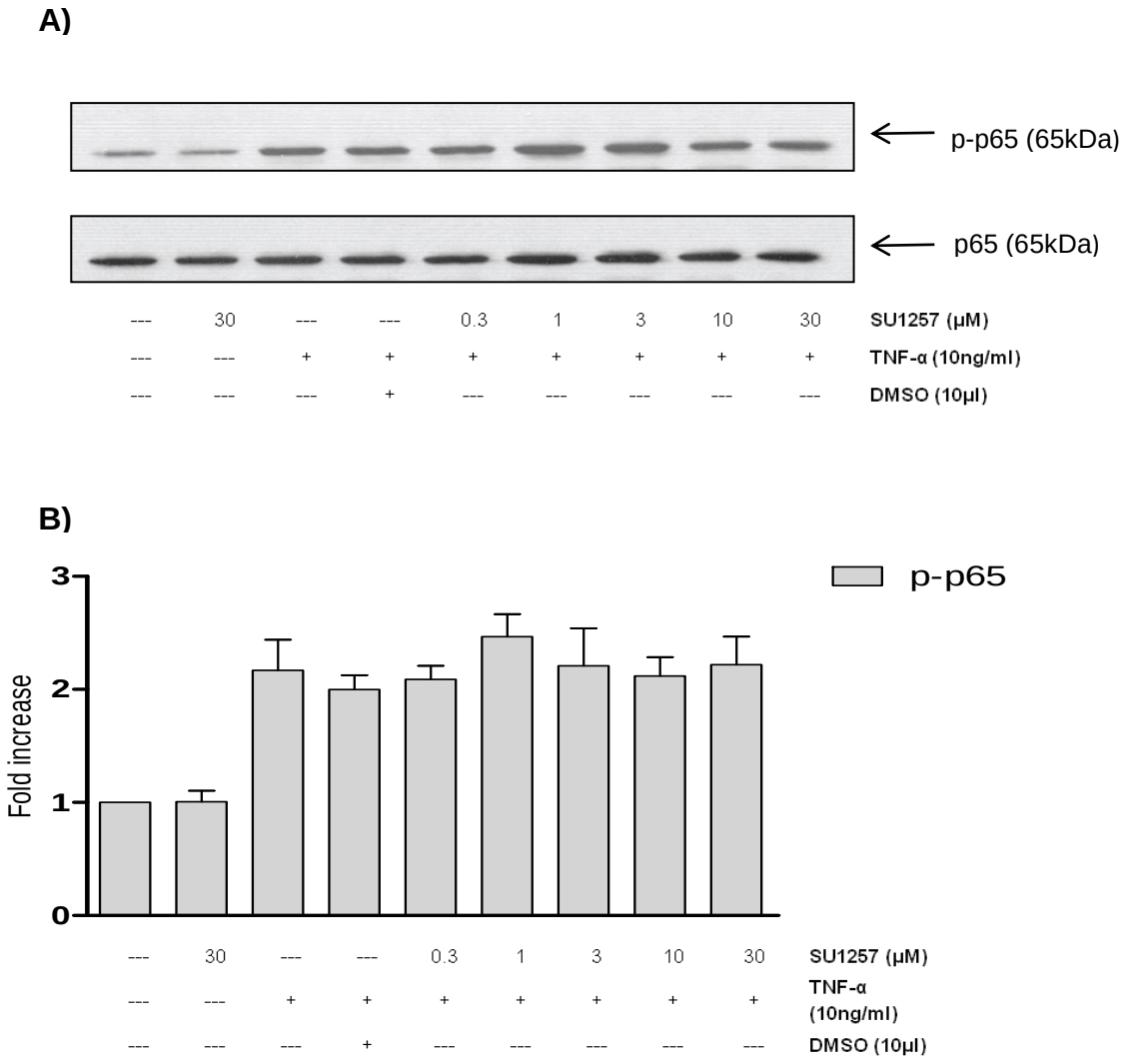


**Figure 3.3: The effect of SU1257 upon TNF-α-mediated p65 phosphorylation in PC3M-luc-C6.** Cells were pre-treated with SU1257 for 1 hr prior to the stimulation with TNF-α (10ng/ml) for 30 min. A) Whole cell lysates were prepared, separated by SDS PAGE and assessed for p-p65 (65kDa) and p65 (65kDa). B) Blots were quantified for % expression by scanning densitometry; each value represents the mean ± S.E.M. The results are representative of three independent experiments.

- **Effect of SU1261 on canonical NF-κB pathway**

Figures 3.4 and 3.5 show the effect of SU161 on TNF-α induced IκB-α degradation and p65 phosphorylation in PC3M-luc-C6 cells. Stimulation of cells with TNF-α (10ng/ml) induced the degradation of IκB-α significantly by more than 80% (% of basal expression=17.27% ±3.61, $P$<0.001) compared with control cells. Pre-treatment of cells with SU1261 in doses ranging from 0.3 to 10μM did not cause any statistically significant changes to TNF-α (10ng/ml) induced IκB-α degradation compared to cells stimulated with TNF-α alone (Figure 3.4, $P$>0.05). However, in the presence of TNF-α (10ng/ml) stimulation, administration of 30μM of SU1261 significantly increased the expression of IκB-α to 57.33% (±7.01, $P$<0.01) compared with 17.27% (±3.61) induced by TNF-α alone. Nonetheless, this highest dose of SU1261 (30μM) did not alter the expression of IκB-α in the absence of TNF-α compared with the untreated control group ($P$>0.05).

Similar to its effect on IκB-α level, SU1261 (0.3-10μM) did not alter the phosphorylation of p65 level induced by TNF-α (10ng/ml) stimulation (Figure 3.5, $P$>0.05) compared with TNF-α stimulated cells. However, post-stimulation with TNF-α (10ng/ml), 30μM of SU1261 returned the level of the phosphorylated p65 close to the control basal level of the untreated control group (fold increase=0.87±0.48, $P$<0.01). Without TNF-α stimulation, SU1261 (30μM) did not affect the phosphorylation measurement of p65 in cells (fold increase=0.90 ±0.08, $P$>0.05) compared with untreated control cells.

These findings demonstrated that SU1261 (0.3-10μM) did not exert a major effect on the canonical NF-κB pathway. However, the maximum tested concentration of SU1261 (30μM) engaged the canonical pathway by targeting the IκB-α degradation and the phosphorylation of p65 which was induced by TNF-α (10ng/ml).

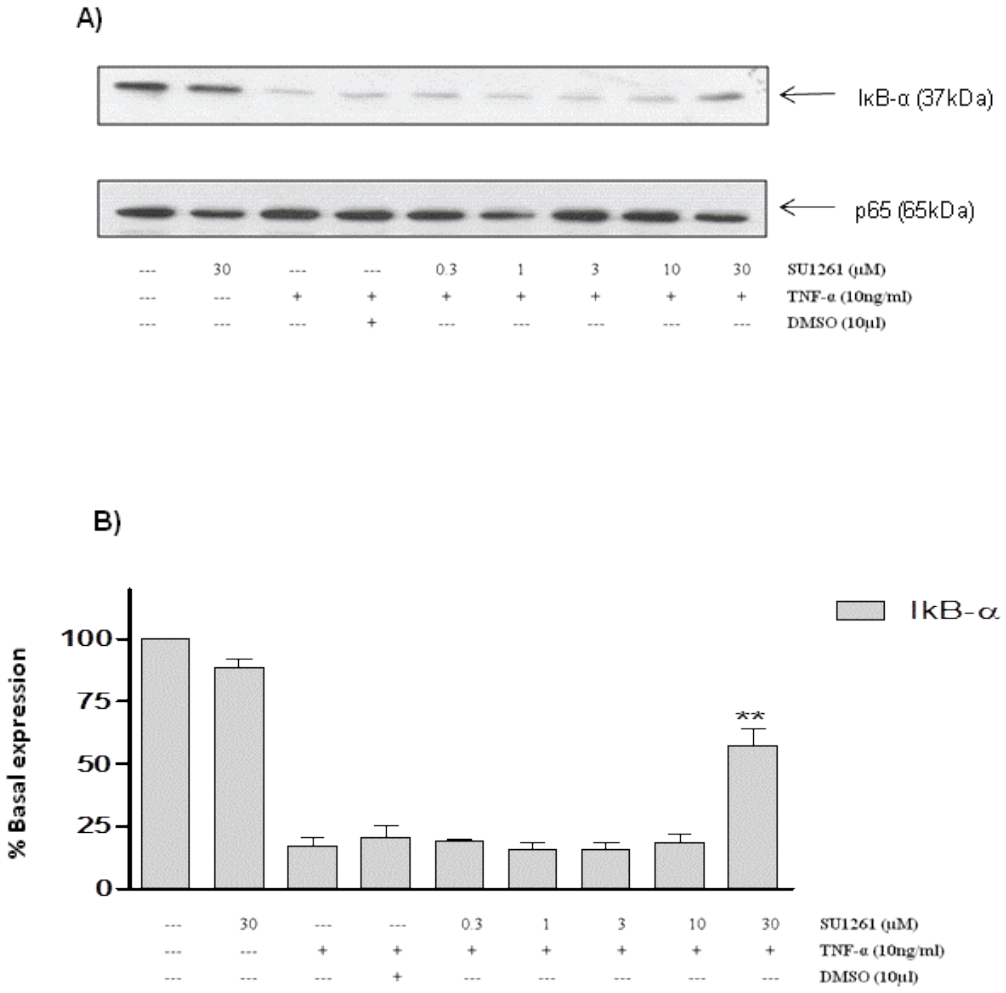


**Figure 3.4: The effect of SU1261 upon TNF-α-mediated IκB-α degradation in PC3M-luc-C6.** Cells were pre-treated with SU1261 for 1 hr prior to the stimulation with TNF-α (10ng/ml) for 30 min. A) Whole cell lysates were prepared, separated by SDS PAGE and assessed for IκB-α (37kDa) and p65 (65kDa). B) Blots were quantified for % expression by scanning densitometry; each value represents the mean ± S.E.M. The results are representative of three independent experiments. ***P*<0.01 compared with TNF-α stimulated control.

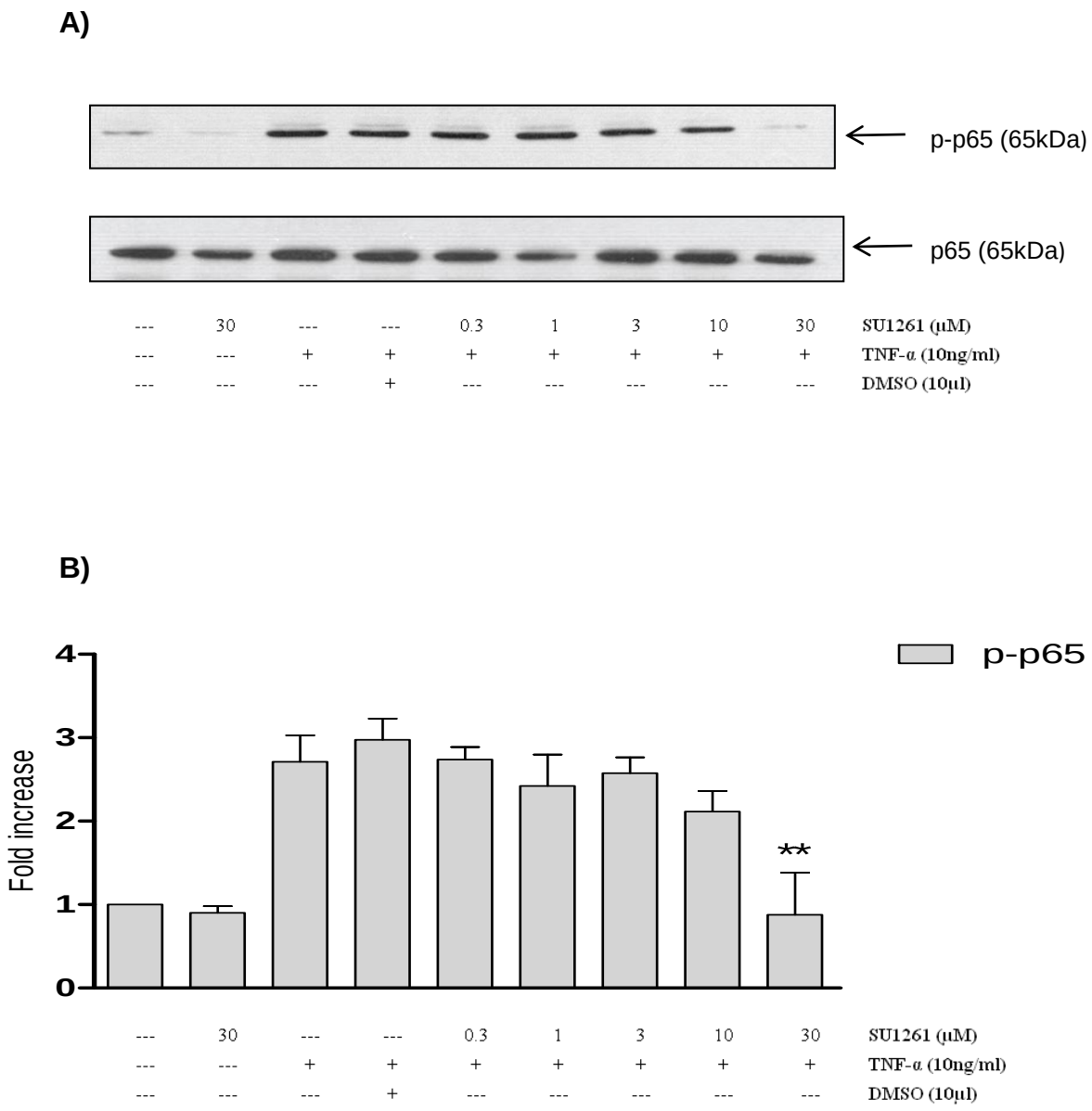


**Figure 3.5: The effect of SU1261 upon TNF-α-mediated p65 phosphorylation in PC3M-luc-C6.** Cells were pre-treated with SU1261 for 1 hr prior to the stimulation with TNF-α (10ng/ml) for 30min. A) Whole cell lysates were prepared, separated by SDS PAGE and assessed for p-p65 (65kDa) and p65 (65kDa). B) Blots were quantified for % expression by scanning densitometry; each value represents the mean ± S.E.M. The results are representative of three independent experiments. ***P*<0.01 compared with TNF-α stimulated control.

- **Effect of SU1361 on canonical NF-κB pathway**

SU1361 was the third compound tested in this group. Compared with SU1261, SU1361 demonstrated a greater inhibitory effect on IκB-α loss and phosphorylation of p65 (Figures 3.6 and 3.7). In Figure 3.6, SU1361 administered in the concentration range (0.3-1μM) did not show any statistically significant change in IκB-α degradation ($P$>0.05) following TNF-α (10ng/ml) stimulation compared with the group stimulated with TNF-α alone. However, starting from administration of 3μM of SU1361 the degradation of IκB-α was gradually inhibited after stimulation with TNF-α (10ng/ml) compared with unstimulated control cells. Doses of 3μM and 10μM inhibited the degradation of IκB-α significantly following TNF-α (10ng/ml) stimulation to 47.45% (±7.36, $P$<0.05) and 61.93% (±6.57, $P$<0.01) respectively, compared with control cells. Moreover, treatment of cells with SU1361 (30μM) followed by TNF-α (10ng/ml) stimulation increased the IκB-α expression significantly, to 84% (±5.39, $P$<0.001) of the basal control level. However, compared with the untreated control group, no significant alterations were observed on IκB-α expression when non-TNF-α stimulated cells were treated with 30μM of SU1361 alone ($P$>0.05).

In Figure 3.7, SU1361 (0.3-1μM) did not demonstrate any significant change in p65 phosphorylation level post-stimulation with TNF-α (10ng/ml) compared with TNF-α (10ng/ml) treatment alone ($P$>0.05). Nevertheless, increasing concentrations of SU1361 (3-30μM) showed a dose-inhibitory effect on TNF-α induced p65 phosphorylation. Doses of 3μM and 10μM of SU1361 reduced the

fold increase in phosphorylated p65 level induced by TNF-α (10ng/ml) from 3.29 (±0.77) to 2.40 fold (±0.56, $P>0.05$) and 1.79 fold (±0.19, $P<0.05$) respectively, compared with the TNF-α stimulated group. The maximum concentration of SU1361 (30μM) diminished the phosphorylated p65 level (fold increase=1.12 ± 0.31, $P<0.05$) compared with TNF-α treated cells nearly to the level of the control group.

Unlike SU1257 or SU1261, these data indicated that SU1361 in a dose range of 3-10μM engaged the canonical pathway by counteracting the effect of TNF-α-induced IκB-α degradation and p65 phosphorylation.

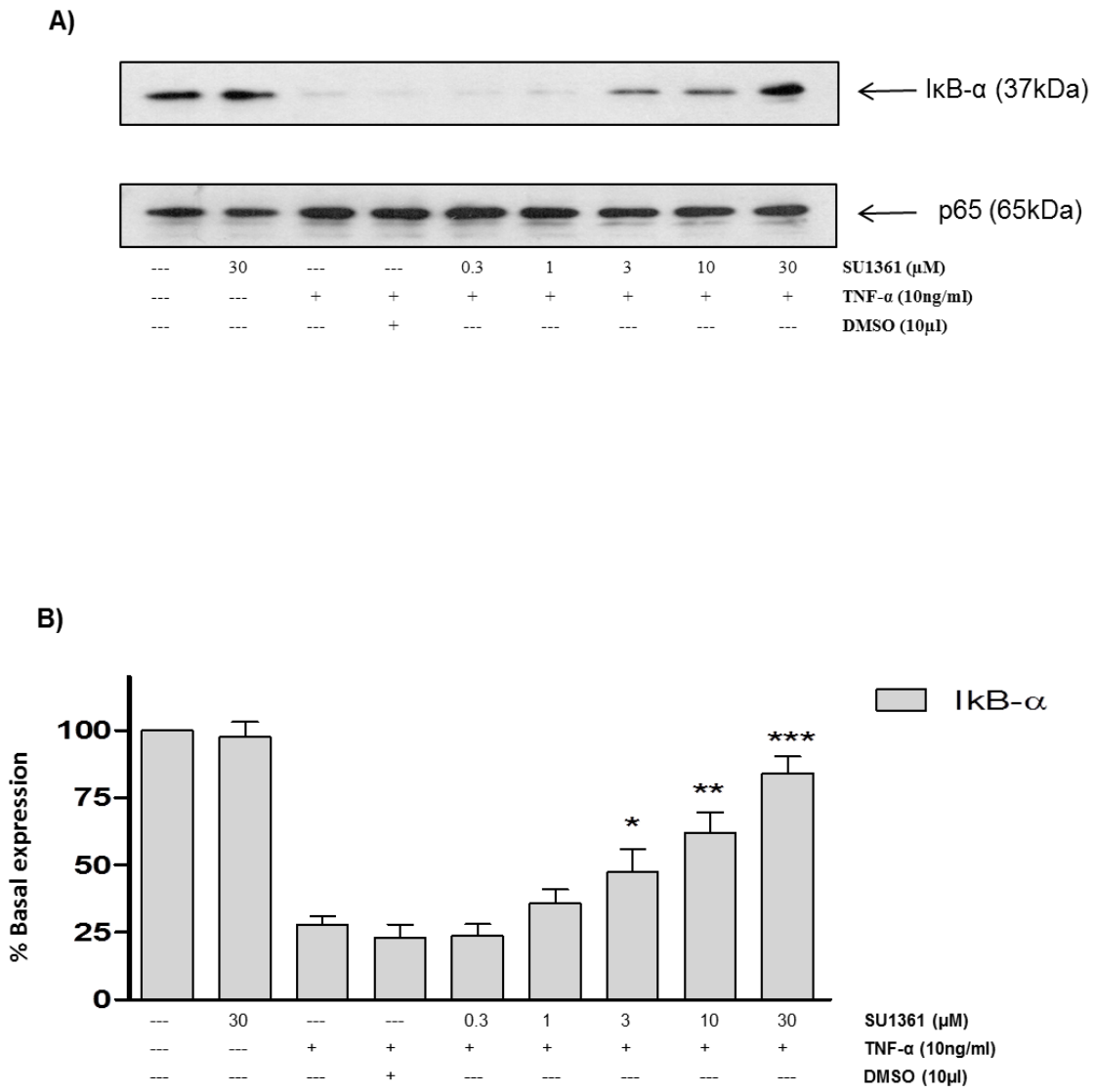


**Figure 3.6: The effect of SU1361 upon TNF-α-mediated IκB-α degradation in PC3M-luc-C6.** Cells were pre-treated with SU1361 for 1 hr prior to the stimulation with TNF-α (10ng/ml) for 30min. A) Whole cell lysates were prepared, separated by SDS PAGE and assessed for IκB-α (37kDa) and p65 (65kDa). B) Blots were quantified for % expression by scanning densitometry; each value represents the mean ± S.E.M. The results are representative of three independent experiments. **P*<0.05 ***P*<0.01 ***P*<0.001 compared with TNF-α stimulated control.

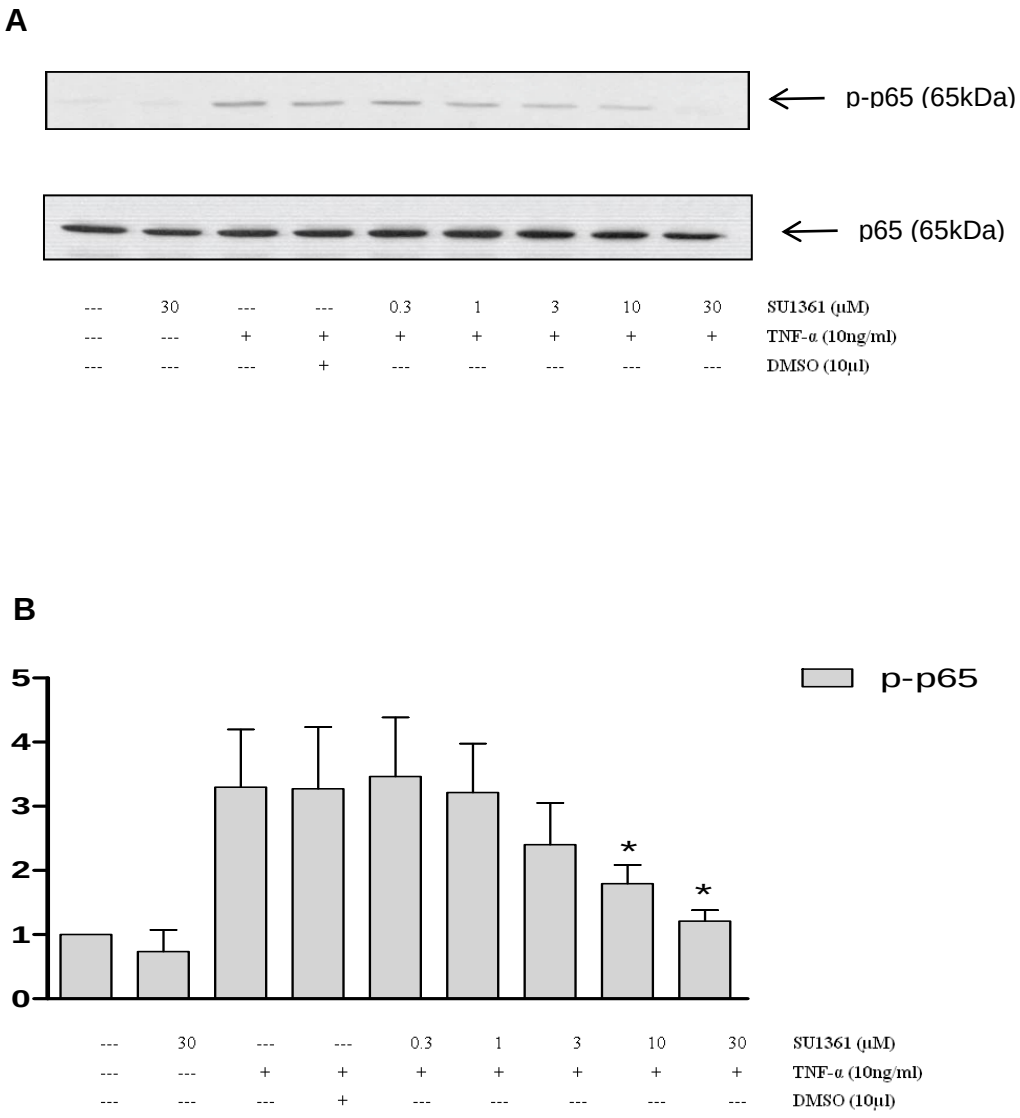


**Figure 3.7: The effect of SU1361 upon TNF-α-mediated p65 phosphorylation in PC3M-luc-C6**. Cells were pre-treated with SU1361 for 1 hr prior to the stimulation with TNF-α (10ng/ml) for 30min. A) Whole cell lysates were prepared, separated by SDS PAGE and assessed for p-p65 (65kDa) and p65 (65kDa). B) Blots were quantified for % expression by scanning densitometry; each value represents the mean ± S.E.M. The results are representative of three independent experiments. *$P$<0.05 compared with TNF-α stimulated control.

- **Effect of SU11337 on canonical NF-κB pathway**

The final SU compound examined in this group was SU1337. As shown in Figure 3.8, treatment of cells with SU1337 in concentrations ranging from 0.3μM to 3μM did not alter the TNF-α induced IκB-α degradation or p65 phosphorylation significantly ($P$>0.05). However, when cells were treated with 10μM and 30μM of SU1337 followed by TNF-α (10ng/ml) stimulation, the degradation of the IκB-α subunits decreased insignificantly to 49.83% (±12.60, $P$>0.05) and significantly to 78.29% (±8.17, $P$<0.01) respectively, compared with the control basal expression level. No significant effect on IκB-α expression levels were observed when cells exposed to 30μM of SU1337 without TNF-α (10ng/ml) stimulation ($P$>0.05) compared with unstimulated control cells.

Figure 3.9 demonstrates the effect of SU1337 on p65 phosphorylation induced by TNF-α (10ng/ml) stimulation. In a similar fashion, a concentration range of 1-10μM of SU1337 caused a decrease in the phosphorylation of p65 level induced by TNF-α stimulation which was not statistically significant ($P$>0.05) compared with TNF-α treated cells alone. However, 30μM of SU1337 reduced the expression of the phosphorylated p65 significantly by 70% (fold increase=1.57 ± 1.41, $P$<0.05), compared with cells stimulated by TNF-α alone (fold increase=5.05 ± 2.39). These data revealed that SU1337 inhibited the canonical pathway stimulated with TNF-α (10ng/ml). Similarly to SU1361, 10μM and 30μM of SU1337 decreased the degradation of IκB-α. However, starting from administration of only 1μM of SU1337, the expression of phosphorylated p65 declined but was largely inhibited when doses were increased to10 and 30μM.

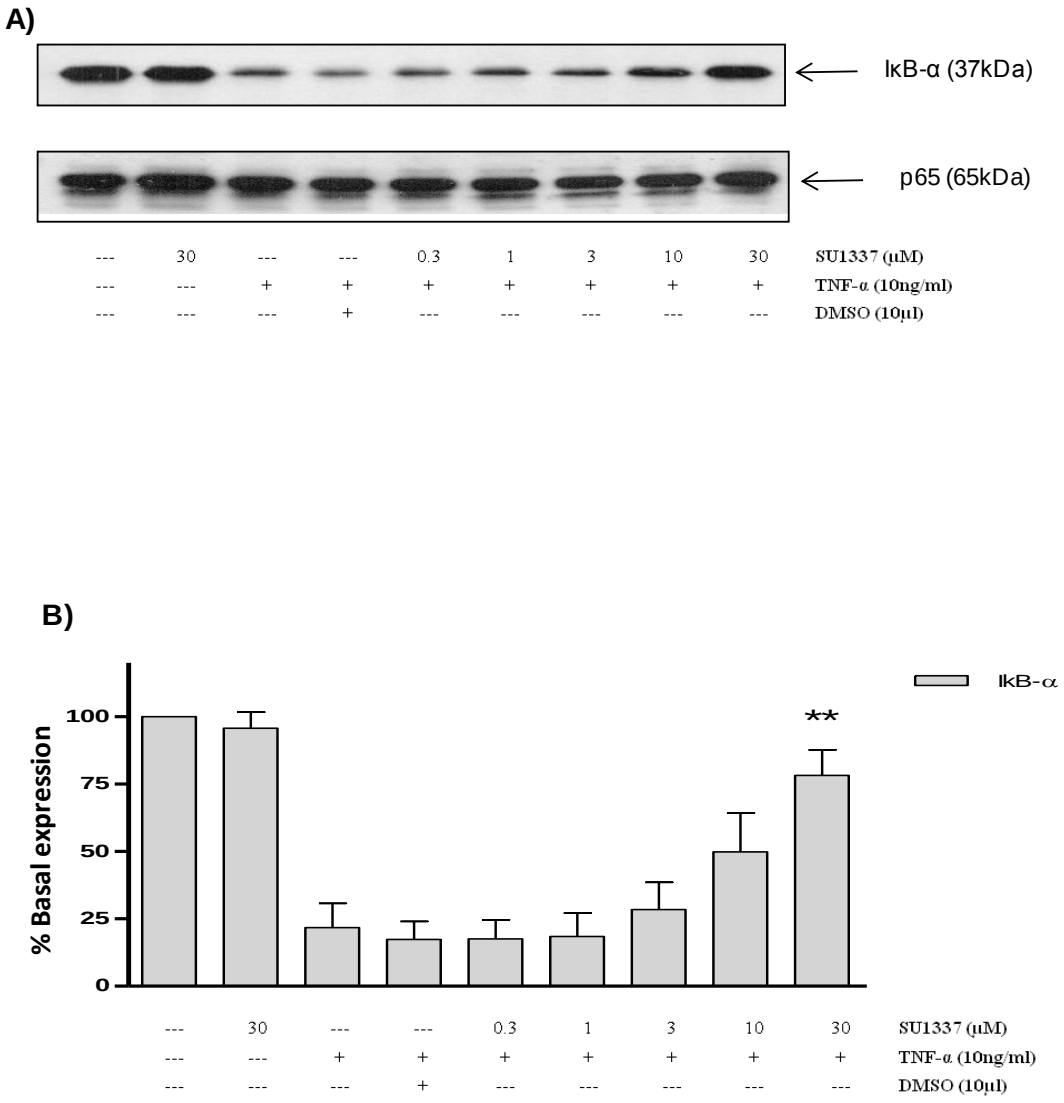


**Figure 3.8: The effect of SU1337 upon TNF-α-mediated IκB-α degradation in PC3M-luc-C6.** Cells were pre-treated with SU1337 for 1 hr prior to stimulation with TNF-α (10ng/ml) for 30 min. A) Whole cell lysates were prepared, separated by SDS PAGE and assessed for IκB-α (37kDa) and p65 (65kDa). B) Blots were quantified for % expression by scanning densitometry; each value represents the mean ± S.E.M. The results are representative of three independent experiments. ***P*<0.01 compared with TNF-α stimulated control.

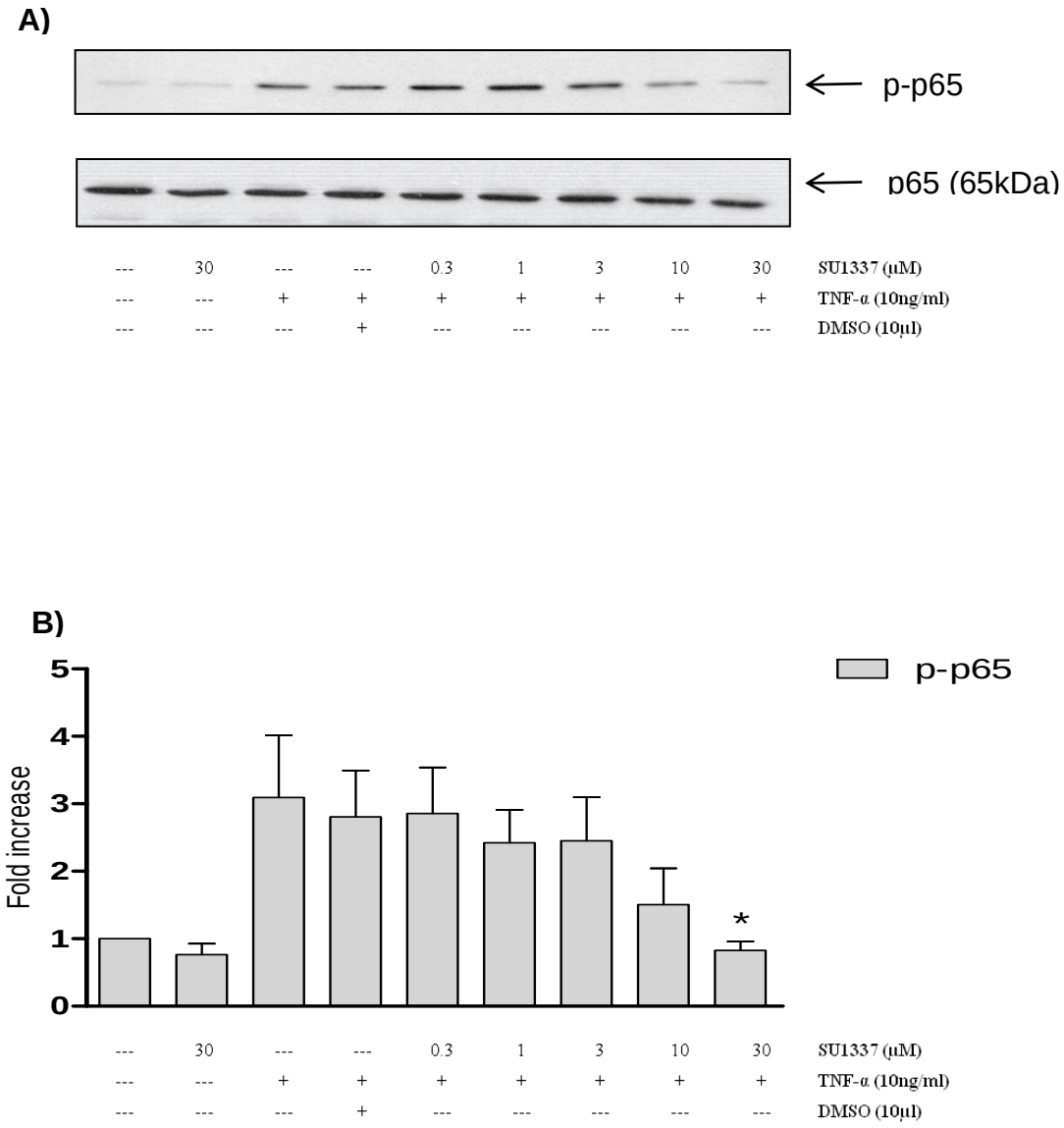


**Figure 3.9: The effect of SU1337 upon TNF-α-mediated p65 phosphorylation in PC3M-luc-C6.** Cells were pre-treated with SU1337 for 1 hr prior to the stimulation with TNF-α (10ng/ml) for 30 min. A) Whole cell lysates were prepared, separated by SDS PAGE and assessed for p-p65 (65kDa) and p65 (65kDa). B) Blots were quantified for % expression by scanning densitometry; each value represents the mean ± S.E.M. The results are representative of three independent experiments. *$P$<0.05 compared with TNF-α stimulated control.

### *3.2.2.3 The $IC_{50}$ values of SU compounds for IκB-α degradation and p65 phosphorylation following TNF-α stimulation*

Next, the data obtained from the Western blot analysis of SU compounds (Figures 3.2 - 3.9) were fitted in a sigmoidal dose-response curve and the $IC_{50}$ values were calculated using GraphPad Prism software, version 6.0 (Figure 3.10 A-D). The $IC_{50}$ values of each SU compound for both IκB-α degradation and p65 phosphorylation were determined in PC3-luc-C6 cells after stimulation with TNF-α (10ng/ml). The $IC_{50}$ for IκB-degradation is the concentration that induces inhibition of the IκB-α degradation by 50%, while the $IC_{50}$ for p65 phosphorylation is the concentration that decreases the phosphorylation of p65 by 50%.

The $IC_{50}$ of SU1261 for IκB-α degradation was >30 μM ($IC_{50}$=35.65μM (±7.22)), while for p65 phosphorylation was >10μM ($IC_{50}$=16.83μM(±5.04)). However, the $IC_{50}$ values of the negative control SU1257 were not detected for IκB-α degradation and p65 phosphorylation as the concentration-inhibition curve showed no alteration in both protein expression levels in the range of doses investigated (0.3-30μM). In contrast, SU1361 and SU1337 documented lower $IC_{50}$ values compared with SU1261. The $IC_{50}$ values of SU1361 were <3μM ($IC_{50}$=2.754μM (±2.75)) for IκB-α degradation and <30μM ($IC_{50}$=20.07μM(±6.33)) for p65 phosphorylation. Also, <10μM ($IC_{50}$=8.055 (±3.04)) and <30μM ($IC_{50}$=11.79μM (±3.13)) were the $IC_{50}$ concentrations of SU1337 for IκB-α degradation and p65 phosphorylation respectively.

These data indicated that concentrations >30μM and >10μM of SU1261 were needed to achieve the $IC_{50}$ concentrations for IκB-α degradation and p65 phosphorylation respectively. SU1257 did not show any detectable $IC_{50}$ values against either IκB-α degradation or p65 phosphorylation. However, SU1361 inhibited the phosphorylation of p65 more strongly ($IC_{50}$=2.754μM) than SU1337 ($IC_{50}$=8.055 μM). In contrast, SU1337 showed about twice the inhibitory effect against IκB-α degradation ($IC_{50}$=11.79μM) compared with SU1361 ($IC_{50}$=20.07μM).

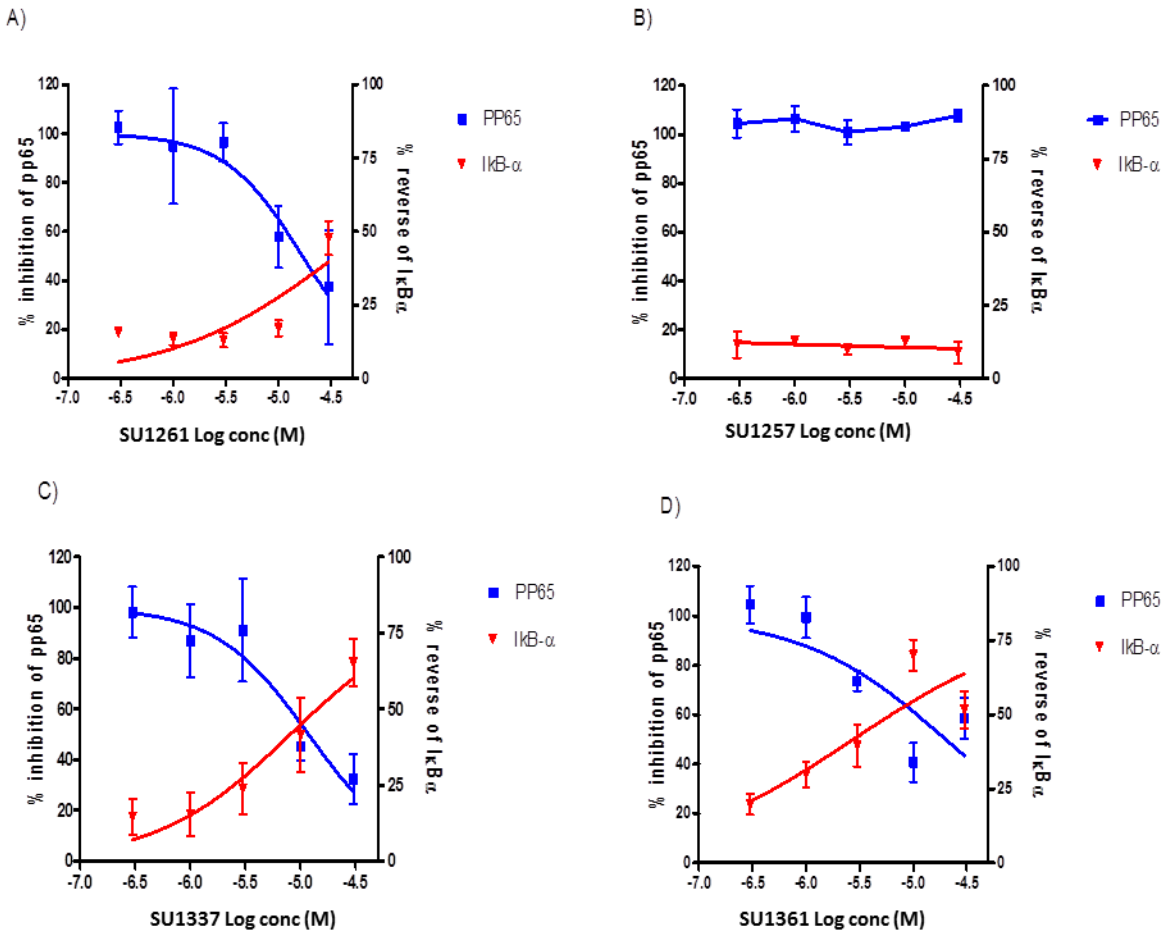


**Figure 3.10: The $IC_{50}$ values of SU compounds for IκB-α degradation and p65 phosphorylation following TNF-α stimulation on PC3M-luc-C6 cells.** The data obtained from Western blot analysis of SU compounds were fitted in a sigmoidal dose-response curve using GraphPad Prism software, version 6.0, for A) SU1261, B) SU1257, C) SU1361 and D) SU1337.

**Table 3.2: The $IC_{50}$ values for IκB-α degradation and p65 phosphorylation were determined in PC3M-luc-C6 cells after stimulation with TNF-α (10ng/ml).** NA: Not achieved.

| SU compounds | $IC_{50}$ (±SEM) for IκB-α degradation (μM) | $IC_{50}$ (±SEM) for p-p65 (μM) |
|---|---|---|
| SU1261 | 35.65 (±7.22) | 16.83 (±5.04) |
| SU1257 | NA | NA |
| SU1361 | 2.75 (±1.65) | 20.07 (±6.33) |
| SU1337 | 8.05 (±3.04) | 11.79 (±3.13) |

### 3.2.3 Characterisation of SU compounds on LTα1β mediated p52 formation of the non-canonical NF-κB pathway in PC3M-luc-C6 cell lines

Once again, the SU compounds (SU1261, SU1361, SU1337 and SU1257) were assessed for their selectivity against the non-canonical NF-κB pathway in PC3M-luc-C6 cell lines. Cells were treated with SU compounds for an hour followed by stimulation of the non-canonical NF-κB pathway using lymphotoxin-α LTα1β (30ng/ml) for 24 hrs. The cytoplasmic extracts were then blotted for processing of p100 to p52 expression as a marker for non-canonical NF-κB pathway engagement. Moreover, the total p65 level was used as indicator for the total protein loading.

#### *3.2.3.1 LTα1β induced p52 expression in PC3M-luc-C6 cell lines in a time-dependent manner*

Figure 3.11 A and B show a time course ranging from 1 to 24hr, for LTα1β (30ng/ml) induced processing of p100 to p52 in PC3M-luc-C6 cell lines using two blots. The stimulation of p52 expression with LTα1β (30ng/ml) was found to be delayed-onset, with no stimulatory effect of LTα1β (30ng/ml) on p52 and p100 proteins expression seen at lag 6hr and below compared with unstimulated cells. However, the expression of p52 was gradually increased following 8hr of LTα1β (30ng/ml) by one and half fold (fold increase=1.52) and reached the maximum level after 24hr of LTα1β (30ng/ml) by almost two-fold (fold increase=1.96) compared with the control group. However, there was no detectable change in p100 expression during the time course between LTα1β (30ng/ml) stimulated and untreated control group.

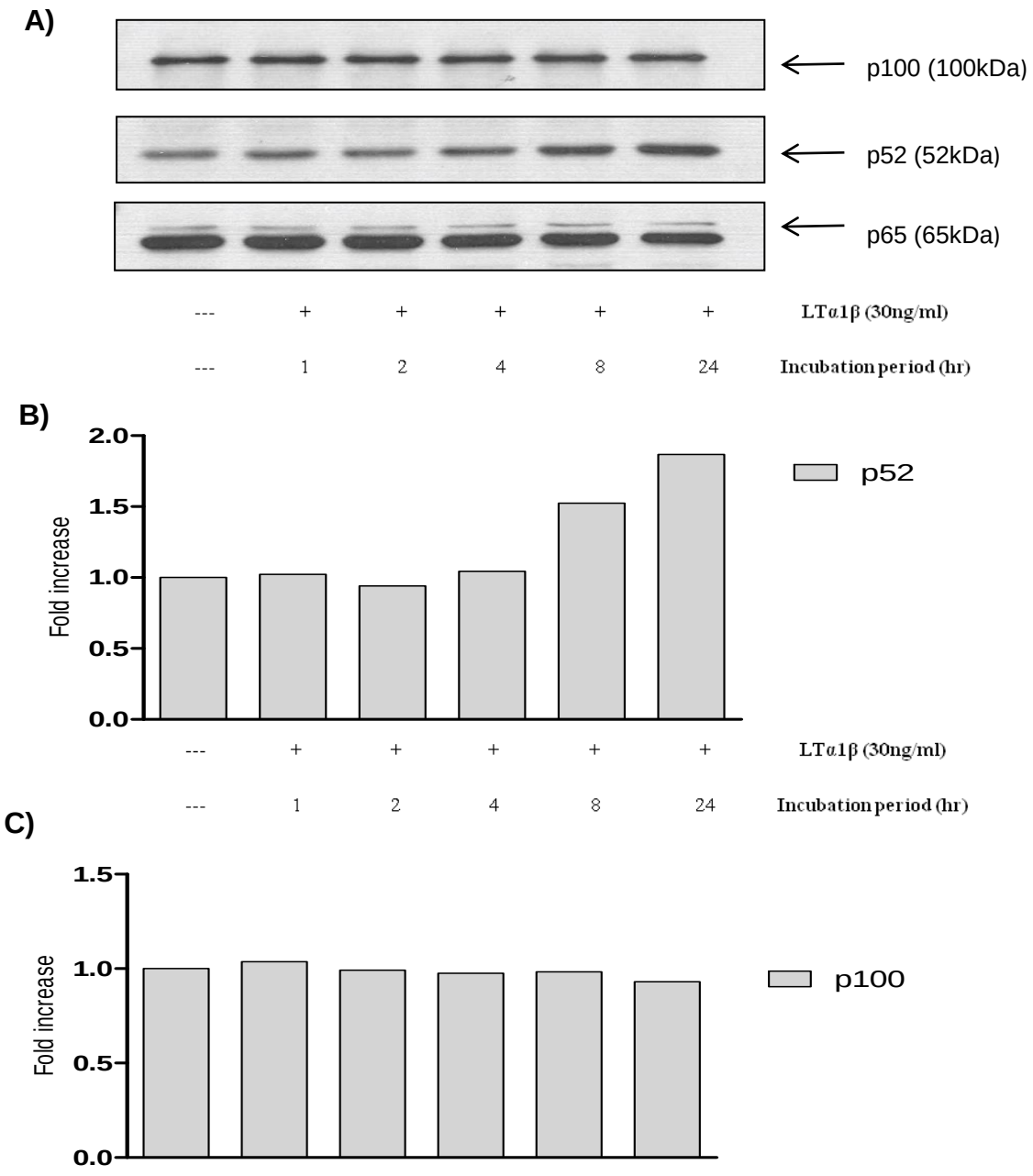


**Figure 3.11: Time course of LTα1β-mediated p100 processing in PC3M-luc-C6.** Cells were stimulated with LTα1β (30ng/ml) for the indicated time points. Whole cell lysates were prepared, separated by SDS-PAGE, and then assessed for A) p100 (100kDa), p52 (52kDa) formation and total p65 (65kDa). Blots were quantified by scanning densitometry for fold stimulation of B) p52 and C) p100. The results are representative of one independent experiment.

### *3.2.3.2 Effect of SU compounds on LTα1β induced p52 expression of the non-canonical NF-κB pathway in PC3M-luc-C6 cell lines*

In order to assess the inhibitory effects of SU compounds (SU1261, SU1361, SU1337 and the negative control, SU1257) on the non-canonical NF-κB pathway, the PC3M-luc-C6 cell lines were treated with the same dose range (0.3 to 30μM) of SU compounds, followed by LTα1β (30ng/ml) stimulation for 24hr. Expressions of p100 and p52 were then assessed by western blotting as markers for the non-canonical NF-κB pathway.

- **Effect of SU1257 on non-canonical NF-κB pathway**

Figure 3.12 (A and B) demonstrates the impact of administration of various range of SU1257 (0.3-30μM) on LTα1β induced p52 formation in PC3M-luc-C6. When the cells were treated with LTα1β (30ng/ml) alone for 24hrs, the formation of the p52 doubled (fold increase=1.91 ± 0.41, $P<0.01$) compared with the untreated control group. However, treatment of cells with different doses of SU1257 (0.3-30μM) followed by stimulation with LTα1β (30ng/ml) did not statistically significantly alter the expression of the p52 compared with LTα1β (30ng/ml) treated alone ($P>0.05$). Furthermore, stimulation of cells with LTα1β (30ng/ml) for 24hrs resulted in no change in p100 expression level compared with untreated control cells (Figure 3.12 A and C, $P>0.05$). In addition, exposure of cells to SU1257 (0.3-30μM) followed by LTα1β (30ng/ml) for 24hrs did not affect the level of p100 expression ($P>0.05$).

These results showed that the negative control SU1257 (0.3-30μM) had no impact on the cells p52 formation or p100 expression when stimulated with LTα1β (30ng/ml) compared to cells stimulated with LTα1β alone. Hence, SU1257 is an ideal negative control against other SU compounds for further study on the non-canonical pathway.

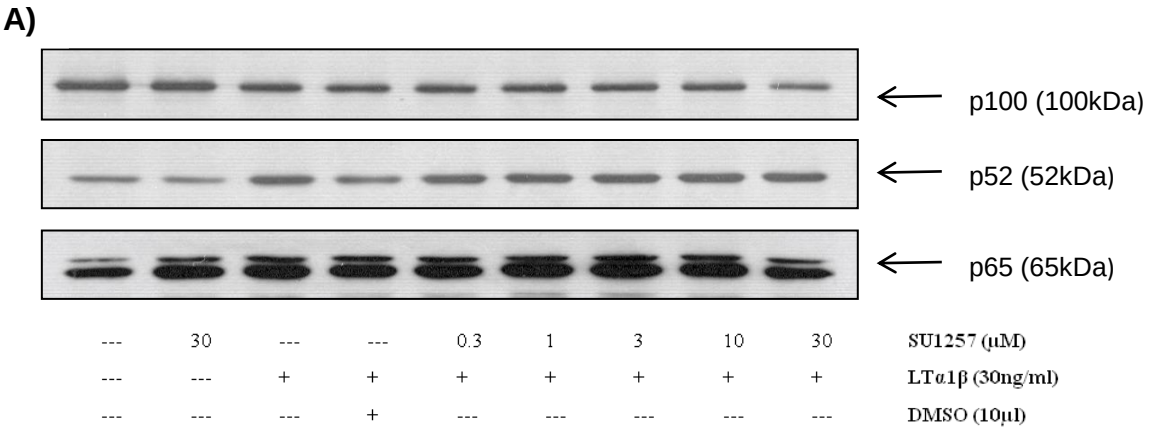


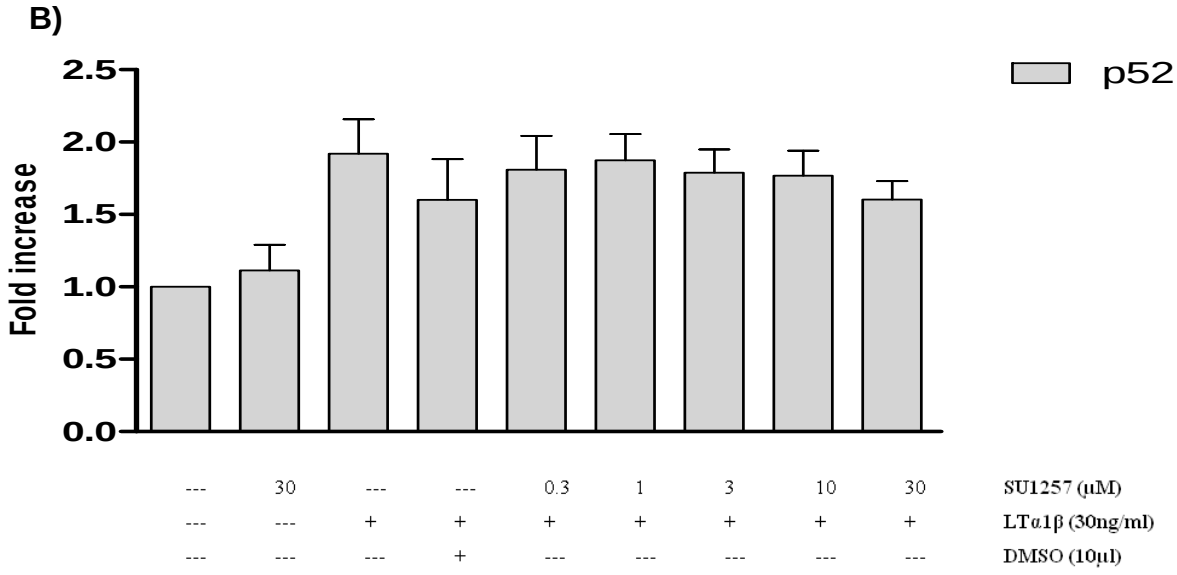

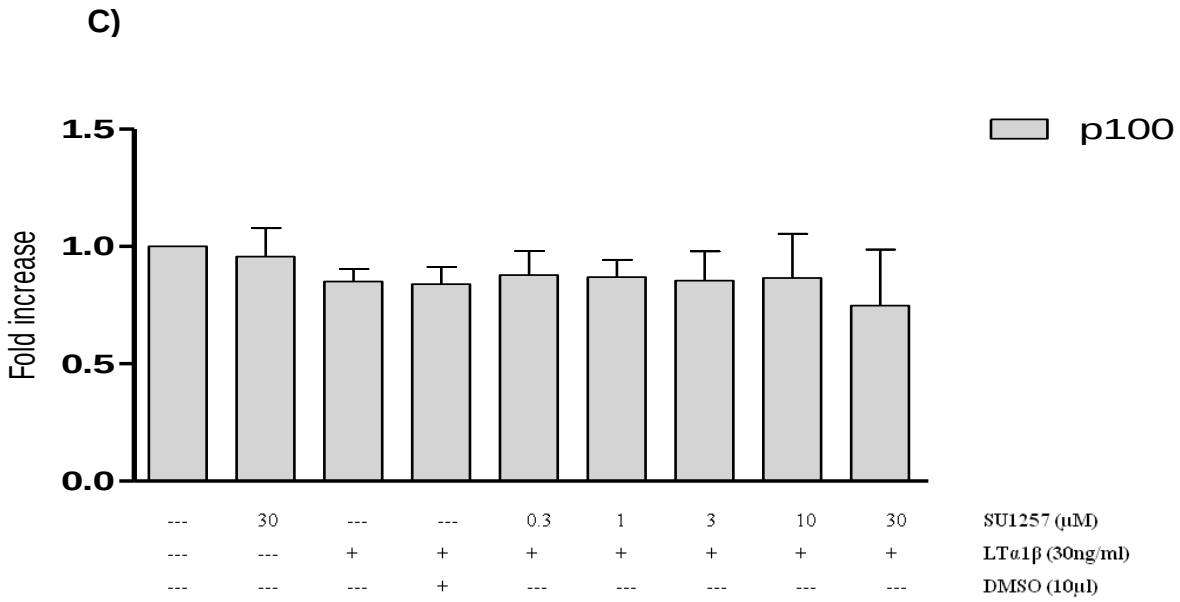


**Figure 3.12: The effect of SU1257 upon LTα1β-mediated p100 processing in PC3M-luc-C6.** Cells were pre-treated with SU1257 for 1h prior to stimulation with LTα1β (30ng/ml) for 24hrs. A) Whole cell lysates were prepared, separated by SDS PAGE and assessed for p100 (100kDa), p52 (52kDa) and p65 (65kDa). Blots were quantified by scanning densitometry for fold stimulation of B) p52 and C) p100; each value represents the mean ± S.E.M. The results are representative of three independent experiments.

- **Effect of SU1261 on non-canonical NF-κB pathway**

Figure 3.13 shows the effect of SU1261 on LTα1β induced p52 formation and p100 expression in PC3M-luc-C6s cells. As shown in Figures 3.12 A and B, stimulation with LTα1β (30ng/ml) alone resulted in 1.53 fold increase (±0.12, $P<0.05$) in p52 formation compared with untreated control group. In the absence of stimulation, SU1261 decreased the formation of p52 by about 30% (fold increase=0.71 ± 0.04) compared with untreated control cells but this was not statistically significant relative to control cells ($P>0.05$). However, in the presence of LTα1β (30ng/ml), increasing concentrations of SU1261 caused a statistically significant gradual decrease in p52 formation with significance achieved at 3, 10 and 30μM (SU1261 3μM: Fold increase = 0.71 ± 0.07, $P<0.05$, SU1261 10μM: Fold increase = 0.54 ± 0.05, $P<0.01$ and SU1261 30μM: Fold increase = 0.42 ± 0.13, $P<0.001$) compared with LTα1β treated alone cells. As presented in Figures 3.12 A and C, the p100 levels were not changed significantly compared with control cells in dose range from 0.3 to 10μM of SU1261 ($P>0.05$); however a statistically insignificant decrease in p100 measurement was recorded with the maximum concentration (30μM) of SU1261 followed by LTα1β (30ng/ml) stimulation (fold increase = 0.65± 0.08, $P>0.05$) compared with untreated control cells.

These data suggested that SU1261 largely inhibited the non-canonical pathway of PC3M-luc-C6 cells in dose-dependent manner. At as little as 3μM of SU1261, p52 formation was completely inhibited to less than the control basal level.

**A)**

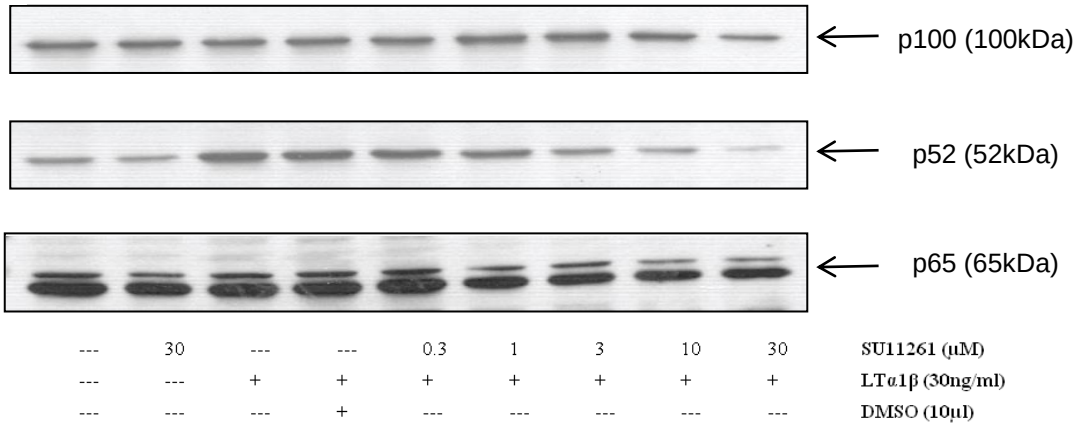
p100 (100kDa)
p52 (52kDa)
p65 (65kDa)
--- 30 --- --- 0.3 1 3 10 30 SU11261 (μM)
--- --- + + + + + + + LTα1β (30ng/ml)
--- --- --- + --- --- --- --- --- DMSO (10μl)

**B)**

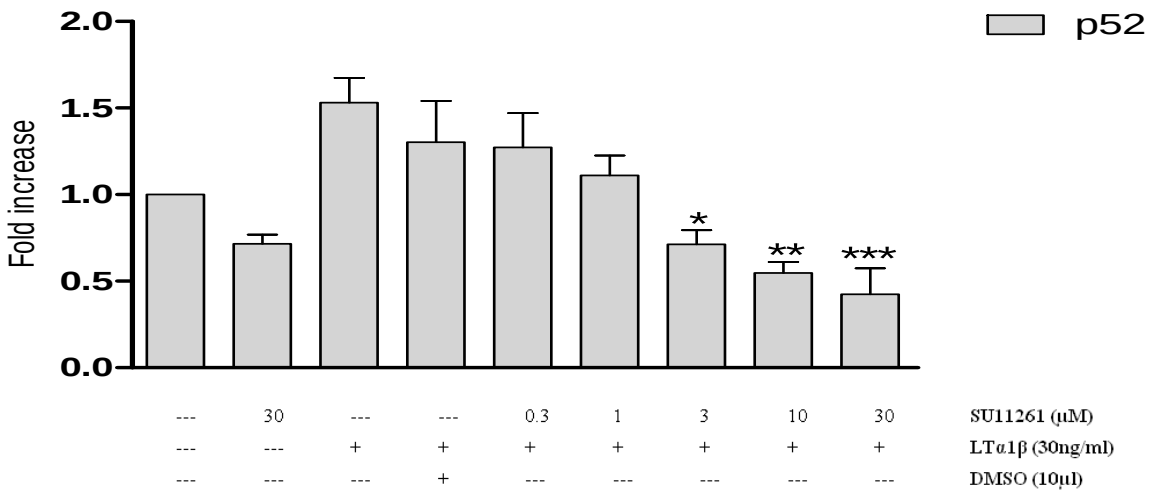
p52
Fold increase
2.0
1.5
1.0
0.5
0.0
*
**
***
--- 30 --- --- 0.3 1 3 10 30 SU11261 (μM)
--- --- + + + + + + + LTα1β (30ng/ml)
--- --- --- + --- --- --- --- --- DMSO (10μl)

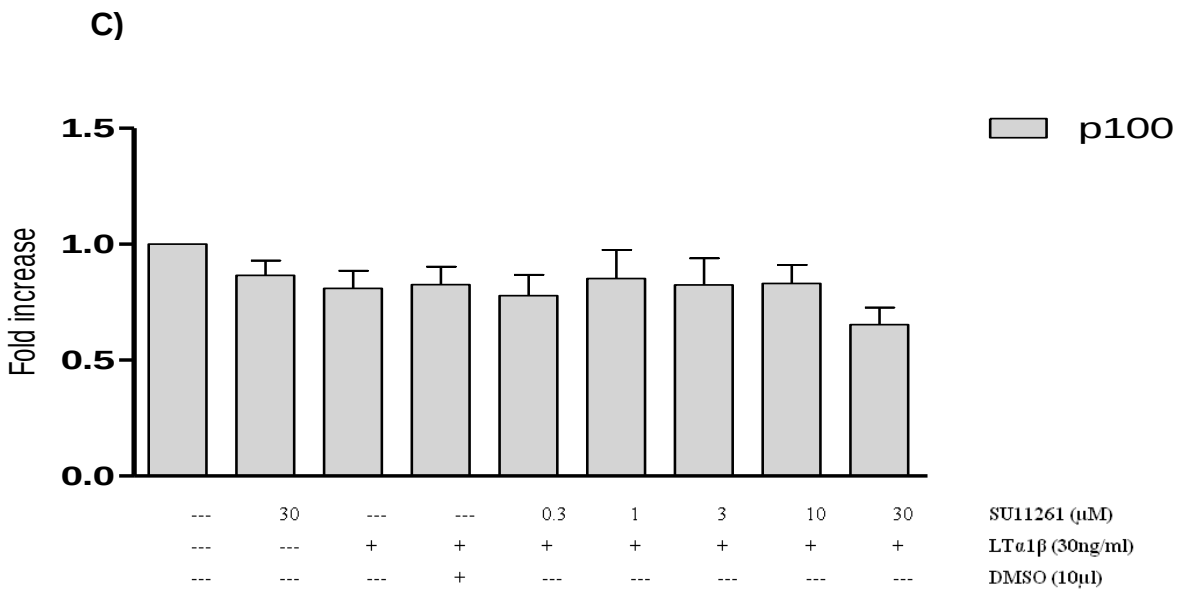


**Figure 3.13: The effect of SU1261 upon LTα1β-mediated p100 processing in PC3M-luc-C6.** Cells were pre-treated with SU1261 for 1h prior to the stimulation with LTα1β (30ng/ml) for 24hrs. A) Whole cell lysates were prepared, separated by SDS PAGE and assessed for p100 (100kDa), p52 (52kDa) and p65 (65kDa). Blots were quantified by scanning densitometry for fold stimulation of B) p52 and C) p100; each value represents the mean ± S.E.M. The results are representative of three independent experiments. **P*<0.05, ***P*<0.01 and ****P*<0.001 compared with LTα1β stimulated control.

- **Effect of SU1361 on non-canonical NF-κB pathway**

The effect of SU1361 on p52 formation and p100 expression is illustrated in Figure 3.14. LTα1β (30ng/ml) stimulated the formation of p52 significantly by almost two-fold (fold increase = 1.92 ± 0.25, $P<0.001$) compared with untreated control cells. Pre-treatment cells with 30μM of SU1361 alone reduced the p52 expression level insignificantly by 30% (Fold increase= 0.70 ± 0.58, $P>0.05$) compared with the control group. However, with increasing concentrations of SU1361 to 10μM in presence of LTα1β, p52 formation was not altered significantly compared with the LTα1β (30ng/ml) stimulated group. Furthermore, a maximum concentration of SU1361 (30μM) followed by LTα1β (30ng/ml) stimulation inhibited the p52 formation significantly (fold increase= 0.99 ± 0.11, $P<0.05$) compared with the LTα1β (30ng/ml) stimulated group. However, the expression of the p100 was not changed significantly when cells were treated with SU3161 (0.3-30μM) followed by LTα1β compared with LTα1β stimulated cells ($P>0.05$).

These data revealed that the maximum concentration of SU1361 (30μM) largely retarded the non-canonical NF-κB pathway stimulation; however, the dose range from 0.3 to 10μM did not show any major inhibitory effect.

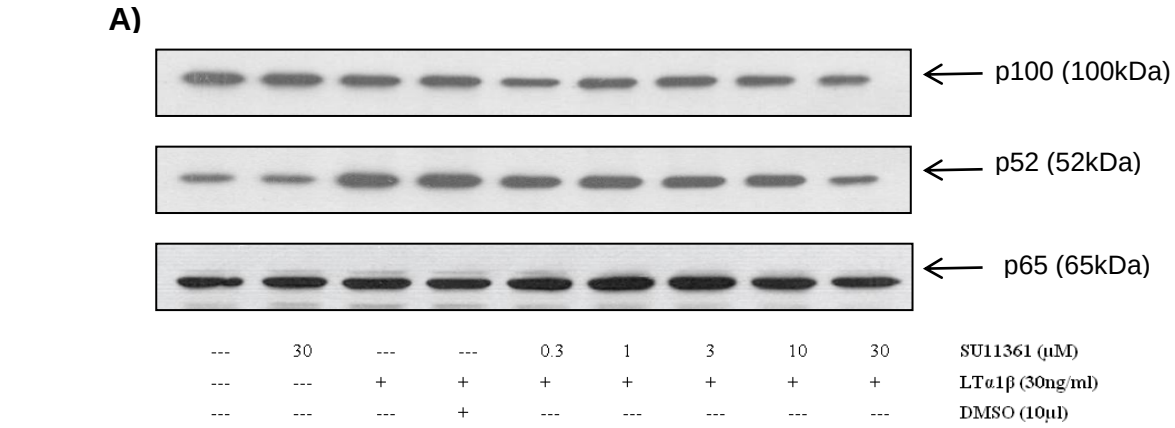
A)
p100 (100kDa)
p52 (52kDa)
p65 (65kDa)
--- 30 --- --- 0.3 1 3 10 30 SU11361 (μM)
--- --- + + + + + + + LTα1β (30ng/ml)
--- --- --- + --- --- --- --- --- DMSO (10μl)

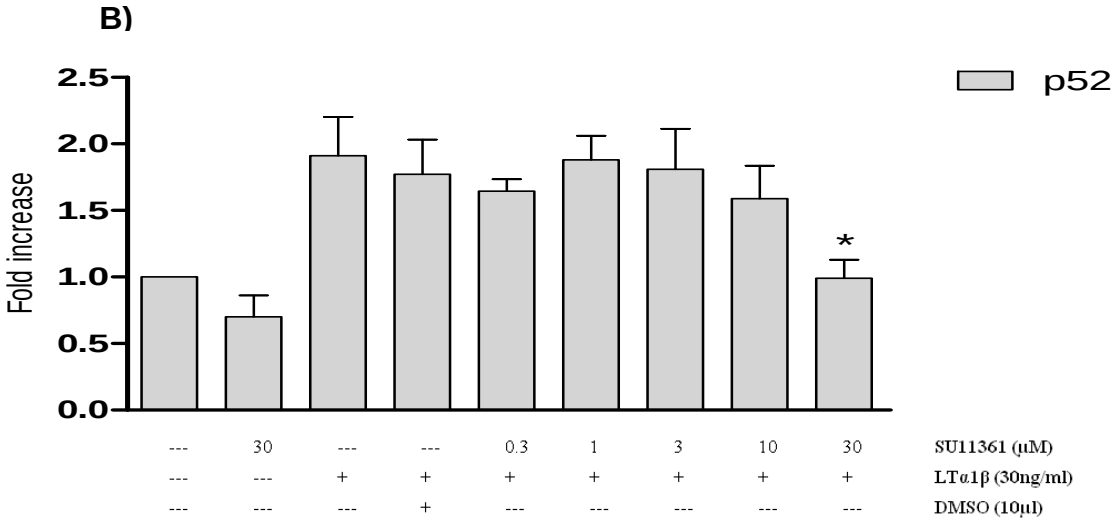
B)
p52
Fold increase
2.5
2.0
1.5
1.0
0.5
0.0
*
--- 30 --- --- 0.3 1 3 10 30 SU11361 (μM)
--- --- + + + + + + + LTα1β (30ng/ml)
--- --- --- + --- --- --- --- --- DMSO (10μl)

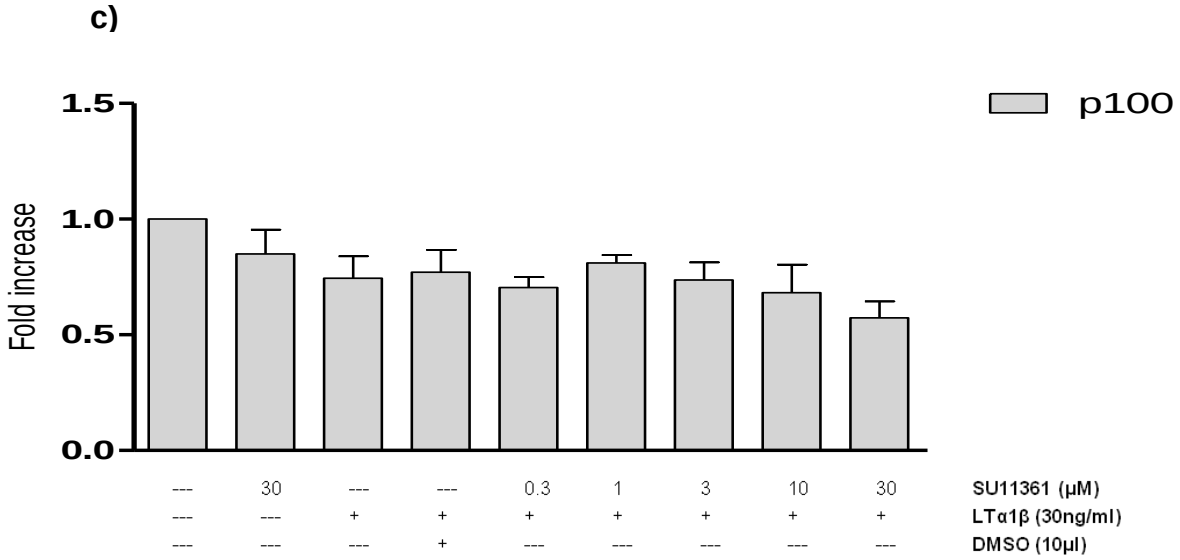


**Figure 3.14: The effect of SU1361 upon LTα1β-mediated p100 processing in PC3M-luc-C6.** Cells were pre-treated with SU1361 for 1hr prior to the stimulation with LTα1β (30ng/ml) for 24hrs. A) Whole cell lysates were prepared, separated by SDS PAGE and assessed for p100 (100kDa), p52 (52kDa) and p65 (65kDa). Blots were quantified by scanning densitometry for fold stimulation of B) p52 and C) p100; each value represents the mean ± S.E.M. The results are representative of three independent experiments. **P*<0.05 compared with LTα1β stimulated control.

- **Effect of SU1337 on non-canonical NF-κB pathway following LTα1β induced p52 expression**

Figure 3.15 demonstrates the effect of SU1337 on LTα1β (30ng/ml) induced non-canonical NF-κB pathway stimulation in PC3M-luc-C6. Stimulation of cells with LTα1β (30ng/ml) induced p52 formation significantly by more than two fold (Fold increase = 2.19 ± 0.67, $P<0.01$) but without significant change on p100 processing ($P>0.05$) compared to control unstimulated cells. Furthermore, exposure cells to SU1337 (0.3-3μM) did not show any detectable or statistically significant change on LTα1β (30ng/ml) induced p52 formation compared to LTα1β (30ng/ml) stimulated cells ($P>0.05$). However, treatment of cells with 10μM of SU1337 followed by stimulation with LTα1β (30ng/ml) decreased both the p52 formation expression (fold increase = 1.44 ± 0.78) and p100 expression (fold increase= 0.49 ± 0.17) compared to cells treated with LTα1β (30ng/ml) alone, but this change was again insignificant statistically ($P>0.05$). Compared to cells stimulated with LTα1β (30ng/ml), a significant inhibition response was achieved in p52 (fold increase= 0.31 ± 0.20, $P<0.05$) and p100 expression (fold increase= 0.16 ± 0.12, $P<0.001$) when cells were treated with the maximum concentration of SU1337 (30μM) followed by LTα1β (30ng/ml) stimulation.

These findings showed that SU1337 at 10μM decreased the p52 and p100 formation but this decrease was not statistically significant relative to LTα1β stimulated cells; however in presence of LTα1β stimulation, a 30μM significantly inhibited the expression of both proteins compared with the LTα1β treated

group. The lower doses of SU1337 (0.3-3μM) did not exert any significant effect on this pathway.

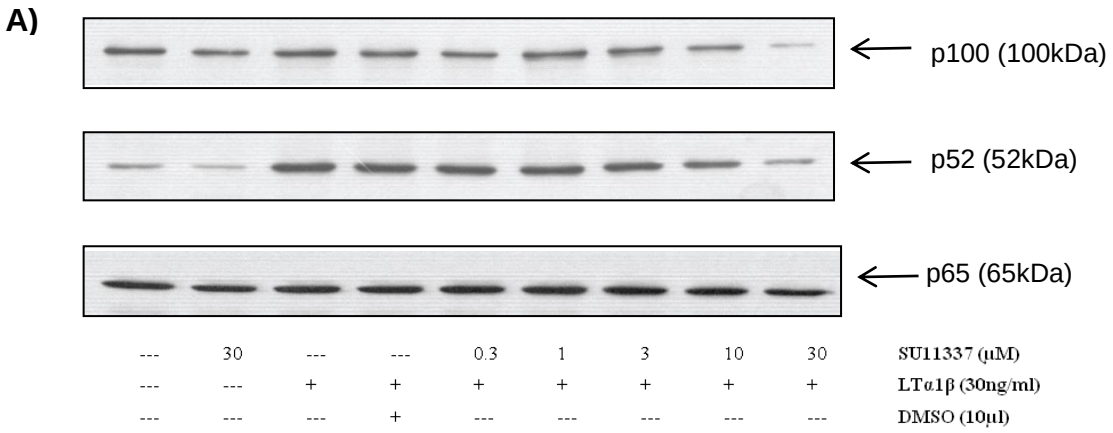


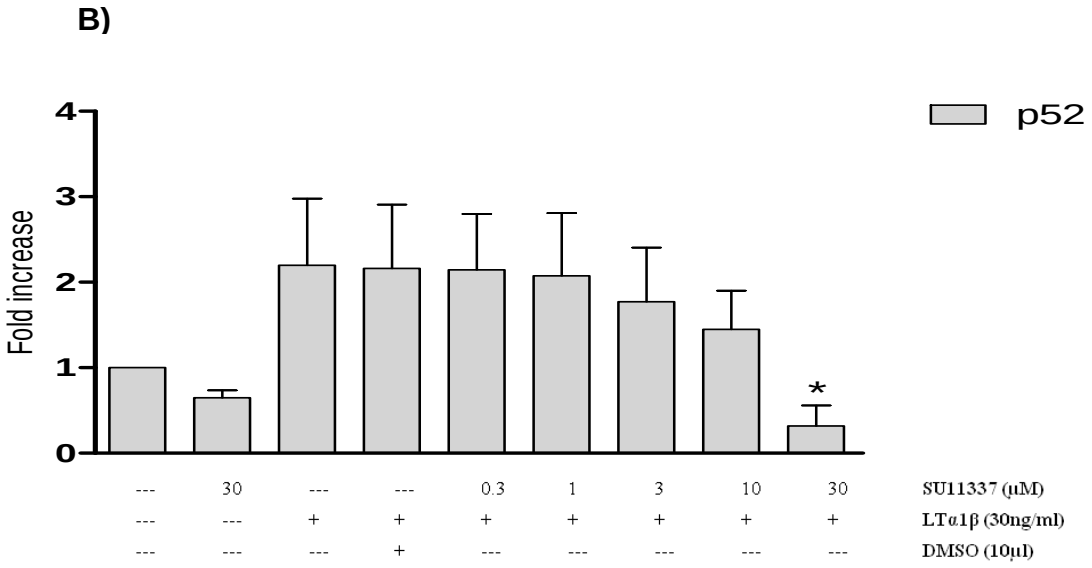

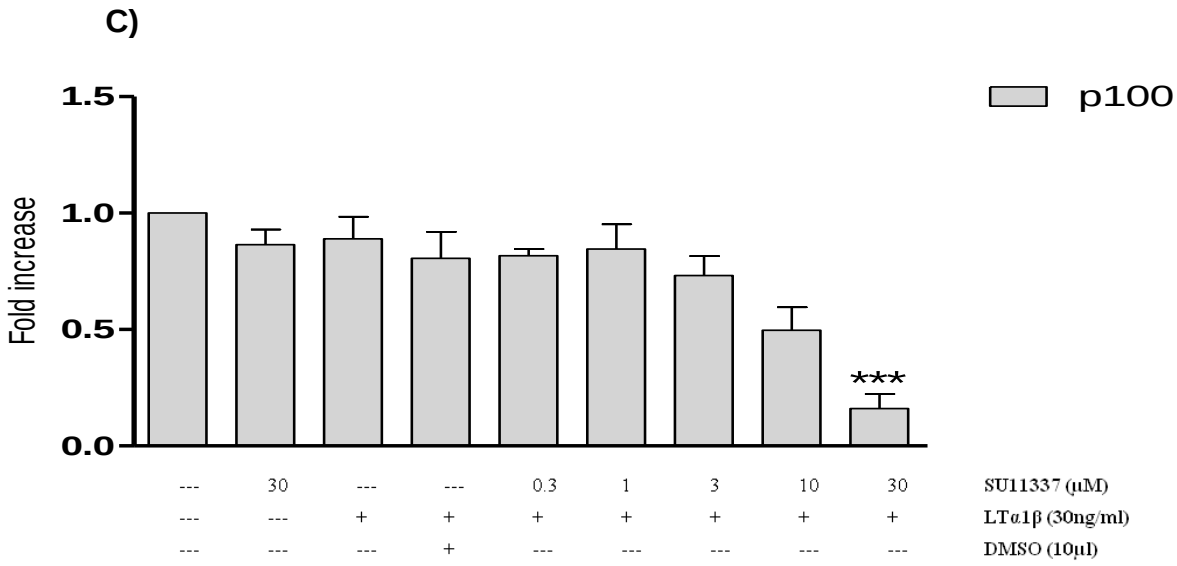


**Figure 3.15: The effect of SU1337 upon LTα1β-mediated p100 processing in PC3M-luc-C6.** Cells were pre-treated with SU1337 for 1hr prior to the stimulation with LTα1β (30ng/ml) for 24hrs. A) Whole cell lysates were prepared, separated by SDS PAGE and assessed for p100 (100kDa), p52 (52kDa) and p65 (65kDa). Blots were quantified by scanning densitometry for fold stimulation of B) p52 and C) p100; each value represents the mean ± S.E.M. The results are representative of three independent experiments. *$P$<0.05 and ***$P$<0.001 compared with LTα1β stimulated control.

### *3.2.3.3 The $IC_{50}$ values of SU compounds for p52 formation following LTα1β stimulation*

In order to calculate the $IC_{50}$ values of SU compounds on p52 formation, the protein levels determined on after treatment with the SU compounds (Figures 3.12-3.15) were fitted in a sigmoid concentration-response curve and the $IC_{50}$ values were calculated using GraphPad Prism software, version 6.0 (Figure 3.16 A-D). The $IC_{50}$ values of each agent for p52 formation were determined in PC3-luc-C6 cells after stimulation with LTα1β (30ng/ml). The $IC_{50}$ for p52 formation was the concentration that inhibited the p52 formation by 50%.

The $IC_{50}$ of SU1261 for p52 formation was only 3.92µM (±2.12) (Figure 3.16 A). However, the $IC_{50}$ values of the negative control SU1257 were not achieved for p52 formation inhibition as the concentration-inhibition curve showed a steep pattern and inhibition of 50% of growth was not obtained (Figure 3.16 B). In contrast, SU1361 and SU1337 recorded relatively high $IC_{50}$ values compared to SU1261. The $IC_{50}$ value of SU1361 was >30µM ($IC_{50}$=33.82µM (±4.12)), Figure 3.16 C) for p52 formation, while it was 24.01µM (±8.23) for SU1337 (Figure 3.16D).

These data showed that as little as 3.925µM of SU1261 was enough to inhibit the non-canonical NF-κB pathway and induce inhibition of the p52 formation by 50%. However, SU13317 inhibited the p52 formation by 50% in a lower concentration ($IC_{50}$=24.01µM) than SU1361 ($IC_{50}$=33.82µM), although both concentrations were relatively high. The order of potency of these compounds for p52 formation was SU1261>SU1337>SU1361>SU1257.

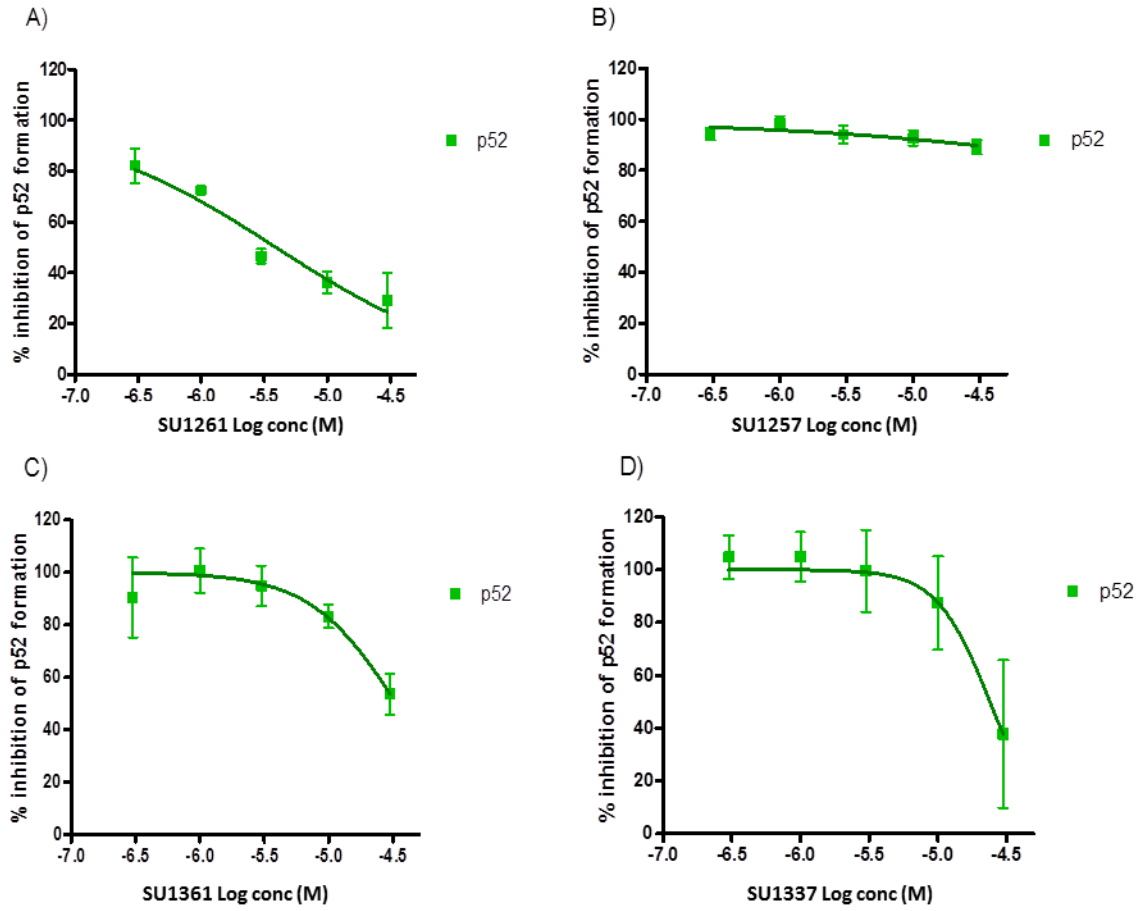


**Figure 3.16: The $IC_{50}$ values of SU compounds for p52 formation and following LTα1β stimulation on PC3M-luc-C6 cells.** Using GraphPad Prism software, version 6.0, the data obtained from Western blot analysis of SU compounds were fitted in a sigmoidal dose-response curve for A) SU1261, B) SU1257, C) SU1361 and D) SU1337.

**Table 3.2: The $IC_{50}$ values for p52 formation which were determined in PC3M-luc-C6 cells after stimulation with LTα1β (30ng/ml).** NA: Not achieved

| SU compounds | $IC_{50}$ (±SEM) for p52 formation (μM) |
|---|---|
| SU1261 | 3.92 (±2.12) |
| SU1257 | NA |
| SU1361 | 33.82 (±4.12) |
| SU1337 | 24.01 (±8.23) |

## 3.3 Discussion

As mentioned in the introduction (Chapter 1), the NF-κB signalling pathway is strongly associated with disorders and diseases that involve inflammation, such as autoimmune diseases, neurodegenerative diseases and cancer (Meffert *et al*., 2003; Giuliani *et al*., 2001; Karin, 2006). Inhibition of NF-κB has therefore become a new strategy for the treatment of various diseases, including cancer. One of the most studied and best-known strategies to target NF-κB is the use of proteasome inhibitors. For instance, bortezomib has been used in chemotherapeutic regimens for the treatment of multiple leukaemia and myeloma (Picot *et al.,* 2011; Zheng *et al.,* 2012; Richardson *et al.,* 2004). In addition, there is evidence to show that bortezomib inhibits proliferation by inducing apoptosis of the androgen-dependant (LNCaP) and androgen-independent (PC-3 and DU145) PCa cell lines (Zheng *et al.,* 2015; Papandreou and Logothetis, 2004). MG-13 is another example of a proteasome inhibitor which has been used in PCa combination therapy. It inhibits NF-κB activity through reducing IκB-α degradation (Shirley *et al.,* 2005). Further, a natural proteasome inhibitor, apigenin (5,7,4-trihydroxyflavone), has been found to inhibit the viability and induce apoptosis in the PC-3 PCa cell line (Singh *et al.,* 2015). Moreover, the proteosome inhibitor PS-341 induces growth arrest and apoptosis of LNCaP cells by down-regulating the androgen receptor (AD) signalling pathway (Ikezoe *et al.,* 2004). Dehydroxymethylepoxyquinomicin (DHMEQ) is a unique NF-κB inhibitor which acts by preventing the nuclear

translocation of NF-κB p65 (Ariga *et al.,* 2002), leading to the induction of apoptotic cell death in Adult T-cell leukaemia/lymphoma (ATL) (Horie *et al.,* 2006). Finally, PMS1077 has been found to inhibit NF-κB activity by counteracting TNF-α induced lκB-α degradation as well as p65 phosphorylation leading to induction of apoptosis in PCa cell lines (Shi *et al.,* 2013).

These positive studies suggest a role for NF-κB inhibition in PCa and the aim of this project was to further dissect the components of the NF-κB pathway by targeting the IKKβ complex as a new and a more specific target than non-specific NF-κB inhibitors. Various studies have shown that pharmacological inhibition of IKK inhibitors induces cancer cell cytotoxicity or triggers apoptosis in response to different stimuli such as TNF-α (Romieu-Mourez *et al.,* 2001). Different IKK inhibitor compounds have been discovered. These inhibitors have been found to be either IKK inhibitors (IKKα/β) or more IKKβ inhibitors. However, to date there has been no specific pharmacological inhibitors of IKKα. Examples of agents targeting IKKα/β are a β-carboline natural product PS-1145 and ML120B (Castro *et al.,* 2003; Wen *et al.,* 2006), BMS-345541 (Burke *et al.,* 2003; McIntyre *et al.,* 2003), SPC-839 (Palanki *et al.,* 2002), plant flavone, apigenin (4′, 5, 7-trihydroxyflavone) (Shukla *et al.,* 2015) and CHS828 (Olsen *et al.,* 2004; Hjarnaa *et al.,* 1999). It was found that PS-1145 and ML120B demonstrated potent anti-tumour effect against different cancers including multiple myeloma, chronic myelogenous leukemia, diffuse large B-cell lymphoma and PCa (Cilloni *et al.,* 2006; Yemelyanov *et al.,* 2006; Lam *et al.,*

2005). PS-1145 was also found to sensitise PCa DU145 and PC3 cells to death by apoptosis following TNF-α stimulation (Yemelyanov *et al.,* 2006). Moreover, plant flavone apigenin (4′, 5, 7-trihydroxyflavone) has been found to inhibit carcinogenesis and metastasis in transgenic adenocarcinoma of the mouse prostate (TRAMP) mice (Shukla *et al.,* 2007) and inhibits proliferation and invasiveness in PC-3 and 22Rv1 human PCa cells (Shukla *et al.,* 2015). To date, however, none of the previous IKKβ inhibitors have been used clinically due to serious associated complications such as chronic inflammatory disorders, immunosuppression, infectious disease and fatal hepatotoxicity (Chariot, 2009, Li *et al*., 1999).

An alternative strategy is inhibition of IKKα. IKKα have been involved in various types of cancer, including PCa (Fernandez-Majada *et al.,* 2007; Park *et al.,* 2005; Shiah *et al.,* 2006; Hirata *et al.,* 2006; Luo *et al.,* 2007). In PCa, the silencing of IKKα with siRNA in PCa cell lines PC3 and DU-145 was found to inhibit their invasion and metastasis (Mahato *et al.,* 2011), as well as delay the progression of castration-resistant PCa in the murine myc-CaP cell line (Ammirante *et al.,* 2010). In addition, IKKα inhibition via siRNA has been demonstrated to inhibit maspin, the tumour suppressor gene that induces PCa metastasis (Luo *et al.,* 2007). Furthermore, expression of the inactive mutant form of IKKα ($IKK\alpha^{AA/AA}$) in transgenic adenocarcinoma of mouse prostate (TRAMP) model of PCa inhibited metastases, delayed the cancer's progression and improved survival compared with wild type TRAMP mice (Luo *et al.,* 2007).

Therefore, targeting PCa using a selective inhibitor of IKKα might be a promising approach for the development of a novel treatment of PCa. However, as mentioned, compared with the previous large number of non-selective IKK inhibitors, no compounds currently available have a selective inhibitory effect on IKKα. Asamitsu *et al*. (2008) synthesised the noraristeromycin (NAM) as an anti-HIV virus agent. NAM was tested for IKK selectivity by an *in vitro* kinase assay using immunoprecipitated IKK complex from HEK293 cells. Asamitsu *et al*. (2008) published the finding that NAM inhibited the kinase activity of IKKα more than that of IKKβ. However, when HEK293 cells were treated with NAM, they found this agent to inhibit p65 phosphorylation and IκBα degradation, suggesting that this effect takes place through the canonical NF-κB pathway inhibition. In addition, no effect of NAM on p100 phosphorylation or p52 formation was demonstrated. Similarly, it has been claimed that a glucosamine derivative, 2-(N-Acetyl)-L-phenylalanylamido-2-deoxy-beta-D-glucose (NAPA), inhibits the IKKα kinase activity, as confirmed by an *in vitro* kinase assay. NAPA has been shown to decrease IKKα nuclear re-localisation in human chondrocytes, but in very high doses (250-500μM) (Scotto d'Abusco *et al.,* 2010). However, currently there are no selective IKKα inhibitors commercially or clinically available.

Within the Univesity of Strathclyde we have developed a multidisciplinary team (small molecule drug discovery group led by Professor Simon MacKay) to generate first in class of IKKα inhibitor compounds. In this project, I worked with three different selective IKKα inhibitor compounds, SU1261, SU1361 and

SU1337, in addition to the negative control SU1257, which lacks a kinase inhibitory effect. These agents have been successfully assessed by an *in vitro* kinase assay to have higher affinity and selectivity for purified IKKα protein than for IKKβ. As is shown in Table 3.1, the dissociation constant values (Ki value) of SU1261, SU1361 and SU1337 indicate that the selectivity of these agents was higher on IKKα than on IKKβ. SU compounds contain an azole ring which specifically binds to the ATP binding domain of the IKKα amino-terminal kinase, inhibiting kinase activity. The main objective of this chapter was to test the inhibitory effects and the selectivity of SU compounds on a cellular level. These agents were tested in a highly metastatic PCa cell line, PC3M-luc-C6. We hypothesised that these compounds, as selective IKKα inhibitors, would affect the non-canonical NF-κB pathway rather than the NF-κB canonical pathway, meaning that they reduce p52 formation rather than inhibiting IκB-α loss and p65 phosphorylation.

Selective IKKα inhibitors of SU compounds should not affect the canonical NF-κB pathway as IKKα is not the main player in this cascade. Stimulation of the canonical NF-κB pathway with TNF-α activated the IKK complex by phosphorylation, leading to the activation of the IκB-α degradation and the translocation of p65 into the nucleus (Oeckinghaus and Ghosh, 2009). The negative control SU1257 (0.3-30μM) did not influence in TNF-α induced IκB-α degradation or phosphorylation of p65 in PC3M-luc-C6. These results are ideal for a negative control as there was no effect when there should be no effect, or,

in other words, any other effects which could have been exerted from different parts of the structure were excluded. These findings were expected, as SU1257 lacks the kinase inhibitory effect. However, SU1261 (>10μM) was found to impact the canonical NF-κB pathway by inhibiting p65 phosphorylation ($IC_{50}$= 16.83μM), while treatment with more than 30μM was needed to decrease the degradation of IκB-α ($IC_{50}$= >30μM). On the other hand, SU1361 and SU1337 affected the canonical NF-κB pathway in lower doses than SU1261. The $IC_{50}$ values of SU1361 against p65 phosphorylation and IκB-α degradation were 20.07μM and 2.75μM respectively, whereas these values were 11.79μM and 8.05μM for SU1337 in the same respect. Therefore, of the SU compounds, SU1261 (0.3-10μM) had no effect on IKKβ as no changes were found in IκB-α loss and p65 phosphorylation.

The non-canonical NF-κB pathway is controlled mainly by IKKα homodimers. Stimulation of this pathway by lymphotoxin β (LTβ) resulted in the processing of p100 and the generation of active p52-RelB heterodimers through the phosphorylation of IKKα subunits (Oeckinghaus and Ghosh, 2009). As expected, the negative control SU1257 did not alter the response of LTα1β induced p52 formation. Interestingly, the $IC_{50}$ value of SU1261 was as little as 3.92μM for p52 inhibition. Unexpectedly, the $IC_{50}$ values of SU1361 and SU1337 for p52 formation inhibition were >30μM and 24μM respectively, therefore SU1261 was the most selective IKKα inhibitor agent of the tested compounds as the inhibition in p52 formation started with a low dose (3μM). However, the

negative control SU1257 did not cause any change in p52 formation levels following stimulation with LTα1β, making this compound an ideal negative control for this group.

In conclusion, SU1261 showed a novel IKKα inhibitory effect on the tested SU compounds. SU1261 is inhibited by p52 formation, the marker of the non-canonical NF-κB pathway, in low doses ($IC_{50}$=3.92μM) in the presence of LTα1β stimulation. Moreover, SU1261 did not inhibit the canonical NF-κB pathway in doses from 0.3-10μM after TNF-α induced p65 phosphorylation and IκB-α degradation. In addition, SU1257 demonstrated itself to be an ideal negative control compound as it did not affect the stimulated NF-κB pathways. Furthermore, SU compounds were able to bind the intracellular kinase domains of IKKα and IKKβ, which indicated the stability of these agents in the cellular setting. Thus, it was of interest and of value to assess the cytotoxicity of SU1261 as a novel IKKα inhibitor in highly metastasis androgen-insensitive PCa cell lines against its negative control, SU1257.

# Chapter 4

# Assessing the Cytotoxicity of Novel IKKα Inhibitor (SU1261) as Single Agents and in Combination with External Beam Radiation (XBR) in Prostate Cancer Cell Lines

## 4.1 Introduction

Prostate cancer (PCa) is the second most commonly diagnosed cancer in males worldwide, representing the second leading cause of mortality-related cancer (Torre *et al*., 2015). In the early stages of the cancer, curative therapies are available, including radical prostatectomy (surgery) and radiation and in some cases, hormonal ablation for androgen-dependent PCa. However, within 12-18 months from androgen ablation therapy, PCa can develop to the highly metastatic castration-resistance (CRPC) carcinoma stage, which is associated with serious complications and a high mortality rate (Maroto *et al*., 2016). Currently no curative therapies are available for CRPC and the only available options are palliative.

The non-canonical (alternative) NF-κB pathway is controlled solely by the IKKα homodimer. IKKα has been found to regulate numerous genes involved in cancer cell transformation, tumour progression and angiogenesis (Huang *et al*., 2007, Luo *et al*., 2007). The simulation of the non-canonical NF-κB pathway can be achieved in response to several stimuli of the TNF superfamily of cytokines, such as lymphotoxin β (LTβ), CD40 ligand (CD40L) and BAFF. There is a large body of evidence to support the influence of IKKα in tumour progression in various types of cancer, such as colorectal, breast, pancreatic, gastric and prostate cancer (Fernandez-Majada *et al*., 2007; Park *et al*., 2005; Shiah *et al*., 2006; Hirata *et al*., 2006; Luo *et al*., 2007). Following androgen deprivation therapy, it has been published that lymphotoxin β, the activator of non-canonical

pathway, is an essential factor of CRPC development and tumour progression (Ammirante *et al*., 2010). In addition, knockdown of IKKα with siRNA in androgen-independent prostate cell lines PC3 and DU-145 has resulted in inhibition of PCa invasion and metastasis (Mahato *et al*., 2011), and delayed the development of CRPC in the murine myc-CaP cell line (Ammirante *et al*., 2010). Furthermore, IKKα has been found to induce PCa metastasis by inhibiting maspin, the tumour suppressor gene that inhibits tumour metastasis (Luo *et al*., 2007).

Although strong evidence links IKKα and PCa progression, to date no selective pharmacological IKKα inhibitors are currently available. The pharmaceutical industry has worked hardly to generate various compounds targeting IKK-NF-κB pathways; however these inhibitors have either been IKKβ/α pan-inhibitors or IKKβ selective. Examples of these compounds are a β-carboline natural product PS-1145 and ML120B (Castro *et al*., 2003; Wen *et al*., 2006), BMS-345541 (Burke *et al*., 2003; McIntyre *et al*., 2003), and SPC-839 (Palanki *et al*., 2002). In spite of showing cytotoxicity against cancer cells, inhibition of IKKβ is not a desirable target as it has been associated with a number of serious toxicities in normal cells and/or lethality. For example, an early study of Li and co-workers demonstrated that creating IKKβ knockout mice resulted in massive liver apoptosis leading to embryonic death at mid-gestation (Li *et al*., 1999). Clinical trial use of different IKK inhibitors has also been associated with immunosuppression and infectious diseases (Chariot, 2009). Therefore, targeting PCa using a selective inhibitor of IKKα over IKKβ might be a promising

approach to the treatment of CRPC as it may result in lower toxicities and could have considerable clinical and commercial potential.

Our findings in Chapter 3 suggested that our lead compound, SU1261, demonstrated a high potency and selectivity on IKKα over IKKβ, as confirmed by *in vitro* kinase assay and on the regulation of non-canonical NF-κB pathway biomarkers in PC3M-luc-C6s, the highly metastasis androgen-independent PCa cell line. Kinase activity assay for SU1261 showed a potent activity against IKKα (Ki = 10nM), which was 70x more selective over IKKβ (Ki = 680nM). SU1261 also recorded a high selectivity on IKKα over IKKβ in PC3M-luc-C6 NFκB pathway via biomarker assessment (p52 formation (IKKα) $IC_{50}$ = 3.925μM; IκBα degradation (IKKβ) $IC_{50}$ > 30μM: p65 phosphorylation (IKKβ) $IC_{50}$ > 10μM); i.e. in concentrations ranging from 0.3 to 10μM, SU1261 inhibited the non-canonical NF-κB pathway without affecting the canonical NF-κB pathway.

Radiotherapy, such as external beam radiotherapy (XBR) is a mainstay in the treatment of advanced PCa (Dulaney *et al*., 2016). The therapeutic efficacy of radiation therapy is highly dose-dependent; however, toxicity to normal cells increases as the dose of radiation increases (Kozakai *et al*., 2012). Furthermore, the development of radioresistance in cancers cells have been found to be associated with therapeutic failure and subsequently tumour relapse (Li and Sethi, 2010; Wu *et al*., 2011). In particular, advanced stage androgen-insensitive PCa cells are known to be radioresistant compared with hormone-sensitive cells in early stage of PCa (Xie *et al*., 2010). This characteristic of androgen-insensitive behaviour towards radiation has been documented to occur through

activation of NF-κB pathways subunits following radiation exposure (Kim *et al*., 2006; Baud and Karin, 2009; Li and Sethi, 2010). However, the alternative NF-κB pathway subunits (RelB and p52) are among the proteins involved in the resistance of PCa cells to radiation-induced cytotoxicity. For instance, inhibition of the p52/p100 dimer in PCa cells using STI571, an inhibitor of tyrosine kinase, resulted in enhancement of the sensitivity of these cells to radiation therapy (Xu *et al*., 2010). In addition, transfected human PC3 cells and mouse RM-1 cells (highly aggressive androgen-insensitive mouse prostatic cancer cells) with RelB siRNA, sensitised both cell lines to radiation-induced cell death (Holley *et al*., 2010; Zhu *et al*., 2015). We demonstrated in Chapter 3 that SU1261, a novel IKKα inhibitor, inhibited the non-canonical NF-κB pathway, as confirmed by the large inhibition of p52 formation in PC3M-luc-C6 cells. Therefore, new therapies based on radiosensitisation are required to increase the sensitivity of cancer cells to radiation, subsequently resulting in enhancing radiation-induced cytotoxicity and reducing related toxicity to normal cells.

In this chapter, we aimed to investigate the cytotoxic effect of SU1261, as a novel selective IKKα inhibitor, as a single agent and its negative control SU1257 in prostate cells PC3, PC3M-luc-C6 (androgen-insensitive human prostate carcinoma prostate cell lines) and PNT2A (normal human epithelial prostate cell line). Cytotoxicity was assessed by a cell growth analysis (Chapter 2, section 2.6), an alamar blue cell viability assay (Chapter 2, section 2.7), clonogenic survival assay (Chapter 2, section 2.8), cell cycle progression analysis (Chapter

2, section 2.9) and caspase-3 activity analysis (Chapter 2, section 2.10). Furthermore, by using a combination index analysis model (Chapter 2, section 2.11), we aimed in this study to assess the radiosensitisation effect of SU126 on PCa PC3M-luc-C6 cell line. To the best of our knowledge, ours is the first work studying the cytotoxicity and the radiosensitising effect of IKKα inhibition using pharmacological inhibition in cancer, particularly in PCa cells.

## 4.2 Results

### 4.2.1 Growth of PC3M-luc-C6, PC3 and PNT2A cells following administration of SU1261 and SU1257

In order to determine the effect of SU1261 and SU1257 on the growth rate of PC3M-luc-C6, PC3 and PNT2A cells, a cell growth assay of the three prostate cell lines following SU compounds administration, as described in materials and methods (Chapter 2, section 2.6), was undertaken. The cells were incubated and exposed to different doses (0-10μM) of SU1261 and SU1257 at 5 time points (0h, 24h, 48h, 72h and 96h). The number of cells for each dose at each time point was counted and the percentage of growth AUC (mean ± sd) compared with the control for each dose, measured using GraphPadPrism, version 6.01.

#### *4.2.1.1 Growth of PC3M-luc-C6 cells following administration of SU1261 and SU1257*

Figure 4.1 shows the effect of SU1261 and the negative control SU1257 on growth AUC of PC3M-luc-C6 cells. SU1257 did not significantly affect growth

AUC of PC3M-luc-C6 in all doses (0.1-10μM) during the period of treatment compared to the untreated controls ($P$>0.05). However, starting from a low dose of 1μM of SU1261, the PC3M-luc-C6 cell growth AUC was significantly inhibited in a dose inhibition response compared with control cells. Compared with untreated cells, concentrations of 1, 3 and 10 μM showed highly statistically significant inhibition of PC3M-luc-C6 cell growth AUC by 30% (% of AUC = 70.30 ± 5.01, $P$ < 0.01), 46% (% of AUC = 54.38 ± 10.2, $P$ < 0.001) and 73% (% of AUC = 27.01 ± 8, $P$ < 0.001) respectively. However, low concentrations of SU1261 (0.1-0.3) did not statistically significantly affect the normal growth pattern of PC3M-luc-C6 cells ($P$ > 0.05).

#### *4.2.1.2 Growth of PC3 cells following administration with SU1261 and SU1257*

As demonstrated in Figure 4.2, the presence of SU1257 (0.1-10 μM) or low concentrations of SU1261 (0.1-0.3 μM) did not affect the growth AUC of PC3 cells compared to untreated cells ($P$>0.05). However, exposure of these cells to 1-10μM of SU1261 resulted in a decrease in the growth AUC in a dose-dependent manner. Compared with untreated cells, the growth AUC significantly decreased ($P$>0.001) by 33% (% of AUC = 67.07 ± 6.21), 50% (% of AUC = 49.25 ± 8.12) and 70% (% of AUC = 30.67 ± 6.01) following treatment with 1, 3 and 10μM of SU1261 respectively.

#### *4.2.1.3 Growth of PNT2A cells following administration with SU1261 and SU1257*

In PNT2A cells, no statistically significant change in the growth AUC was observed when cells were exposed to SU1257 (0.1-10μM) compared with untreated cells ($P$>0.5, Figure 4.3). Similarly and in contrast to treatment of PC3M-luc-C6 and PC3 cells, treatment of PNT2A cells with 0.1-1μM of SU1261 did not alter the growth AUC of cells significantly compared with control cells ($P$>0.05). Conversely, there was a highly significant decrease in the growth AUC by 41% (% of AUC= 59.19 ±12.01) when cells were treated with 3μM of SU1261 and further inhibition in growth curve by 71% (% of AUC= 29.29 ±9.23) compared to control cells ($P$<0.001).

These findings suggested that SU1261, our lead novel IKKα inhibitor, strongly inhibited the growth of PCa PC3M-luc-C6 and PC3 cells in a concentration range from 1-10μM. Similarly, 3 and 10μM SU1261 reduced the growth of the normal prostate PNT2A cells but to a lesser extent. The negative control SU1257 did not interfere with the growth rate of any PCa cell line interrogated (PC3M-luc-C6, PC3 and PNT2A cells).

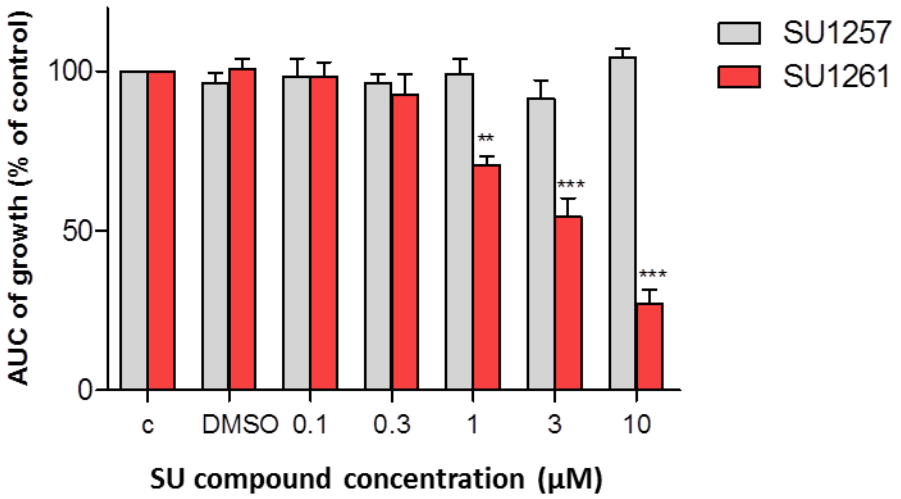


**Figure 4.1: The effect of SU compounds on PC3M-luc-C6 growth curve**. Cells were treated with different concentrations of SU1257 and SU1261 compounds (0.1-10 µM) for 96 hrs. Then Area Under the Curve (AUC) of cell growth for each dose following 96 hrs of treatment was measured and normalised to control. Statistical analysis was carried out using a one-way ANOVA with Bonferroni correction post-test to compare to untreated control. Data shown are expressed as percentage of AUC of control growth, and each value represents the mean (±sd) of three separate experiments. ***P*<0.01 and ****P*<0.001 compared with the non-treated control group.

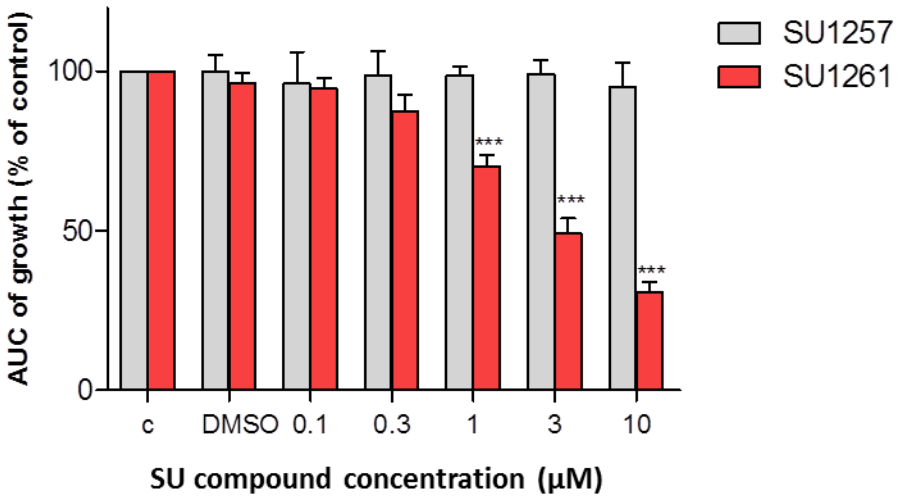


**Figure 4.2: The effect of SU compounds on PC3 growth curve**. Cells were treated with different concentrations of SU1257 and SU1261 compounds (0.1-10 µM) for 96 hrs. Then Area Under the Curve (AUC) of cell growth for each dose following 96 hrs of treatment was measured and normalised to control. Statistical analysis was carried out using a one-way ANOVA with Bonferroni correction post-test to compare to untreated control. Data shown are expressed as percentage of AUC of control growth, and each value represents the mean (±sd) of three separate experiments. ****P*<0.001 compared with the non-treated control group.

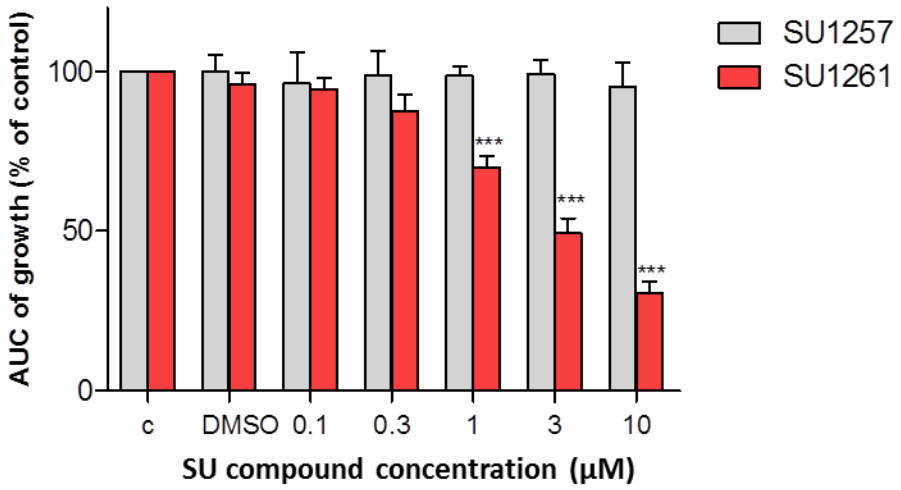


**Figure 4.3: The effect of SU compounds on PNT2A growth curve**. Cells were treated with different concentrations of SU1257 and SU1261 compounds (0.1-10 µM) for 96 hrs. Then Area Under the Curve (AUC) of cells growth for each dose following 96 hrs of treatment was measured and normalised to control. Statistical analysis was carried out using a one-way ANOVA with Bonferroni correction post-test to compare to untreated control. Data shown are expressed as percentage of AUC of control growth, and each value represents the mean (±sd) of three separate experiments. ****P*<0.001 compared with the non-treated control group.

### 4.2.2 Cell viability of PC3M-luc-C6, PC3 and PNT2A cells following administration of SU1261 and SU1257

To evaluate the cytotoxic effect of SU1261 and SU1257 on cell viability of PC3-luc-C6, PC3 and PNT2A cells, an Alamar blue assay was conducted, as described in the materials and methods (Chapter 2, section 2.7). Cells were incubated with varying concentrations (0.-10µM) of SU1261 and SU1257 for 72

hrs. Following this duration, Alamar blue reagent (10% v/v) in media was added and cells incubated for an additional 4 hrs. Fluorescence intensity was then measured with an excitation wavelength of 570 nm and an emission wavelength of 580nm. The results were plotted as a percentage of cell viability (mean ± sd) compared to untreated control cells on the y-axis against the logarithmic dose of SU compounds on x-axis, and $IC_{50}$ values (the concentration which decreased the cell viability of PC3M-luc-C6 by 50%) were calculated using non-linear regression curve fitting of cell viability using GraphPadPrism software, version 6.01.

#### *4.2.2.1 Cell viability of PC3M-luc-C6 cells following administration of SU1261 and SU1257*

As shown in Figure 4.4A, following treatment with 0.1-1µM of SU1261 for 72 hrs, there was no statistically significant decrease in PC3M-luc-C6 cells viability compared to the control group ($P$>0.05). However, the percentage of viable cells significantly decreased in the PC3M-luc-C6 cells by 33% (% cell viability=67.93 ± 11.97) following exposure to 3µM of SU1261 compared with the untreated group($P$<0.01). When the concentration of SU1261 was increased to 10µM, the viability of PC3M-luc-C6 cells was highly statistically significantly decreased ($P$<0.001) by 63% (% cell viability=37.92 ± 8.55) compared to the control cells. The concentration which decreased the cell viability of PC3M-luc-C6 by 50% ($IC_{50}$ concentration) of SU1261 on PC3M-luc-C6 was 6.81µM (±1.03). However, incubation of the PC3M-luc-C6 with SU1257 (0.1-10µM) for

72 hrs did not exert any significant change in cell viability compared to the control group (*P*>0.05, Figure 4.4B).

#### *4.2.2.2 Cell viability of PC3 cells following administration with SU1261 and SU1257*

In PC3 cells, SU1261 also demonstrated an inhibitory effect on cell viability (Figure 4.5A). Treatment of PC3 cells with 1µM of SU1261 for 72 hrs resulted in a small decrease in the viable cells by 17% (% cell viability=83.92 ± 20.68); however this inhibition was not statistically significant (*P*>0.05) when compared to control cells. Incubation of PC3 cells with the highest concentrations of SU1261 (3-10µM) resulted in a further statistically significant decrease in the viable cells. Following exposure of PC3 cells with 3 and 10µM of SU1261, the viability of these cells declined significantly to 55.36±16.78 (*P*<0.01) and 41.56±10.57 (*P*<0.001) respectively compared to the control cells. The calculated $IC_{50}$ value of SU1261 against PC3 cells viability was 5.24µM(±1.95). However, incubation of PC3 cells with the negative control SU1257 (0.1-10µM) did not change the viability of these cells significantly (*P*>0.05) compared to untreated group (Figure 4.5B).

#### *4.2.2.3 Cell viability of PNT2A cells following administration of SU1261 and SU1257*

The cytotoxic-inhibitory effect of SU1261 on PNT2A cell line viability is shown in Figure 4.6A. Incubation of cells with 0.1-1µM of SU1261 resulted in no

statistically significant reduction in PNT2A cell viability compared with the untreated cells ($P$>0.05). However, incubation with 3µM of SU1261 induced a statistically significant inhibition of PNT2A cells viability by 27% (% cell viability=73.88 ± 17.06) compared to the control cells ($P$<0.01). When the concentration of SU1261 was increased to 10µM, the inhibition in cells viability was similar to 3µM of SU1261 (% cell viability=71.82 ± 18.32) but still significant lower compared to the control cells ($P$<0.01). The $IC_{50}$ concentration of SU1261 on PNT2A cells viability was 19.80µM (±3.22). Similar to previous findings, Figure 4.6B demonstrated that the negative control SU1257 had no significant impact ($P$>0.05) on PNT2A cells viability in any tested concentration (0.1-10µM).

In conclusion, the data demonstrated that SU1261 (3-10µM) significantly reduced the viability of prostate cells (PC3M-luc-C6, PC3 and PNT2A cells). However, the obtained $IC_{50}$ values indicated a therapeutic advantage of SU1261 as they showed high toxicity to prostate cancer cells (PC3M-luc-C6=6.81µM; PC3=5.24µM) over normal prostate cells (PNT2A=19.80). In addition, SU1257 our negative had no cytotoxic effect against any prostate cell line (PC3M-luc-C6, PC3 and PNT2A cells). The $IC_{50}$ values of SU compounds against PC3M-luc-C6, PC3 and PNT2A cells are shown in Table 4.1.

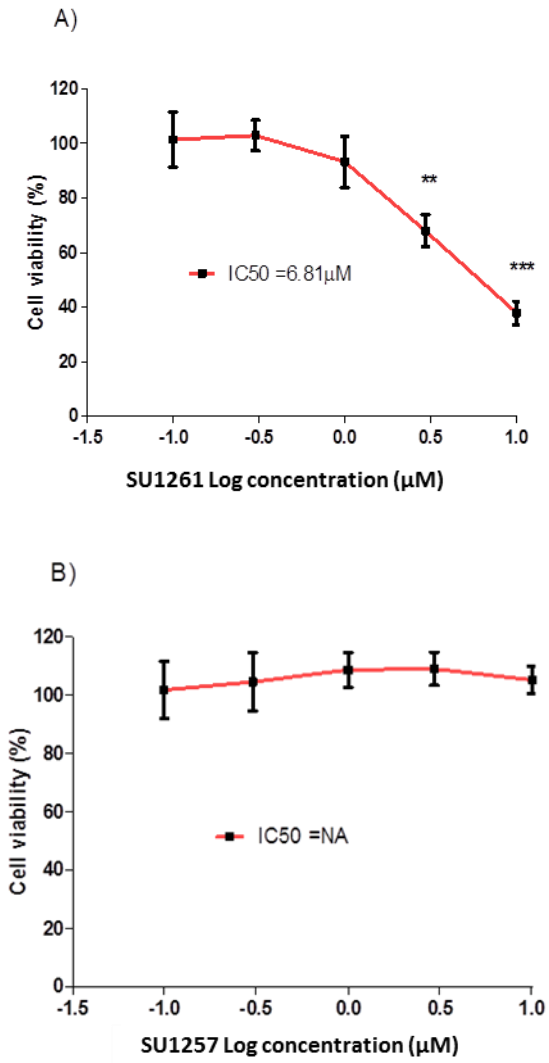


**Figure 4.4: Effect of SU compounds on cell viability of PC3M-luc-C6 cell line.** Cells were exposed to 0.1-10 µM of A) SU1261, B) SU1257 for 72 hrs and then cell viability was measured by an Alamar blue assay. Data shown are expressed as percentage of cell viability compared to the control group. Statistical analysis was carried out using a one-way ANOVA with Bonferroni correction post-test to compare to untreated control. Statistical analysis was carried out using a one-way ANOVA with Bonferroni correction post-test to compare to untreated control. Each value represents the mean (± sd) of three independent experiments. *$P$<0.05, **$P$<0.01 and ***$P$<0.001 compared with the non-treated control group. NA: not achieved

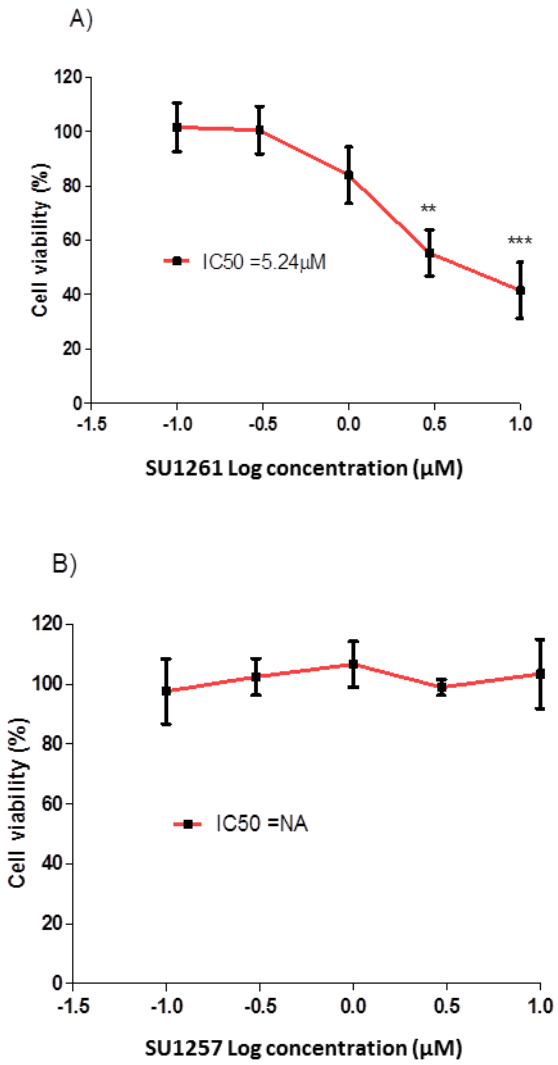


**Figure 4.5: Effect of SU compounds on cell viability of PC3 cell line.** Cells were exposed to 0.1-10 µM of A) SU1261, B) SU1257 for 72 hr and then cell viability was measured by an Alamar blue assay. Data shown are expressed as percentage of cell viability compared to the control group. Statistical analysis was carried out using a one-way ANOVA with Bonferroni correction post-test to compare to untreated control. Statistical analysis was carried out using a one-way ANOVA with Bonferroni correction post-test to compare to untreated control. Each value represents the mean (± sd) of three independent experiments. *$P$<0.05, **$P$<0.01 and ***$P$<0.001 compared with the non-treated control group.

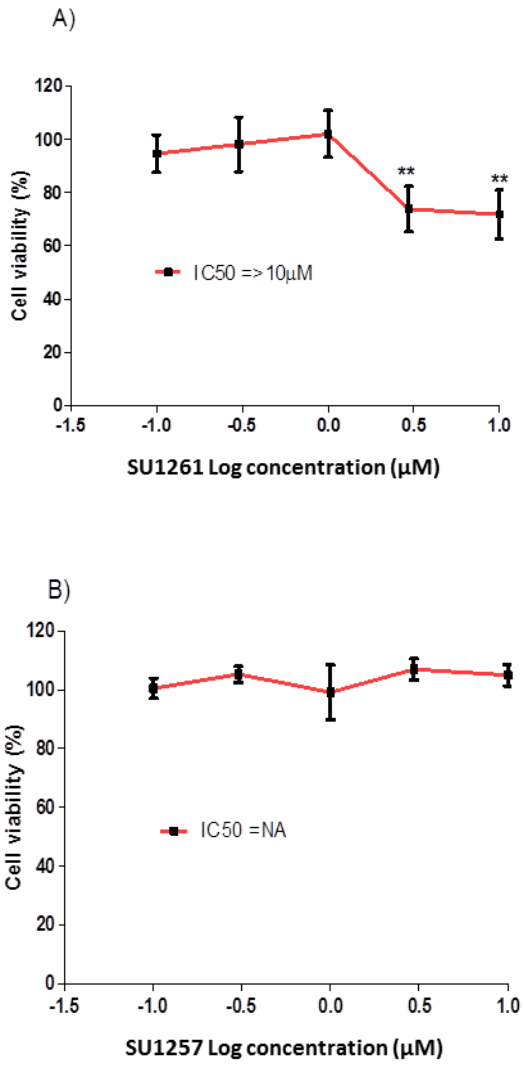


**Figure 4.6: Effect of SU compounds on cell viability of PNT2A cell line.** Cells were exposed to 0.1-10 µM of A) SU1261, B) SU1257 for 72 hr and then cell viability was measured by an Alamar blue assay. Data shown are expressed as percentage of cell viability compared to the control group. Statistical analysis was carried out using a one-way ANOVA with Bonferroni correction post-test to compare to untreated control. Statistical analysis was carried out using a one-way ANOVA with Bonferroni correction post-test to compare to untreated control. Each value represents the mean (± sd) of three independent experiments. *$P$<0.05, **$P$<0.01 and ***$P$<0.001 compared with the non-treated control group. NA: not achieved.

**Table 4.1: $IC_{50}$ values (μM) of SU compounds on PC3M-luc-C6, PC3 and PNT2A cell lines.** Data from cell viability experiments as described before being analysed to calculate the $IC_{50}$ values of each SU compound (SU1261, SU1361, SU1337 and SU1257) on PC3M, PC3 and PNT2A, using nonlinear regression GraphPadPrism 5. NA: not achieved.

| SU compounds | Cell line | $IC_{50}$ (±sd) |
|---|---|---|
| SU1261 | PC3M-luc-C6 | 6.81 (1.03) |
| SU1257 | PC3M-luc-C6 | NA |
| SU1261 | PC3 | 5.24 (±1.95) |
| SU1257 | PC3 | NA |
| SU1261 | PNT2A | >10 (19.80 (±3.22)) |
| SU1257 | PNT2A | NA |

### 4.2.3 Clonogenic survival of PC3-M-luc-C6 and PC3 cells following treatment with SU 1261 and SU1257

Following on from short term cytotoxicity analysis of cell growth and cell viability using the Alamar blue assay, the ultimate fate of cells following drug treatment was then assessed by clonogenic assay (more details in Chapter 2, section 2.8). While clonogenic cells will undergo unlimited proliferation, exposure of cells to cytotoxic agents could affect their division and ability to form colonies. Following 24 hrs of treatment with SU compounds (0.1-10μM), PCa cells (PC3M-luc-C6 and PC3 cells) were re-seeded for assessment of colony formation and incubated for 10-14 days to assess the delayed cytotoxicity in term of cell division and colony formation. The experimental results were fitted to a

concentration-response curve as the mean SF (± sd) on the y-axis against the logarithmic dose of SU compounds on x-axis of three independent experiments. However, the effect on PNT2A cells was not tested in this experiment as this cell line did not form colonies and is unsuitable for this particular assay.

#### *4.2.3.1 Clonogenic survival of PC3M-luc-C6 cells following administration with SU1261 and SU1257*

The effect of SU1261 and 1257 on the survival fraction of PC3M-luc-C6 cells following a 24hr treatment period with different concentrations of these agents is shown in Figures 4.7 A and B. It was observed that at the lower concentrations of SU1261 (0.1 and 0.3μM) there was no statistically significant reduction in PC3M-luc-C6 cells survival compared with control untreated cells ($P$>0.05). However, there was a marked decline in survival fraction (SF) at higher administered concentrations of SU1261 (1, 3 and 10 μM). Concentrations of 1 and 3 μM exerted a significant inhibition of the survival by 30% (SF= 0.70 ±0.07) and 33 % (SF=0.67 ±0.12) respectively compared with the untreated cells ($P$<0.01). Furthermore administration of 10μM of SU1261 resulted in a highly statistically significant decline in the PC3M-luc-C6 SF by 45% (SF=0.55 ±0.9) compared with the control cells ($P$<0.001). In contrast, the negative control SU1257 showed no effect on survival of PC3M-luc-C6, even with the highest administered concentration ($P$>0.05).

#### *4.2.3.2 Clonogenic survival of PC3 cells following treatment with SU1261 and SU1257*

Similarly, PC3 cells were incubated with same concentrations range of SU1261 and SU1257 (0.1-10μM) for 24 hrs (Figures 4.8 A and B). The clonogenic SF of PC3 cells did not show a significant decrease following incubation with 0.1-0.3μM of SU1261 compared with the untreated control cells ($P>0.05$). However, a concentration-dependent decrease in the PC3 clonogenic survival was detected with a concentration range from 1 to 10μM of SU1261. Compared with the control cells, concentrations of 1, 3 and 10μM of SU1261 decreased the SF of PC3 significantly to 0.85 ±0.06 ($P<0.05$), 0.64 ±0.04 ($P<0.001$) and 0.38 ±0.05 ($P<0.001$) respectively. In contrast, PC3 cells did not demonstrate any significant reduction in cell survival following exposure to increasing concentrations of SU1257 (0.1-10μM) ($P>0.05$).

From these data, it can be concluded that SU1261 showed a concentration dependent cytotoxic effect against PCa PC3M-luc-C6 and PC3 cells clonogenicity. Compared to the control wells, concentration ranges of 1-10μM of SU1261 inhibited the both PCa cells (PC3M-luc-C6 and PC3) survival significantly in a concentration-dependent manner, whereas the negative control SU1257 showed a negligible effect on the survival of these cells.

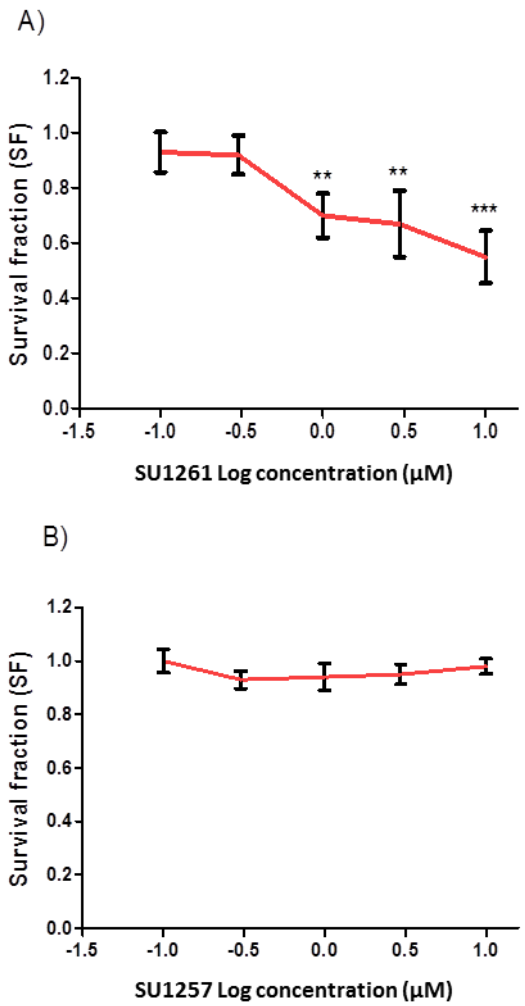


**Figure 4.7: The effect of SU compounds on PC3M-luc-C6 cells clonogenicity.** Cells were incubated with different concentrations of SU compounds (0.1-10 µM) A) SU1261, and B) SU1257, for 24 hrs and then clonogenic survival assays were performed. Data shown are expressed as the average survival fraction (SF) compared to control group. Statistical analysis was carried out using a one-way ANOVA with Bonferroni correction post-test to compare to untreated control. Each value represents the mean (± sd) of three independent experiments. ***P*<0.01 and ****P*<0.001 compared with the non-treated control group.

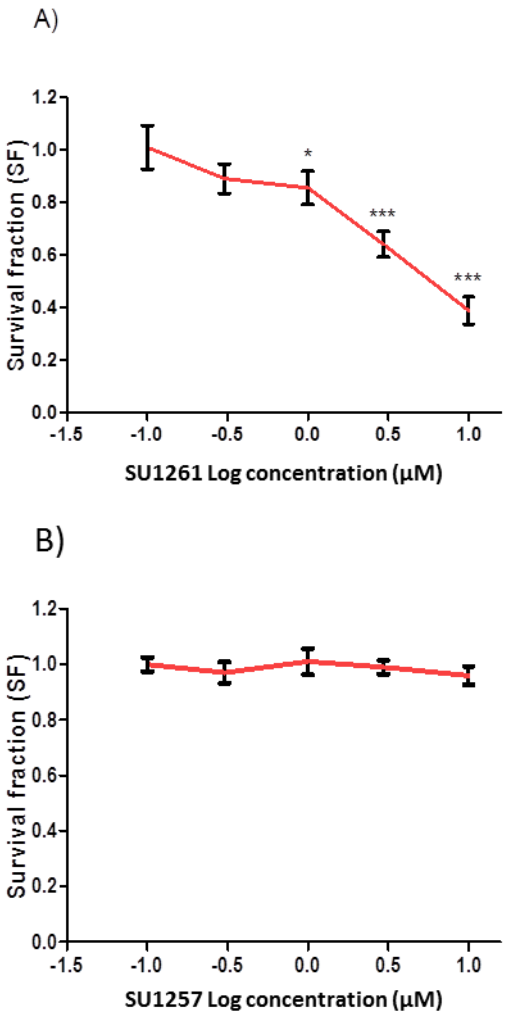


**Figure 4.8: The effect of SU compounds on PC3 cells clonogenicity.** Cells were incubated with different concentrations of SU compounds (0.1-10 µM) A) SU1261, and B) SU1257, for 24hr and then clonogenic survival assays performed. Data shown are expressed as the average survival fraction (SF) compared to control group. Statistical analysis was carried out using a one-way ANOVA with Bonferroni correction post-test to compare to untreated control. Each value represents the mean (± sd) of three separate experiments. *$P$<0.05 and ***$P$<0.001 compared with the non-treated control group.

### 4.2.4 Effect of SU126 and SU1257 treatment on caspase-3 activation as a marker of apoptosis in PC3M-luc-C6, PC3 and PNT2A cells

Apoptosis (programmed cell death) is one of the major death pathways in mammalian cells. However, suppression of apoptosis in cancer cells is critical in malignancy initiation and progression (Sarosiek and Letai, 2016). Our previous findings demonstrated that SU1261 showed cytotoxicity against prostate cancer cell lines as confirmed by the growth assay, cell viability and the clonogenic assays; therefore it was crucial to assess the mechanism involved in SU1261-induced cell death. To do this, caspase-3 activity as a hallmark of apoptosis was measured following exposure of prostate cell lines (PC3-luc-C6, PC3 and PNT2A cell lines) to SU1261, and the negative control SU1257, in addition to the Staurosporine, a positive control drug known to induce apoptotic cell death through a caspase-dependent mechanism (Flanagan *et al*., 2016). As described in the methods and materials section (Chapter 2, section 2.10), cells were incubated with these agents for 4 hrs, then the fluorescence intensity of caspase-3 activity was read with an excitation wavelength of 360nm, and an emission wavelength of 460nm. The results were presented as the mean fold increase (mean ± sd) in caspase-3 activity by normalising and comparing the mean fluorescence intensity for each treated group with the fluorescence intensity of untreated control wells in three independent experiments.

#### *4.2.4.1 Effect of Staurosporine treatment on caspase-3 activation as a marker of apoptosis in PC3M-luc-C6, PC3 and PNT2A cells*

The aim of this initial experiment was to determine the optimal time period for the positive control Staurosporine-induced caspase-3 activity in PC3M-luc-C6 cell lines during 24 hrs of administration. As shown in Figure 4.9A, caspase-3 activity was largely induced 4 hrs following Staurosporine (30µM) treatment and caspase-3 levels were sustained over 8 hrs. Subsequently, the induction of caspase-3 decreased towards control level values by 24 hrs (70.66% of control basal expression), however the fold increase in caspase-3 activity was still statistically significantly higher compared to untreated control group ($P<0.01$).

We then investigated if our prostate cells could produce caspase-3 in response to apoptosis induction. Therefore, PC3M, PC3 and PNT2A cells were treated with increasing concentrations of Staurosporine (1-30µM) for 4 hrs (Figure 4.9B). Compared with control cells, exposure of both PC3M and PNT2A cells to 3µM of Staurosporine resulted in a small but statistically significant increase in caspase-3 levels by 1.58 fold (± 0.22, $P<0.01$) and 1.54 fold (± 0.14, $P<0.01$) respectively, but this concentration did not show any statistical significant change relative to control cells in PC3 cells($P>0.05$). However, Staurosporine-induced apoptosis was significantly increased when the concentration was increased to 10 and 30µM in all prostate cell lines. Treatment of PC3M-luc-C6, PC3 and PNT2A cells with Staurosporine (10µM) resulted in a significant induction in caspase-3 level to 2.12 fold (± 0.29), 1.91 fold (± 0.51), and 2.22 fold (± 0.24) respectively compared with control cells ($P<0.001$). A further

significant increase was observed in the level of caspase-3 following exposure to Staurosporine (30µM) in PC3M-luc-C6 by 2.93 fold (± 0.44), PC3 by 2.59 fold (± 0.45) and PNT2A by 3.09 fold (± 0.24) compared with untreated cells (*P*<0.001).

Therefore, a 30µM of Staurosporine for 4hrs treatment are the proper concentration and time which were applied in each experiment when we investigated the effect of SU compounds on caspase-3 activation in prostate cell lines.

#### *4.2.4.2 Effect of SU126 and SU1257 treatment on caspase-3 activation as a marker of apoptosis in PC3M-luc-C6 cells*

We investigated the apoptosis induction potential of SU1261 and SU1257 in PC3M-luc-C6 cells with a range of administered concentrations (1-10µM) for 4 hrs (Figure 4.10). Exposure of cells to 0.1-1µM did not affect the level of caspase-3 significantly compared to the control group (*P*>0.05). However, pre-treatment of cells with higher doses of SU1261 (3-10µM) showed a statistically significant induction of apoptosis in PC3M-luc-C6 cells relative to control cells. Administration of 3µM induced the activation of caspase-3 significantly by 35% (fold increase=1.35 ± 0.11) compared with the untreated control cells *(P*<0.01). Furthermore a statistically significant increase was detected in caspase-3 levels (fold increase=1.70 ± 0.14) when cells were exposed to the maximum concentration of SU1261 (10µM) compared to the control cells *(P*<0.001). However, incubation of PC3M-luc-C6 cells with the negative control SU1257 did

not result in any statistically significant alteration in caspase-3 activity compared with the control cells (*P*>0.05).

#### *4.2.4.3 Effect of SU126 and SU1257 treatment on caspase-3 activation as a marker of apoptosis in PC3 cells*

Figure 4.11 demonstrates the fold increase in caspase-3 levels in PC3 cells following administration of SU1261 and SU1257 compared with control cells. Pre-treatment of cells with SU1261 (0.1-1µM) resulted in no statistically significant induction in caspase-3 measurement compared to the control cells (*P*>0.05). However, when the concentration of SU1261 increased to 3µM, the caspase-3 level significantly increased by 43% (fold increase=1.43 ± 0.18) compared with the control cells *(P*<0.001). Furthermore, an almost two-fold increase in caspase-3 activity (Fold increase=1.91 ± 0.19) was achieved compared with the control cells (*P*<0.001) following exposure with 10µM of SU1261. As hypothesised, pre-treatment with the negative control SU1257 did not cause a significant change in PC3 cells caspase-3 level compared with the control group (*P*>0.05).

#### *4.2.4.4 Effect of SU126 and SU1257 treatment on caspase-3 activation as a marker of apoptosis in PNT2A cells*

The caspase-3 activity levels following treatment with various concentrations (0.1-10µM) of both SU1261 and SU1257 on normal prostate PNT2A cells is shown in Figure 4.12. Incubation of cells with 0.1-3µM of SU1261 resulted in no

statistically significant induction caspase-3 level in PNT2A cell compared with the untreated cells ($P$>0.05). Treatment of PNT2A cells with the highest concentration of SU1261 (10µM) induced more than a two-fold increase (fold increase=2.15 ±0.21) in the caspase-3 activity compared to control cells *(*$P$<0.001). Similar to its previous effects, the negative control SU1257 did not induce caspase-3 in PNT2A cells in any of the tested concentrations (0.1-10µM) compared with the control cells ($P$>0.05).

In conclusion, these data indicated that SU1261 (3-10µM) significantly induced apoptosis in PCa cells (PC3M-luc-C6 and PC3 cell lines). Interestingly, only the maximum dose of SU1261 (10µM) showed activation of the apoptosis marker (caspase- 3) against the normal prostate PNT2A cells. However, the negative control SU12517 (0.1-10µM) did not trigger apoptosis in any tested prostate cell line (PC3M-luc-C6, PC3 and PNT2A cells).

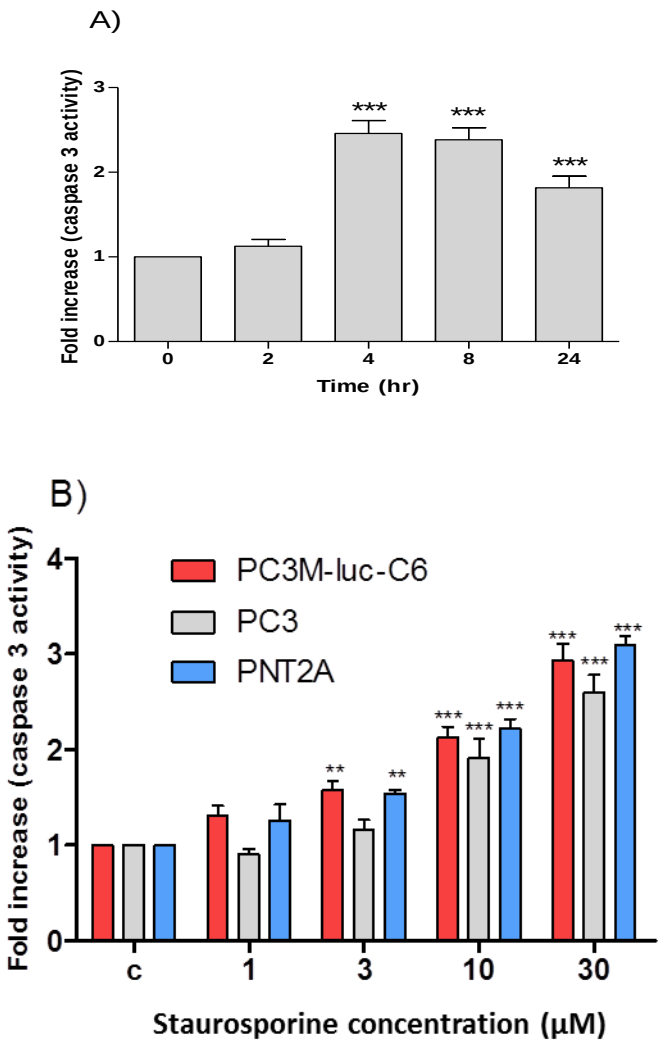


**Figure 4.9: Effect of Staurosporine-mediated caspase-3 activity on PC3M-luc-C6 cell lines.** A) PC3M-luc-C6 cells were treated with 30 µM of Staurosporine for the indicated time points. B) PC3M-luc-C6, PC3 and PNT2A cells were treated with increasing concentrations of Staurosporine (0.1-30µM) for 4 hrs, then caspase-3 activity was measured using a caspase-3 fluorometric assay. Data shown are expressed as fold increase in caspase-3 activity compared to the control group. Statistical analysis was carried out using a one-way ANOVA with Bonferroni correction post-test to compare to the untreated control. Each value represents the mean (±sd) of three separate experiments. ***P*<0.01 and ****P*<0.001 compared with the non-treated control group.

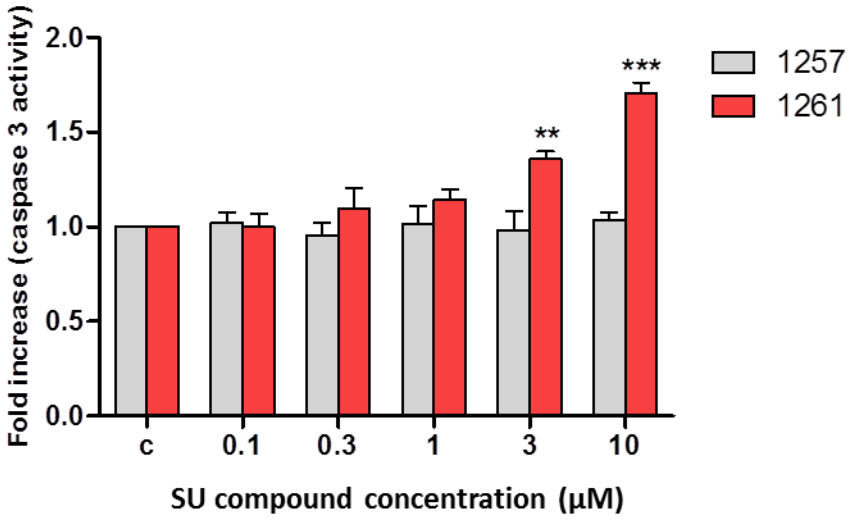


**Figure 4.10: Effect of SU compounds on caspase-3 activity in PC3M-luc-C6 cells.** Cells were treated with different concentrations of SU1261 and SU1257 compounds (1-10 µM) for 4 hrs, and then caspase-3 activity was measured using caspase-3 fluorometric assay. The chart shows the data as fold increase following treatment in caspase-3 level compared with control. Statistical analysis was carried out using a one-way ANOVA with Bonferroni correction post-test to compare to the untreated control. Each value represents the mean (±sd) of three separate experiments. $^{**}P<0.01$ and $^{***}P<0.001$ compared with the non-treated control group.

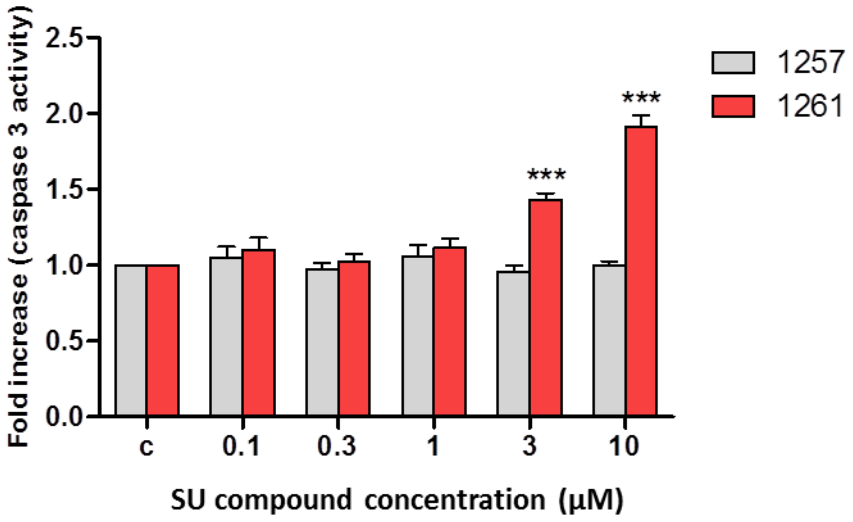


**Figure 4.11: Effect of SU compounds on caspase-3 activity in PC3 cells.** Cells were treated with different concentrations of SU compounds (1-10 µM) A) SU1261, and B) SU1257, for 4 hrs, and then caspase-3 activity was measured using a caspase-3 fluorometric assay. The chart shows the data as fold increase following treatment in caspase-3 level compared to the control. Statistical analysis was carried out using a one-way ANOVA with Bonferroni correction post-test to compare to the untreated control. Each value represents the mean (±sd) of three separate experiments. ****P*<0.001 compared with the non-treated control group.

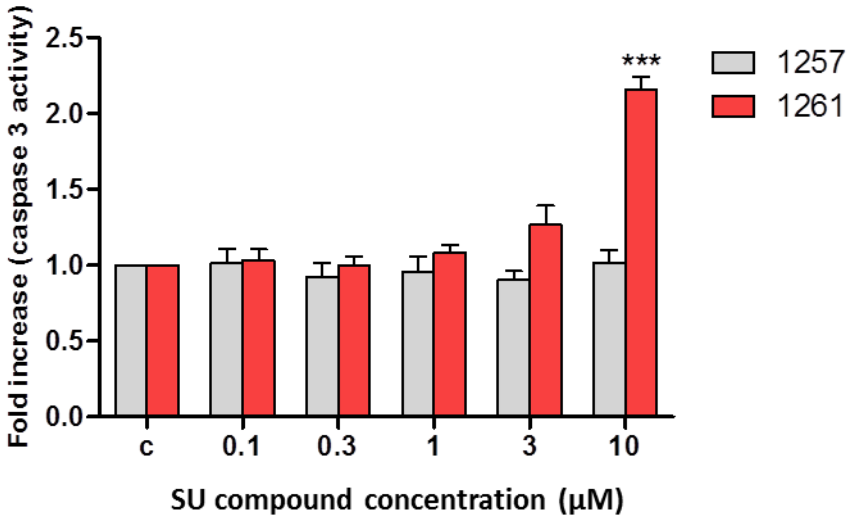


**Figure 4.12: Effect of SU compounds on caspase-3 activity in PNT2A cells.** Cells were treated with different concentrations of SU compounds (1-10 µM) A) SU1261, and B) SU1257, for 4 hrs, and then caspase-3 activity was measured using a caspase-3 fluorometric assay. The chart shows the data as fold increase following treatment in caspase-3 level compared with the control. Statistical analysis was carried out using a one-way ANOVA with Bonferroni correction post-test to compare to the untreated control. Each value represents the mean (± sd) of three separate experiments. ****P*<0.001 compared with the non-treated control group.

### 4.2.5 Effect of SU126 and SU1257 treatment on cell cycle progression of PC3M-luc-C6 cells

Following assessment of the cytotoxic effect of SU1261 on cell growth assay, cell viability, clonogenic assay and caspase-3 activity, we next planned to analyse whether the observed effects could be accompanied by induction of cell cycle arrest. This was undertaken by assessing the spread of cells within the

stages of the cell cycle using flow cytometry following propidium iodide (PI) staining. As described in methods and materials (Chapter 2, section 2.9), PC3M-luc-C6 cells were treated with various concentrations (0.1-10μM) of SU1261 and the negative control SU1257 for 24 hrs prior to cell cycle analysis. Cell cycle analysis was carried out using a FACScan (Becton Dickinson Systems, Cowley, UK) and data were analysed using Fluorescence-Activated Cell Sorting Analysis (FACS) BD. Three independent experiments were carried out with a minimum of 1000cells/sample and results presented as the percentage of the cell cycle phases (mean ± sd).

As is shown in Figure 4.13.A, incubation of PC3M-luc-C6 cells with increasing concentrations (0.1-10μM) of SU1261 for 24 hrs did not cause any significant changes ($P>0.05$) in cell cycle distribution of G0/G1, G2/M and S phases. However, the highest administered concentration of SU1261 (10μM) caused a statistically significant increase ($P<0.01$) in the percentage of cells in subG0 phase from 2.43% (± 0.11) in the control cells to 12.80% (± 5.16) in the treatment group. Conversely, treatment PC3M-luc-C6 cells with the negative control SU1257 for 24 hrs did not affect cell cycle progression in any concentration used (Figure 4.13.B). It can be concluded that the highest concentration used of SU1261 (10μM) significantly increased the proportions of PC3M-luc-C6 cells in subG0 phase, but with no influence in G0/G1, G2/M and S phase of cell cycle. However, the negative control SU1257 (0.1-10μM) did not change the normal cell cycle progression of PC3M-luc-C6 cells.

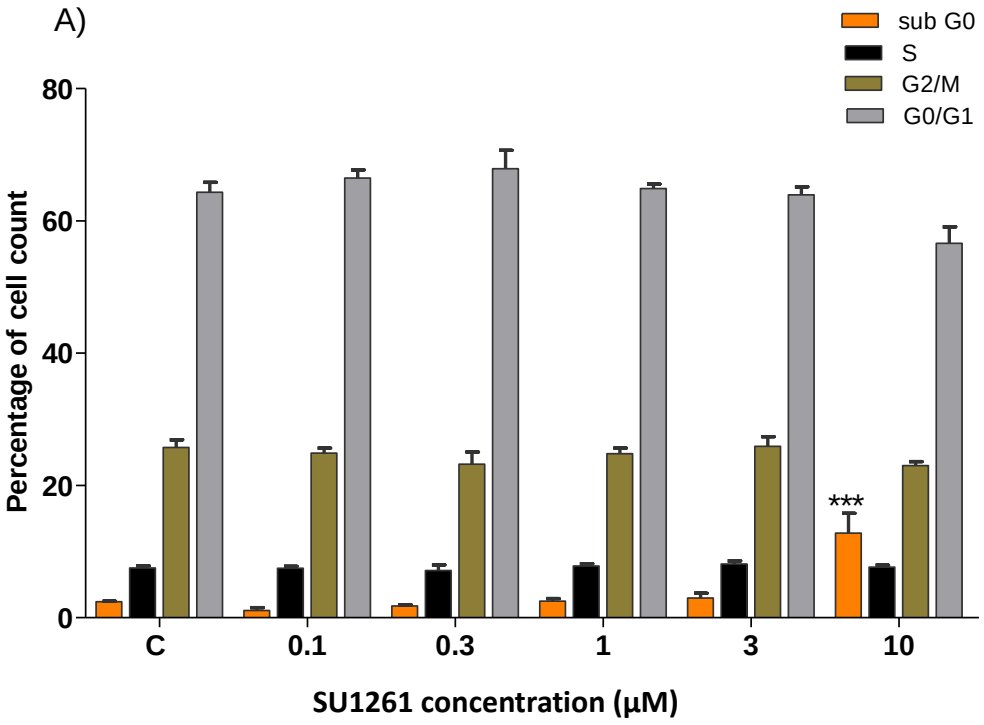
A)
sub G0
S
G2/M
G0/G1
80
60
40
20
0
Percentage of cell count
***
C
0.1
0.3
1
3
10
SU1261 concentration (µM)

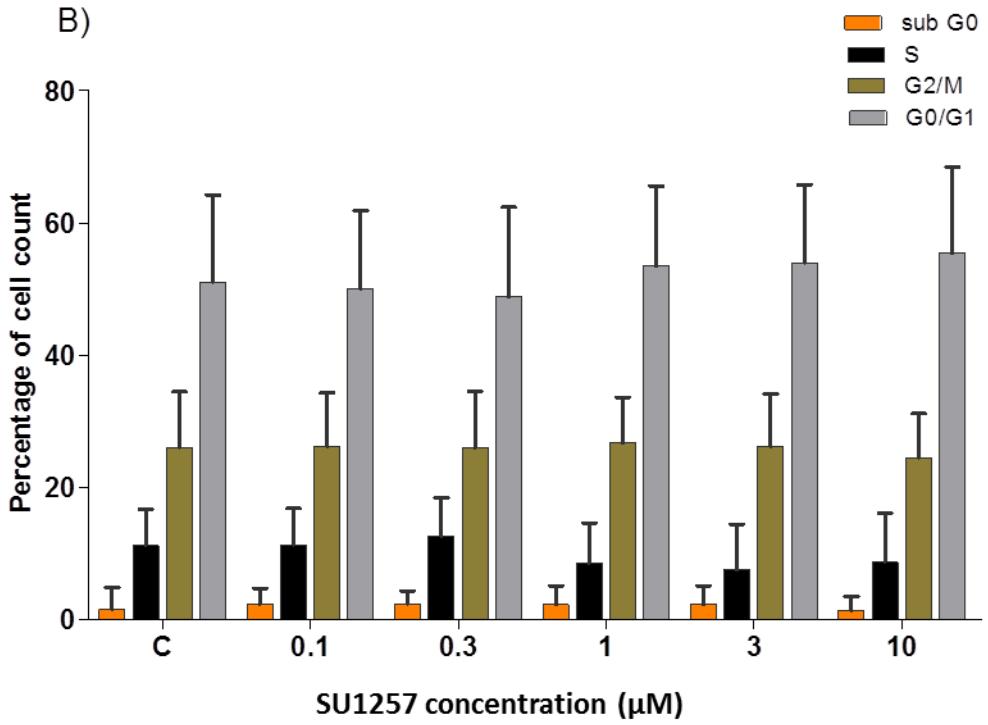


**Figure 4.13: Effect of SU compounds on cell cycle progression in PC3M-luc-C6 cell lines.** Cells were treated with different concentrations of SU compounds (1-10 µM) A) SU1261, and B) SU1257, for 24 hrs, then the cell cycle assessed by flow cytometry using propidium iodide (PI) for the determination of total DNA content. The chart demonstrates the distribution of cells in the different phases of the cell cycle following treatment. Statistical analysis was carried out using a one-way ANOVA with Bonferroni post-test to compare to untreated control. Each value represents the mean (± sd) of three separate experiments. ****P*<0.001 compared with the non-treated control group.

### 4.2.6 Investigation of the radiosensitisation potential of SU1261 in combination with External Beam Radiation (XBR)

In this experiment, we investigated whether inhibition of IKKα by SU1261 before radiation exposure could enhance the cytotoxicity of radiation in the highly aggressive androgen-insensitive PC3M-luc-C6 cells compared to each therapy alone. To achieve this, a clonogenic assay was undertaken to assess the survival fraction of SU1261 and XBR combination treatment in PC3M-luc-C6 cells (for more details, see methods and materials, Chapter 2, section 2.8). The clonogenic survival fraction findings of this combination were analysed using a combination index analysis to assess the interaction and the therapeutic efficacy of the two therapies (for more details, see methods and materials in Chapter 2, section 2.11). The impact of this combination on the cell cycle progression of PC3M-luc-C6cells was also investigated through the cell cycle analysis (for more details, see methods and materials in Chapter 2, section 2.9). The experimental results were carried out in three independent experiments (mean ± sd).

#### *4.2.6.1 Determination of the effect of XBR exposure on clonogenic survival of PC3M-luc-C6 cells*

The effect of XBR exposure as a single treatment on the clonogenic survival of PC3M-luc-C6 cells was initially examined to assess the sensitivity of these cells to radiation, as well as to determine the dose range of XBR to be used in combination with SU1261 compound in the radiosensitisation study.

As demonstrated in Figure 4.14, exposure of PC3M-luc-C6 cells to increasing doses of XBR (0-6Gy) resulted in a dose-dependent reduction in clonogenic survival in PC3M-luc-C6 cells. Exposure of cells to 0.5Gy of radiation inhibited the survival fraction of PC3M-luc-C6 significantly, by 23% (SF=0.78 ±0.05) compared with untreated cells *(P*<0.01). Doses of 1, 2 and 4 Gy induced further statistically significant decreases in the clonogenic survival of cells compared to the control cells (*P*<0.001) by 31% (SF=0.69 ± 0.06), 47% (SF=0.53 ± 0.08) and 62% (SF=0.38 ± 0.04) respectively. Furthermore, treatment of these cells with the highest dose of radiation (6 Gy), resulted in a significant decline in survival, by 70% (SF=0.3 ± 0.07) compared with untreated control cells *(P*<0.001). The calculated $IC_{50}$ for XBR against the PC3M-luc-C6 cells was 2.41Gy (±0.64).

These results indicated that XBR induced cytotoxicity in PC3M-luc-C6 cells in a dose-dependent manner. The purpose of this study was to assess the radiosensitisation potential of SU1261 in PC3M-luc-C6 cells. Based on the $IC_{50}$ value (2.41Gy) of XBR, a dose range below this value (0-2Gy) was used for combination study with SU1261 in PC3M-luc-C6 cells.

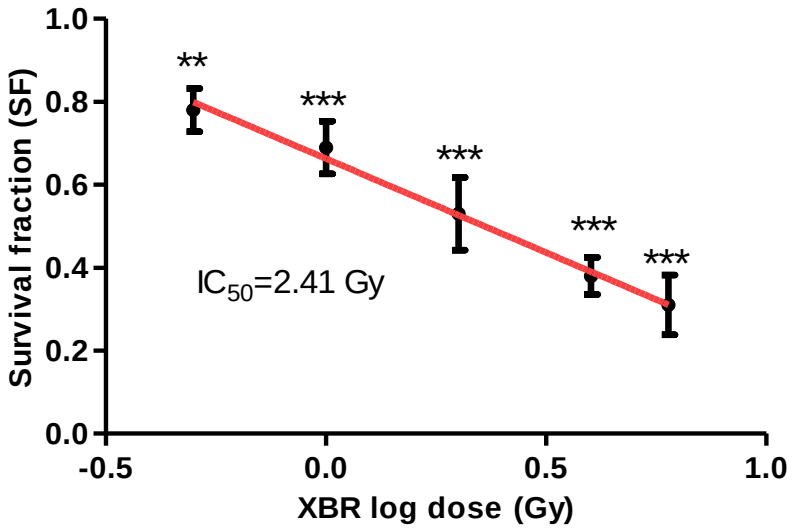


**Figure 4.14: Clonogenic survival of PC3M-luc-C6 cells exposed to increasing doses of XBR.** Cells were exposed to increasing concentrations of radiation (0-6 Gy), followed by clonogenic survival assay. Statistical analysis was carried out using a one-way ANOVA with Bonferroni post-test to compare to untreated control. Data shown are expressed as the average survival fraction compared to control group. Each value represents the mean (±sd) of three separate experiments. ***P*<0.01 and ****P*<0.001 compared with the untreated control group.

### *4.2.6.2 Determination of the effect of SU1261 in combination with XBR exposure on clonogenic survival of PC3M-luc-C6 cells*

To assess the radiosensitisation effect of SU1261, PC3M-luc-C6 cells were pretreated with various concentrations of SU1261 (0.1-10μM) for 24hr followed by XBR exposure (0-2Gy). Cytotoxicity was analysed by clonogenic survival

assay (Figure 4.15). In the absence of XBR treatment, the lower doses of SU1261 (0.1 and 0.3μM) had no significant effect on the clonogenic survival of PC3M-luc-C6 cells compared with control cells ($P$>0.05). However, treatment of cells with 1 and 3μM of SU1261 resulted in a statistically significant inhibition of clonogenic survival by 30% (SF= 0.70 ±0.07) and 33% (SF=0.67 ±0.12) respectively compared with untreated cells ($P$<0.01). Further significant inhibition in SF was observed when cells were incubated with 10μM of SU1261 (SF=0.55 ±0.9) compared with control cells ($P$<0.001). Exposure of cells to low doses of SU1261 (0.1 and 0.3μM) followed by 1Gy of XBR resulted in no statistically significant inhibition in SF of cells compared to the group treated with 1Gy alone ($P$>0.05). However, when the cells were treated with 1, 3 and 10μM of SU1261 followed by 1Gy irradiation, this combination resulted in a statistically significant decrease in survival fraction to 0.52 ±0.04 ($P$<0.01), 0.42 ±0.06 ($P$<0.001) and 0.29 ±0.07 ($P$<0.001) respectively compared to the effects of 1Gy alone (SF=0.79 ±0.03). When the dose of XBR was increased to 2Gy, combination with low doses of SU1261 (0.1-0.3μM) did not change the SF in cells significantly compared to cells treated with 2Gy alone ($P$>0.05). However, again, compared to cells exposed to 2Gy alone, co-administration of 1, 3 and 10μM of SU1261 resulted in a statistically significant inhibition in the SF of PC3M-luc-C6 cells from 0.61 ±0.03 to 0.34 ±0.04 ($P$<0.01), 0.24 ±0.07 ($P$<0.001) and 0.08 ±0.03 ($P$<0.001) respectively.

These data indicated that combined treatments of XBR with SU1261 (1-10µM) significantly reduced survival compared to the non-irradiated control cells. Subsequently, combination index analysis was carried out, in order to assess potential synergy arising from the interaction of XBR and SU1261 in PC3M-luc-C6 cell line.

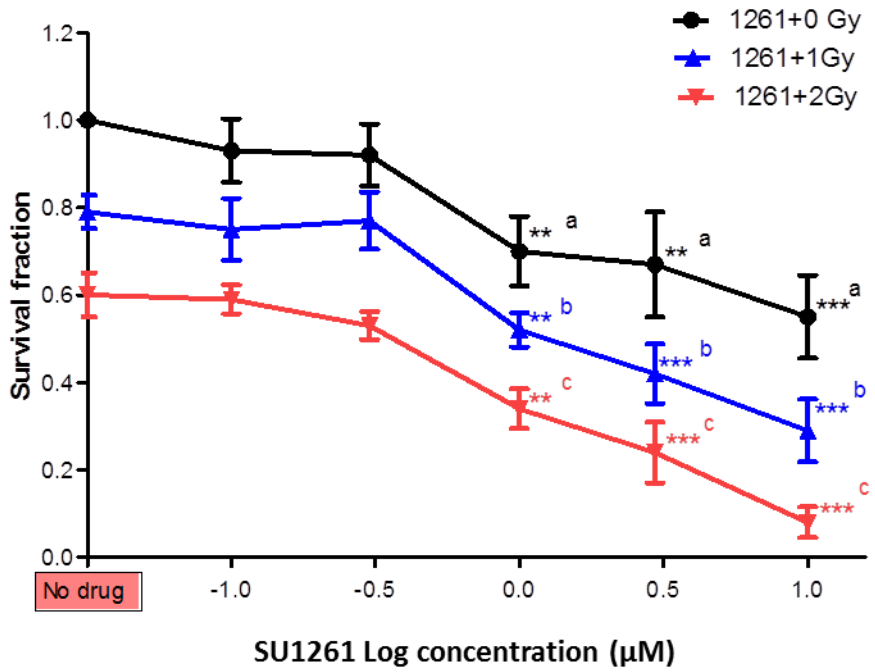


**Figure 4.15: Effect of combination of SU1261 and radiation on clonogenic survival of PC3M-luc-C6 cells.** Cells were treated with SU1261 (0.1-10µM) for 24 hrs followed by XBR exposure (0-2Gy), and then clonogenic survival assays were performed. Statistical analysis was carried out using a one-way ANOVA with Bonferroni correction post-test to compare to (a) untreated control (b) 1Gy-treated or (c) 2Gy-treated group. Data shown are expressed as the average survival fraction compared to the control group. Each value represents the mean (± sd) of three separate experiments. $^{**}P<0.01$ and $^{***}P<0.001$ compared to the indicated groups.

#### *4.2.6.3 Determination of the radiosensitising effect of SU1261 in combination*

To assess the radiosensitisation potential of SU1261 on PC3M-luc-C6, the clonogenic survival interaction between SU1261 (0.1-10μM) and radiation (0-2Gy) from Figure 4.15 was fitted using combination index analysis (Figures 4.16 A and B). The cytotoxicity of combinations of SU1261 and radiation was then analysed by calculating a combination index value (CI) at different levels of cytotoxicity, where $CI < 1$, $CI = 1$ and $CI > 1$ indicate synergism, additivity and antagonism, respectively.

As demonstrated in Figure 4.16A, a combination of 1Gy of XBR and low doses of SU1261 (0.1-0.3μM) demonstrated cytotoxicity that was supra-additive to antagonistic against PC3M-luc-C6 cells (CI=0.92 ±0.13 for 0.1μM+1Gy and CI=1.14 ±0.07 for 0.3μM+1Gy). In contrast, a dose dependant synergistic cytotoxic effect was achieved when cells were exposed to higher concentrations of SU1261 prior to 1Gy exposure. Treatment with 1μM, 3μM and 10μM resulted in CI values of 0.49 ±0.04, 0.45 ±0.07 and 0.38 ±0.09 respectively.

Increasing the radiation dose to 2Gy following 0.1μM SU1261 treatment resulted in an additive effect (CI=1.01 ±0.08). However, cells exposed to 0.3μM, 1μM, 3μM and 10μM of SU1261 followed by 2Gy exhibited a highly synergistic combination effect (CI=0.46 ±07 for 1μM + 2Gy; CI=0.34 ±0.6 for 3μM + 2Gy; CI=0.13 ±0.05 for 10μM + 2Gy).

The CI analysis data indicates that pre-treatment PC3-luc-C6 cells with SU1261 for 24hr followed by XBR exposure resulted in a concentration-dependent increase in toxicity on PC3-luc-C6 cells suggesting a synergistic effect (at certain combination doses) compared to each agent alone.

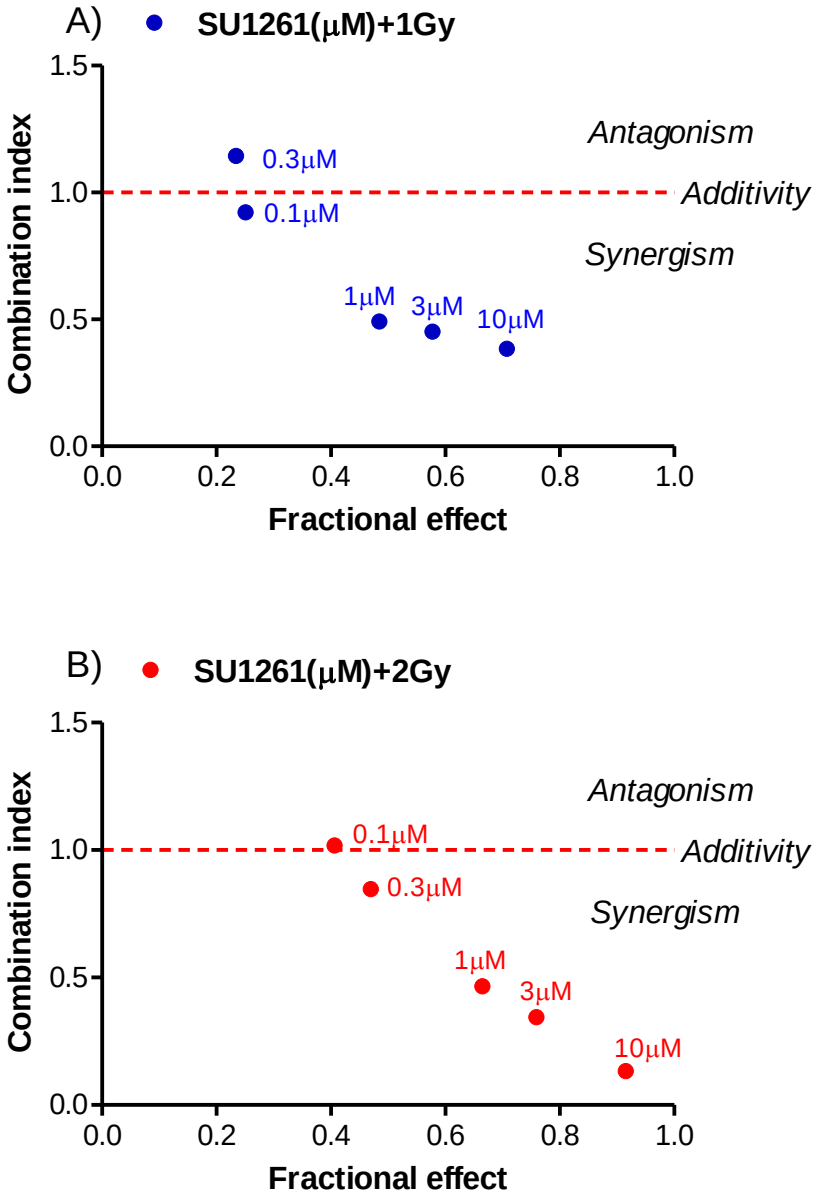


**Figure 4.16: Combination index (C.I.) data analysis of the combined effect of SU1261 and radiation on clonogenic survival of PC3M-luc-C6 cells.** Clonogenic survival data of SU1261 and radiation on PC3M-luc-C6 cells from Figure 4.15 were analysed using combination index analysis, where panel (A) for the C.I effect of SU1261 + 1Gy and panel (B) for the C.I effect of SU1261 + 2Gy. CI < 1, CI = 1 and CI > 1 indicated synergism, additivity and antagonism respectively. Each value represents the CI of three separate experiments.

### *4.2.6.4 The effect of SU1261 in combination with XBR on the cell cycle progression of PC3M-luc-C6 cells*

For further investigation of the cytotoxicity of SU1261 and XBR combination, the progression of PC3M-luc-C6 cells was determined through cell cycle analysis to assess whether this combination therapy caused an abrogation to the normal cycling of PC3M-luc-C6 cells. The effect of SU1261 (0.1-10μM) in combination with XBR (0-2Gy) on the cell cycle progression was determined at 24 hrs following radiation treatment (Figures 4.17A and B).

Single treatment of cells with SU1261 (10μM) or XBR (1Gy) had no effect in normal progression of PC3M-luc-C6 cells compared with the control cells ($P$>0.05). Similarly, a combination of SU1261 (0.1-0.3μM) and 1Gy of radiation did not significantly affect the cell cycle progression of the PC3M-luc-C6 compared with the untreated control group ($P$>0.05). Despite showing a decrease in clonogenic survival and synergistic cytotoxic effect in PC3M-luc-C6 cells, a combination treatment of SU1261 (1μM) and 1Gy of XBR resulted in no statistically significant change in the distribution of PC3M-luc-C6 in the various phases of the cell cycle compared to the control cells ($P$>0.05). However, exposure of cells to 3μM of SU1261 followed by 1Gy of XBR led to significant increase ($P$<0.001) in the number cells within the G2/M phase from 29.07(±3.77) to 40.60 (±2.81) and a significant decrease ($P$<0.01) in G0/G1 cell fraction from 60.20 (±5.29) to 49.30 (±3.21) compared to the untreated cells. Similarly, a combination of SU1261 (10μM) and XBR (1Gy) significantly increased

(*P*<0.001) the accumulation of cells in the G2/M phase and also significantly decreased (*P*<0.01) the fraction of cells in the G0/G1 phase to 38.86 (±3.70) and 48.901(±2.78) respectively, compared to the control measurement (% of G2/M cells=29.07 ±3.77; % of G0/G1 cells=60.20 ±5.29).

When PC3M-luc-C6 cells were treated with either SU1261 (10μM) or XBR (2Gy) as a single agent, the cell cycle progression of PC3M-luc-C6 cells was not affected compared to the control cells (*P*>0.05). However, exposure of PC3M-luc-C6 cells to SU1261 (0.1-10μM) and XBR (2Gy) combination, resulted in a statistically significant accumulation of cells within the G2/M phase of the cell cycle compared with the control cells. Concentrations of 0.1μM and 0.3μM of SU1261 in combination with 2Gy of XBR increased the percentage of cells in G2/M significantly from 29.07 (±3.77) in control cells to 39.10 (±2.55, *P*<0.05) and 41.40 (± 2.53, *P*<0.01) respectively. Similarly, treatment with 1, 3 and 10μM of SU1261 followed by exposure to 2Gy, increased the accumulation of cells in G2/M significantly (*P*<0.001) to 47.46 (±1.65), 46.10 (±4.50) and 44.50 (±4.34) respectively, compared with the control cells (% of G2/M cells=29.07 ±3.77). Furthermore, this increase in cells in the G2/M phase was accompanied by a significant decrease (*P*<0.01) in G0/G1 to 42.26 (±1.85), 44.20 (±3.61) and 43.50 (±4.75) compared with 60.20 (± 5.29) in the control cells.

In conclusion, analysis of the progression of cells through the cell cycle demonstrated that the combination of SU1261 (3-10μM) with 1Gy XBR as well as a combination of SU1261 (0.1-10μM) with 2Gy resulted in a statistically

significant arrest of cells in the G2/M phase of the cell cycle compared to the control cells. This increase in the percentage of cells in G2/M was also accompanied by a decrease in the percentage of cells in G0/G1.

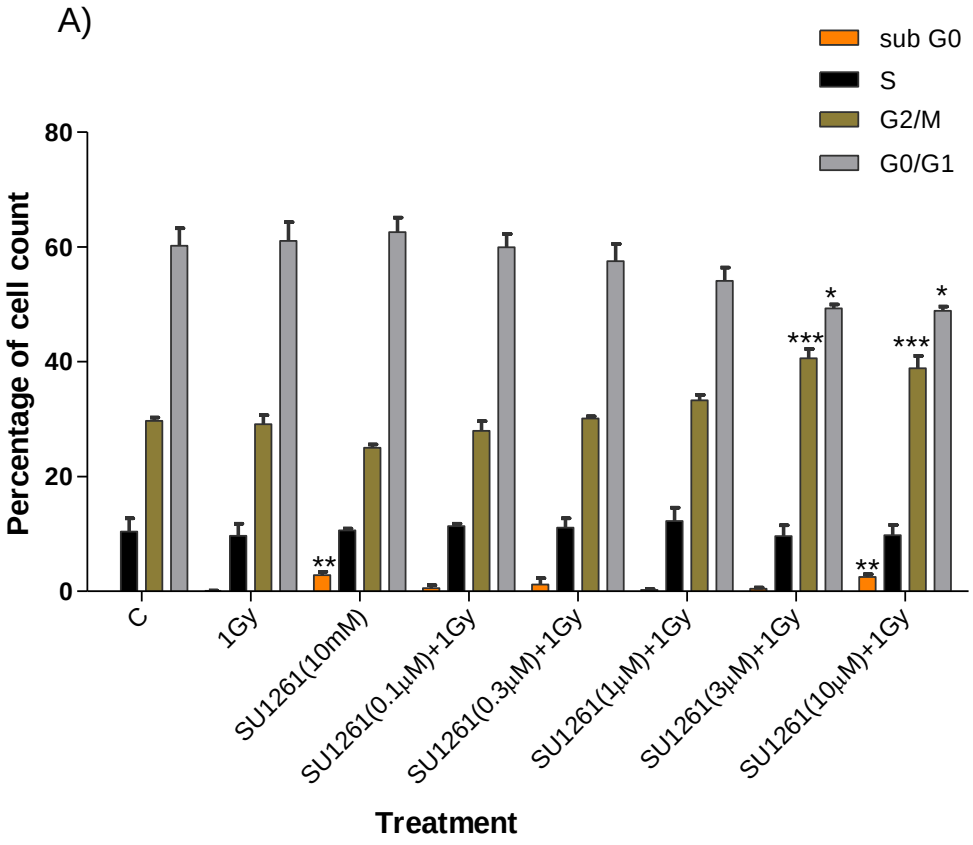

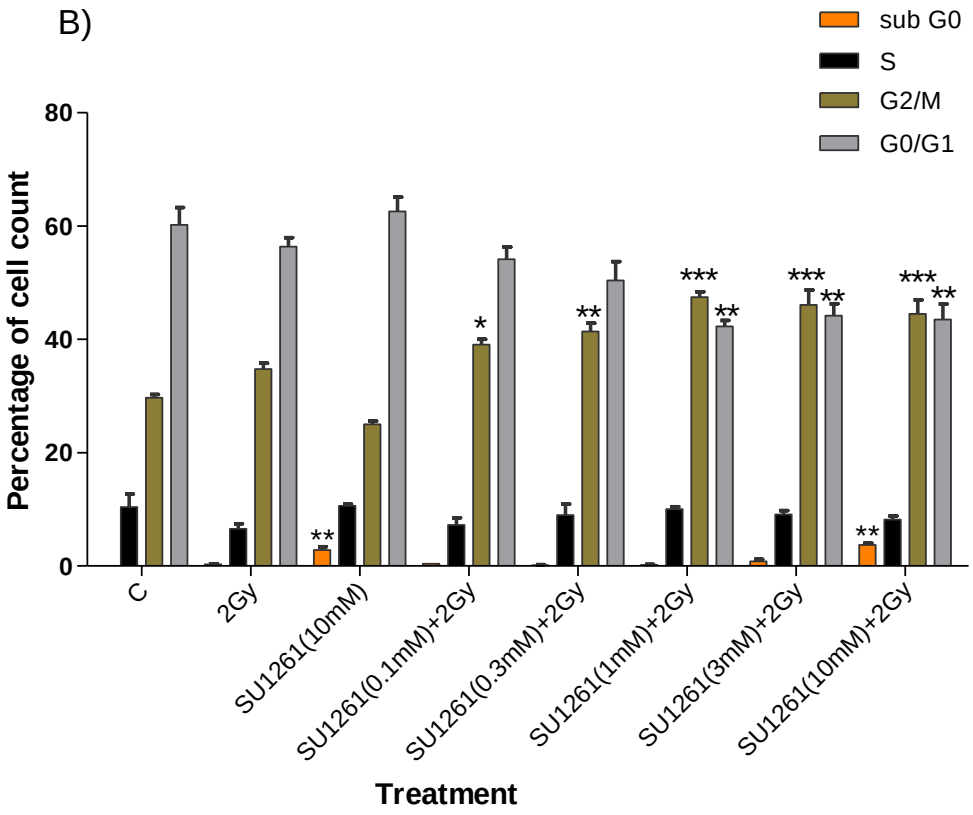


**Figure 4.17: Effect of the combination of SU1261 in combination with XBR on cell cycle progression of PC3M-luc-C6 cell lines.** Cells were treated with SU1261 (0.1-10μM) for 24 hrs following XBR of radiation; after 24 hrs, cells were assessed by flow cytometry using propidium iodide (PI) for determination of total DNA content. The chart demonstrates the distribution of cells in the different phases of the cell cycle following treatment. Data shown are expressed as % of cell count. Each value represents the mean (± sd) of three separate experiments. *$P$<0.05 and ***$P$<0.001 compared with the non-treated control group.

## 4.3 Discussion

CRPC is an advanced stage of PCa which is associated with poor therapeutic outcome and high mortality rate in men worldwide. Currently, palliative therapy is the only available treatment option as no complete cure is available for patients suffering from CRPC (Maroto *et al.*, 2016). Aberrant activation of the IKK-NF-κB pathway has been associated with the tumourigenesis of many cancers, including PCa (Nguyen *et al*., 2014). Further, highly constitutive NF-κB protein levels have been linked with survival of cancer cells following radiation and chemotherapy treatment (Haffner et al., 2006). Thus, developing IKK inhibitors which target the NF-κB pathways has become an interesting area for many researchers in the cancer field. Numerous IKK inhibitor compounds have been developed: a β-carboline natural product PS-1145 and ML120B (Castro *et al.,* 2003; Wen *et al.,* 2006), BMS-345541 (Burke *et al.,* 2003; McIntyre *et al.,* 2003), SPC-839 (Palanki *et al.,* 2002). While these and similar agents have been extensively studied, their value in cancer treatment is limited due to the non-selectivity of these agents against IKKα and IKKβ, leading to potential harmful toxicities to normal cells and/or lethality (Chariot, 2009; Li *et al*., 1999; Shukla *et al.,* 2015).

An alternative approach that is gaining interest is to target IKKα. A growing body of evidence suggests that IKKα play a role in pathogenesis of number of cancer types including PCa (Luo *et al.*, 2007; Ammirante *et al.*, 2010; Mahato *et al.*, 2011; Jain *et al.*, 2012). In PCa, IKKα is a key mediator in the tumourigenesis of

PCa and development of CRPC (Luo *et al*., 2007; Ammirante *et al.*, 2010; Mahato *et al*., 2011; Jain *et al.*, 2012). However, no potent selective IKKα pharmacological inhibitor has been identified to date. Our study is the first to demonstrate the anti-cancer cytotoxicity of the pharmacological inhibition of IKKα against highly metastatic androgen-insensitive PCa cells PC3-luc-C6 and PC3 cells. The effect on normal cells was also considered; thus the cytotoxicity screening on normal prostatic epithelial cell line (PNT2A) was tested.

As confirmed by Western blot analysis in the previous chapter (Chapter 3), our lead IKKα inhibitor, SU1261 (1-10μM), showed a highly selective inhibition on the non-canonical NF-κB pathway (p52 formation (IKKα) $IC_{50}$ = 3.925μM) in a concentration-dependent manner (Chapter 3, Figure 3.13) without affecting the canonical NF-κB pathway (IκBα degradation (IKKβ) $IC_{50}$ > 30μM: p65 phosphorylation (IKKβ) $IC_{50}$ > 10μM) (Chapter 3, Figures 3.4 and 3.5). Interestingly, in this study, the same concentration range of SU1261 (1-10μM) showed a significant cytotoxic effect against PCa cell lines, the PC3M-luc-C6 and PC3, and to a lesser extent against the normal prostatic epithelial cells, PNT2A. SU1261 (1-10 μM) induced a concentration dependant reduction in the growth rate of PC3M-luc-C6 and PC3 cells (Figures 4.1 and 4.2) as well as a concentration dependant reduction in cell viability (Figure 4.4A and Figure 4.5A). Furthermore, the delayed cytotoxic effect following SU1261 (1-10μM) treatment was assessed by a clonogenic survival assay showed a significant inhibition in the cell survival of PC3M-luc-C6 and PC3 cells (Figures 4.7A and 4.8A).

However, a higher concentration range of SU1261 (3-10μM) was required to inhibit growth and viability in normal PNT2A cells (Figures 4.3 and 4.6A), suggesting a shifting for the curve to the right and hence a potential therapeutic window for the treatment of PCa over non-cancerous cells.

We found that SU1261 inhibited the growth of PCa PC3M-luc-C6 and PC3 cells. This is in agreement with previous publications which link IKKα with PCa growth and development. One illustration of this link is the observation that when IKKα is knocked down by siRNA, STAT3 protein, a transcription factor, is inhibited, delaying the growth of castration-resistant PCa in the murine myc-CaP cell line (Ammirante *et al*., 2010). STAT3 protein is an important event for the mediation of growth proliferation, survival and development via regulation of different anti-apoptotic and survival gene expression such as Bcl-xL and survivin genes (Yue and Turkson, 2009; Darnell, 1997). Pharmacological inhibition of STAT3 activity resulted in growth inhibition and induction of apoptosis of human non-small cell lung cancer (NSCLC) bearing mice *in vivo* (Weerasinghe *et al*., 2007). Other possible mechanism of SU1261-induced PC3M-luc-C6 and PC3 cells growth inhibition is through upregulation of the tumour suppressor gene maspin. It is involved in metastasis and growth in some cancers. Overexpression of maspin protein inhibits the growth and metastasis in breast cancer in transgenic mice model (Shi et al., 2001). In PCa, Luo and his group showed that a mutation that deactivated IKKα in TRAMP mice inhibits both PCa growth and metastasis. It also correlates with upregulation in maspin protein expression (Luo *et al*., 2007).

Also, siRNA knockdown of IKKα in androgen-independent prostate cell lines PC3 and DU-14 resulted in the expression of maspin protein and inhibition of invasion and metastasis of these cells (Mahato *et al*., 2011). Moreover, growth inhibition of PCa can be argued that it acts through the non-canonical NF-κB pathway inhibitory effect of SU1261. For example, transfecting PC3 cells with a dominant-negative p100 mutant, there is a delay in nuclear RelB protein level translocation and an inhibition in the growth of these cells in xenograft model (Xu *et al*., 2010). All these explanations are possible mechanisms of IKKα inhibition induced cytotoxicity by SU1261. In future studies, by measuring the expression levels of such mentioned molecular changes, we can further our understanding on the mechanism of how IKKα inhibition acts on the growth of our PCa cells.

SU1261 showed less cytotoxic effect on normal prostate cell, PNT2A, in higher doses than observed against PCa PC3M-luc-C6 and PC3 cells. The normal development and growth of prostate is androgen dependent. Androgen (testosterone) is synthesised in testicles and then converted to the active metabolite, 5α-dihydrotestosterone (DHT), by 5α-reductase enzyme. It is taken up by prostate cells through the androgen receptors (AR) (Heinlein and Chang, 2004). Androgen-induced prostate regeneration is through activation of progenitor/stem cells (English *et al.*, 1987). Similar to its effect on PCa cell, IKKα activation is implicated in androgen-induced regeneration of the normal prostate through B lymphocytes. It has been found that B lymphocytes activate IKKα

within progenitor cells which subsequently activates the nuclear translocation of E2F1, a transcription factor. E2F1 binds to the promoters regions of the Bmi1 gene, the regulator of progenitor cell proliferation (Ammirante *et al.,* 2013). Although PNT2A cells originate from adult normal prostatic epithelial cells, these cells have been transfected with a plasmid containing SV40 genome to immortalise. This genetic modification could alter the normal biological characteristics of these cells and it should be taken into consideration. A range of normal cell lines should be investigated; however the initial findings in the PNT2A cells are encouraging.

Lack of cell growth and cell viability could be either due to either inhibition in proliferation or cell death, mainly by apoptosis. Most cytotoxic agents have been shown to induce apoptosis. Therefore, we first investigated if apoptosis was occurring by measuring the activity of caspase-3 as marker for apoptotic cell death. In this current study, we demonstrated that SU1261 (3-10µM) induces apoptosis in PC3M-luc-C6 and PC3 cell lines over a range of doses (Figures 4.10 and 4.11). In the PNT2A normal prostatic epithelial cell line, apoptosis only occurred at the maximum dose tested (10µM) (Figure 4.12).

Inhibiting IKKα also induces apoptosis in different cancer cells. Knocking IKKα by small hairpin RNA (shRNA) inhibited growth and induced apoptosis in human colorectal cancer cells, HCT116 and Ls174T cells *in vitro* and in nude mice *in vivo* (Margalef *et al.*, 2012). Similarly, it has been demonstrated that siRNA silencing of IKKα induces apoptosis in liver cancer cells, MHCC97H (Jiang *et al.*,

2010). Different scenarios can be contribute to apoptosis induction via IKKα. Huang *et al*. (2007) found that IKKα can downregulate the expression of the pro-apoptotic p53 protein. They revealed that IKKα-mediated CREB-binding protein (CBP) phosphorylation leads to switching the binding affinity of CBP, a histone acetyltransferase, from p53 to NF-κB, which concomitantly promotes tumour survival and inhibits cell apoptosis in human lung cancer A549 cells. STAT3, which is regulated by IKKα, contributes in PCa growth and is also found to control anti-apoptotic gene expression such as Bcl-xL (Ammirante *et al*., 2010; Yue and Turkson, 2009). The induction of apoptosis through inhibition of non-canonical NF-κB pathway is another possibility. For example, RelB has been demonstrated to upregulate the expression of the anti-apoptotic proteins, cIAP2, Bcl-2 and Bcl-xl in multiple myeloma cell lines (RMPI-8226, U266 and LP1 cells) (Cormier *et al*., 2013). In the same study, the knockdown of RelB expression in multiple myeloma LP1 cells with lentivirus carrying a shRNA directed against RelB markedly decreased the expression of cIAP2, Bcl-2 and Bcl-xl proteins and induced apoptosis. Similar, siRNA targeting of RelB in the PCa androgen-independent RM-1 cells was found to correlate with an inhibition in expression of the Bcl-xl anti-apoptotic protein (Zhu *et al.*, 2014). Further mechanistic studies considering the expression level of mentioned anti-apoptotic proteins following SU1261 is needed to verify their contribution in apoptosis induction of PC3M-luc-C6 cells.

For further investigation of the mechanisms involved in growth inhibition caused by SU1261, we assessed the cell cycle progression of PC3M-luc-C6 cells following SU1261 treatment. We observed no significant changes in the percentage of PC3M-luc-C6 cells in the various phases of the cell cycle. The highest administered dose of SU1261 (10μM) only caused an increase in the percentage of cells in subG1 (Figure 4.13A) but did not alter the proportion of cells in any other phase of the cell cycle at any dose tested. These results suggest that in our system in these cell lines and following pharmacological inhibition of IKKα, these drugs do not exert their effect through cell cycle arrest. In some studies, IKKα has been found to regulate the cell cycle protein such as cyclin D1 and Aurora-A protein (Cao *et al*., 2001; Demicco *et al.*, 2005; Prajapati *et al.*, 2006). However, the regulatory function of IKKα in cell cycle seems to be more tumour- and cell-type specific. For example, our result is in agreement with the findings of Mahato *et al.* (2011), who found that siRNA silencing of IKKα in two PCa cell lines, PC3 and DU145, did not alter the cell cycle. On the other hand, a recent study by Shukla *et al*. (2015) demonstrated that knockdown IKKα in PCa PC-3 and 22Rv1 cells using short hairpin RNA (shRNA) resulted in accumulation of cells in the G1 phase. However, knockdown of IKKα by siRNA did not affect the cell cycle progression in the breast cancer cell line, SKBr3 (Merkhofer *et al.,* 2010). In contrast, Tu *et al*. (2006) concluded that silencing of IKKα by siRNA impaired the cell cycle the breast cancer cell line, MCF7 in the S-phase. However, in our results the PC3M-luc-C6 cells were incubated with the drugs for 24hr and this period was not enough to induce any significant change

on cell cycle distribution of the PC3M-luc-C6 cells. We need to examine the effect of these IKKα inhibitors for longer incubation periods as well as using different PCa cell lines.

External beam radiation therapy in combination with chemotherapy has been documented for many years as an effective treatment in metastatic CRPC patients (Dulaney *et al*., 2016). In advanced metastatic cases of CRPC, high doses of radiation may be needed to improve the outcome in these patients. Nevertheless, the use of high doses of radiotherapy is limited due to harmful acute and chronic toxicities and complications (White *et al.*, 2015). In addition, CRPC cells are hormone insensitive and more radio-resistant compared with hormone sensitive cells in early stage of PCa (Xie *et al.,* 2010). One of the well-known mechanisms involved in the development of radiation resistance in PCa cells is through activation of the classical (RelA and p50) and the alternative (RelB and p52) NFκB pathways following radiation exposure (Kim *et al.*, 2006; Baud and Karin, 2009; Li and Sethi, 2010). Radiation has been documented to activate both NF-κB pathways and increase its nuclear transcription level *in vitro* and *in* vivo models (Rithidech *et al*., 2005; Ahmed *et al.*, 2006; Natarajan *et al.,* 2006; Lewis and Spandau, 2007). Therefore, we hypothesised that inhibition of NF-κB classical and alternative pathways in PCa cells would improve the sensitivity of these cells to radiation therapy and subsequently improve the therapeutic efficacy by decreasing the therapeutic doses and decreasing the associated toxicities.

Numerous reports have demonstrated that suppression of the classical NFκB subunits (p65) and inhibition of their activator (IKKβ) improves the radiosensitisation of various cancer cells (Egan *et al*., 2004). However, in addition to the serious potential toxicities against normal cells, inhibition of the classical NF-κB pathway will also potentiate the radiation-induced toxicity to normal tissue. NF-κB genes and proteins are pivotal for the radioresistance of normal tissues as they regulate various anti-apoptosis genes and antioxidant enzymes which protect normal tissues against radiation-induced DSBs damage (Guo *et al*., 2003; Kim *et al*., 2015). Similar to malignant cells, ionising radiation stimulates NF-κB proteins expression and their DNA activity in normal cells (Zhou *et al*., 1999). Hence overall advantages from targeting of this pathway are not the best choice.

Interestingly, in addition to its role in PCa progression, the alternative NFκB pathway has also been found to contribute to the radio-resistance of PCa cells (Zhu *et al*., 2015). As demonstrated in Chapter 3, the selective IKKα inhibitor SU1261 induced a potent inhibitory effect on the alternative pathway and decreased the expression of the non-canonical regulatory subunit p52 in a concentration-dependent manner without affecting the classical pathway, as measured by IκB-α degradation (Chapter 3, Figure 3.13 and Figure 3.5). Based on these data, it was hypothesised that inhibition of the alternative NF-κB pathway by the novel IKKα inhibitor SU1261 in PC3M-luc-C6 prior to XBR exposure would improve the radiosensitivity of these cells and potentiate the

effective therapeutic dose of radiation therapy. The results presented in this chapter demonstrated that combinations of the novel IKKα inhibitor SU1261 and XBR resulted in supra-additive levels of toxicity (CI<1, Figure 4.16). This suggests that treatment of PC3M-luc-C6 cells with SU1261 (1-10μM) for 24 hrs followed by XBR exposure (0-2Gy) potentiated the radiation-induced reduction in clonogenic survival, compared with XBR treatment alone (Figure 4.15). Furthermore, both SU1261 (10μM) and radiation (0-2Gy) were independently found not to cause cell cycle arrest (Figure 4.17). However, pre-treatment of cells with SU1261 (1-10μM) prior to radiation exposure (0-2Gy) led to cells accumulating in the G2/M phase of the cell cycle- i.e. induced a G2/M arrest. These results suggest that the IKKα inhibitor, SU1261 sensitised the PC3M-luc-C6s to radiation induced cytotoxicity and G2/M phase arrest.

This interaction is in agreement with previous studies that demonstrated that inhibition of non-canonical NF-κB pathway prior to radiation increased the radiosensitivity of androgen-insensitive PCa cell lines. For instance, silencing of RelB using siRNA or prevention of its nuclear translocation by p100 dominant negative mutation on RM 1 and PC3 respectively enhanced cell kill as measured by clonogenic assay and increased the sensitivity of these cells to radiation (Zhu *et al*., 2015; Holley *et al*., 2010). Furthermore, inhibiting the nuclear import of the RelB/p52 dimer using SN52, a cell-permeable small peptide, in PC3 and DU145 androgen-independent cells resulted in strong cytotoxicity on colony formation and radiosensitisation effect on PCa cells (Xu *et al*., 2008). This effect is

believed to be mediated mainly by RelB protein. RelB protein is highly expressed in PCa biopsies and associated with high Gleason scores in PCa patients (Lessard *et al*., 2005). In addition, RelB upregulates the expression of cIAP2, Bcl-2 and Bcl-xl anti-apoptotic proteins and MnSOD anti-oxidant enzyme. However, radiation interacts with DNA, directly or by generating free radicals in the cellular water content, which leads to DSBs and subsequently kill the cancer cells by apoptosis (Baskar *et al.*, 2012a; Verheij, 2008). Thus, inhibiting the RelB protein prior to radiation exposure will decrease the anti-apoptotic and anti-oxidant system within the cells, leaving the cells more susceptible to radiation-induced DSBs and apoptosis. This mechanism is suggested for SU1261-induced PC3M-luc-C6s radiosensitisation.

Cells that arrest in G2/M phase is a cytotoxic sign of radiation-induced DSBs (Fernet *et al*., 2010). We observed, pre-treatment of PC3M-luc-C6s with SU1261 prior to radiation exposure led to cells accumulating in the G2/M phase of the cell cycle. Following radiation, the presence of DSBs in tumour cells activates G2/M checkpoints that accumulate irradiated cells in G2 phases (Fernet *et al*., 2010). Cell cycle arrest is mediated by the ataxia telangiectasia mutated (ATM) kinase. It activates the checkpoint kinases (Chk) 1 and 2, which subsequently inhibit cyclin-dependent kinase (Cdk) 1/cyclin B1 activities, resulting in cell cycle arrest and preventing the progression from G2 phase into mitosis (Niida and Nakanishi, 2006). Thus, the G2/M arrest of PC3M-luc-C6s cell cycle induced by

the combination of SU1261 and radiation is probably due to the enhanced efficacy of radiation.

Although a large number of studies correlated the tumorigenesis of PCa and the expression of IKKα kinase, generation of selective IKKα inhibitor compounds which can be used clinically remains a dilemma. In the current study, for the first time, we present a pre-clinical cytotoxicity investigation of our lead novel IKKα inhibitor compound, SU1261, against aggressive androgen independent PCa PC3M-luc-C6 and PC 3 cell lines. In both cell lines, SU1261 induced an anti-tumour effect in the form of a decrease in growth rate, inhibition of cell viability and clonogenicity, mainly through the induction of apoptosis. SU1261 also showed lower toxicity against the normal epithelium prostate cells, PNT2A, compared with PCa cells. Despite the fact that radiotherapy is the major approach in PCa treatment, resistance of androgen-insensitive PCa cells to the radiation and the toxicity towards normal cells are two factors which limit its usefulness in current cancer treatment. Thus, combination therapies in cancer treatment using radiation have many advantages over mono-therapies. These advantages include an increase in anti-tumour activity against cancer cells, a decrease in cytotoxicity to normal cells, and reduced development of therapy resistance. Interestingly, the clonogenic survival assay and combination index analysis findings revealed that inhibition of IKKα kinase in PCa PC3M-luc-C6 cells by SU1261 prior to radiation exposure, resulted in a synergistic effect and induced accumulation of cells in the G2/M phase of cell cycle compared with the

effect of each therapy alone. Hence, these results suggest that targeting IKKα by SU1261 in combination with radiation is a promising therapeutic regimen in PCa treatment.

Overall, SU1261, or its derivative compounds which inhibit IKKα, is a promising compound for advanced CRPC therapy as a single therapy or in combination with radiotherapy. In our preclinical investigations, the new IKKα inhibitor, SU1261, is a novel molecule that has shown to have anti-cancer activity as a single compound and synergism in combination with radiation therapy on CRPC. These encouraging findings from this study provide a novel foundation for a possible future translation of these therapies into a clinical trial study. In the subsequent chapter, we investigate the cytotoxic consequences of the non-pharmacological inhibition of IKKα and IKKβ using siRNA silencing molecules, and the potential of this knockdown on the radiosensitivity towards the highly aggressive androgen-insensitive PCa cells, PC3M-luc-C6 cells.

# Chapter 5

# Study of the Cytotoxicity Effect of IKKα and IKKβ siRNA Silencing Alone or in Combination with External Beam Radiation (XBR) in Prostate Cancer Cell Lines

## 5.1 Introduction

As demonstrated in Chapters 3, SU1261 is a highly selective IKKα inhibitor and a novel agent in this class. Additionally, the unique pharmacological inhibition effect of SU1261 on IKKα over IKKβ was also accompanied by high levels of cytotoxicity against the PCa PC3M-luc-C6 and PC3 cell lines. This cytotoxicity included inhibition of growth; cell viability, clonogenicity, and the induction of caspase-3 activity in prostate cell lines (see Chapter 4). Furthermore, SU1261 was demonstrated to be a potent radiosensitiser in PC3M-luc-C6 cells (see Chapter 4, section 4.2.6). These data supported our hypothesis in section 1.4, which stated that IKKα is strongly implicated in PCa progression; suggesting that inhibition of this kinase could be a promising target in PCa therapy. Thus, an important line of enquiry was to find out more about the impact of inhibition of both IKKs kinases (IKKα and IKKβ) on prostate cancer cytotoxicity and radiosensitivity by employing non-pharmacological inhibition strategies.

Rather than the classical pharmacological inhibition strategy using pharmacological agents, inhibition of gene expression is an advanced and valuable method in molecular biology to study the roles of particular genes or proteins in mammalian cells. Among these strategies is using the small interference RNA (siRNA). SiRNA is a double-stranded RNA (20-25 base pairs) which inhibits the expression of targeted genes with complementary nucleotide sequences, subsequently leading to protein translation and synthesis inhibition (Elbashir *et al*., 2001). In this current study, we targeted the expression of IKKβ

and IKKα by employing specific synthetic siRNA targeting both kinases. In addition, a non-targeting (NT) siRNA negative control was used to distinguish the actual effect of the silencing of the IKKs from the general effects of the transfection procedure (more details can be seen in Chapter 2, section 2.4).

As discussed in the introduction (Chapter 1), IKKβ and IKKα are the main activators of the canonical and non-canonical NF-κB pathways respectively (Hacker and Karin, 2006; Huang and Hung, 2013). These pathways have been found to be highly expressed in PCa cells (Suh *et al*., 2002). IKKα has been implicated in PCa carcinogenesis (Luo *et al*., 2007; Ammirante *et al*., 2010; Mahato *et al*., 2011; Jain *et al*., 2012). However, because IKKβ controls the major classical NF-κB pathway, inhibition of this kinase has also been found to induce cytotoxicity in various PCa cell lines (Yemelyanov *et al*., 2006; Lee and Hung, 2008; Jain *et al*., 2012; Kong *et al*., 2015).

Ionizing radiation (IR) is one of the major therapies for various cancers, including PCa. However, the radioresistant nature of cancer cells often results in poor treatment outcome (Li and Sethi, 2010; Wu *et al*., 2011). The IKK-NF-κB pathways have been found to play a critical role in the development of radioresistance in cancer cells (Kim *et al*., 2006; Baud and Karin, 2009; Li and Sethi, 2010). As mentioned above, the NF-κB pathway has been found to be highly activated in PCa cells (Suh *et al*., 2002). Inhibition of IKKβ by siRNA or agents (BMS, SC-514 and TPCA-1) has been found to sensitise breast cancer and lung cancer cells to radiation therapy (Wu *et al*., 2011). Similarly, it was

found that canonical NF-κB pathway was inhibited by the IKKβ inhibitor PS-341, or by the use of an adenovirus encoding IκBα in colorectal cancer cells (Russo *et al*., 2001). However, inhibition of the non-canonical NF-κB pathway has also been demonstrated to sensitise PCa cells to radiation-induced cytotoxicity. Targeting the p52;p100 dimer using STI571, an inhibitor of tyrosine kinase, has been shown to enhance the prostate cancer DU-145 and PC-3 cells to radiation therapy (Xu *et al*., 2010). Similarly, we documented in Chapter 4 that SU1261, a novel IKKα inhibitor, inhibited the p52 formation and radiosensitised the PC3M-luc-C6 cells.

Therefore, we aimed to investigate the impact of IKKα and IKKβ silencing in PCa PC3M-luc-C6 cells using specific synthetic siRNAs and to evaluate its effects on cancer cell growth, cell cycle progression and caspase-3 induction. Further, using linear quadratic analysis model (more details can be seen in section 2.12), we aimed to study the radiosensitisation effect of direct non-pharmacological inhibition of both IKKβ and IKKα using siRNA in PCa PC3M-luc-C6. Western blot analysis was used to measure the protein expression of both IKKα and IKKβ using specific primary antibodies, and the expression of the p65 level for the total loaded protein sample.

## 5.2 Results

### 5.2.1 SiRNA silencing of IKKα and IKKβ in PC3M-luc-C6 cells

In order to optimise the knockdown of the IKKs with the siRNA, different concentrations of IKKα and IKKβ siRNA (25-100nM) were transfected into the PC3M-luc-C6 cells for 72 hrs which was found to be the optimal duration for silencing. The same doses of the negative control non-targeting (NT) siRNA were also employed to exclude any effect on the phenotype which could be due to the transfection process.

Figure 5.1 demonstrates the expression level of IKKα in PC3M-luc-C6 cells after 72 hrs of transfection. IKKα expression was significantly reduced using all siRNA concentrations. Surprisingly, as little as 25nM of siRNA against IKKα efficiently knocked down endogenous IKKα expression by approximately 65% (% of basal expression = 34.98 ± 14.01, $P<0.001$). In addition, transfection with higher siRNA IKKα concentrations (50-100nM) greatly decreased the IKKα expression by more than 95% ($P<0.001$). Moreover, treatment of cells with siRNA IKKα (25-100nM) did not have an off-target effect on IKKβ expression, even at the maximum concentration (100nM).

Similarly, Figure 5.2 shows the expression level of IKKβ following transfection with siRNA against IKKβ in PC3M-luc-C6 cells. The same duration (72hrs) and concentration of siRNA IKKβ (25-100nM) were used. Surprisingly, the lowest concentration (25nM) caused a statistically significant reduction in the level of IKKβ expression by more than 95% compared to the control basal levels (% of

basal expression = 6.17 ±4.82, *P*<0.001). This inhibition was further increased to more than 98% (% of basal expression = 1.68 ±2.38) with the highest siRNA concentration (100nM) compared with control cells (*P*<0.001). Furthermore, siRNA against IKKβ did not show any non-selectivity targeting on the IKKα level. In addition, (NT) as a negative control, did not target either IKKα or IKKβ; neither were any changes in the loading protein detected, as confirmed by assessment of p65 levels.

These results suggest that IKKα and IKKβ siRNAs in PC3M-luc-C6 cells are highly effective and selective, acting specifically without off-target inhibition even at the maximum concentration used. Thus, siRNA IKKα and IKKβ were used for non-pharmacological knockdown of IKKα and IKKβ levels for further studies, which are discussed in this chapter.

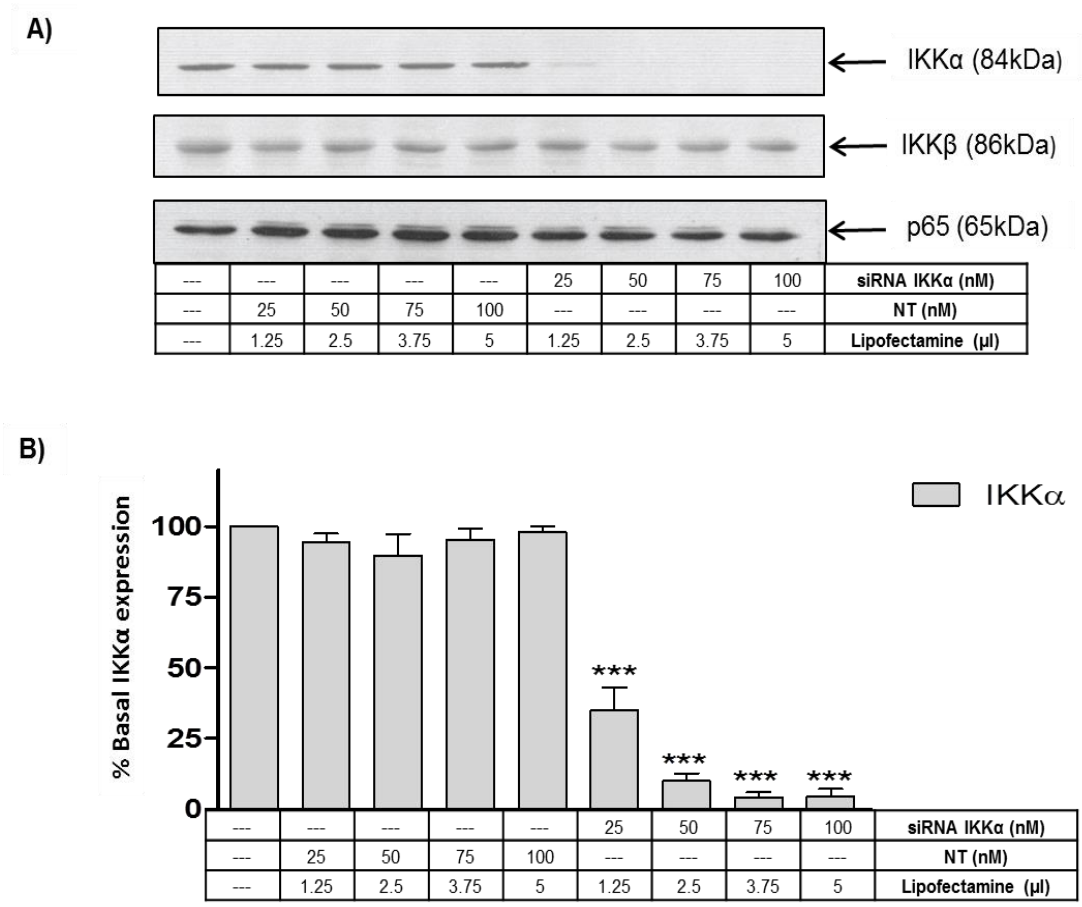


**Figure 5.1: The effect of siRNA IKKα on IKKα expression in PC3M-luc-C6.** Cells were transfected with non-targeting scramble sequence or siRNA IKKα up to a concentration of 100nM. Whole cell lysates were prepared, separated by SDS-PAGE, and then assessed for A) IKKα (84kDa), IKKβ (86kDa) and p65 (65kDa). B) Blots were quantified for percentage of basal IKKα expression by scanning densitometry. Each value represents the mean (±sd) of three independent experiments. Statistical analysis was carried out using a one-way ANOVA with Bonferroni correction post-test to compare with untreated control. ****P*<0.001 compared with the control.

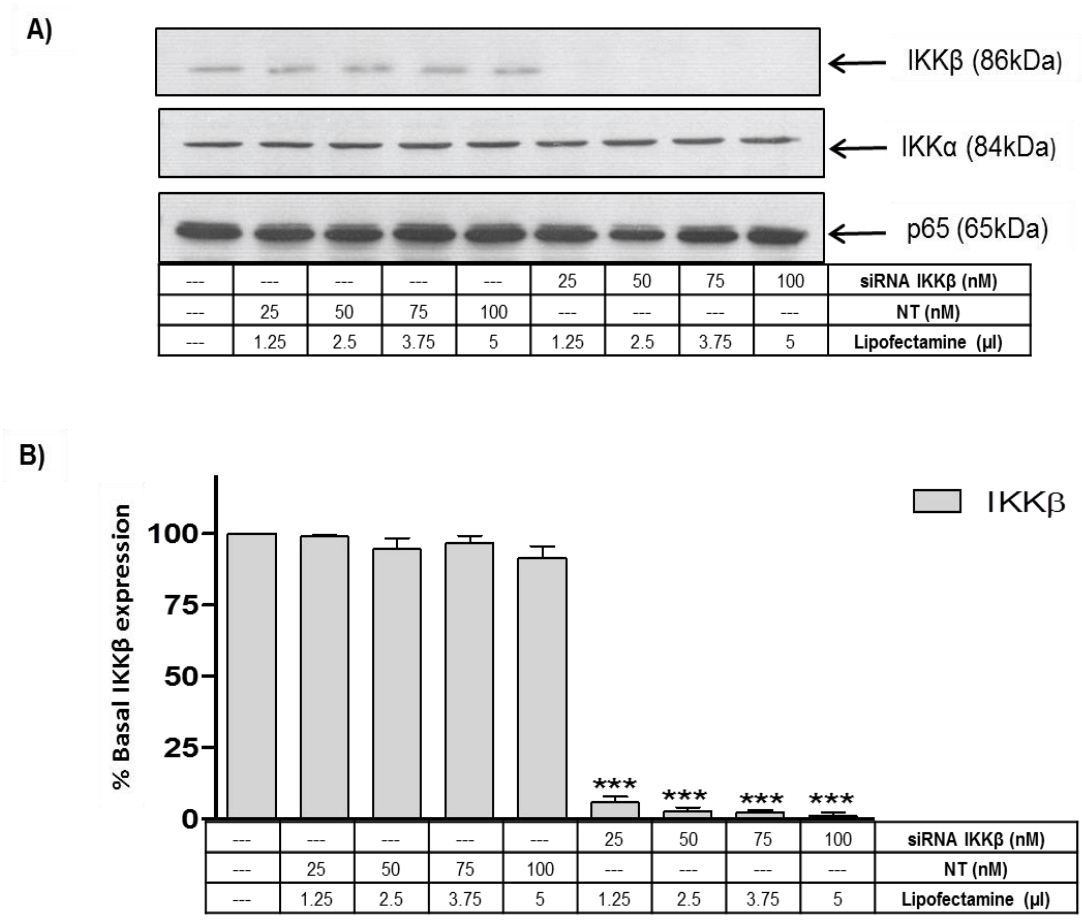


**Figure 5.2: The effect of siRNA IKKβ on IKKβ expression in PC3M-luc-C6.** Cells were transfected with non-targeting scramble sequence or siRNA IKKβ up to a concentration of 100nM. Whole cell lysates were prepared, separated by SDS-PAGE, and then assessed for A) IKKβ (86kDa), IKKα (84kDa) and p65 (65kDa). B) Blots were quantified for percentage of basal IKKα expression by scanning densitometry; Each value represents the mean (±sd) of three independent experiments. Statistical analysis was carried out using a one-way ANOVA with Bonferroni correction post-test to compare with untreated control. ****P*<0.001 compared with the control.

### 5.2.2 Effect of silencing the IKKs on PC3M-luc-C6 cells cytotoxicity

Two different doses of siRNA (50 and 100nM) were used to study the cytotoxic effect of IKKα and IKKβ knockdown by the relevant siRNAs in PC3M-luc-C6 cells. Before proceeding to the cytotoxicity assay, we first validated the expression levels of IKKα and IKKβ in each set of experiments to confirm that the silencing had occurred successfully.

#### *5.2.2.1 Validation of IKKα and IKKβ silencing*

For each set of cytotoxicity experiments, PC3M-luc-C6 cells were transfected with two different concentrations (50 and 100nM) of IKKα and IKKβ siRNA in addition to the negative control (NT). The whole cell extracts were then subject to Western blot to determine the basal expression of IKKα and IKKβ.

Figure 5.3 shows the blots of IKKα and IKKβ following transfection of the cells with 50nM siRNA. Similarly to our previous results (Figures 5.1 and 5.2), siRNA markedly diminished the expression of IKKα and IKKβ by approximately 95% (% of IKKα basal expression = 4.76 ± 0.94, $P<0.001$; % of IKKβ basal expression = 5.51 ± 4.06, $P<0.001$). However, as Figure 5.4 demonstrates, 100nM of siRNA totally inhibited the IKKα expression (% of basal expression = 1.1 ± 3.23) and largely reduced the IKKβ to almost 5% (% of basal expression = 4.97 ± 1.74) compared to untreated control cells ($P<0.001$). Additionally, no differences in loaded protein were noted as the total p65 levels of blots were similar.

These results confirmed our previous findings (Figures 5.1 and 5.2), which showed the highly selectivity of the used siRNAs against IKKα and IKKβ knockdown in PC3M-luc-C6 cells. Both concentrations of siRNAs (50 and 100nM) caused significant inhibition of IKKα and IKKβ expression compared to the control cells ($P$<0.001).

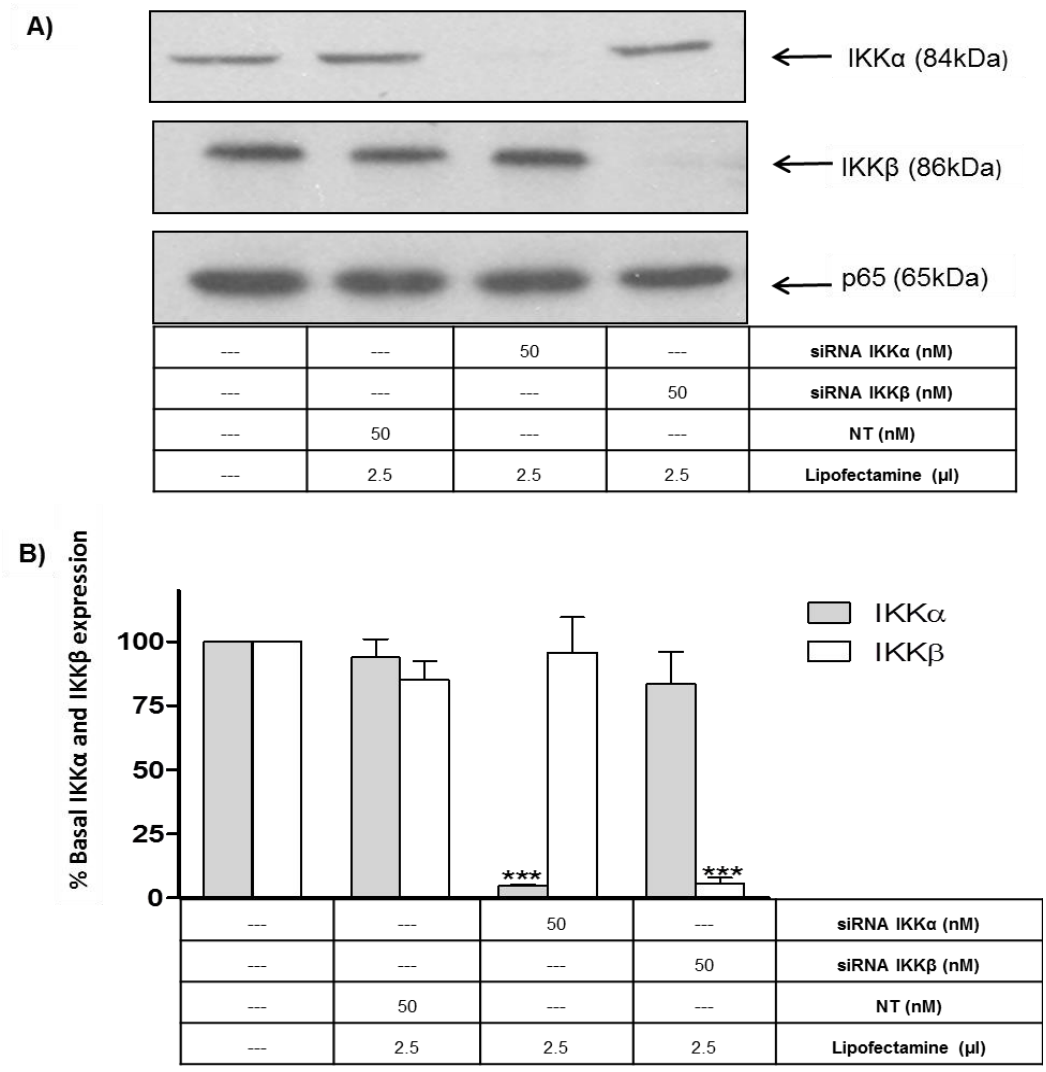


**Figure 5.3: The effect of siRNA IKKα and siRNA IKKβ on IKKα and IKKβ expression in PC3M-luc-C6.** Cells were transfected with 50nm of non-targeting scramble sequence or siRNA IKKα or siRNA IKKβ for 72 hrs. Whole cell lysates were prepared, separated by SDS-PAGE, and then assessed for A) IKKα (84kDa), IKKβ (86kDa) and p65 (65kDa). B) Blots were quantified for percentage of basal IKKα and IKKβ expression by scanning densitometry. Each value represents the mean (±sd) of three independent experiments. Statistical analysis was carried out using a one-way ANOVA with Bonferroni correction post-test to compare with untreated control. ****P*<0.001 compared with control.

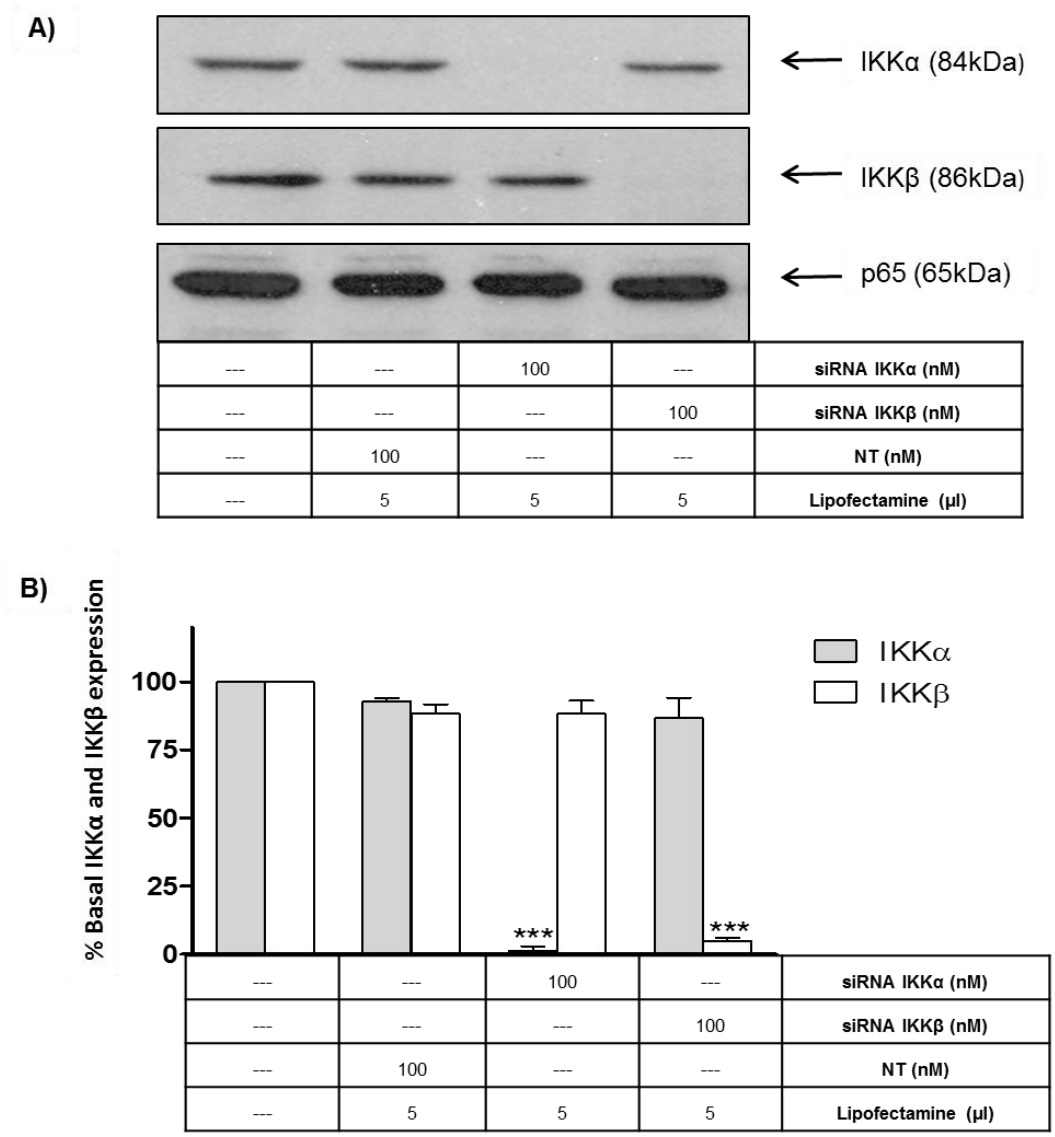


**Figure 5.4: The effect of siRNA IKKα and siRNA IKKβ on IKKα and IKKβ expression in PC3M-luc-C6.** Cells were transfected with 100nM of non-targeting scramble sequence or siRNA IKKα or siRNA IKKβ for 72 hrs. Whole cell lysates were prepared, separated by SDS-PAGE, and then assessed for A) IKKα (84kDa), IKKβ (86kDa) and p65 (65kDa). B) Blots were quantified for % of basal IKKα and IKKβ expression by scanning densitometry. Each value represents the mean (±sd) of three independent experiments. Statistical analysis was carried out using a one-way ANOVA with Bonferroni correction post-test to compare with untreated control. ****P*<0.001 compared with control.

#### *5.2.2.2 Effect of IKKα and IKKβ silencing on PC3M-luc-C6 cells growth*

In order to assess the effect of IKKα and IKKβ silencing on PC3M-luc-C6 cells growth, cells were treated with two different concentrations of IKKα and IKKβ siRNA (50 and 100nM). Following 72 hrs of silencing, the total number of cells in each well was counted using a haemocytometer and then normalised to the untreated control group.

As demonstrated in Figure 5.5, transfecting cells with 50nM of siRNA IKKα and IKKβ led to a significant reduction in cell number by approximately 50% (normalised cell number= 0.51 ± 0.04) and 40% (normalised cell number = 0.62 ± 0.02) for IKKα and IKKβ respectively compared with control group ($P$<0.001). Furthermore, transfecting cells with 100nM of siRNA IKKα resulted in a further significant decline in cell numbers of 60% (normalised cell number = 0.40 ± 0.18 compared with control cells ($P$<0.01). Similarly, less than half the number of cells were found in wells treated with 100nM of siRNA IKKβ (normalised cell number = 0.42 ± 0.08) compared with control group ($P$<0.01). Conversely, transfection of the PC3M-luc-C6 cells with 50nM and 100nM of the negative control (NT) resulted in only a slight inhibition in cell numbers by 8% (normalised cell number = 0.92 ± 0.04) and 15% (normalised cell number = 0.85 ± 0.15) respectively; however this reduction was not significant ($P$>0.05). We can conclude that the silencing of both kinases with two different siRNA concentrations resulted in a statistically significant reduction in the cell numbers of PC3M-luc-C6 cells compared with non-treated control wells. These

observations suggested that knockdown of both IKKα and IKKβ resulted in an inhibition of PC3M-luc-C6 cell growth.

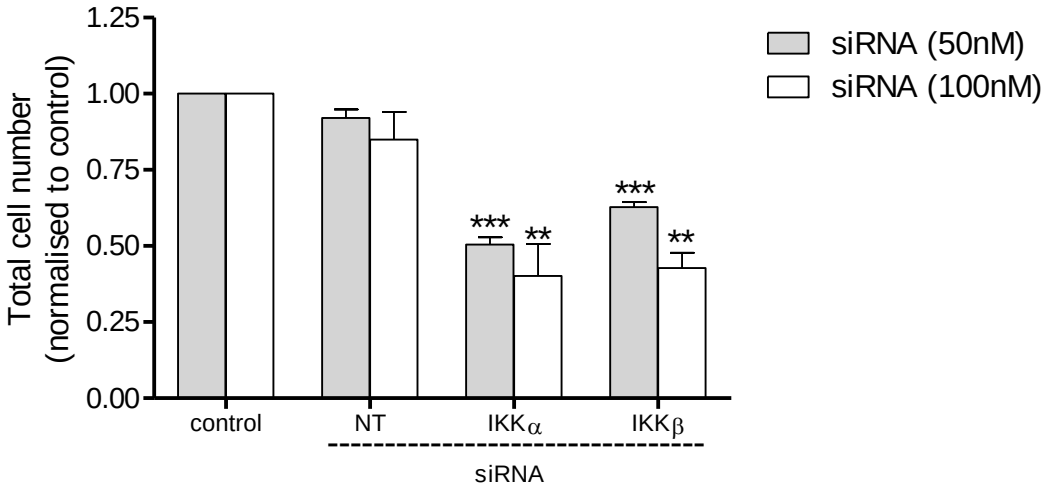


**Figure 5.5: Effect of siRNA IKKα and IKKβ transfection on PC3M-luc-C6 cells number.** Cells were transfected with 50 and 100nM of non-targeting (NT) scramble DNA, siRNA IKKα or IKKβ for 72 hrs, and then cells were counted using a haemocytometer for each treated group. Data shown are expressed as the average total cell number normalised to control group. Each value represents the mean (±sd) of three independent experiments. Statistical analysis was carried out using a one-way ANOVA with Bonferroni correction post-test to compare with untreated control. ***P*<0.01 and ****P*<0.001 compared with the non-treated control group.

#### *5.2.2.3 Effect of IKKα and IKKβ silencing on PC3M-luc-C6 cells clonogenicity*

In order to perform a more robust assessment of the effect of genetic knockdown of IKKα and IKKβ, we next investigated the effects of IKKα and IKKβ siRNA on the clonogenicity of PC3M-luc-C6 cells. Following 72 hrs of transfection with 50 and 100nM of siRNA, cells were re-seeded for assessment of colony formation and incubated for 10-14 days to assess the delayed cytotoxicity in terms of cells division and colony formation.

At both 50nM and 100nM siRNA administered concentrations, inhibition of IKKα expression caused a small but not significant decrease in cell survival fraction by 16% (SF = 0.84 ± 0.10) and 14% (SF = 0.86 ± 0.09) respectively compared to the untreated control group *(P*<0.01). Conversely, we observed a significant reduction in PC3M-luc-C6 survival fraction in the IKKβ transfected groups (Figure 5.6). Almost 30% of the inhibition in survival fraction was caused by the addition of 50nM IKKβ siRNA (SF = 0.72 ± 0.10) and a further reduction with 100nM IKKβ siRNA (SF = 0.64 ± 0.12) compared with control cells (*P*<0.01). In contrast, transfection of the cell with the scrambled siRNA (NT) did not show any significant change in the survival fraction of PC3M-luc-C6 (*P*>0.05).

These results demonstrated that IKKβ silencing has a significant impact on the colony formation capacity of PC3M-luc-C6 prostate cancer cells. Furthermore, knockdown of IKKα expression in these cells caused a small reduction in PC3M-luc-C6 cell survival fraction but was not statistically significant.

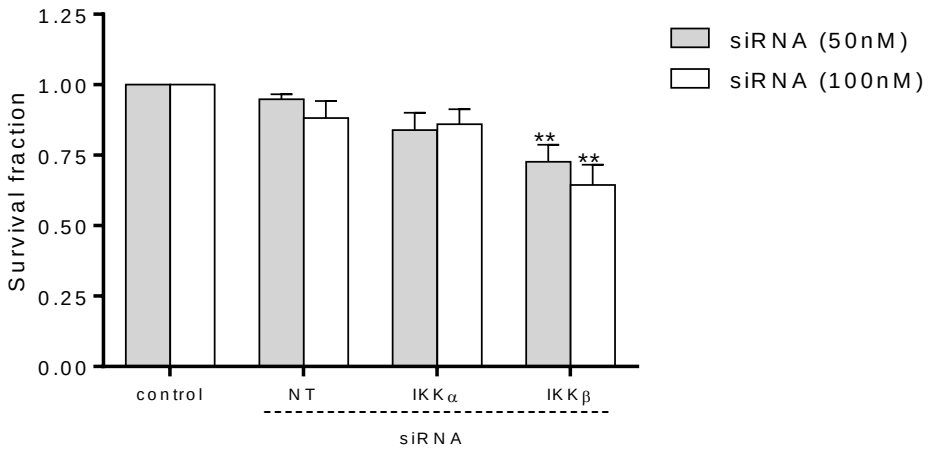


**Figure 5.6: Effect of siRNA IKKα and IKKβ transfection on PC3M-luc-C6 cell clonogenic survival.** Cells were transfected with 50 and 100nM of non-targeting (NT) scrambled, IKKα or IKKβ siRNAs for 72 hrs, and then clonogenic survival assays were performed for each treated group. Data shown are expressed as the average survival fraction compared to control group. Each value represents the mean (±sd) of three independent experiments. Statistical analysis was carried out using a one-way ANOVA with Bonferroni correction post-test to compare with untreated control. ***P*<0.01 compared with non-treated control group.

#### *5.2.2.4 Effect of IKKα and IKKβ silencing on caspase-3 activation as a marker of apoptosis in PC3M-luc-C6 cells*

We next interrogated whether IKKα and IKKβ had a role on PC3M-luc-C6 cells apoptosis. Therefore, we examined the level of caspase-3 induction as a marker of apoptosis following IKKα and IKKβ knockdown with siRNA treatment. As caspase-3 is induced in the early stages of apoptosis, we assessed caspase -3 levels 48hr and 72hr after transfection.

PC3M-luc-C6 cells treated with 50nM and 100nM of NT siRNA or IKKα siRNA did not show a significant difference in caspase-3 activity after 48hr and 72hr post-transfection when compared to untreated control cells ($P$>0.05, Figures 5.7 and 5.8). Similarly, following transfection with 50nM IKKβ siRNA for 48hr, no significant change in the caspase-3 levels were recorded compared with control group ($P$>0.05, Figures 5.7). Conversely, the same concentration of IKKβ siRNA (50nM) caused a significant increase in caspase-3 levels by 70% compared with control cells (caspase-3 fold increase = 1.69 ± 0.0.25, $P$<0.001, Figure 5.8) 72hrs after transfection. However, silencing IKKβ with 100nM siRNA increased apoptosis significantly after 48hr by 23% (caspase-3 fold increase = 1.23 ± 0.02, $P$<0.01, Figure 5.7) compared with control group. Additionally, caspase-3 activity significantly increased by nearly 60% (caspase-3 fold increase = 1.60 ± 0.06, Figure 5.8) compared to control cells ($P$<0.001) after 72hr of IKKβ siRNA (100nM) transfection.

These results indicate that neither NT siRNA nor IKKα siRNA are involved in the apoptosis process of PC3M-luc-C6 cells. However, IKKβ silencing induced the level of caspase-3 activity which suggests its major role in apoptosis in these cells.

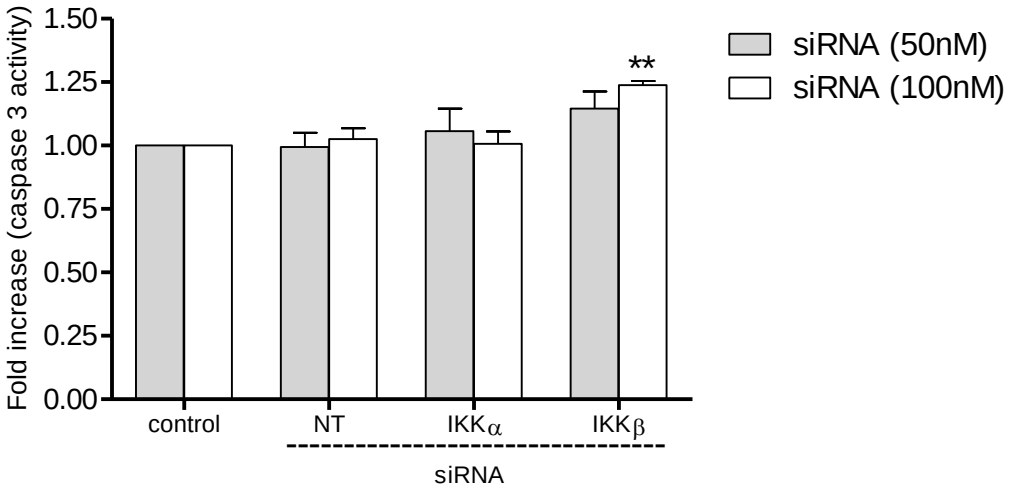


**Figure 5.7: Effect of siRNA IKKα and IKKβ transfection after 48 hr on caspase 3 activity on PC3M-luc-C6 cell lines.** Cells were transfected with 50 and 100nM of non-targeting (NT) scramble DNA, siRNA IKKα or IKKβ for 48hr, and then caspase 3 levels were measured using caspase 3 fluorometric assay. The chart shows the data as fold increase following treatment in caspase 3 level compared with control. Each value represents the mean (±sd) of three independent experiments. Statistical analysis was carried out using a one-way ANOVA with Bonferroni correction post-test to compare with untreated control. ***P*<0.01 compared with non-treated control group.

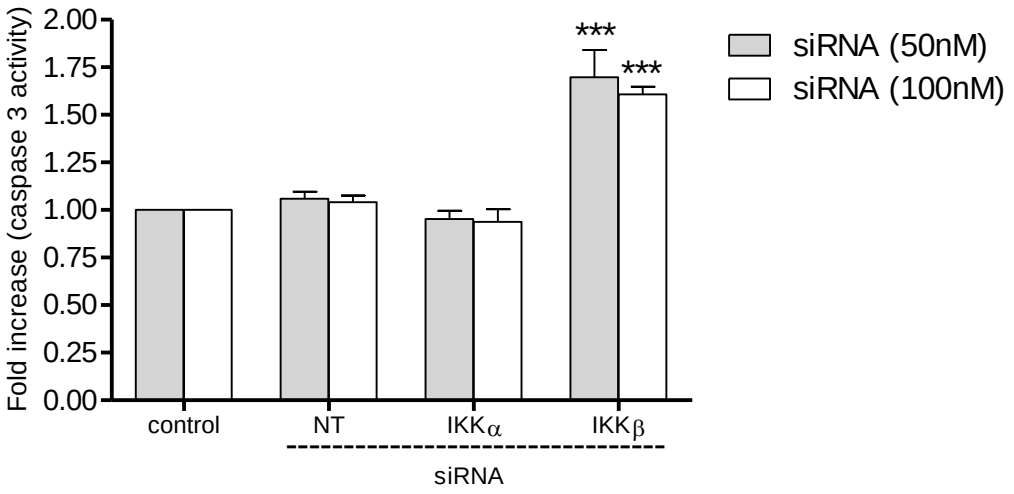


**Figure 5.8: Effect of siRNA IKKα and IKKβ transfection for 72 hr on caspase 3 activity on PC3M-luc-C6 cell lines.** Cells were transfected with 50 and 100nM of non-targeting (NT) scramble DNA, siRNA IKKα or IKKβ for 72 hrs, and then caspase 3 levels were measured using caspase 3 fluorometric assay. The chart shows the data as fold increase following treatment in caspase 3 level compared to control. Each value represents the (mean ± SD, n=3). Statistical analysis was carried out using a one-way ANOVA with Bonferroni correction and Dunnett's post-test to compare with untreated control. ****P*<0.001 compared with non-treated control group.

#### *5.2.2.5 Effect of IKKα and IKKβ silencing on PC3M-luc-C6 cell cycle progression*

We further examined whether the knockdown of IKKα and IKKβ using siRNA leads to alterations in the cell cycle distribution of PCa cells by assessing cell cycle population using flow cytometry following propidium iodide (PI) staining (see section 2.8) after transfection. Again, two concentrations of siRNA were used (50nM and 100nM). As Figures 5.9 and 5.10 demonstrate, cells transfected with both concentrations (50nM and 100nM) of NT, IKKα and IKKβ siRNAs showed no change the distribution of cells in the various cell cycle phases (G0/G1, G2/M and S phases) compared with control cells. However, a significant increase in subG0 fractions were found in cells transfected with both concentrations of IKKβ siRNA. Doses of 50nM and 100nM increased the percentage of cells subG0 phase significantly from 0.55 (± 0.56) in the control group to 2.30 (± 0.70, $P<0.05$, Figure 5.9) and 4.30 (± 0.42, $P<0.01$, Figure 5.10) respectively.

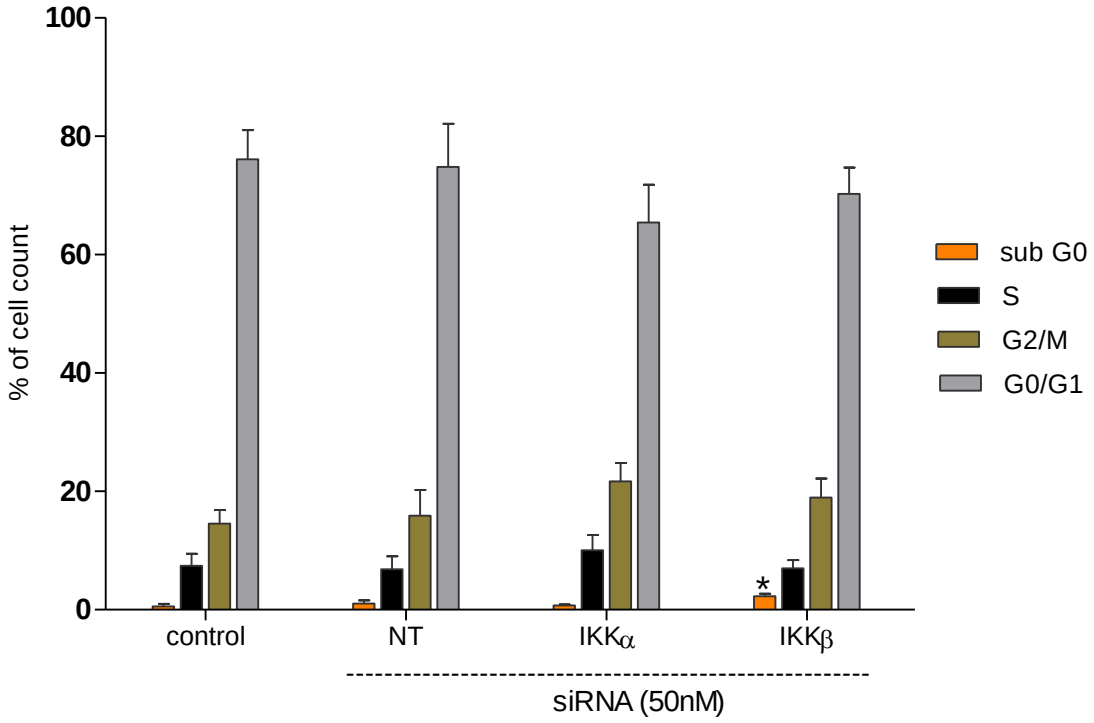


**Figure 5.9: Effect of 50nM of siRNA IKKα and IKKβ on cell cycle progression in PC3M-luc-C6 cell lines.** Cells were transfected with 50nM of non-targeting (NT) scramble DNA, siRNA IKKα or IKKβ for 72 hrs, then assessed by flow cytometry using propidium iodide (PI) for determination of total DNA content. The chart demonstrates the distribution of cells in the different phases of the cell cycle following treatment. Data shown is expressed as % of cell count. Each value represents the mean (±sd) of three independent experiments. Statistical analysis was carried out using a one-way ANOVA with Bonferroni correction post-test to compare with untreated control. **P*<0.05 compared with non-treated control group.

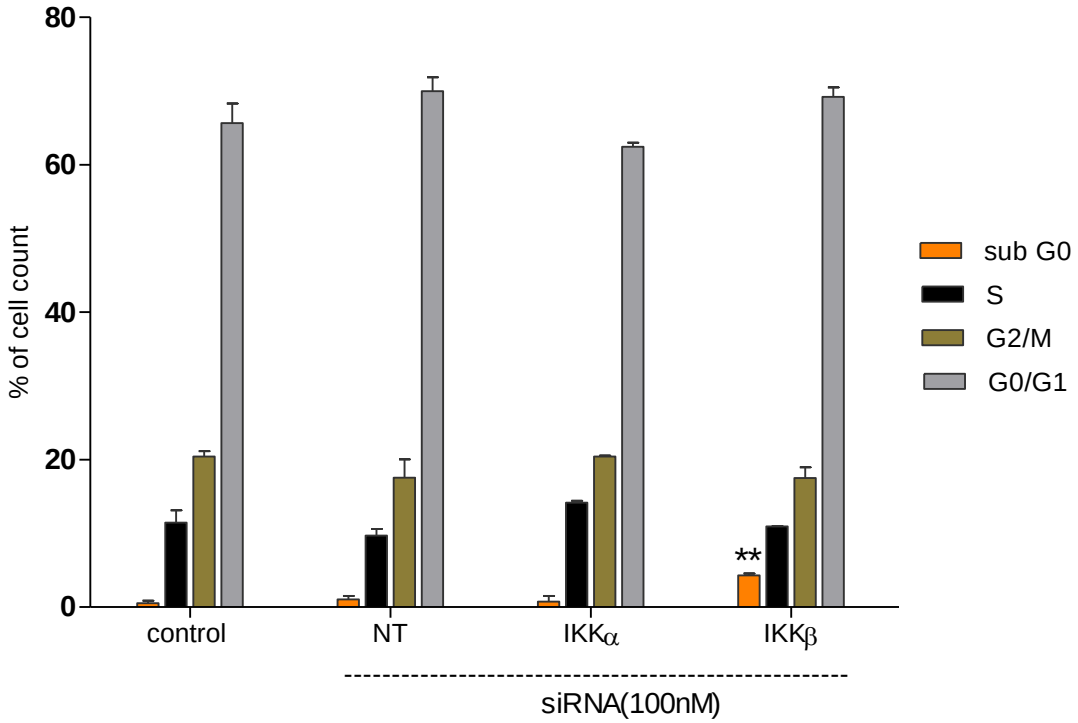


**Figure 5.10: Effect of 100nM of siRNA IKKα and IKKβ on cell cycle progression in PC3M-luc-C6 cell lines.** Cells were transfected with 100nM of non-targeting (NT) scramble DNA, siRNA IKKα or IKKβ for 72 hrs, then assessed by flow cytometry using propidium iodide (PI) for determination of total DNA content. The chart demonstrates the distribution of cells in the different phases of the cell cycle following treatment. Data shown are expressed as % of cell count. Each value represents the mean (±sd) of three independent experiments. Statistical analysis was carried out using a one-way ANOVA with Bonferroni correction post-test to compare with untreated control. ***P*<0.01 compared with non-treated control group.

### 5.2.3 Investigation of the radiosensitisation potential of silencing the IKKs in combination with External Beam Radiation (XBR) on PC3M-luc-C6 cells cytotoxicity

#### *5.2.3.1 Introduction*

Activation of the IKK-NFκB pathway plays an essential role in the development of cancer resistance to ionizing radiation (Baud and Karin, 2009, Li and Sethi, 2010). It has been published that pharmacological inhibition of IKKβ by the low molecular weight compound BMS-345541, as well as knockdown of IKKβ by lentiviral short hairpin RNAs (shRNAs), inhibits the repair of ionizing radiation induced Double Strand Breaks (DSB) in breast MCF-7 cells and human lung cancer cells H1299 and H1648 (Wu *et al*., 2011). In PCa, it has been found that Curcumin, which interferes with IKK activation, improved radiation-induced cytotoxicity of PC-3 cells (Chendil *et al*., 2004). Similar findings were also detected in IKKα and/or IKKβ knockout mouse embryonic fibroblasts (Shao *et al*., 2012).

To the best of our knowledge, none of the previous studies analysed the radiosensitisation effect of IKKα and IKKβ silencing by siRNA in combination with radiation in prostate cancer PC3M-luc-C6 cells. Thus, we aimed in this study to assess the radiosensitisation potential of silencing IKKα and IKKβ in combination with external beam radiation (XBR) by examining the clonogenic cell survival of IKK-silenced prostate cancer PC3M-luc-C6 cells. In addition, we investigated the impact of this combination on cell cycle progression. For clonogenic and cell cycle assays, cells were transfected with 50nM or 100nM of

IKKα and IKKβ siRNA for 72hr. Then plates were irradiated with 1 or 2 Gy. For radiosensitivity analysis, GraphPad Prism software, version 6.0, 2014 (GraphPad Software Inc, CA, USA) was used to fit clonogenic survival data to the linear quadratic curve as described previously in the methods and materials (section 2.12).

#### *5.2.3.2 Determination of the radiosensitising effect of silencing IKKα in combination with External Beam Radiation (XBR) on PC3M-luc-C6 using the linear quadratic model*

Groups of PC3M-luc-C6 cells were irradiated (0-2Gy), transfected with siRNA IKKα (50nM and100nM) for 72hr, or transfected with siRNA IKKα (50nM and 100nM) for 72 hrs followed by irradiation (0-2Gy). Clonogenic assays were then performed and survival fractions (SF) normalised to the untreated control groups (Figure 5.11). The obtained survival data was then fitted to the linear quadratic model (Figure 5.12).

Table 5.1 summarises the SF values of all treated groups. The SF fraction of PC3M-luc-C6 cells decreased by about 20% relative to control cells following irradiation with 1Gy (SF = 0.79 ± 0.04, $P>0.05$) and fell proportionally by 37% with 2Gy of radiation (SF = 0.63 ± 0.13, $P<0.01$). Cells transfected with 50nM and 100nM of siRNA IKKα showed insignificant inhibition in colony number by 19% (SF = 0.81 ± 0.019) and 26% (SF = 0.74 ± 0.016) respectively compared with the control group *(*$P>0.05$).

However, irradiation with 1Gy and 2Gy of XBR following 50nM siRNA IKKα transfection reduced the SF values to 0.67 (± 0.16, *P* <0.05) and 0.53 (± 0.14, *P* <0.001) respectively compared with untreated cells: these values were not statistically significant when compared with 1Gy or 2Gy irradiated group, but non-transfected treated cells (*P*>0.05). Similarly, silencing cells with 100nM of IKKα siRNA followed by XBR resulted in survival fractions of 0.58 (± 0.07, *P* <0.01) with 1Gy and 0.45 (± 0.11, *P* <0.001) with 2Gy. Again, there was no statistically significant difference in survival fraction compared with XBR alone treated group (*P*>0.05).

The clonogenic survival data (Figure 5.11) was fitted to the linear quadratic model (Figure 5.12 A) and the $IC_{50}$ and $DEF_{50}$ were calculated (Figure 5.12 B). The $IC_{50}$ (the dose of radiation that caused an inhibition of 50%) in PC3M-luc-C6 cells was 3.03 ±0.66. When cells were transfected with 50nM siRNA IKKα followed by radiation therapy, no significant change was found in the $IC_{50}$ value ($IC_{50}$ = 3.06 ±0.36). However, a very small reduction (12%) in the $IC_{50}$ ($IC_{50}$=2.88 ±0.23) was observed when PC3M-luc-C6 cells were transfected with 100nM siRNA IKKα followed by radiation but this change was not significant compared to cells treated by XBR alone (*P*>0.05). The dose enhancement factor at 50% cell death ($DEF_{50}$) was calculated. No statistically significant change was observed in the $DEF_{50}$ value ($DEF_{50}$ = 0.98 ±0.03) with the 50nM siRNA IKKα group compared to the radiation alone treated group. However, a very small increase in the $DEF_{50}$ value ($DEF_{50}$ = 1.05 ±0.04, *P*>0.05) for cells

transfected with 100nM of siRNA IKKα followed by radiation was observed, but once again this was not statistically significant.

The $DEF_{50}$ and $IC_{50}$ values indicated that transfecting cells with 50nM or 100nM siRNA IKKα did not enhance the cytotoxic potential of radiation. While 100nM of siRNA IKKα followed by XBR treatment resulted in a small enhancement of radiation-induced toxicity, it was insignificant statistically.

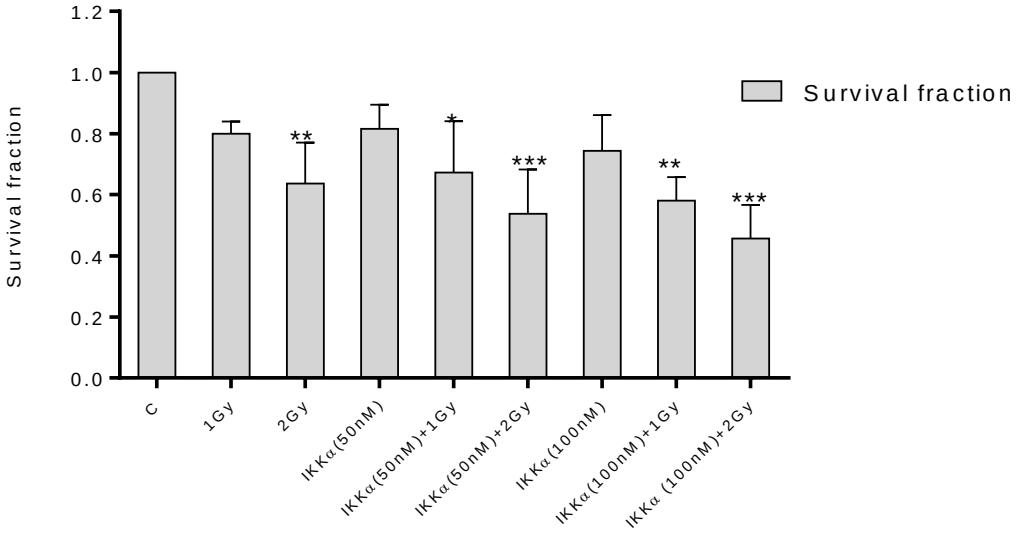


**Figure 5.11: Effect of combination of radiation and siRNA IKKα transfection on PC3M-luc-C6 cell clonogenicity.** Cells were irradiated with 1 or 2Gy, or transfected with 50nM or 100nM of siRNA IKKα for 72 hrs following by radiation with 1 or 2Gy, and then clonogenic survival assays were performed. Data shown are expressed as the average survival fraction compared to control group. Data shown are expressed as % of cell count. Each value represents the mean (±sd) of three independent experiments. Statistical analysis was carried out using a one-way ANOVA with Bonferroni correction post-test to compare with untreated control. *$P$<0.05, **$P$<0.01 and ***$P$<0.001 compared with the non-treated control group.

**A)**

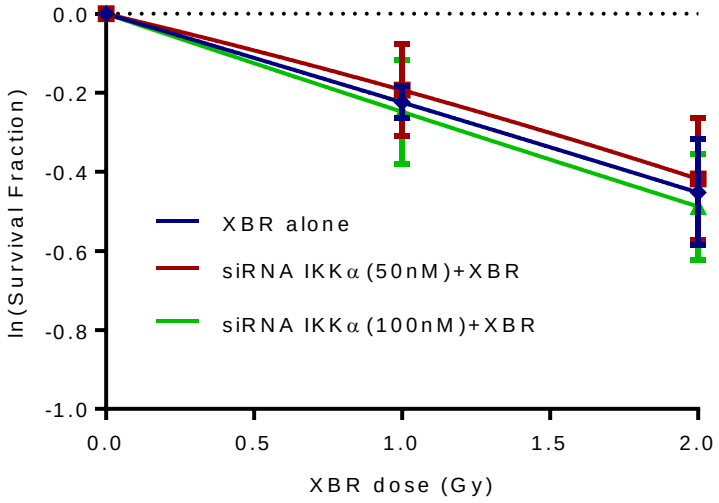


**B)**

| | Rx alone | siRNA IKKα (50nM) +Rx | siRNA IKKα (100nM) +Rx |
|---|---|---|---|
| $IC_{50}$ | 3.03 ±0.66 | 3.06 ±0.36 | 2.88 ±0.23 |
| $DEF_{50}$ | 1 | 0.98 ±0.03 | 1.05 ±0.04 |

**Figure 5.12: Radiosensitising effect of transfected PC3M-luc-C6 cells with siRNA IKKα to radiation.** Cells were irradiated with 1 or 2 Gy, or transfected with 50nM and 100nM of siRNA IKKα for 72 hrs following by irradiation with 1 or 2 Gy, then clonogenic survival assays were performed. **A)** Obtained clonogenic SF data was normalised to untreated control (radiation alone) or siRNA treated controls (50nM and 100nM alone) and fitted to a linear quadratic survival curve (Y axis is natural log of the normalised mean SF, and X axis is dose of radiation in Gy) **B)** and the $IC_{50}$ and the $DEF_{50}$ values of all treatment groups were calculated.

#### *5.2.3.3 Determination of the radiosensitising effect of silencing IKKβ in combination with External Beam Radiation (XBR) on PC3M-luc-C6 using the linear quadratic model*

As with the previous IKKα experiment (section 5.2.2.2), PC3M-luc-C6 Cells were irradiated (0-2Gy), transfected with of siRNA IKKβ (50nM and100nM) for 72 hrs, or transfected with of siRNA IKKβ (50nM and 100nM) for 72 hrs following by irradiation with XBR (0-2Gy). Clonogenic assays were then performed and survival fractions (SF) were normalised to the untreated control groups (Figure 5.13). The obtained survival data was then fitted to the linear quadratic model (Figure 5.14).

The SF values (± sd) of all treated groups are listed in Table 5.2. The cells treated with XBR (0-2Gy) in this experiment were from the same groups as for the previous results. Results were described in the previous section (section 5.2.3.2).

Our results indicated that the SFs were inhibited significantly by approximately 32% (SF = 0.68 ± 0.17) in cells transfected with 50nM of siRNA IKKβ compared with the control group ($P$<0.01). In addition, cells transfected with 100nM of siRNA IKKβ, demonstrated more than 40% inhibition (SF = 0.58 ± 0.03) of the colony formation of PC3M-luc-C6 cells compared with untreated cells ($P$<0.001). However, when 50nM of siRNA IKKβ transfected cells were treated with 1 and 2Gy irradiation, SFs values further declined significantly by 48% (SF = 0.52 ± 0.11) and 59% (SF = 0.41 ± 0.06) respectively compared to the control group ($P$<0.001). Similarly, co-treatment of cells with 100nM of siRNA IKKβ and 1Gy

XBR caused a highly significant inhibition of survival by more than 50% (SF = 0.47 ± 0.13) and with 2Gy to more than 60% (SF = 0.36 ± 0.03) compared to the control cells (*P*<0.001). However, statistically there was no significant change of SF when we compared the cells treated by radiation alone (1 and 2Gy) with the transfected cells (50 and 100nM siRNA) followed by XBR (*P*>0.05).

The data obtained from the linear quadratic model show that exposure of cells to XBR radiation following IKKβ knockdown with 50nM siRNA did not sensitise PC3M-luc-C6 cells to X-ray irradiation at any of the tested doses (Figure 5.13). Similarly, $IC_{50}$ values were calculated for XBR exposure alone ($IC_{50}$=3.03 ±0.66) and in combination with 50nM siRNA IKKβ ($IC_{50}$=2.95 ±0.84). Similarly, the $DEF_{50}$ value of 50nM siRNA IKKβ in combination with XBR ($DEF_{50}$ =1.02 ±0.07) indicated that there was a minimal, insignificant enhancement in cytotoxicity compared with XBR treated groups (*P*>0.05). However, when the concentration of siRNA IKKβ was increased to 100nM followed by irradiation, this led to a further decrease in the XBR dose required to kill 50% of the cell population from 3.03Gy to $IC_{50}$=2.67 ±0.64 as well as an increase in $DEF_{50}$value from 1 to 1.13 ±0.09 compared with radiation treatment alone.

In conclusion, the obtained values of $IC_{50}$ and $DEF_{50}$ indicate that treating siRNA IKKβ (100nM) PC3M-luc-C6 transfected cells with XBR at 1 and 2Gy showed a small sensitisation to radiation therapy and resulted in slight enhanced radiation-induced cytotoxicity compared to XBR alone. Nevertheless the *P* value indicates that this enhancement is not significant (*P*>0.05).

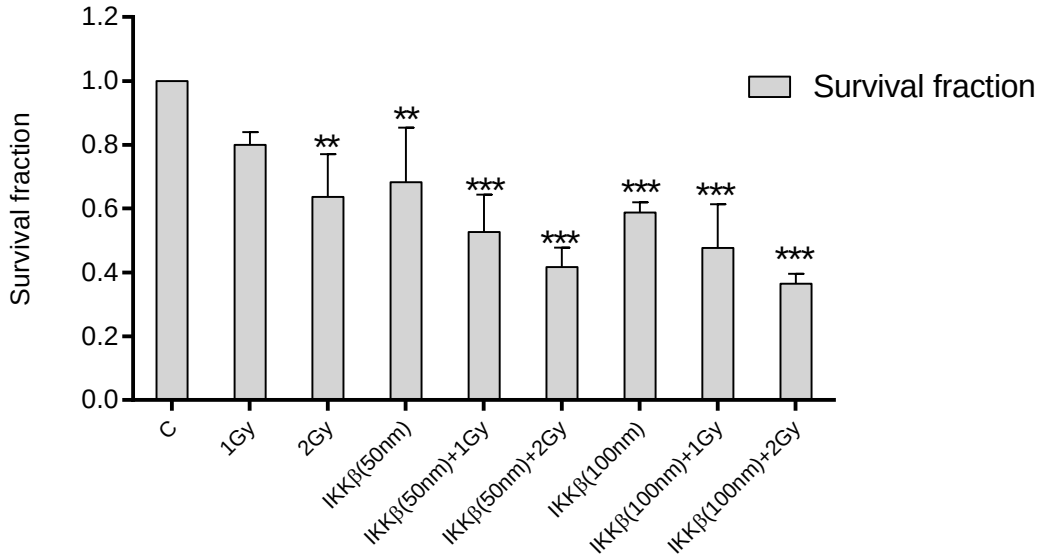


**Figure 5.13: Effect of combination of radiation and siRNA IKKβ transfection on PC3M-luc-C6 cell clonogenicity.** Cells were irradiated with 1 or 2Gy, or transfected with 50nM or 100nM of siRNA IKKβ for 72 hrs followed by radiation with 1 or 2Gy, and then clonogenic survival assays were performed. Data shown are expressed as the average survival fraction compared to the control group. Each value represents the mean (±sd) of three independent experiments. Statistical analysis was carried out using a one-way ANOVA with Bonferroni correction post-test to compare with untreated control. *$P$<0.05, **$P$<0.01 and ***$P$<0.001 compared with the non-treated control group.

**A)**

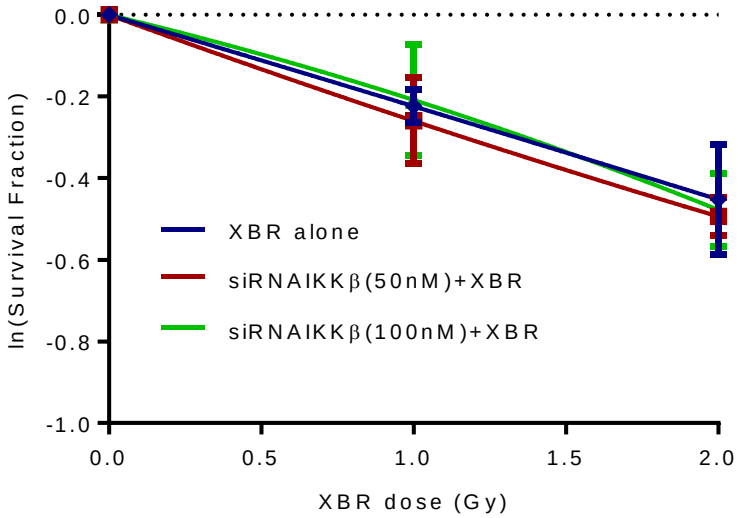


**B)**

| | Rx alone | siRNA IKKβ (50nM) +Rx | siRNA IKKβ (100nM) +Rx |
|---|---|---|---|
| **$IC_{50}$** | 3.03 ±0.66 | 2.95 ±0.84 | 2.67 ±0.64 |
| **$DEF_{50}$** | 1 | 1.02 ±0.07 | 1.13 ±0.09 |

**Figure 5.14: Radiosensitising effect of transfected PC3M-luc-C6 cells with siRNA IKKβ to radiation.** Cells were irradiated with 1 or 2Gy, or transfected with 50nM and 100nM of siRNA IKKβ for 72 hrs, followed by radiation with 1 or 2Gy, and then clonogenic survival assays were performed. **A)** Obtained clonogenic SF data was normalised to untreated control (radiation alone) or siRNA-treated controls (50nM and 100nM alone) and fitted to a linear quadratic survival curve (Y axis is the natural log of the normalised mean SF, and X axis is dose of radiation in Gy) **B)** and the $IC_{50}$ and the $DEF_{50}$ values of all treatment groups were calculated.

#### *5.2.3.4 Effect of IKKα and IKKβ silencing effect in combination with External Beam Radiation (XBR) on PC3M-luc-C6 cells cycle progression*

The progression of PC3M-luc-C6 cells through the cell cycle was investigated next in order to assess whether the XBR radiation following IKKs silencing could cause an abrogation of the normal cycling of cells. Our previous results showed that neither silencing the IKKs nor XBR alone affected the normal cell cycle of PC3M-luc-C6 cells. In this analysis, cells were either exposed to XBR alone (0-2Gy) or transfected with siRNA (50nM and 100nM) for 72 hrs. For combination treatment, cells were transfected with siRNA (50nM and100nM) for 72 hrs followed by XBR (0-2Gy). After 24 hrs of radiation, cells were assessed by flow cytometry using propidium iodide (PI) for determination of total DNA content, as described in section 2.8. Figures 5.15 and 5.16 show the effect of siRNA IKKα and IKKβ respectively in combination with XBR therapy on the percentage of cells in each phase of the cell cycle. Generally, none of the treatment groups exhibited any significant changes in the G0/G1, G2/M and S phases of the cell cycle ($P>0.05$). However, a change was observed in the subG0 peak, which represents the fraction of non-viable cells. Exposure of the cells to radiation significantly increased the percentage of cells in the subG0 phase from 0.36 (± 0.28) in untreated control group to 1.40 (± 0.26, $P<0.01$) and 2.06 (± 0.11, $P<0.001$) with 1 and 2Gy respectively. No other major changes were observed in the pattern of cell cycle phases among any of the treatment groups.

This suggests that exposure of the PC3M-luc-C6 IKKs siRNA transfected cells to radiation did not cause any major changes in the cell cycle progression.

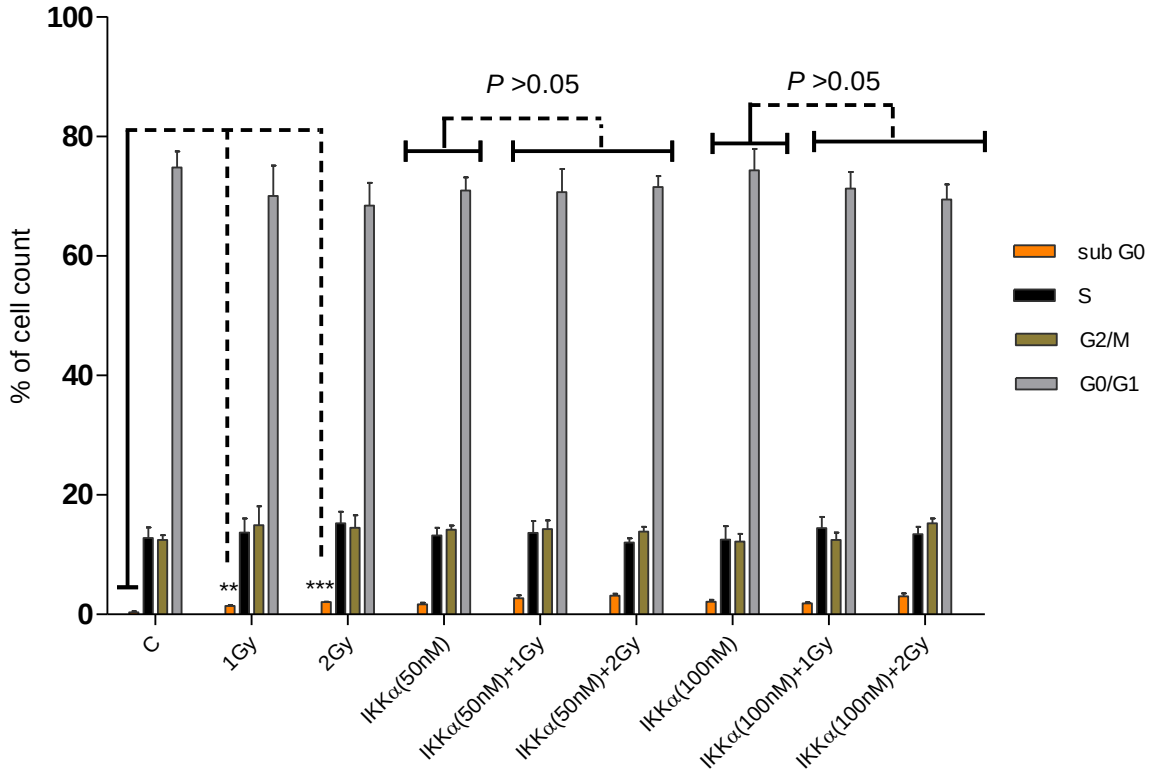


**Figure 5.15: Effect of the combination of radiation and siRNA IKKα on cell cycle progression in PC3M-luc-C6 cell lines.** Cells were irradiated with 1 or 2 Gy, or transfected with 50nM or 100nM of siRNA IKKα for 72 hrs and then irradiated with 1 or 2 Gy. After 24 hr cells were assessed by flow cytometry using propidium iodide (PI) for determination of total DNA content. The chart demonstrates the distribution of cells in the different phases of the cell cycle following treatment. Data shown are expressed as a percentage of cell count. Each value represents the mean (±sd) of three independent experiments. Statistical analysis was carried out using a one-way ANOVA with Bonferroni post-test to compare to the untreated control (for radiation treated groups) or to the IKKα treated group (for combination treated groups). ***P*<0.01 and ****P*<0.001 compared with the indicated group in the figure.

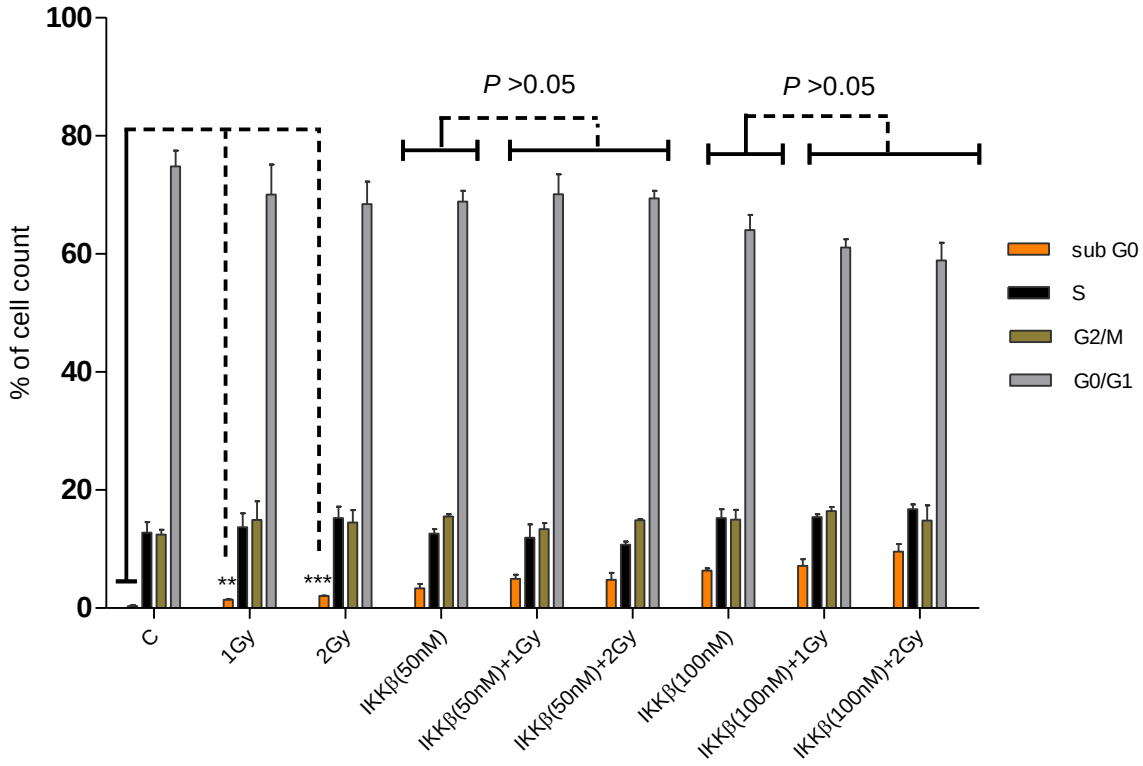


**Figure 5.16: Effect of the combination of radiation and siRNA IKKβon cell cycle progression in PC3M-luc-C6 cell lines.** Cells were irradiated with 1 or 2 Gy, or transfected with 50nm or 100nm of siRNA IKKβ for 72 hrs and then irradiated with 1 or 2 Gy, after 24 hr cells were assessed by flow cytometry using propidium iodide (PI) for the determination of total DNA content. The chart demonstrates the distribution of cells in the different phases of the cell cycle following treatment. Data shown are expressed as a percentage of cell count. Each value represents the mean (±sd) of three independent experiments. Statistical analysis was carried out using a one-way ANOVA with Bonferroni post-test to compare to the untreated control (for radiation treated groups) or to the IKKβ treated group (for combination treated groups). ***P*<0.01 and ****P*<0.001 compared with the indicated group on the figure.

## 5.3 Discussion

In the previous chapter (Chapter 4) the cytotoxicity of the first in class novel SU1261 was demonstrated to be selective against IKKα in PCa cells. Thus, in this chapter the aim was to compare and assess the impact of inhibition of the major kinases IKKα and IKKβ at the protein level and, to determine the effect of this inhibition on cell growth rate, clonogenic survival, induction of apoptosis, cell cycle progression and also to determine radiosensitisation effect which was carried out by treatment of increasing doses of ionising radiation, as measured by the clonogenic capacity and cell cycle distribution of PCa cells. To achieve these aims, siRNA specific for IKKα and IKKβ were used to knockdown expression of both kinases in PC3M-luc-C6s cells.

Efficiently, by using siRNA transfection the expression of both IKKα and IKKβ kinases were largely inhibited in PC3M-luc-C6 cells as confirmed by Western blot analysis. Using a dose range of 50-100nM, both siRNAs exhibited a potent inhibition in IKKs protein expression in PC3M-luc-C6 cells by more than 90% (Figures 5.1 and 5.2). Also, no off-target effects were detected of siRNA IKKα on IKKβ expression and vice-versa as confirmed by the expression levels of both kinases following transfection. Therefore, the knockdown strategy using siRNA was efficient at silencing IKKα and IKKβ expression and optimal conditions were established.

Similar to SU1261, silencing of IKKα reduced the total number of cells (Figure 5.3) and displayed no effect on the cell cycle distribution (Figure 5.5) of PC3M-

luc-C6 following 72hr of transfection. However, in contrast to SU1261, knockdown of IKKα did not result in a significant change in clonogenicity (Figure 5.7), caspase-3 activity (Figure 5.8) or radiosensitivity (Figure 5.9) on PC3M-luc-C6 cells. These results suggest that non-pharmacological inhibition of IKKα using siRNA technique does not show similar cytotoxicity profile in PC3M-luc-C6 cells similar to our previous finding when IKKα is inhibited pharmacologically by SU1261.

This conflict in the cytotoxicity results between the effect IKKα inhibition by SU1261 compound and siRNA on PC3M-luc-C6 could be explained mainly by the different inhibition strategy between the two agents. The molecular inhibition mechanism following RNA interference method and small-molecule compound is greatly different, thus correlating phenotypes between the two agents is not always straightforward (Weiss *et al*., 2007). While both SU1261 and siRNA IKKα are targeting IKKα kinase, the inhibitory mechanisms involved for siRNA and SU compounds not the same: SU compounds contain an azole ring which specifically binds to the ATP binding domain of the IKKα amino-terminal kinase inhibiting the kinase activity but not affecting the protein level, whereas, siRNA suppresses the IKKα protein expression totally by targeting mRNA cleavage and interacting with the double-stranded Tat RNA-binding protein (TRBP) or PACT (PKR activating protein). Our previous results within our group (data not shown) showed that using siRNA IKKα 100nM in PC3M-luc-C6 cells or 200nM in Panc1 cells (pancreatic cancer cell line) did not inhibit the formation of p52 in both cell

lines. These data suggested that knockdown of IKKα using our siRNA transfection reagent did not subsequently inhibit the non-canonical NF-κB pathway in PC3M-luc-C6 cells. This could explained in part the difference of phenotypic profiles on PC3M-luc-C6 cells between the pharmacological inhibition of IKKα using small-molecule SU1261 and non-pharmacological by siRNA. Therefore, using different siRNA transfection reagents or different RNA interference (RNAi) method such as using small hairpin RNA (shRNA) could be useful in the future.

The compensatory mechanism between IKKα and IKKβ could be also play a critical role in the negative cytotoxic impact following inhibition of IKKα by siRNA. It has been found that the both kinases compensate each other and, but not exclusively involve IKKβ in the classical and IKKα in the alternative NF-κB pathway. In our results, IKKα expression was greatly inhibited (more than 90%). The inhibition of the non-canonical pathway can lead to induction of the canonical NF-κB pathway which is a known survival pathway. It has been demonstrated in lymphoma ABC DLBCL cells that neither the knocking down IKKα using shRNA nor a small molecule IKKβ inhibitor individually caused a phenotypic effect, however using a small molecule IKKβ inhibitor in silenced IKKα cells induced a synergetic effect on cell death and caspase 3/7 activation suggesting the compensatory mechanism between the two kinases (Lam *et al*., 2008). Therefore, this compensatory phenomenon between IKKα IKKβ might be contributing in the negative phenotypic effect of knockdown IKKα using siRNA in

PC3M-luc-C6 cells. So, dual inhibition of both IKK pathways could be useful in the future to study the compensation and augmentation properties between the both IKKs in PC3M-luc-C6.

In addition to the previous argument, one explanation for the negative impact of knockdown IKKα on PC3M-luc-C6 cytotoxicity is that the presence of a truncated form of IKKα of 45 kDa (referred to as p45- IKKα). The truncated IKKα is a nuclear isoform of active IKKα which contains the kinase domain but lacks several regulatory regions. It has been found to be associated with advanced human colorectal cancer (Margalef *et al*., 2012; Luo *et al*., 2007). When we performed the transfection process with siRNA followed by western blot analysis of PC3M-luc-C6 cells cytoplasmic samples, we observed that most of the IKKα was according to the expected size of 84 kDa. Unexpectedly, the same primary anti-IKKα antibody recognized a double band of around 45 kDa that was highly expressed in the cytoplasmic fraction and was not inhibited along with wild type IKKα (data not shown). Truncated p45-IKKα has been demonstrated to prevent apoptosis and stimulate the growth of colorectal cancer cells *in vitro* and in xenograft mice (Margalef *et al*., 2012). This could explain in part why transfection of PC3M-luc-C6 cells with siRNA IKKα did not induce apoptosis. However, further investigation using specific primary antibody for p45-IKKα is needed to clarify this possibility: is it a truncated p45 or just non-specific binding?

As we mentioned in the introduction, IKKβ is critical for the main NF-kB classical pathway activation. IKKβ phosphorylates the inhibitor of NF-κB (IκBα) leading to its rapid degradation, and induces p65/RELA nuclear translocation, where it binds to its target DNA sequence, and induces the expression of numerous genes which are involved in inflammation (TNFα, IL-1 and COX2), cell proliferation (cyclin D1, cyclin D2, c-MYC and JUNB), angiogenesis (VEGF, IL-6, and IL-8), anti-apoptotic 'cell survival' (XIAP, BCL-xL, c-IAP2), invasion and metastasis (matrix metalloproteinase-9 and urokinase-type plasminogen activator) (Basseres and Baldwin, 2006; Lee and Hung, 2008). Previous studies showed that transfection of PCa PC3 and LNCaP cells with siRNA IKKβ resulted in a high reduction of viable cells number, migration and invasion however the inhibition of the siRNA IKKβ treated group was higher than siRNA IKKα treated group (Jain *et al*., 2012; Kong *et al*., 2015). Based on these facts, it was hypothesized that silencing of IKKβ expression in PC3M-luc-C6 cells using specific siRNA will also inhibit their growth. As expected, we found that knockdown of IKKβ expression at the optimal concentration (100nM) showed inhibition in PC3M-luc-C6 total cell number (Figure 5.5) and significantly decreased the colonies survival fraction (Figure 5.6). In addition, we demonstrated that the same concentration (100nM) caused a significant elevation in caspase-3 activity after 48hr of transfection (Figure 5.7) and further after 72hr (Figure 5.8), however no significant change observed in cell cycle progression (Figure 5.9). This data revealed that knockdown of IKKβ by siRNA

in PC3M-luc-C6 cells induced cell death mainly by apoptosis but with no effect on cell cycle progression.

IKKβ is implicated in cell cycle progression genes (cyclin D1, cyclin D2, c-MYC, and JUNB) through activation of the NF-κB p65/RELA heterodimer degradation and its nuclear translocation (Basseres and Baldwin, 2006; Lee and Hung, 2008). However, no significant changes of cell cycle were observed when we transfected the PC3M-luc-C6 with siRNA IKKβ. This might be because the effect is, in part, the regulatory function of IKKβ in cell cycle seems to be a cell-type-specific. For example, inhibition of IKKβ showed inhibition of the S-phase of prostate cancer cell line DU145; however no effect was detected in the cell cycle of PC3 cells (Yemelyanov *et al*., 2006). Our findings demonstrated that silencing of IKKβ by siRNA transfection does not alter the normal cell cycle progression of PC3M-luc-C6s. Further investigation using wide range of PCa cell lines is needed to indentify the effect of IKKβ in cell cycle regulation.

As discussed in the previous chapter (Chapter 4), the classical NFκB containing p65 and IκB-α proteins regulate anti-apoptosis genes and antioxidant enzymes which protect cells against radiation-induced DSBs damage (Baskar *et al*., 2012b). Inhibition of IKKβ improves the radiosensitisation of some cancer cells (Egan *et al*., 2004). Thus, it was hypothesised that knockdown of IKKβ using siRNA might sensitise PC3M-luc-C6s to radiation and potentiate radiation induced cell death. By analysing the dose required to induce 50% clonogenic cell kill ($IC_{50}$) and the dose enhancement factors at 50% clonogenic cell kill

($DEF_{50}$) of XBR exposure alone as shown in Figure 5.13, down regulation of IKKβ expression reduced the $IC_{50}$ value of XBR from 3.03Gy to 2.67Gy, and increased the $DEF_{50}$ from 1 to 1.13, however this effect was insignificant statically. These data suggests that silencing of IKKβ in PC3M-luc-C6s using our system did not significantly potentiate the radiation-induced cytotoxicity.

In conclusion, silencing of IKKβ demonstrated a greater cytotoxic effect on PC3M-luc-C6 compare to IKKα knockdown. Inhibition of IKKβ expression showed inhibition of growth and clonogenicity, induction of apoptosis, but with no radiosensitisiation potential. On the other hand, silencing of IKKα showed only inhibition in PC3M-luc-C6s total cell number. Despite IKKβ exerting high cytotoxicity in cancer cells it is not a safe target in cancer therapy. As IKKβ controls different important physiological functions through activation of the main NF-κB signalling pathway, inhibition of this kinase could lead to serious toxicity in normal cells and/or lethality. An early study of Li *et al.* demonstrated that, creating IKKβ knockout mice resulted in embryonic death at mid-gestation (Li *et al*., 1999). The authors demonstrated this lethality was due to massive apoptosis of the liver. Clinically, the use of different IKK inhibitors is associated with high toxicity in term of severe and chronic inflammation, immunosuppression and infection (Chariot, 2009).

# Chapter 6

# General Discussion

# and Conclusion

## 6.1 General discussion

PCa is one of the most commonly diagnosed cancers in men and remains the second leading cause of cancer-related deaths in the UK with 30 deaths every day (Cancer Research UK, 2016). In its early stages, PCa is treatable under the standard approaches including surgical prostatectomy, radiotherapy, hormonal therapy and chemotherapeutic agents. However, the vast majority of men with metastatic PCa develop CRPC which is associated with a high mortality rate (Maroto *et al*., 2016). To date, there is still no cure available to patients with advanced metastasis CRPC and the only available treatment options are palliative (Maroto *et al*., 2016). Effective new therapeutic agents and combinations are therefore critically needed to improve treatment and outcomes for these patients. Developing new therapies and identifying novel targets requires an understanding of the molecular mechanisms underlying PCa progression.

Since the discovery in 1986 by Nobel Prize winner David Baltimore's group of NF-KB as a major driver of immunity and survival in cells, it has been an attractive target for scientists in oncology (Hoesel and Schmid, 2013). While IKKβ regulates the major canonical NF-KB pathway involving phosphorylation and degradation of IκB-α and the nuclear translocation of p65, the IKKα homodimer regulates the non-canonical NF-KB pathway by mediating the processing of p100 to p52 to generate active p52-RelB heterodimers which then translocate into the nucleus (Solan *et al*., 2002). Both pathways lead to

expression of different genes involved in immunity, inflammation, and anti-apoptotic survival in normal and cancerous cells (Oeckinghaus and Ghosh, 2009).

The first logical step by many researchers in cancer treatment was to inhibit the NF-KB signalling pathway by targeting the major regulatory kinase IKKβ, which resulted in the development of a reasonable number of compounds such as PS-1145, ML120B, BMS-345541 and SPC-839 (Castro *et al*., 2003; Wen *et al*., 2006; Burke *et al*., 2003; McIntyre *et al*., 2003; Palanki *et al*., 2002). These agents showed a high regression impact on PCa experimentally (Yemelyanov *et al*., 2006; Jain *et al*., 2012; Kong *et al*., 2015). However, inhibition of IKKβ could not been clinically applied due to the associated serious side effects and toxicities that occurred due to severe reduction in anti-apoptotic protein expression in normal cells (Chariot, 2009; Li *et al*., 1999; Shukla *et al*., 2015; Gamble *et al*., 2012). Thus IKKβ or classical NF-κB (p65) inhibitors may not be safe targets for the treatment of cancer.

In the last decade, a growing body of evidence suggests that IKKα plays a critical role in tumorigenesis of a number of cancer types including colorectal, breast, pancreatic and prostate cancer (Fernandez-Majada *et al*., 2007; Park *et al*., 2005; Shiah *et al*., 2006; Luo *et al*., 2007). In PCa, IKKα is a key mediator in growth, metastasis and development of CRPC (Luo *et al*., 2007; Ammirante *et al*., 2010; Mahato *et al*., 2011; Jain *et al*., 2012). This cancer promoting effect of IKKα is believed to be via the regulation of non-canonical NF-KB pathway

subunits (RelB;p52 hetrodimer) or via regulation of numerous genes involved in prostate tumour growth and metastasis such as the *BMI1* and *maspin* genes (Ammirante *et al*., 2013; Luo *et al*., 2007). This evidence indicates an alternative and potentially less toxic approach than targeting IKKβ in PCa treatment. Despite accumulated data that suggest that IKKα is involved in the tumourigenesis of PCa, no potent selective pharmacological IKKα inhibitors have been identified to date. Due to the structural similarity between IKKα and IKKβ, which share 52% overall sequence homology within N-terminal kinase domains, development of a selective IKKα inhibitor compound is chemically challenging (DiDonato *et al*., 1997; Gamble *et al*., 2012). This is due to the fact that selective IKKα inhibitor molecules can also bind to the IKKβ kinase domain which limits their selectivity (Gamble *et al*., 2012). However, we have now developed in-house a novel class of IKKα inhibitor compounds as part of a CRUK small molecule drug discovery programme (led by Professor Simon MacKay).

The selectivity of these novel IKKα inhibitors SU compounds was assessed by an *in vitro* kinase assay and our lead compounds were demonstrated to have higher affinity and selectivity for purified IKKα protein than for IKKβ. Therefore, we aimed in Chapter 3 to assess the pharmacological characteristics of these novel IKKα inhibitors (SU compounds) in terms of their selectivity and potency against canonical and non-canonical NFκB pathways in the metastatic PCa cell line PC3M-luc-C6. Among these inhibitors, SU1261 was the most selective

compound against the IKKα kinase as it inhibits the non-canonical NF-κB pathway biomarker (p52 protein) in lower concentrations than that required to inhibit the canonical NF-κB pathway biomarkers (p65 and IκB-α degradation). Furthermore, data within our group also demonstrated the selectivity of SU1261 for IKKα in osteosarcoma U2OS and pancreatic Panc-1 cell lines (data not shown) indicating the high selectivity of this compound in different cancer cell lines. Although SU1261 showed a unique selectivity for IKKα over IKKβ in PC3M-luc-C6s, this compound still has potential to inhibit IKKβ at higher concentrations. Therefore, our team continues to strive to create more selective IKKα inhibitors. Nevertheless, SU1261 remains the most promising IKKα selective drug available worldwide.

In Chapter 4, SU1261 showed inhibition in the growth rate, cell viability, and clonogenicity by inducing apoptosis in two highly metastatic aggressive forms of androgen-resistant PCa cell lines, PC3 and PC3M-luc-C6 cells. SU1261 also demonstrated less cytotoxicity in normal prostate cells (PNT2A) compared with PCa cells. These findings suggest that the IKKα inhibitor, SU1261, which selectivity inhibits the non-canonical NF-KB pathway, is a promising compound for advanced CRPC therapy. However, several studies reported that IKKα is involved in metastasis independently of NF-κB (Huang and Hung, 2013; Huang *et al*., 2007; Solan *et al*., 2002). For instance, in both *in vivo* and *in vitro* models, IKKα is implicated in PCa metastasis by promoting transcriptional activity of *maspin* gene expression (Luo *et al*., 2007; Mahato *et al*., 2011). Furthermore,

IKKα also plays an important role in the regulation of angiogenesis. Angiogenesis is the process of the development and branching of blood vessels (Birbrair *et al*., 2015). In colorectal cancer for example, IKKα was found to induce expression of angiogenic genes such as interleukin-8 (IL-8), vascular endothelial growth factor (VEGF) and matrix metallo-proteinases-9 (MMP-9) (Agarwal *et al*., 2005). Furthermore, stimulation of fibrosarcoma tumours with lymphotoxin, a known activator of IKKα, was demonstrated to promote the release of macrophage inflammatory protein 2 (MIP-2), an angiogenic CXC chemokine, in a xenograft model (Hehlgans *et al*., 2002). Therefore, future investigations are required in this area to examine the impact of IKKα inhibition by SU1261 on metastasis and angiogenesis of PCa using additional experiments such as wound healing and cell migration assays. All of these genes are possible targets of SU1261, so further investigation using Western blot and gene array methods is needed to identify potential additional markers of IKKα besides non-canonical NFkB pathway biomarkers.

Combination therapies in cancer treatment have many advantages over monotherapies. These advantages include an increase in anti-tumour activity against cancer cells and reduced development of therapy-resistance (Komarova and Boland, 2013). Basically, an ideal combination therapy should have the following characteristics: 1) each single drug should exhibit anti-tumour activity without cross-resistance with other agents; 2) the synergistic activity between the drugs should be approved pre-clinically and 3) the combined drugs should

not exhibit additive toxicity to normal cells (Miles *et al*., 2002). In Chapter 4, we demonstrated that, aside from its anti-tumour effect as a single agent, SU1261 exhibits unique synergism in combination with radiation therapy on PCa cells. IKKα contributes to radiation resistance in PCa cells through the activation of nuclear translocation of RelB protein. RelB, which is highly expressed in PCa biopsies, drives the radioresistance in PCa through upregulation of cIAP2, Bcl-2 and Bcl-xl anti-apoptotic proteins and MnSOD anti-oxidant enzyme (Lessard *et al*., 2005; Zhu *et al*., 2015). Therefore, a study of the consequences of these genes following combination treatment is necessary to understand the mechanism involved in this effect. The encouraging findings from this study provide a novel foundation for a possible future translation of these therapies into a clinical trial study.

Despite CRPC being androgen-independent, growth of cancer cells remains stimulated by the expression of AR (Dutt and Gao, 2009). Overexpression of AR is correlated with cancer progression, hormonal resistance, as well as the development of androgen-resistant PCa (Zhang *et al*., 2009). Once cytoplasmic AR is activated by androgen, it translocates to the nucleus and stimulates transcription of genes that regulate survival and proliferation of PCa cells (Lamont and Tindall, 2010). One of the potent hormonal therapies used in PCa is enzalutamide. Enzalutamide is a potent AR antagonist which inhibits both AR nuclear translocation and transcriptions of its target genes (Tran *et al*., 2009; Zhang *et al*., 2011). Inhibition of AR nuclear translocation by enzalutamide leads

to regression in tumour CRPC in xenograft models (Guerrero *et al*., 2013). Interestingly, knockdown of IKKα by siRNA has been found to reduce AR activity, nuclear androgen receptor levels and AR gene expression in PCa cells (Lessard *et al*., 2007; Jain *et al*., 2012). In light of these facts, it would be interesting in future studies, although beyond the scope of the current investigations, to investigate if SU1261 had any inhibitory effect on AR expression. Furthermore, investigation of the combination of SU1261 and AR inhibitors such as enzalutamide in PCa cells' cytotoxicity would be interesting future work to assess the possible synergistic interaction between the two compounds.

RNAi (RNA interference) is an advanced analysis of loss-of-function cytotoxicity; however correlating this phenotypic impact with pharmacological small-molecule inhibition profiles is not always consistent (Weiss *et al*., 2007). Although our results further evidence that pharmacological inhibition of IKKα by our novel inhibitor, SU1261, may be a potential target in PCa as a single agent or in combination with radiation, transfection of IKKα with siRNA did not show a similar effect. Inhibition of IKKα by our siRNA duplex resulted only in inhibition in PCa growth rate but did not affect clonogenicity, apoptosis or radiosensitisation of PCa cells. As we discussed in Chapter 5, the difference between inhibitory mechanisms of SU1261 and siRNA agents and the compensatory mechanism between IKKα and IKKβ may all have contributed in this controversial difference between SU1261 and siRNA IKKα phenotypes. In

addition, the results within our group (data not shown) indicated that using our siRNA did not inhibit the non-canonical NF-kB in PCa PC3M-luc-C6 and pancreatic Panc-1 cells. Therefore, we suggest this transfection agent is not the best one in pharmacological and phenotype studies of IKKα inhibition in our cells. Further investigation is needed using a different siRNA reagent, as well as using other RNAi methods such as small hairpin RNA (shRNA). While siRNA duplex are introduced directly into the cytosol of cells for short-term knockdown of protein expression (days), shRNA molecules composed of two complementary RNA sequences are delivered to cells through viral vectors, allowing long-term knockdown (months) of targeted gene (Moore *et al*., 2010).

## 6.2 Conclusion

In conclusion, in this thesis we demonstrated that SU1261 is a novel first-in-class IKKα inhibitor compound. SU1261 shows selectivity of IKKα over IKKβ in highly metastatic androgen-insensitive PCa cells. In our preclinical investigations, the novel IKKα inhibitor, SU1261, has been shown to be a promising compound for advanced castration-resistant prostate cancer treatment as a single therapy or in combination with radiotherapy. These encouraging findings from this study provide a novel foundation for a possible future translation of these therapies into *in vivo* study and then a clinical trial study. IKKα kinase contributes to tumourigenesis in different cancers such as pancreatic, colorectal and breast. Therefore, the SU compounds may have therapeutic potential in the treatment of a range of different cancers.

# Chapter 7: REFERENCES


ACOSTA, A. M., SENSENG, C., KIM, G., SEKOSAN, M. & REE, N. 2016. Sarcomatoid carcinoma of the prostate with adenocarcinoma, squamous cell carcinoma, and heterologous components. *APMIS*.

AGARWAL, A., DAS, K., LERNER, N., SATHE, S., CICEK, M., CASEY, G. & SIZEMORE, N. 2005. The AKT/IκB kinase pathway promotes angiogenic/metastatic gene expression in colorectal cancer by activating nuclear factor-κB and β-catenin. *Oncogene,* 24**,** 1021-1031.

AHMED, K. M., DONG, S., FAN, M. & LI, J. J. 2006. Nuclear factor-kappaB p65 inhibits mitogen-activated protein kinase signaling pathway in radioresistant breast cancer cells. *Mol Cancer Res,* 4**,** 945-55.

AKANNI, E., OLOKE, J. & FAKUNLE, E. 2010. Haematological characterization in N-Nitroso-N ethylurea induced tumour bearing rats on oral administration of pleurotus pulmonarius and pleurotus ostreatus metabolites. *International Journal of Research and Reviews in Applied Sciences,* 3**,** 343-348.

ALBANESE, C., WU, K., D'AMICO, M., JARRETT, C., JOYCE, D., HUGHES, J., HULIT, J., SAKAMAKI, T., FU, M. & BEN-ZE'EV, A. 2003. IKKα regulates mitogenic signaling through transcriptional induction of cyclin D1 via Tcf. *Molecular biology of the cell,* 14**,** 585-599.

AMARAL, T. M. S., MACEDO, D., FERNANDES, I. & COSTA, L. 2012. Castration-resistant prostate cancer: mechanisms, targets, and treatment. *Prostate cancer,* 2012.

AMMIRANTE, M., KURAISHY, A. I., SHALAPOUR, S., STRASNER, A., RAMIREZ-SANCHEZ, C., ZHANG, W., SHABAIK, A. & KARIN, M. 2013. An IKKalpha-E2F1-BMI1 cascade activated by infiltrating B cells controls prostate regeneration and tumor recurrence. *Genes Dev,* 27**,** 1435-40.

AMMIRANTE, M., LUO, J. L., GRIVENNIKOV, S., NEDOSPASOV, S. & KARIN, M. 2010. B-cell-derived lymphotoxin promotes castration-resistant prostate cancer. *Nature,* 464**,** 302-5.

ARIGA, A., NAMEKAWA, J., MATSUMOTO, N., INOUE, J. & UMEZAWA, K. 2002. Inhibition of tumor necrosis factor-alpha -induced nuclear translocation and activation of NF-kappa B by dehydroxymethylepoxyquinomicin. *J Biol Chem,* 277**,** 24625-30.

ARISTA-NASR, J., MARTINEZ-BENITEZ, B., BORNSTEIN-QUEVEDO, L., AGUILAR-AYALA, E., ALEMAN-SANCHEZ, C. N. & ORTIZ-BAUTISTA, R. 2016. Low grade urothelial carcinoma mimicking basal cell hyperplasia and transitional metaplasia in needle prostate biopsy. *Int Braz J Urol,* 42**,** 247-52.

ASAMITSU, K., YAMAGUCHI, T., NAKATA, K., HIBI, Y., VICTORIANO, A. F., IMAI, K., ONOZAKI, K., KITADE, Y. & OKAMOTO, T. 2008. Inhibition of human immunodeficiency virus type 1 replication by blocking IkappaB kinase with noraristeromycin. *J Biochem,* 144**,** 581-9.

BAGLIETTO, L., SEVERI, G., ENGLISH, D. R., HOPPER, J. L. & GILES, G. G. 2006. Alcohol consumption and prostate cancer risk: results from the Melbourne collaborative cohort study. *International journal of cancer,* 119**,** 1501-1504.

BALK, S. P., KO, Y. J. & BUBLEY, G. J. 2003. Biology of prostate-specific antigen. *J Clin Oncol,* 21**,** 383-91.

BANIN, S., MOYAL, L., SHIEH, S., TAYA, Y., ANDERSON, C. W., CHESSA, L., SMORODINSKY, N. I., PRIVES, C., REISS, Y., SHILOH, Y. & ZIV, Y. 1998. Enhanced phosphorylation of p53 by ATM in response to DNA damage. *Science,* 281**,** 1674-7.

BARBIE, D. A., TAMAYO, P., BOEHM, J. S., KIM, S. Y., MOODY, S. E., DUNN, I. F., SCHINZEL, A. C., SANDY, P., MEYLAN, E. & SCHOLL, C. 2009. Systematic RNA interference reveals that oncogenic KRAS-driven cancers require TBK1. *Nature,* 462**,** 108-112.

BARENDSEN, G. W. 1997. Parameters of linear-quadratic radiation dose-effect relationships: dependence on LET and mechanisms of reproductive cell death. *Int J Radiat Biol,* 71**,** 649-55.

BASKAR, R., LEE, K. A., YEO, R. & YEOH, K.-W. 2012. Cancer and radiation therapy: current advances and future directions. *Int J Med Sci,* 9**,** 193-199.

BASSERES, D. & BALDWIN, A. S. 2006. Nuclear factor-κB and inhibitor of κB kinase pathways in oncogenic initiation and progression. *Oncogene,* 25**,** 6817-6830.

BASSERES, D. S., EBBS, A., COGSWELL, P. C. & BALDWIN, A. S. 2014. IKK is a therapeutic target in KRAS-Induced lung cancer with disrupted p53 activity. *Genes Cancer,* 5**,** 41-55.

BAUD, V. & KARIN, M. 2009. Is NF-kappaB a good target for cancer therapy? Hopes and pitfalls. *Nat Rev Drug Discov,* 8**,** 33-40.

BIRBRAIR, A., ZHANG, T., WANG, Z.-M., MESSI, M. L., MINTZ, A. & DELBONO, O. 2015. Pericytes at the intersection between tissue regeneration and pathology. *Clinical Science,* 128**,** 81-93.

BOLAND, M. P., FITZGERALD, K. A. & O'NEILL, L. A. 2000. Topoisomerase II is required for mitoxantrone to signal nuclear factor κB activation in HL60 cells. *Journal of Biological Chemistry,* 275**,** 25231-25238.

BONIZZI, G. & KARIN, M. 2004. The two NF-κB activation pathways and their role in innate and adaptive immunity. *Trends in immunology,* 25**,** 280-288.

BORGES, G. T., VENCIO, E. F., QUEK, S. I., CHEN, A., SALVANHA, D. M., VENCIO, R. Z., NGUYEN, H. M., VESSELLA, R. L., CAVANAUGH, C., WARE, C. B., TROISCH, P. & LIU, A. Y. 2016. Conversion of Prostate Adenocarcinoma to Small Cell Carcinoma-Like by Reprogramming. *J Cell Physiol,* 231**,** 2040-7.

BOSTWICK, D. G., BURKE, H. B., DJAKIEW, D., EULING, S., HO, S. M., LANDOLPH, J., MORRISON, H., SONAWANE, B., SHIFFLETT, T., WATERS, D. J. & TIMMS, B. 2004. Human prostate cancer risk factors. *Cancer,* 101**,** 2371-490.

BOURS, V., BONIZZI, G., BENTIRES-ALJ, M., BUREAU, F., PIETTE, J., LEKEUX, P. & MERVILLE, M.-P. 2000. NF-κB activation in response to toxical and therapeutical agents: role in inflammation and cancer treatment. *Toxicology,* 153**,** 27-38.

BRAUNSTEIN, S., FORMENTI, S. C. & SCHNEIDER, R. J. 2008. Acquisition of stable inducible up-regulation of nuclear factor-κB by tumor necrosis factor exposure confers increased radiation resistance without increased transformation in breast cancer cells. *Molecular Cancer Research,* 6**,** 78-88.

BRENNER, D. J., HLATKY, L. R., HAHNFELDT, P. J., HUANG, Y. & SACHS, R. K. 1998. The linear-quadratic model and most other common radiobiological models result in similar predictions of time-dose relationships. *Radiat Res,* 150**,** 83-91.

BRUNI-CARDOSO, A., JOHNSON, L. C., VESSELLA, R. L., PETERSON, T. E. & LYNCH, C. C. 2010. Osteoclast-derived matrix metalloproteinase-9 directly affects angiogenesis in the prostate tumor-bone microenvironment. *Mol Cancer Res,* 8**,** 459-70.

BURKE, J. R., PATTOLI, M. A., GREGOR, K. R., BRASSIL, P. J., MACMASTER, J. F., MCINTYRE, K. W., YANG, X., IOTZOVA, V. S., CLARKE, W., STRNAD, J., QIU, Y. & ZUSI, F. C. 2003. BMS-345541 is a highly selective inhibitor of I kappa B kinase that binds at an allosteric site of the enzyme and blocks NF-kappa B-dependent transcription in mice. *J Biol Chem,* 278**,** 1450-6.

CANCER_RESEARCH_UK. 2016. *CancerStats - Incidence 2013 - UK.* [Online]. Available: http://publications.cancerresearchuk.org/cancerstats/statsincidence/incidence.html. [Accessed May 2016].

CANMAN, C. E., LIM, D. S., CIMPRICH, K. A., TAYA, Y., TAMAI, K., SAKAGUCHI, K., APPELLA, E., KASTAN, M. B. & SILICIANO, J. D. 1998. Activation of the ATM kinase by ionizing radiation and phosphorylation of p53. *Science,* 281**,** 1677-9.

CAO, Y., BONIZZI, G., SEAGROVES, T. N., GRETEN, F. R., JOHNSON, R., SCHMIDT, E. V. & KARIN, M. 2001. IKKα provides an essential link between RANK signaling and cyclin D1 expression during mammary gland development. *Cell,* 107**,** 763-775.

CARAYOL, N. & WANG, C.-Y. 2006. IKKα stabilizes cytosolic β-catenin by inhibiting both canonical and non-canonical degradation pathways. *Cellular signalling,* 18**,** 1941-1946.

CASTRO, A. C., DANG, L. C., SOUCY, F., GRENIER, L., MAZDIYASNI, H., HOTTELET, M., PARENT, L., PIEN, C., PALOMBELLA, V. & ADAMS, J. 2003. Novel IKK inhibitors: beta-carbolines. *Bioorg Med Chem Lett,* 13**,** 2419-22.

CAVANAGH, H. & ROGERS, K. M. 2015. The role of BRCA1 and BRCA2 mutations in prostate, pancreatic and stomach cancers. *Hereditary cancer in clinical practice,* 13**,** 1.

CHARIOT, A. 2009. The NF-κB-independent functions of IKK subunits in immunity and cancer. *Trends in cell biology,* 19**,** 404-413.

CHI, K. N., BJARTELL, A., DEARNALEY, D., SAAD, F., SCHRODER, F. H., STERNBERG, C., TOMBAL, B. & VISAKORPI, T. 2009. Castration-resistant prostate cancer: from new pathophysiology to new treatment targets. *Eur Urol,* 56**,** 594-605.

CHOU, T. C. & TALALAY, P. 1984. Quantitative analysis of dose-effect relationships: the combined effects of multiple drugs or enzyme inhibitors. *Adv Enzyme Regul,* 22**,** 27-55.

CHUU, C.-P., KOKONTIS, J. M., HIIPAKKA, R. A., FUKUCHI, J., LIN, H.-P., LIN, C.-Y., HUO, C. & SU, L.-C. 2011. Androgens as therapy for androgen receptor-positive castration-resistant prostate cancer. *Journal of biomedical science,* 18**,** 1.

CILLONI, D., MESSA, F., ARRUGA, F., DEFILIPPI, I., MOROTTI, A., MESSA, E., CARTURAN, S., GIUGLIANO, E., PAUTASSO, M. & BRACCO, E. 2006. The NF-κB pathway blockade by the IKK inhibitor PS1145 can overcome imatinib resistance. *Leukemia,* 20**,** 61-67.

COHEN–JONATHAN, E., BERNHARD, E. J. & MCKENNA, W. G. 1999. How does radiation kill cells? *Current opinion in chemical biology,* 3**,** 77-83.

CONDE MORENO, A. J., FERRER ALBIACH, C., MUELAS SORIA, R., GONZALEZ VIDAL, V., GARCIA GOMEZ, R. & ALBERT ANTEQUERA, M. 2014. Oligometastases in prostate cancer: restaging stage IV cancers and new radiotherapy options. *Radiat Oncol,* 9**,** 258.

CORMIER, F., MONJANEL, H., FABRE, C., BILLOT, K., SAPHARIKAS, E., CHEREAU, F., BORDEREAUX, D., MOLINA, T. J., AVET-LOISEAU, H. & BAUD, V. 2013. Frequent engagement of RelB activation is critical for cell survival in multiple myeloma. *PLoS One,* 8**,** e59127.

CUNNINGHAM, S., BOYD, M., BROWN, M., CARLIN, S., MCCLUSKEY, A., LIVINGSTONE, A., MAIRS, R. & WHELDON, T. 2000. A gene therapy approach to enhance the targeted radiotherapy of neuroblastoma. *Medical and pediatric oncology,* 35**,** 708-711.

DARNELL, J. E., JR. 1997. STATs and gene regulation. *Science,* 277**,** 1630-5.

DASGUPTA, S., SRINIDHI, S. & VISHWANATHA, J. K. 2012. Oncogenic activation in prostate cancer progression and metastasis: Molecular insights and future challenges. *J Carcinog,* 11**,** 4.

DE BONO, J. S., OUDARD, S., OZGUROGLU, M., HANSEN, S., MACHIELS, J.-P., KOCAK, I., GRAVIS, G., BODROGI, I., MACKENZIE, M. J. & SHEN, L. 2010. Prednisone plus cabazitaxel or mitoxantrone for metastatic castration-resistant prostate cancer progressing after docetaxel treatment: a randomised open-label trial. *The Lancet,* 376**,** 1147-1154.

DE NUNZIO, C., PRESICCE, F., LOMBARDO, R., CANCRINI, F., PETTA, S., TRUCCHI, A., GACCI, M., CINDOLO, L. & TUBARO, A. 2015. Physical activity as a risk factor for prostate cancer diagnosis: a prospective biopsy cohort analysis. *BJU Int*.

DEARNALEY, D. P. Radiotherapy of prostate cancer: established results and new developments. Seminars in surgical oncology, 1995. Wiley Online Library, 50-59.

DEJARDIN, E. 2006. The alternative NF-κB pathway from biochemistry to biology: pitfalls and promises for future drug development. *Biochemical pharmacology,* 72**,** 1161-1179.

DEMICCO, E. G., KAVANAGH, K. T., ROMIEU-MOUREZ, R., WANG, X., SHIN, S. R., LANDESMAN-BOLLAG, E., SELDIN, D. C. & SONENSHEIN, G. E. 2005. RelB/p52 NF-κB complexes rescue an early delay in mammary gland development in transgenic mice with targeted superrepressor IκB-α expression and promote carcinogenesis of the mammary gland. *Molecular and cellular biology,* 25**,** 10136-10147.

DENK, A., GOEBELER, M., SCHMID, S., BERBERICH, I., RITZ, O., LINDEMANN, D., LUDWIG, S. & WIRTH, T. 2001. Activation of NF-κB via the IκB kinase complex is both essential and sufficient for proinflammatory gene expression in primary endothelial cells. *Journal of Biological Chemistry,* 276**,** 28451-28458.

DIDONATO, J. A., HAYAKAWA, M., ROTHWARF, D. M., ZANDI, E. & KARIN, M. 1997. A cytokine-responsive IκB kinase that activates the transcription factor NF-κB. *Nature,* 388**,** 548-554.

DIDONATO, J. A., MERCURIO, F. & KARIN, M. 2012. NF-κB and the link between inflammation and cancer. *Immunological reviews,* 246**,** 379-400.

DOMINGO-DOMENECH, J., MELLADO, B., FERRER, B., TRUAN, D., CODONY-SERVAT, J., SAULEDA, S., ALCOVER, J., CAMPO, E., GASCON, P. & ROVIRA, A. 2005. Activation of nuclear factor-κB in human prostate carcinogenesis and association to biochemical relapse. *British journal of cancer,* 93**,** 1285-1294.

DULANEY, C. R., OSULA, D. O., YANG, E. S. & RAIS-BAHRAMI, S. 2016. Prostate radiotherapy in the era of advanced imaging and precision medicine. *Prostate cancer,* 2016.

DUTT, S. S. & GAO, A. C. 2009. Molecular mechanisms of castration-resistant prostate cancer progression. *Future Oncol,* 5**,** 1403-13.

EDDY, S. F., GUO, S., DEMICCO, E. G., ROMIEU-MOUREZ, R., LANDESMAN-BOLLAG, E., SELDIN, D. C. & SONENSHEIN, G. E. 2005. Inducible IκB kinase/IκB kinase ε expression is induced by CK2 and promotes aberrant nuclear factor-κB activation in breast cancer cells. *Cancer research,* 65**,** 11375-11383.

EGAN, L. J., ECKMANN, L., GRETEN, F. R., CHAE, S., LI, Z.-W., MYHRE, G. M., ROBINE, S., KARIN, M. & KAGNOFF, M. F. 2004. IκB-kinaseβ-dependent NF-κB activation provides radioprotection to the intestinal epithelium. *Proceedings of the National Academy of Sciences of the United States of America,* 101**,** 2452-2457.

ELBASHIR, S. M., HARBORTH, J., LENDECKEL, W., YALCIN, A., WEBER, K. & TUSCHL, T. 2001. Duplexes of 21-nucleotide RNAs mediate RNA interference in cultured mammalian cells. *Nature,* 411**,** 494-8.

ENGLISH, H. F., SANTEN, R. J. & LSAACS, J. T. 1987. Response of glandular versus basal rat ventral prostatic epithelial cells to androgen withdrawal and replacement. *The Prostate,* 11**,** 229-242.

FERLAY, J., SHIN, H. R., BRAY, F., FORMAN, D., MATHERS, C. & PARKIN, D. M. 2010. Estimates of worldwide burden of cancer in 2008: GLOBOCAN 2008. *International journal of cancer,* 127**,** 2893-2917.

FERNÁNDEZ-MAJADA, V., PUJADAS, J., VILARDELL, F., CAPELLA, G., MAYO, M. W., BIGAS, A. & ESPINOSA, L. 2007. Aberrant cytoplasmic localization of N-CoR in colorectal tumors. *Cell cycle,* 6**,** 1748-1752.

Fernet, M., Megnin-Chanet, F., Hall, J., and Favaudon, V. 2010. Control of the G2/M checkpoints after exposure to low doses of ionising radiation: implications for hyperradiosensitivity. *DNA Repair*, 9, (1) 48-57.

FICARRA, V., NOVARA, G., ROSEN, R. C., ARTIBANI, W., CARROLL, P. R., COSTELLO, A., MENON, M., MONTORSI, F., PATEL, V. R., STOLZENBURG, J. U., VAN DER POEL, H., WILSON, T. G., ZATTONI, F. & MOTTRIE, A. 2012. Systematic review and meta-analysis of studies reporting urinary continence recovery after robot-assisted radical prostatectomy. *Eur Urol,* 62**,** 405-17.

FINE, S. W., AL-AHMADIE, H. A., GOPALAN, A., TICKOO, S. K., SCARDINO, P. T. & REUTER, V. E. 2007. Anatomy of the anterior prostate and extraprostatic space: a contemporary surgical pathology analysis. *Adv Anat Pathol,* 14**,** 401-7.

FINNBERG, N. & EL-DEIRY, W. S. 2004. Activating FOXO3a, NF-kappaB and p53 by targeting IKKs: an effective multi-faceted targeting of the tumor-cell phenotype? *Cancer biology & therapy,* 3**,** 614-616.

FLANAGAN, L., MEYER, M., FAY, J., CURRY, S., BACON, O., DUESSMANN, H., JOHN, K., BOLAND, K., MCNAMARA, D. & KAY, E. 2016. Low levels of Caspase-3 predict favourable response to 5FU-based chemotherapy in advanced colorectal cancer: Caspase-3 inhibition as a therapeutic approach. *Cell death & disease,* 7**,** e2087.

FOWKE, J. H., MCLERRAN, D. F., GUPTA, P. C., HE, J., SHU, X.-O., RAMADAS, K., TSUGANE, S., INOUE, M., TAMAKOSHI, A. & KOH, W.-P. 2015. Associations of body mass index, smoking, and alcohol consumption with prostate cancer mortality in the Asia Cohort Consortium. *American Journal of Epidemiology,* 182**,** 381-389.

FRANKEN, N. A., VAN BREE, C., VELTMAAT, M. A., RODERMOND, H. M., HAVEMAN, J. & BARENDSEN, G. W. 2001. Radiosensitization by bromodeoxyuridine and hyperthermia: analysis of linear and quadratic parameters of radiation survival curves of two human tumor cell lines. *J Radiat Res,* 42**,** 179-90.

FRIEDMAN, M. V., HILLEN, T. J., WESSELL, D. E., HILDEBOLT, C. F. & JENNINGS, J. W. 2014. Hip chondrolysis and femoral head osteonecrosis: a complication of periacetabular cryoablation. *Journal of Vascular and Interventional Radiology,* 25**,** 1580-1588.

FRIELING, J. S., BASANTA, D. & LYNCH, C. C. 2015. Current and emerging therapies for bone metastatic castration-resistant prostate cancer. *Cancer control: journal of the Moffitt Cancer Center,* 22**,** 109.

FULDA, S. 2014. Molecular pathways: targeting inhibitor of apoptosis proteins in cancer—from molecular mechanism to therapeutic application. *Clinical Cancer Research,* 20**,** 289-295.

FURUYA, K., OZAKI, T., HANAMOTO, T., HOSODA, M., HAYASHI, S., BARKER, P. A., TAKANO, K., MATSUMOTO, M. & NAKAGAWARA, A. 2007. Stabilization of p73 by nuclear IkappaB kinase-alpha mediates cisplatin-induced apoptosis. *J Biol Chem,* 282**,** 18365-78.

GALALAE, R. M., MARTINEZ, A., MATE, T., MITCHELL, C., EDMUNDSON, G., NUERNBERG, N., EULAU, S., GUSTAFSON, G., GRIBBLE, M. & KOVACS, G. 2004. Long-term outcome by risk factors using conformal high-dose-rate brachytherapy (HDR-BT) boost with or without neoadjuvant androgen suppression for localized prostate cancer. *Int J Radiat Oncol Biol Phys,* 58**,** 1048-55.

GAMBLE, C., MCINTOSH, K., SCOTT, R., HO, K. H., PLEVIN, R. & PAUL, A. 2012. Inhibitory kappa B Kinases as targets for pharmacological regulation. *Br J Pharmacol,* 165**,** 802-19.

GARDAM, S., SIERRO, F., BASTEN, A., MACKAY, F. & BRINK, R. 2008. TRAF2 and TRAF3 signal adapters act cooperatively to control the maturation and survival signals delivered to B cells by the BAFF receptor. *Immunity,* 28**,** 391-401.

GASPARIAN, A. V., YAO, Y. J., KOWALCZYK, D., LYAKH, L. A., KARSELADZE, A., SLAGA, T. J. & BUDUNOVA, I. V. 2002. The role of IKK in constitutive activation of NF-κB transcription factor in prostate carcinoma cells. *Journal of cell science,* 115**,** 141-151.

GIULIANI, C., NAPOLITANO, G., BUCCI, I., MONTANI, V. & MONACO, F. 2001. Nf-kB transcription factor: role in the pathogenesis of inflammatory, autoimmune, and neoplastic diseases and therapy implications. *La Clinica Terapeutica,* 152**,** 249-253.

GLEASON, D. F., MELLINGER, G. T. & VETERANS ADMINISTRATION COOPERATIVE UROLOGICAL RESEARCH, G. 2002. Prediction of prognosis for prostatic adenocarcinoma by combined histological grading and clinical staging. 1974. *J Urol,* 167**,** 953-8; discussion 959.

GLOECKNER, H., JONULEIT, T. & LEMKE, H. D. 2001. Monitoring of cell viability and cell growth in a hollow-fiber bioreactor by use of the dye Alamar Blue. *J Immunol Methods,* 252**,** 131-8.

GLOIRE, G., HORION, J., EL MJIYAD, N., BEX, F., CHARIOT, A., DEJARDIN, E. & PIETTE, J. 2007. Promoter-dependent effect of IKKα on NF-κB/p65 DNA binding. *Journal of Biological Chemistry,* 282**,** 21308-21318.

GODL, K., GRUSS, O. J., EICKHOFF, J., WISSING, J., BLENCKE, S., WEBER, M., DEGEN, H., BREHMER, D., ŐRFI, L. & HORVÁTH, Z. 2005. Proteomic characterization of the angiogenesis inhibitor SU6668 reveals

multiple impacts on cellular kinase signaling. *Cancer research,* 65**,** 6919-6926.

GOGVADZE, V., ORRENIUS, S. & ZHIVOTOVSKY, B. 2006. Multiple pathways of cytochrome c release from mitochondria in apoptosis. *Biochim Biophys Acta,* 1757**,** 639-47.

GOMPERTS, B. & STRIETER, R. 2006. Chemokine-directed metastasis. *Infection and Inflammation: Impacts on Oncogenesis.* Karger Publishers.

GONG, Y., CHIPPADA-VENKATA, U. D. & OH, W. K. 2014. Roles of matrix metalloproteinases and their natural inhibitors in prostate cancer progression. *Cancers (Basel),* 6**,** 1298-327.

GONG, Z., AGALLIU, I., LIN, D. W., STANFORD, J. L. & KRISTAL, A. R. 2007. Obesity is associated with increased risks of prostate cancer metastasis and death after initial cancer diagnosis in middle-aged men. *Cancer,* 109**,** 1192-202.

GORIS GBENOU, M. C., PELTIER, A., SCHULMAN, C. C. & VELTHOVEN, R. V. 2016. Increased body mass index as a risk factor in localized prostate cancer treated by radical prostatectomy. *Urol Oncol*.

GREEN, A. K., CORTY, R. W., WOOD, W. A., MEENEGHAN, M., REEDER-HAYES, K. E., BASCH, E., MILOWSKY, M. I. & DUSETZINA, S. B. 2015. Comparative effectiveness of mitoxantrone plus prednisone versus prednisone alone in metastatic castrate-resistant prostate cancer after docetaxel failure. *The oncologist,* 20**,** 516-522.

GUERRERO, J., ALFARO, I. E., GÓMEZ, F., PROTTER, A. A. & BERNALES, S. 2013. Enzalutamide, an androgen receptor signaling inhibitor, induces tumor regression in a mouse model of castration-resistant prostate cancer. *The Prostate,* 73**,** 1291-1305.

GUO, G., YAN-SANDERS, Y., LYN-COOK, B. D., WANG, T., TAMAE, D., OGI, J., KHALETSKIY, A., LI, Z., WEYDERT, C., LONGMATE, J. A., HUANG, T. T., SPITZ, D. R., OBERLEY, L. W. & LI, J. J. 2003. Manganese superoxide dismutase-mediated gene expression in radiation-induced adaptive responses. *Mol Cell Biol,* 23**,** 2362-78.

GUO, J.-P., SHU, S.-K., HE, L., LEE, Y.-C., KRUK, P. A., GRENMAN, S., NICOSIA, S. V., MOR, G., SCHELL, M. J. & COPPOLA, D. 2009. Deregulation of IKBKE is associated with tumor progression, poor prognosis, and cisplatin resistance in ovarian cancer. *The American journal of pathology,* 175**,** 324-333.

GURTU, V., KAIN, S. R. & ZHANG, G. 1997. Fluorometric and colorimetric detection of caspase activity associated with apoptosis. *Anal Biochem,* 251**,** 98-102.

HAAS, G. P., DELONGCHAMPS, N., BRAWLEY, O. W., WANG, C. Y. & DE LA ROZA, G. 2008. The worldwide epidemiology of prostate cancer: perspectives from autopsy studies. *Can J Urol,* 15**,** 3866-71.

HAFFNER, M. C., BERLATO, C. & DOPPLER, W. 2006. Exploiting our knowledge of NF-κB signaling for the treatment of mammary cancer. *Journal of mammary gland biology and neoplasia,* 11**,** 63-73.

HALL, E. J., GIACCIA, A. J., 2006. Radiobiology for the radiologist. 6th ed. Lippincott Williams & Wilkins, Philadelphia.

HANAHAN, D. & WEINBERG, R. A. 2000. The hallmarks of cancer. *cell,* 100**,** 57-70.

HARALDSDOTTIR, S., HAMPEL, H., WEI, L., WU, C., FRANKEL, W., BEKAII-SAAB, T., DE LA CHAPELLE, A. & GOLDBERG, R. M. 2014. Prostate cancer incidence in males with Lynch syndrome. *Genetics in Medicine,* 16**,** 553-557.

HARRINGTON, K., KAZI, R., BHIDE, S., NEWBOLD, K. & NUTTING, C. 2010. Novel therapeutic approaches to squamous cell carcinoma of the head and neck using biologically targeted agents. *Indian journal of cancer,* 47**,** 248.

HARRIS, W. P., MOSTAGHEL, E. A., NELSON, P. S. & MONTGOMERY, B. 2009. Androgen deprivation therapy: progress in understanding mechanisms of resistance and optimizing androgen depletion. *Nature clinical practice Urology,* 6**,** 76-85.

HAYDEN, M. S. & GHOSH, S. 2008. Shared principles in NF-kappaB signaling. *Cell,* 132**,** 344-62.

HEGARTY, J., BEIRNE, P. V., WALSH, E., COMBER, H., FITZGERALD, T. & WALLACE KAZER, M. 2010. Radical prostatectomy versus watchful waiting for prostate cancer. *The Cochrane Library*.

HEHLGANS, T., STOELCKER, B., STOPFER, P., MÜLLER, P., CERNAIANU, G., GUBA, M., STEINBAUER, M., NEDOSPASOV, S. A., PFEFFER, K. & MÄNNEL, D. N. 2002. Lymphotoxin-β receptor immune interaction promotes tumor growth by inducing angiogenesis. *Cancer research,* 62**,** 4034-4040.

HEINLEIN, C. A. & CHANG, C. 2004. Androgen receptor in prostate cancer. *Endocrine reviews,* 25**,** 276-308.

HIDESHIMA, T., CHAUHAN, D., RICHARDSON, P., MITSIADES, C., MITSIADES, N., HAYASHI, T., MUNSHI, N., DANG, L., CASTRO, A., PALOMBELLA, V., ADAMS, J. & ANDERSON, K. C. 2002. NF-kappa B as a therapeutic target in multiple myeloma. *J Biol Chem,* 277**,** 16639-47.

HIRAI, M., KONISHI, T., SAITO, K., WASHINO, S., KOBAYASHI, Y., NOKUBI, M. & MIYAGAWA, T. 2015. Small cell carcinoma of the prostate: A case report of relative long-term survival. *Nihon Hinyokika Gakkai Zasshi,* 106**,** 280-4.

HIRATA, Y., MAEDA, S., OHMAE, T., SHIBATA, W., YANAI, A., OGURA, K., YOSHIDA, H., KAWABE, T. & OMATA, M. 2006. Helicobacter pylori induces IκB kinase α nuclear translocation and chemokine production in gastric epithelial cells. *Infection and immunity,* 74**,** 1452-1461.

HJARNAA, P. J., JONSSON, E., LATINI, S., DHAR, S., LARSSON, R., BRAMM, E., SKOV, T. & BINDERUP, L. 1999. CHS 828, a novel pyridyl cyanoguanidine with potent antitumor activity in vitro and in vivo. *Cancer Res,* 59**,** 5751-7.

HOESEL, B. & SCHMID, J. A. 2013. The complexity of NF-kappaB signaling in inflammation and cancer. *Mol Cancer,* 12**,** 86.

HOLLEY, A. K., XU, Y., ST CLAIR, D. K. & ST CLAIR, W. H. 2010. RelB regulates manganese superoxide dismutase gene and resistance to ionizing radiation of prostate cancer cells. *Ann N Y Acad Sci,* 1201**,** 129-36.

HORIE, R., WATANABE, T. & UMEZAWA, K. 2006. Blocking NF-kappaB as a potential strategy to treat adult T-cell leukemia/lymphoma. *Drug News Perspect,* 19**,** 201-9.

HU, M. C.-T., LEE, D.-F., XIA, W., GOLFMAN, L. S., OU-YANG, F., YANG, J.-Y., ZOU, Y., BAO, S., HANADA, N. & SASO, H. 2004. IκB kinase promotes tumorigenesis through inhibition of forkhead FOXO3a. *Cell,* 117**,** 225-237.

HU, Y., BAUD, V., DELHASE, M., ZHANG, P., DEERINCK, T., ELLISMAN, M., JOHNSON, R. & KARIN, M. 1999. Abnormal morphogenesis but intact IKK activation in mice lacking the IKKα subunit of IκB kinase. *Science,* 284**,** 316-320.

HUANG, S., PETTAWAY, C. A., UEHARA, H., BUCANA, C. D. & FIDLER, I. J. 2001. Blockade of NF-κB activity in human prostate cancer cells is associated with suppression of angiogenesis, invasion, and metastasis. *Oncogene,* 20.

HUANG, W.-C., JU, T.-K., HUNG, M.-C. & CHEN, C.-C. 2007. Phosphorylation of CBP by IKKα promotes cell growth by switching the binding preference of CBP from p53 to NF-κB. *Molecular cell,* 26**,** 75-87.

HUANG, W. C. & HUNG, M. C. 2013. Beyond NF-kappaB activation: nuclear functions of IkappaB kinase alpha. *J Biomed Sci,* 20**,** 3.

HUMMEL, S., SIMPSON, E., HEMINGWAY, P., STEVENSON, M. & REES, A. 2010. Intensity-modulated radiotherapy for the treatment of prostate cancer: a systematic review and economic evaluation.

HUSSON, O., STEENBERGEN, L. N., KOLDEWIJN, E. L., POORTMANS, P. M., COEBERGH, J. W. W. & JANSSEN-HEIJNEN, M. L. 2014. Patients with prostate cancer continue to have excess mortality up to 15 years after diagnosis. *BJU international,* 114**,** 691-697.

HUTTI, J. E., SHEN, R. R., ABBOTT, D. W., ZHOU, A. Y., SPROTT, K. M., ASARA, J. M., HAHN, W. C. & CANTLEY, L. C. 2009. Phosphorylation of the tumor suppressor CYLD by the breast cancer oncogene IKKε promotes cell transformation. *Molecular cell,* 34**,** 461-472.

IKEDA, F., HECKER, C. M., ROZENKNOP, A., NORDMEIER, R. D., ROGOV, V., HOFMANN, K., AKIRA, S., DÖTSCH, V. & DIKIC, I. 2007. Involvement of the ubiquitin-like domain of TBK1/IKK-i kinases in regulation of IFN-inducible genes. *The EMBO journal,* 26**,** 3451-3462.

IKEZOE, T., YANG, Y., SAITO, T., KOEFFLER, H. P. & TAGUCHI, H. 2004. Proteasome inhibitor PS-341 down-regulates prostate-specific antigen

(PSA) and induces growth arrest and apoptosis of androgen-dependent human prostate cancer LNCaP cells. *Cancer Sci,* 95**,** 271-5.
ISRAËL, A. 2010. The IKK complex, a central regulator of NF-κB activation. *Cold Spring Harbor perspectives in biology,* 2**,** a000158.
JAIN, G., VOOGDT, C., TOBIAS, A., SPINDLER, K.-D., MÖLLER, P., CRONAUER, M. V. & MARIENFELD, R. B. 2012. IκB kinases modulate the activity of the androgen receptor in prostate carcinoma cell lines. *Neoplasia,* 14**,** 178-IN6.
JIANG, R., XIA, Y., LI, J., DENG, L., ZHAO, L., SHI, J., WANG, X. & SUN, B. 2010. High expression levels of IKKα and IKKβ are necessary for the malignant properties of liver cancer. *International journal of cancer,* 126**,** 1263-1274.
JIN, R., YI, Y., YULL, F. E., BLACKWELL, T. S., CLARK, P. E., KOYAMA, T., SMITH, J. A. & MATUSIK, R. J. 2014. NF-κB gene signature predicts prostate cancer progression. *Cancer research,* 74**,** 2763-2772.
JIN, R. J., LHO, Y., CONNELLY, L., WANG, Y., YU, X., SAINT JEAN, L., CASE, T. C., ELLWOOD-YEN, K., SAWYERS, C. L. & BHOWMICK, N. A. 2008. The nuclear factor-κB pathway controls the progression of prostate cancer to androgen-independent growth. *Cancer research,* 68**,** 6762-6769.
JONES, M. R., JOSHU, C. E., KANAREK, N., NAVAS-ACIEN, A., RICHARDSON, K. A. & PLATZ, E. A. 2016. Cigarette Smoking and Prostate Cancer Mortality in Four US States, 1999–2010. *Preventing Chronic Disease,* 13.
JOSSON, S., XU, Y., FANG, F., DHAR, S. K., ST CLAIR, D. K. & ST CLAIR, W. H. 2006. RelB regulates manganese superoxide dismutase gene and resistance to ionizing radiation of prostate cancer cells. *Oncogene,* 25**,** 1554-9.
KAN, Z., JAISWAL, B. S., STINSON, J., JANAKIRAMAN, V., BHATT, D., STERN, H. M., YUE, P., HAVERTY, P. M., BOURGON, R. & ZHENG, J. 2010. Diverse somatic mutation patterns and pathway alterations in human cancers. *Nature,* 466**,** 869-873.
KARIN, M. 2006. Nuclear factor-κB in cancer development and progression. *Nature,* 441**,** 431-436.
KARIN, M. 2009. NF-κB as a critical link between inflammation and cancer. *Cold Spring Harbor perspectives in biology,* 1**,** a000141.
KARIN, M., CAO, Y., GRETEN, F. R. & LI, Z.-W. 2002. NF-κB in cancer: from innocent bystander to major culprit. *Nature reviews cancer,* 2**,** 301-310.
KAUR, S., SINGH, G. & KAUR, K. 2014. Cancer stem cells: An insight and future perspective. *Journal of cancer research and therapeutics,* 10**,** 846.
KHEMLINA, G., IKEDA, S. & KURZROCK, R. 2015. Molecular landscape of prostate cancer: Implications for current clinical trials. *Cancer treatment reviews,* 41**,** 761-766.

KICINSKI, M., VANGRONSVELD, J. & NAWROT, T. S. 2011. An epidemiological reappraisal of the familial aggregation of prostate cancer: a meta-analysis. *PLoS One,* 6**,** e27130.

KIM, B. M., HONG, Y., LEE, S., LIU, P., LIM, J. H., LEE, Y. H., LEE, T. H., CHANG, K. T. & HONG, Y. 2015. Therapeutic implications for overcoming radiation resistance in cancer therapy. *Int J Mol Sci,* 16**,** 26880-913.

KIM, H. J., HAWKE, N. & BALDWIN, A. S. 2006. NF-kappaB and IKK as therapeutic targets in cancer. *Cell Death Differ,* 13**,** 738-47.

KISSELEV, A. F. & GOLDBERG, A. L. 2001. Proteasome inhibitors: from research tools to drug candidates. *Chemistry & biology,* 8**,** 739-758.

KNIGHT, S. J. & LATINI, D. M. 2009. Sexual side effects and prostate cancer treatment decisions: patient information needs and preferences. *The Cancer Journal,* 15**,** 41-44.

KOHLI, M. & TINDALL, D. J. New developments in the medical management of prostate cancer. Mayo Clinic Proceedings, 2010. Elsevier, 77-86.

KOMAROVA, N. L. & BOLAND, C. R. 2013. Cancer: calculated treatment. *Nature,* 499**,** 291-2.

KONG, X. J., DUAN, L. J., QIAN, X. Q., XU, D., LIU, H. L., ZHU, Y. J. & QI, J. 2015. Tumor-suppressive microRNA-497 targets IKKbeta to regulate NF-kappaB signaling pathway in human prostate cancer cells. *Am J Cancer Res,* 5**,** 1795-804.

KOUTSODONTIS, G., VASILAKI, E., CHOU, W. C., PAPAKOSTA, P. & KARDASSIS, D. 2005. Physical and functional interactions between members of the tumour suppressor p53 and the Sp families of transcription factors: importance for the regulation of genes involved in cell-cycle arrest and apoptosis. *Biochem J,* 389**,** 443-55.

KOZAKAI, N., KIKUCHI, E., HASEGAWA, M., SUZUKI, E., IDE, H., MIYAJIMA, A., HORIGUCHI, Y., NAKASHIMA, J., UMEZAWA, K., SHIGEMATSU, N. & OYA, M. 2012. Enhancement of radiosensitivity by a unique novel NF-[kappa]B inhibitor, DHMEQ, in prostate cancer. *Br J Cancer,* 107**,** 652-657.

KRISHAN, A. 1975. Rapid flow cytofluorometric analysis of mammalian cell cycle by propidium iodide staining. *J Cell Biol,* 66**,** 188-93.

KUMAR, V. L. & MAJUMDER, P. K. 1995. Prostate gland: structure, functions and regulation. *Int Urol Nephrol,* 27**,** 231-43.

KVORNING TERNOV, K., KRAG JAKOBSEN, A., BRATT, O. & AHLGREN, G. 2015. Salvage cryotherapy for local recurrence after radiotherapy for prostate cancer. *Scandinavian journal of urology,* 49**,** 115-119.

LAIRD, A. D., VAJKOCZY, P., SHAWVER, L. K., THURNHER, A., LIANG, C., MOHAMMADI, M., SCHLESSINGER, J., ULLRICH, A., HUBBARD, S. R., BLAKE, R. A., FONG, T. A. T., STRAWN, L. M., SUN, L., TANG, C., HAWTIN, R., TANG, F., SHENOY, N., HIRTH, K. P., MCMAHON, G. & CHERRINGTON, J. M. 2000. SU6668 Is a Potent Antiangiogenic and

Antitumor Agent That Induces Regression of Established Tumors. *Cancer Research,* 60**,** 4152-4160.

LAM, L. T., DAVIS, R. E., NGO, V. N., LENZ, G., WRIGHT, G., XU, W., ZHAO, H., YU, X., DANG, L. & STAUDT, L. M. 2008. Compensatory IKKα activation of classical NF-κB signaling during IKKβ inhibition identified by an RNA interference sensitization screen. *Proceedings of the National Academy of Sciences,* 105**,** 20798-20803.

LAM, L. T., DAVIS, R. E., PIERCE, J., HEPPERLE, M., XU, Y., HOTTELET, M., NONG, Y., WEN, D., ADAMS, J. & DANG, L. 2005. Small molecule inhibitors of IκB kinase are selectively toxic for subgroups of diffuse large B-cell lymphoma defined by gene expression profiling. *Clinical cancer research,* 11**,** 28-40.

LAMONT, K. R. & TINDALL, D. J. 2010. Androgen regulation of gene expression. *Advances in cancer research,* 107**,** 137-162.

LEE, D.-F. & HUNG, M.-C. 2008. Advances in targeting IKK and IKK-related kinases for cancer therapy. *American Association for Cancer Research,* 14**,** 5656-5662.

LEE, D.-F., KUO, H.-P., CHEN, C.-T., HSU, J.-M., CHOU, C.-K., WEI, Y., SUN, H.-L., LI, L.-Y., PING, B. & HUANG, W.-C. 2007. IKKβ suppression of TSC1 links inflammation and tumor angiogenesis via the mTOR pathway. *Cell,* 130**,** 440-455.

LEIBEL, S. A., FUKS, Z., ZELEFSKY, M. J., WOLDEN, S. L., ROSENZWEIG, K. E., ALEKTIAR, K. M., HUNT, M. A., YORKE, E. D., HONG, L. X. & AMOLS, H. I. 2002. Intensity-Modulated Radiotherapy. *The Cancer Journal,* 8**,** 164-176.

LESSARD, L., BEGIN, L. R., GLEAVE, M. E., MES-MASSON, A. M. & SAAD, F. 2005. Nuclear localisation of nuclear factor-kappaB transcription factors in prostate cancer: an immunohistochemical study. *Br J Cancer,* 93**,** 1019-23.

LESSARD, L., SAAD, F., LE PAGE, C., DIALLO, J. S., PEANT, B., DELVOYE, N. & MES-MASSON, A. M. 2007. NF-kappaB2 processing and p52 nuclear accumulation after androgenic stimulation of LNCaP prostate cancer cells. *Cell Signal,* 19**,** 1093-100.

LEWIS, D. A. & SPANDAU, D. F. 2007. UVB activation of NF-kappaB in normal human keratinocytes occurs via a unique mechanism. *Arch Dermatol Res,* 299**,** 93-101.

LI, F. & SETHI, G. 2010. Targeting transcription factor NF-kappaB to overcome chemoresistance and radioresistance in cancer therapy. *Biochim Biophys Acta,* 1805**,** 167-80.

LI, Z. W., CHU, W., HU, Y., DELHASE, M., DEERINCK, T., ELLISMAN, M., JOHNSON, R. & KARIN, M. 1999. The IKKbeta subunit of IkappaB kinase (IKK) is essential for nuclear factor kappaB activation and prevention of apoptosis. *J Exp Med,* 189**,** 1839-45.

LICHTENSZTAJN, D. Y., GOMEZ, S. L., SIEH, W., CHUNG, B. I., CHENG, I. & BROOKS, J. D. 2014. Prostate cancer risk profiles of Asian-American

men: disentangling the effects of immigration status and race/ethnicity. *The Journal of urology,* 191**,** 952-956.

LITVINOV, I. V., DE MARZO, A. M. & ISAACS, J. T. 2003. Is the Achilles' heel for prostate cancer therapy a gain of function in androgen receptor signaling? *The Journal of Clinical Endocrinology & Metabolism,* 88**,** 2972-2982.

LUFTIG, M., YASUI, T., SONI, V., KANG, M.-S., JACOBSON, N., CAHIR-MCFARLAND, E., SEED, B. & KIEFF, E. 2004. Epstein–Barr virus latent infection membrane protein 1 TRAF-binding site induces NIK/IKKα-dependent noncanonical NF-κB activation. *Proceedings of the National Academy of Sciences,* 101**,** 141-146.

LUO, J. L., TAN, W., RICONO, J. M., KORCHYNSKYI, O., ZHANG, M., GONIAS, S. L., CHERESH, D. A. & KARIN, M. 2007. Nuclear cytokine-activated IKKalpha controls prostate cancer metastasis by repressing Maspin. *Nature,* 446**,** 690-4.

MAHATO, R., QIN, B. & CHENG, K. 2011. Blocking IKKα expression inhibits prostate cancer invasiveness. *Pharmaceutical research,* 28**,** 1357-1369.

MALEK, S., HUXFORD, T. & GHOSH, G. 1998. IκBα functions through direct contacts with the nuclear localization signals and the DNA binding sequences of NF-κB. *Journal of Biological Chemistry,* 273**,** 25427-25435.

MARGALEF, P., FERNÁNDEZ-MAJADA, V., VILLANUEVA, A., GARCIA-CARBONELL, R., IGLESIAS, M., LÓPEZ, L., MARTÍNEZ-INIESTA, M., VILLÀ-FREIXA, J., MULERO, M. C. & ANDREU, M. 2012. A truncated form of IKKα is responsible for specific nuclear IKK activity in colorectal cancer. *Cell reports,* 2**,** 840-854.

MAROTO, P., SOLSONA, E., GALLARDO, E., MELLADO, B., MOROTE, J., ARRANZ, J. Á., GÓMEZ-VEIGA, F., UNDA, M., CLIMENT, M. Á. & ALCARAZ, A. 2016. Expert opinion on first-line therapy in the treatment of castration-resistant prostate cancer. *Critical Reviews in Oncology/Hematology,* 100**,** 127-136.

MATTIOLI, I., SEBALD, A., BUCHER, C., CHARLES, R.-P., NAKANO, H., DOI, T., KRACHT, M. & SCHMITZ, M. L. 2004. Transient and selective NF-κB p65 serine 536 phosphorylation induced by T cell costimulation is mediated by IκB kinase β and controls the kinetics of p65 nuclear import. *The Journal of Immunology,* 172**,** 6336-6344.

MAY, M. J., MARIENFELD, R. B. & GHOSH, S. 2002. Characterization of the IκB-kinase NEMO binding domain. *Journal of Biological Chemistry,* 277**,** 45992-46000.

MCCALL, P., BENNETT, L., AHMAD, I., MACKENZIE, L., FORBES, I., LEUNG, H., SANSOM, O., ORANGE, C., SEYWRIGHT, M. & UNDERWOOD, M. 2012. NFκB signalling is upregulated in a subset of castrate-resistant prostate cancer patients and correlates with disease progression. *British journal of cancer,* 107**,** 1554-1563.

MCINTYRE, K. W., SHUSTER, D. J., GILLOOLY, K. M., DAMBACH, D. M., PATTOLI, M. A., LU, P., ZHOU, X. D., QIU, Y., ZUSI, F. C. & BURKE, J.

R. 2003. A highly selective inhibitor of I kappa B kinase, BMS-345541, blocks both joint inflammation and destruction in collagen-induced arthritis in mice. *Arthritis Rheum,* 48**,** 2652-9.

MCNEAL, J. 1981. Normal and pathologic anatomy of prostate. *Urology,* 17**,** 11-16.

MEFFERT, M. K., CHANG, J. M., WILTGEN, B. J., FANSELOW, M. S. & BALTIMORE, D. 2003. NF-κB functions in synaptic signaling and behavior. *Nature neuroscience,* 6**,** 1072-1078.

MERKHOFER, E. C., COGSWELL, P. & BALDWIN, A. S. 2010. Her2 activates NF-kappaB and induces invasion through the canonical pathway involving IKKalpha. *Oncogene,* 29**,** 1238-48.

MILES, D., VON MINCKWITZ, G. & SEIDMAN, A. D. 2002. Combination versus sequential single-agent therapy in metastatic breast cancer. *The oncologist,* 7**,** 13-19.

MILLER, E. M., FOWLER, J. F. & KINSELLA, T. J. 1992. Linear-quadratic analysis of radiosensitization by halogenated pyrimidines. II. Radiosensitization of human colon cancer cells by bromodeoxyuridine. *Radiat Res,* 131**,** 90-7.

MOGENSEN, T. H. 2009. Pathogen recognition and inflammatory signaling in innate immune defenses. *Clinical microbiology reviews,* 22**,** 240-273.

MOORE, C. B., TAXMAN, D. J., GUTHRIE, E. H. & HUANG, M. T.-H. 2010. Short hairpin RNA (shRNA): design, delivery, and assessment of gene knockdown. *RNA Therapeutics: Function, Design, and Delivery***,** 139-156.

MOULE, R. N. & HOSKIN, P. J. 2009. Non-surgical treatment of localised prostate cancer. *Surg Oncol,* 18**,** 255-67.

MUNSHI, A., HOBBS, M. & MEYN, R. E. 2005. Clonogenic cell survival assay. *Methods Mol Med,* 110**,** 21-8.

NATARAJAN, M., NAYAK, B. K., GALINDO, C., MATHUR, S. P., ROLDAN, F. N. & MELTZ, M. L. 2006. Nuclear translocation and DNA-binding activity of NFKB (NF-kappaB) after exposure of human monocytes to pulsed ultra-wideband electromagnetic fields (1 kV/cm) fails to transactivate kappaB-dependent gene expression. *Radiat Res,* 165**,** 645-54.

NGUYEN, D. P., LI, J., YADAV, S. S. & TEWARI, A. K. 2014. Recent insights into NF-kappaB signalling pathways and the link between inflammation and prostate cancer. *BJU Int,* 114**,** 168-76.

NICHOLSON, D. W., ALI, A., THORNBERRY, N. A., VAILLANCOURT, J. P., DING, C. K., GALLANT, M., GAREAU, Y., GRIFFIN, P. R., LABELLE, M., LAZEBNIK, Y. A. & ET AL. 1995. Identification and inhibition of the ICE/CED-3 protease necessary for mammalian apoptosis. *Nature,* 376**,** 37-43.

NIIDA, H., NAKANISHI M. 2006. DNA damage checkpoints in mammals*. Mutagenesis*. 21, 3–9.

NOVACK, D. V., YIN, L., HAGEN-STAPLETON, A., SCHREIBER, R. D., GOEDDEL, D. V., ROSS, F. P. & TEITELBAUM, S. L. 2003. The IκB

function of NF-κB2 p100 controls stimulated osteoclastogenesis. *The Journal of experimental medicine,* 198**,** 771-781.

OAKLEY-GIRVAN, I., KOLONEL, L. N., GALLAGHER, R. P., WU, A. H., FELBERG, A. & WHITTEMORE, A. S. 2003. Stage at diagnosis and survival in a multiethnic cohort of prostate cancer patients. *American journal of public health,* 93**,** 1753-1759.

OECKINGHAUS, A. & GHOSH, S. 2009. The NF-κB family of transcription factors and its regulation. *Cold Spring Harbor perspectives in biology,* 1**,** a000034.

OLSEN, L. S., HJARNAA, P. J., LATINI, S., HOLM, P. K., LARSSON, R., BRAMM, E., BINDERUP, L. & MADSEN, M. W. 2004. Anticancer agent CHS 828 suppresses nuclear factor-kappa B activity in cancer cells through downregulation of IKK activity. *Int J Cancer,* 111**,** 198-205.

PAJONK, F., PAJONK, K. & MCBRIDE, W. H. 1999. Inhibition of NF-kappaB, clonogenicity, and radiosensitivity of human cancer cells. *J Natl Cancer Inst,* 91**,** 1956-60.

PALANKI, M. S., GAYO-FUNG, L. M., SHEVLIN, G. I., ERDMAN, P., SATO, M., GOLDMAN, M., RANSONE, L. J. & SPOONER, C. 2002. Structure-activity relationship studies of ethyl 2-[(3-methyl-2,5-dioxo(3-pyrrolinyl))amino]-4-(trifluoromethyl)pyrimidine-5-carbo xylate: an inhibitor of AP-1 and NF-kappaB mediated gene expression. *Bioorg Med Chem Lett,* 12**,** 2573-7.

PAPANDREOU, C. N. & LOGOTHETIS, C. J. 2004. Bortezomib as a potential treatment for prostate cancer. *Cancer Res,* 64**,** 5036-43.

PARK, K.-J., KRISHNAN, V., O'MALLEY, B. W., YAMAMOTO, Y. & GAYNOR, R. B. 2005. Formation of an IKKα-dependent transcription complex is required for estrogen receptor-mediated gene activation. *Molecular cell,* 18**,** 71-82.

PERKINS, N. D. 2006. Post-translational modifications regulating the activity and function of the nuclear factor kappa B pathway. *Oncogene,* 25**,** 6717-6730.

PHAM, C. G., BUBICI, C., ZAZZERONI, F., PAPA, S., JONES, J., ALVAREZ, K., JAYAWARDENA, S., DE SMAELE, E., CONG, R. & BEAUMONT, C. 2004. Ferritin heavy chain upregulation by NF-κB inhibits TNFα-induced apoptosis by suppressing reactive oxygen species. *Cell,* 119**,** 529-542.

PICOT, J., COOPER, K., BRYANT, J. & CLEGG, A. J. 2011. The clinical effectiveness and cost-effectiveness of bortezomib and thalidomide in combination regimens with an alkylating agent and a corticosteroid for the first-line treatment of multiple myeloma: a systematic review and economic evaluation. *Health Technol Assess,* 15**,** 1-204.

PILON, D., QUEENER, M., LEFEBVRE, P. & ELLIS, L. A. 2016. Cost per median overall survival month associated with abiraterone acetate and enzalutamide for treatment of patients with metastatic castration-resistant prostate cancer. *J Med Econ***,** 1-8.

PLOTNIKOV, A., ZEHORAI, E., PROCACCIA, S. & SEGER, R. 2011. The MAPK cascades: signaling components, nuclear roles and mechanisms of nuclear translocation. *Biochimica et Biophysica Acta (BBA)-Molecular Cell Research,* 1813**,** 1619-1633.

POMERANTZ, J. L. & BALTIMORE, D. 1999. NF-κB activation by a signaling complex containing TRAF2, TANK and TBK1, a novel IKK-related kinase. *The EMBO journal,* 18**,** 6694-6704.

POWELL, I. J. 2007. Epidemiology and pathophysiology of prostate cancer in African-American men. *The Journal of urology,* 177**,** 444-449.

PRAJAPATI, S., TU, Z., YAMAMOTO, Y. & GAYNOR, R. B. 2006. IKKalpha regulates the mitotic phase of the cell cycle by modulating Aurora A phosphorylation. *Cell Cycle,* 5**,** 2371-80.

PRESTON, J. N. & TRIVEDI, M. V. 2012. Eribulin: a novel cytotoxic chemotherapy agent. *Annals of Pharmacotherapy,* 46**,** 802-811.

RAO, D. D., VORHIES, J. S., SENZER, N. & NEMUNAITIS, J. 2009. siRNA vs. shRNA: similarities and differences. *Adv Drug Deliv Rev,* 61**,** 746-59.

RAZANI, B., REICHARDT, A. D. & CHENG, G. 2011. Non-canonical NF-κB signaling activation and regulation: principles and perspectives. *Immunological reviews,* 244**,** 44-54.

RICHARDSON, P. G., HIDESHIMA, T., MITSIADES, C. & ANDERSON, K. 2004. Proteasome inhibition in hematologic malignancies. *Ann Med,* 36**,** 304-14.

RITHIDECH, K. N., TUNGJAI, M., ARBAB, E. & SIMON, S. R. 2005. Activation of NF-kappaB in bone marrow cells of BALB/cJ mice following exposure in vivo to low doses of (137)Cs gamma-rays. *Radiat Environ Biophys,* 44**,** 139-43.

ROBINSON, D., VAN ALLEN, E. M., WU, Y.-M., SCHULTZ, N., LONIGRO, R. J., MOSQUERA, J.-M., MONTGOMERY, B., TAPLIN, M.-E., PRITCHARD, C. C. & ATTARD, G. 2015. Integrative clinical genomics of advanced prostate cancer. *Cell,* 161**,** 1215-1228.

ROGERS, S. J., HARRINGTON, K. J., RHYS-EVANS, P., PORNCHAI, O. & ECCLES, S. A. 2005. Biological significance of c-erbB family oncogenes in head and neck cancer. *Cancer and Metastasis Reviews,* 24**,** 47-69.

ROMIEU-MOUREZ, R., LANDESMAN-BOLLAG, E., SELDIN, D. C., TRAISH, A. M., MERCURIO, F. & SONENSHEIN, G. E. 2001. Roles of IKK kinases and protein kinase CK2 in activation of nuclear factor-κB in breast cancer. *Cancer research,* 61**,** 3810-3818.

ROTHWARF, D. M., ZANDI, E., NATOLI, G. & KARIN, M. 1998. IKK-γ is an essential regulatory subunit of the IκB kinase complex. *Nature,* 395**,** 297-300.

RUSSO, S. M., TEPPER, J. E., BALDWIN, A. S., JR., LIU, R., ADAMS, J., ELLIOTT, P. & CUSACK, J. C., JR. 2001. Enhancement of radiosensitivity by proteasome inhibition: implications for a role of NF-kappaB. *Int J Radiat Oncol Biol Phys,* 50**,** 183-93.

SAKON, S., XUE, X., TAKEKAWA, M., SASAZUKI, T., OKAZAKI, T., KOJIMA, Y., PIAO, J. H., YAGITA, H., OKUMURA, K. & DOI, T. 2003. NF-κB inhibits TNF-induced accumulation of ROS that mediate prolonged MAPK activation and necrotic cell death. *The EMBO journal,* 22**,** 3898-3909.

SAKURAI, H., MIYOSHI, H., TORIUMI, W. & SUGITA, T. 1999. Functional interactions of transforming growth factor β-activated kinase 1 with IκB kinases to stimulate NF-κB activation. *Journal of Biological Chemistry,* 274**,** 10641-10648.

SANCAR, A., LINDSEY-BOLTZ, L. A., UNSAL-KACMAZ, K. & LINN, S. 2004. Molecular mechanisms of mammalian DNA repair and the DNA damage checkpoints. *Annu Rev Biochem,* 73**,** 39-85.

SAROSIEK, K. A. & LETAI, A. 2016. Directly targeting the mitochondrial pathway of apoptosis for cancer therapy using BH3 mimetics–recent successes, current challenges and future promise. *The FEBS journal*.

SCHORL, C. & SEDIVY, J. M. 2007. Analysis of cell cycle phases and progression in cultured mammalian cells. *Methods,* 41**,** 143-50.

SCOTTO D'ABUSCO, A., POLITI, L., GIORDANO, C. & SCANDURRA, R. 2010. A peptidyl-glucosamine derivative affects IKKalpha kinase activity in human chondrocytes. *Arthritis Res Ther,* 12**,** R18.

SEMENAS, J., ALLEGRUCCI, C., A BOORJIAN, S., P MONGAN, N. & LIAO PERSSON, J. 2012. Overcoming drug resistance and treating advanced prostate cancer. *Current drug targets,* 13**,** 1308-1323.

SEN, R. & BALTIMORE, D. 1986. Multiple nuclear factors interact with the immunoglobulin enhancer sequences. *cell,* 46**,** 705-716.

SENEGAS, A., GAUTHERON, J., MAURIN, A. G. D. & COURTOIS, G. 2015. IKK-related genetic diseases: probing NF-κB functions in humans and other matters. *Cellular and Molecular Life Sciences,* 72**,** 1275-1287.

SENFTLEBEN, U., CAO, Y., XIAO, G., GRETEN, F. R., KRÄHN, G., BONIZZI, G., CHEN, Y., HU, Y., FONG, A. & SUN, S.-C. 2001. Activation by IKKα of a second, evolutionary conserved, NF-κB signaling pathway. *Science,* 293**,** 1495-1499.

SHAW, P. H. 1996. The role of p53 in cell cycle regulation. *Pathol Res Pract,* 192**,** 669-75.

SHI, H. Y., ZHANG, W., LIANG, R., ABRAHAM, S., KITTRELL, F. S., MEDINA, D. & ZHANG, M. 2001. Blocking tumor growth, invasion, and metastasis by maspin in a syngeneic breast cancer model. *Cancer Res,* 61**,** 6945-51.

SHI, J., CHEN, J., SERRADJI, N., XU, X., ZHOU, H., MA, Y., SUN, Z., JIANG, P., DU, Y., YANG, J., DONG, C. & WANG, Q. 2013. PMS1077 sensitizes TNF-alpha induced apoptosis in human prostate cancer cells by blocking NF-kappaB signaling pathway. *PLoS One,* 8**,** e61132.

SHIAH, H.-S., GAO, W., BAKER, D. C. & CHENG, Y.-C. 2006. Inhibition of cell growth and nuclear factor-κB activity in pancreatic cancer cell lines by a tylophorine analogue, DCB-3503. *Molecular cancer therapeutics,* 5**,** 2484-2493.

SHIMADA, T., KAWAI, T., TAKEDA, K., MATSUMOTO, M., INOUE, J.-I., TATSUMI, Y., KANAMARU, A. & AKIRA, S. 1999. IKK-i, a novel lipopolysaccharide-inducible kinase that is related to IκB kinases. *International Immunology,* 11**,** 1357-1362.

SHIRLEY, R. B., KADDOUR-DJEBBAR, I., PATEL, D. M., LAKSHMIKANTHAN, V., LEWIS, R. W. & KUMAR, M. V. 2005. Combination of proteasomal inhibitors lactacystin and MG132 induced synergistic apoptosis in prostate cancer cells. *Neoplasia,* 7**,** 1104-11.

SHUKLA, S., KANWAL, R., SHANKAR, E., DATT, M., CHANCE, M. R., FU, P., MACLENNAN, G. T. & GUPTA, S. 2015. Apigenin blocks IKKalpha activation and suppresses prostate cancer progression. *Oncotarget,* 6**,** 31216-32.

SHUKLA, S., MACLENNAN, G. T., FLASK, C. A., FU, P., MISHRA, A., RESNICK, M. I. & GUPTA, S. 2007. Blockade of beta-catenin signaling by plant flavonoid apigenin suppresses prostate carcinogenesis in TRAMP mice. *Cancer Res,* 67**,** 6925-35.

SINGH, V., SHARMA, V., VERMA, V., PANDEY, D., YADAV, S. K., MAIKHURI, J. P. & GUPTA, G. 2015. Apigenin manipulates the ubiquitin-proteasome system to rescue estrogen receptor-beta from degradation and induce apoptosis in prostate cancer cells. *Eur J Nutr,* 54**,** 1255-67.

SMITH, R. A., COKKINIDES, V. & EYRE, H. J. 2007. Cancer screening in the United States, 2007: a review of current guidelines, practices, and prospects. *CA Cancer J Clin,* 57**,** 90-104.

SOLAN, N. J., MIYOSHI, H., CARMONA, E. M., BREN, G. D. & PAYA, C. V. 2002. RelB cellular regulation and transcriptional activity are regulated by p100. *J Biol Chem,* 277**,** 1405-18.

SOLT, L. A., MADGE, L. A. & MAY, M. J. 2009. NEMO-binding domains of both IKKα and IKKβ regulate IκB kinase complex assembly and classical NF-κB activation. *Journal of Biological Chemistry,* 284**,** 27596-27608.

SUAREZ, C., MORALES-BARRERA, R., RAMOS, V., NUNEZ, I., VALVERDE, C., PLANAS, J., MOROTE, J., MALDONADO, X. & CARLES, J. 2014. Role of immunotherapy in castration-resistant prostate cancer (CRPC). *BJU Int,* 113**,** 367-75.

SUH, J. & RABSON, A. B. 2004. NF-κB activation in human prostate cancer: Important mediator or epiphenomenon? *Journal of cellular biochemistry,* 91**,** 100-117.

SUN, Z. J., CHEN, G., HU, X., ZHANG, W., LIU, Y., ZHU, L. X., ZHOU, Q. & ZHAO, Y. F. 2010. Activation of PI3K/Akt/IKK-alpha/NF-kappaB signaling pathway is required for the apoptosis-evasion in human salivary adenoid cystic carcinoma: its inhibition by quercetin. *Apoptosis,* 15**,** 850-63.

TANG, G., YANG, J., MINEMOTO, Y. & LIN, A. 2001. Blocking caspase-3-mediated proteolysis of IKKβ suppresses TNF-α-induced apoptosis. *Molecular cell,* 8**,** 1005-1016.

TANNOCK, I. F., OSOBA, D., STOCKLER, M. R., ERNST, D. S., NEVILLE, A. J., MOORE, M. J., ARMITAGE, G. R., WILSON, J. J., VENNER, P. M. &

COPPIN, C. 1996. Chemotherapy with mitoxantrone plus prednisone or prednisone alone for symptomatic hormone-resistant prostate cancer: a Canadian randomized trial with palliative end points. *Journal of Clinical Oncology,* 14**,** 1756-1764.

TENOEVER, B., SHARMA, S., ZOU, W., SUN, Q., GRANDVAUX, N., JULKUNEN, I., HEMMI, H., YAMAMOTO, M., AKIRA, S., YEH, W.-C., LIN, R. & HISCOTT, J. 2004. Activation of TBK1 and IKKε kinases by vesicular stomatitis virus infection and the role of viral ribonucleoprotein in the development of interferon antiviral immunity. *Journal of virology,* 78**,** 10636-10649.

THOBE, M. N., CLARK, R. J., BAINER, R. O., PRASAD, S. M. & RINKER-SCHAEFFER, C. W. 2011. From prostate to bone: key players in prostate cancer bone metastasis. *Cancers,* 3**,** 478-493.

TORRE, L. A., BRAY, F., SIEGEL, R. L., FERLAY, J., LORTET-TIEULENT, J. & JEMAL, A. 2015. Global cancer statistics, 2012. *CA Cancer J Clin,* 65**,** 87-108.

TOWBIN, H., STAEHELIN, T. & GORDON, J. 1979. Electrophoretic transfer of proteins from polyacrylamide gels to nitrocellulose sheets: procedure and some applications. *Proc Natl Acad Sci U S A,* 76**,** 4350-4.

TRAN, C., OUK, S., CLEGG, N. J., CHEN, Y., WATSON, P. A., ARORA, V., WONGVIPAT, J., SMITH-JONES, P. M., YOO, D. & KWON, A. 2009. Development of a second-generation antiandrogen for treatment of advanced prostate cancer. *Science,* 324**,** 787-790.

TRIBIUS, S. & BERGELT, C. 2011. Intensity-modulated radiotherapy versus conventional and 3D conformal radiotherapy in patients with head and neck cancer: is there a worthwhile quality of life gain? *Cancer treatment reviews,* 37**,** 511-519.

TU, Z., PRAJAPATI, S., PARK, K. J., KELLY, N. J., YAMAMOTO, Y. & GAYNOR, R. B. 2006. IKK alpha regulates estrogen-induced cell cycle progression by modulating E2F1 expression. *J Biol Chem,* 281**,** 6699-706.

UEHARA, H., TRONCOSO, P., JOHNSTON, D., BUCANA, C. D., DINNEY, C., DONG, Z., FIDLER, I. J. & PETTAWAY, C. A. 2005. Expression of interleukin-8 gene in radical prostatectomy specimens is associated with advanced pathologic stage. *Prostate,* 64**,** 40-9.

VAN LEENDERS, G. J., DUKERS, D., HESSELS, D., VAN DEN KIEBOOM, S. W., HULSBERGEN, C. A., WITJES, J. A., OTTE, A. P., MEIJER, C. J. & RAAPHORST, F. M. 2007. Polycomb-group oncogenes EZH2, BMI1, and RING1 are overexpressed in prostate cancer with adverse pathologic and clinical features. *European urology,* 52**,** 455-463.

VELDEMAN, L., MADANI, I., HULSTAERT, F., DE MEERLEER, G., MAREEL, M. & DE NEVE, W. 2008. Evidence behind use of intensity-modulated radiotherapy: a systematic review of comparative clinical studies. *The lancet oncology,* 9**,** 367-375.

VERHEIJ, M. 2008. Clinical biomarkers and imaging for radiotherapy-induced cell death. *Cancer and Metastasis Reviews,* 27**,** 471-480.

VLAHOPOULOS, S. A., CEN, O., HENGEN, N., AGAN, J., MOSCHOVI, M., CRITSELIS, E., ADAMAKI, M., BACOPOULOU, F., COPLAND, J. A. & BOLDOGH, I. 2015. Dynamic aberrant NF-κB spurs tumorigenesis: A new model encompassing the microenvironment. *Cytokine & growth factor reviews,* 26**,** 389-403.

WALLACE, T., TORRE, T., GROB, M., YU, J., AVITAL, I., BRUCHER, B., STOJADINOVIC, A. & MAN, Y. 2014. Current approaches, challenges and future directions for monitoring treatment response in prostate cancer. *Journal of Cancer,* 5**,** 3-24.

WALLIS, C. J., MAHAR, A. L., CHOO, R., HERSCHORN, S., KODAMA, R. T., SHAH, P. S., DANJOUX, C., NAROD, S. A. & NAM, R. K. 2016. Second malignancies after radiotherapy for prostate cancer: systematic review and meta-analysis. *bmj,* 352**,** i851.

WATERFIELD, M. R., ZHANG, M., NORMAN, L. P. & SUN, S.-C. 2003. NF-κB1/p105 regulates lipopolysaccharide-stimulated MAP kinase signaling by governing the stability and function of the Tpl2 kinase. *Molecular cell,* 11**,** 685-694.

WEERASINGHE, P., GARCIA, G. E., ZHU, Q., YUAN, P., FENG, L., MAO, L. & JING, N. 2007. Inhibition of Stat3 activation and tumor growth suppression of non-small cell lung cancer by G-quartet oligonucleotides. *Int J Oncol,* 31**,** 129-36.

WEISS, W. A., TAYLOR, S. S. & SHOKAT, K. M. 2007. Recognizing and exploiting differences between RNAi and small-molecule inhibitors. *Nature chemical biology,* 3**,** 739-744.

WEN, D., NONG, Y., MORGAN, J. G., GANGURDE, P., BIELECKI, A., DASILVA, J., KEAVENEY, M., CHENG, H., FRASER, C., SCHOPF, L., HEPPERLE, M., HARRIMAN, G., JAFFEE, B. D., OCAIN, T. D. & XU, Y. 2006. A selective small molecule IkappaB Kinase beta inhibitor blocks nuclear factor kappaB-mediated inflammatory responses in human fibroblast-like synoviocytes, chondrocytes, and mast cells. *J Pharmacol Exp Ther,* 317**,** 989-1001.

WHITE, R., KHOR, R., BRESSEL, M., DUCHESNE, G., WILLIAMS, S., BOWDEN, P., TAI, K. & FOROUDI, F. 2015. Efficacy of high-dose palliative radiotherapy for localised, castration-resistant prostate cancer. *Clinical Oncology,* 27**,** 16-21.

WILLIAMS, S. B., CHAMIE, K. & HU, J. C. 2015. Watchful waiting - active surveillance in low-risk prostate cancer - Reply. *JAMA Oncol,* 1**,** 689-90.

WONG, Y.-N., MITRA, N., HUDES, G., LOCALIO, R., SCHWARTZ, J. S., WAN, F., MONTAGNET, C. & ARMSTRONG, K. 2006. Survival associated with treatment vs observation of localized prostate cancer in elderly men. *Jama,* 296**,** 2683-2693.

WU, L., SHAO, L., AN, N., WANG, J., PAZHANISAMY, S., FENG, W., HAUER-JENSEN, M., MIYAMOTO, S. & ZHOU, D. 2011. IKKbeta regulates the

repair of DNA double-strand breaks induced by ionizing radiation in MCF-7 breast cancer cells. *PLoS One,* 6**,** e18447.

XIE, B.-X., ZHANG, H., YU, L., WANG, J., PANG, B., WU, R.-Q., QIAN, X.-L., LI, S.-H., SHI, Q.-G. & WANG, L.-L. 2010. The radiation response of androgen-refractory prostate cancer cell line C4-2 derived from androgen-sensitive cell line LNCaP. *Asian J Androl,* 12**,** 405-414.

XU, Y., FANG, F., CLAIR, D. K. S., SOMPOL, P., JOSSON, S. & CLAIR, W. H. S. 2008. SN52, a novel nuclear factor-κB inhibitor, blocks nuclear import of RelB: p52 dimer and sensitizes prostate cancer cells to ionizing radiation. *Molecular cancer therapeutics,* 7**,** 2367-2376.

XU, Y., FANG, F., SUN, Y., ST CLAIR, D. K. & ST CLAIR, W. H. 2010. RelB-dependent differential radiosensitization effect of STI571 on prostate cancer cells. *Mol Cancer Ther,* 9**,** 803-12.

XU, Y., JOSSON, S., FANG, F., OBERLEY, T. D., ST CLAIR, D. K., WAN, X. S., SUN, Y., BAKTHAVATCHALU, V., MUTHUSWAMY, A. & ST CLAIR, W. H. 2009. RelB enhances prostate cancer growth: implications for the role of the nuclear factor-kappaB alternative pathway in tumorigenicity. *Cancer Res,* 69**,** 3267-71.

YAMAGUCHI, T., MIKI, Y. & YOSHIDA, K. 2007. Protein kinase C delta activates IkappaB-kinase alpha to induce the p53 tumor suppressor in response to oxidative stress. *Cell Signal,* 19**,** 2088-97.

YANG, J., PAN, W.-H., CLAWSON, G. A. & RICHMOND, A. 2007. Systemic targeting inhibitor of κB kinase inhibits melanoma tumor growth. *Cancer research,* 67**,** 3127-3134.

YANG, J. & RICHMOND, A. 2001. Constitutive IκB kinase activity correlates with nuclear factor-κB activation in human melanoma cells. *Cancer research,* 61**,** 4901-4909.

YANG, J., SPLITTGERBER, R., YULL, F. E., KANTROW, S., AYERS, G. D., KARIN, M. & RICHMOND, A. 2010. Conditional ablation of Ikkb inhibits melanoma tumor development in mice. *The Journal of clinical investigation,* 120**,** 2563-2574.

YE, L., KYNASTON, H. G. & JIANG, W. G. 2007. Bone metastasis in prostate cancer: molecular and cellular mechanisms (Review). *Int J Mol Med,* 20**,** 103-11.

YEMELYANOV, A., GASPARIAN, A., LINDHOLM, P., DANG, L., PIERCE, J. W., KISSELJOV, F., KARSELADZE, A. & BUDUNOVA, I. 2006. Effects of IKK inhibitor PS1145 on NF-kappaB function, proliferation, apoptosis and invasion activity in prostate carcinoma cells. *Oncogene,* 25**,** 387-98.

YIN, L., HU, Q. & HARTMANN, R. W. 2013. Recent progress in pharmaceutical therapies for castration-resistant prostate cancer. *International journal of molecular sciences,* 14**,** 13958-13978.

YUE, P. & TURKSON, J. 2009. Targeting STAT3 in cancer: how successful are we? *Expert Opin Investig Drugs,* 18**,** 45-56.

ZEJNULLAHU, K., AREVALO, M. G., RYAN, C. J. & AGGARWAL, R. Approaches to minimize castration in the treatment of advanced prostate

cancer. Urologic Oncology: Seminars and Original Investigations, 2016. Elsevier.
ZHANG, L., ALTUWAIJRI, S., DENG, F., CHEN, L., LAL, P., BHANOT, U. K., KORETS, R., WENSKE, S., LILJA, H. G., CHANG, C., SCHER, H. I. & GERALD, W. L. 2009. NF-kappaB regulates androgen receptor expression and prostate cancer growth. *Am J Pathol,* 175**,** 489-99.
ZHANG, Y., CASTANEDA, S., DUMBLE, M., WANG, M., MILESKI, M., QU, Z., KIM, S., SHI, V., KRAFT, P. & GAO, Y. 2011. Reduced expression of the androgen receptor by third generation of antisense shows antitumor activity in models of prostate cancer. *Molecular cancer therapeutics,* 10**,** 2309-2319.
ZHENG, B., ZHOU, R., GONG, Y., YANG, X. & SHAN, Q. 2012. Proteasome inhibitor bortezomib overcomes P-gp-mediated multidrug resistance in resistant leukemic cell lines. *Int J Lab Hematol,* 34**,** 237-47.
ZHENG, R. P., WANG, W. & WEI, C. D. 2015. Bortezomib inhibits cell proliferation in prostate cancer. *Exp Ther Med,* 10**,** 1219-1223.
ZHU, H. C., QIU, T., DAN, C., LIU, X. H. & HU, C. H. 2015. Blockage of RelB expression by gene silencing enhances the radiosensitivity of androgen‐independent prostate cancer cells. *Molecular medicine reports,* 11**,** 1167-1173.
ZHU, L., ZHU, B., YANG, L., ZHAO, X., JIANG, H. & MA, F. 2014. RelB regulates Bcl-xl expression and the irradiation-induced apoptosis of murine prostate cancer cells. *Biomed Rep,* 2**,** 354-358.